



TARTU UNIVERSITY



DOUBLE LAYER AND ADSORPTION  
AT SOLID ELECTRODES

IX

Tartu 1991

TARTU UNIVERSITY

**DOUBLE LAYER AND ADSORPTION  
AT SOLID ELECTRODES**

**9th Symposium**

**Tartu, June 6 - 9, 1991**

**Extended Abstracts**

*Symposium is dedicated  
to the memory of  
prof. Uno Palm*

**Tartu 1991**

KUSTUTATUD

Anh

Tartu Olikooli  
RAVVAATUKOGU

112,59

ДЕВЯТЫЙ ВСЕСОЮЗНЫЙ СИМПОЗИУМ "ДВОЙНОЙ СЛОЙ И АДСОРБЦИЯ  
НА ТВЕРДЫХ ЭЛЕКТРОДАХ". Тезисы.

На английском языке.

Тартуский университет.

ЭР, 202400, г.Тарту, ул.Дликооли, 18.

Vastutav toimetaja V. Paast.

Korrektor R. Nells.

Paljundamiseks antud 14.05.1991.

Formaat 60x84/16.

Rotatoripaber.

Masinakiri. Rotaprint.

Tingtrükipoogmaid 14,88.

Arvestuspoogmaid 14,52. Trükipoogmaid 16,0.

Trüklarv 300.

Tell. nr. 256.

Hind rubl. 7.

TÜ trükikoda. EV, 202400 Tartu, Tlgi t. 78.

FORECASTING OF TETRAALKYLAMMONIUM CATIONS' INFLUENCE ON  
HYDROXONIUM CATION AND OXYGEN MOLECULES' DISCHARGE KINETICS

B.N.Afanasiev, L.V.Bykova, Yu.P.Skobochnikina

Leningrad Lensovet Institute of Technology, Leningrad

It has been shown in the reports /1-2/, that the "dielectric continuum" theory describes quantitatively tetra-butylammonium (TBA<sup>+</sup>), tetraethylammonium (TEA<sup>+</sup>) and tetramethylammonium (TMA<sup>+</sup>) cations influence on Zn<sup>2+</sup> and Cr<sup>3+</sup> ions electroreduction rate. Tetraalkylammonium (TAA<sup>+</sup>) cations have been regarded as charged spheres and the following equations have been used for calculations:

$$\ln(k/k_0) = r_1 \ln(1-\theta) - s_1 \quad (1)$$

$$\Delta\psi_1 = 0 \quad (2)$$

$$s_1 = \frac{N_A (ze)^2}{8\pi\epsilon^0 R T R_{ion}} \frac{(\epsilon_0 - \epsilon_1)}{\epsilon_0 \epsilon_1} - \frac{N_A (ze)^2}{16\pi\epsilon^0 R T X_1} \left( \frac{d_1 - X_1}{\epsilon_1' d_1} - \frac{d_0 - X_1}{\epsilon_1' d_0} \right) \quad (3)$$

$$\begin{aligned} \epsilon_0 &= \epsilon_0' = \bar{\epsilon}_0 = C_0 d_0 / \epsilon^0 \\ \epsilon_1 &= \epsilon_1' = \bar{\epsilon}_1 = C_1 d_1 / \epsilon^0 \end{aligned} \quad (4)$$

Here  $\epsilon_0$  and  $\epsilon_1$  are the values of dielectric constant in the plane  $X=X_1$ ;  $\epsilon_0'$  and  $\epsilon_1'$  - average values of dielectric constant in the volume between the planes  $X=X_1$  and  $X=d$ . The rest of the designations are the same as in /1-2/. Equation (4) corresponds to the "steps" model.

As the structure of hydrated  $H_3O^+$  ions is unknown, there appears the problem of choice the values of  $R_{ion}$  and  $X_1$ . Hydroxonium cation radius  $R_{H_3O^+}$  is sufficiently smaller than  $[Cr(H_2O)_6]^{3+}$  and  $[Zn(H_2O)_6]^{2+}$  cations' radii. Since the dielectric constant depends on distance  $X$  from electrode surface,  $\epsilon_1 \neq \bar{\epsilon}_1$  and  $\epsilon_0 + \bar{\epsilon}_0$  not far from electrode surface can be expected.

When predicting surfactants' influence on  $H_3O^+$  discharge

reaction parameter  $s_1$  can be evaluated by two methods.

The first method is to work out the equations of correlation of non-dimensional parameter  $\alpha = H(\varepsilon)/H(\bar{\varepsilon})$  and  $\bar{\varepsilon}_1$  or  $p = R_{TAA}^{refr}/R_{TMA}^{refr}$ . Here  $H(\varepsilon) = (\varepsilon_0 - \varepsilon_1)/\varepsilon_0 \varepsilon_1$  and  $H(\bar{\varepsilon}) = (\bar{\varepsilon}_0 - \bar{\varepsilon}_1)/(\bar{\varepsilon}_0 - \bar{\varepsilon}_1)$  and  $R_{TAA}^{refr}$  and  $R_{TMA}^{refr}$  are the values of molar fractions of any tetraalkylammonium ion and  $TMA^+$  calculated additively.

The experimental data concerning  $H_3O^+$  discharge on dropping mercury electrode give at  $X_1 = 0.06$  nm and  $R_{ion} = 0.25$  nm the following equations:

$$\alpha = 2.852 - 0.05 \bar{\varepsilon}_1 \quad (5)$$

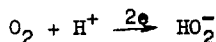
$$\alpha = 2.305 + 0.095 p \quad (6)$$

The equations (5) and (6) were used to predict di-, tri- and tetrasubstituted amines inhibiting action on  $H_3O^+$  discharge reaction in 1 N HCl being previously studied in /3/. It has been shown that calculated parameters  $S_1^{theor}$  are in good agreement with the experimental values for tri- and tetrasubstituted amines. There is no coincidence in case of dialkylamines because these amines cannot be considered as charged spheres.

The second method is described below. It is suggested that the "steps" model (i.e. equation (4)) is realized. The effective value  $X_1^{eff}$  is calculated from equation (4) at the set parameter  $R_{ion}$  with  $S_1^{exper}$  numeral value being used.

The carried calculation has given  $X_1^{eff} = 0.28$  nm in  $TBA^+$  presence. The parameter  $S_1^{theor}$  values, computed by both of the methods are in good coincidence with each other and with the experimental data /4,5/.

The oxygen electroreduction kinetics study has indicated that  $TAA^+$  cations affect the second polarographic wave in the same way as the  $H_3O^+$  cation discharge, i.e. the sequence is  $TBA^+ > TEA^+ > TMA^+$ . The result can be explained in the suggestion of oxygen reduction occurring on the outer Helmholtz plane according to the reaction



at potentials of the second polarographic wave. The ion  $\text{HO}_2^-$  formed is diffusing into the surface layer and being reduced to  $\text{OH}^-$  then. We have calculated the radius  $R_{\text{HO}_2^-}=0.15$  nm by means of equations (1)-(4). This value is quite acceptable if  $R_{\text{H}_2\text{O}}=0.13$  nm.

In the first polarographic wave potentials region corresponding to  $\text{O}_2$  reduction  $\text{TMA}^+$  demonstrates the greatest influence. In this case parameter  $S_1$  value is determined by Van der Waals forces action and we are not able to evaluate parameters  $r_1$  and  $S_1$  with a sufficient reliability.

#### References

1. B.N.Afanasiev, Yu.P.Skobochkina, G.G.Serdyukova, *Elektrokhimiya*, 24 (1988) 503.
2. B.N.Afanasiev, Yu.P.Skobochkina, *Elektrokhimiya*, 27 (1991) 51.
3. E.P.Andreeva, *Zh. Fiz. Khim.*, 29 (1955) 699.
4. B.N.Afanasiev, N.N.Gogolev, *Elektrokhimiya*, 20 (1984) 48.
5. B.N.Afanasiev, E.N.Maiorova, K.T.Kuzovleva, I.A.Chefepkova, Proc. 8th Symp. on Double Layer and Adsorption on Solid Electrodes, Tartu, 1988, p.27.

#### ON STATISTICAL THEORY OF ORGANIC SURFACTANTS' INFLUENCE ON THE KINETICS OF CATIONS ELECTROREDUCTION

N.K.Altayev, Kh.K.Dzhumabekova, M.K.Nauryzbayev

Kazakh Institute of Chemistry and Technology, Chinkent

At present it is well-known that description of experimental data on the influence of organic molecules' adsorption on the reduction kinetics of hydrated and solvated cations is based on Frumkin's equation of 1952:

$$i = k \cdot f(\theta) \cdot \exp\left[-\frac{\beta(\varphi - \varphi_0)nF}{RT}\right] \exp\left[-\frac{\varphi_0 z F}{RT}\right] \quad (1)$$

Later on the following interpretations of the function  $f(\theta)$  have been suggested by various authors:

$$f(\theta) = \exp(-\Delta U/RT) \quad \text{by Lashkarev M.A. ,} \quad (2)$$

$$f(\theta) = (1 - \theta) \quad \text{by Weber-Coryta,} \quad (3)$$

$$f(\theta) = (1 - \theta)^b \quad \text{by Sathyanarayana S.,} \quad (4)$$

$$f(\theta) = (1 - \theta)^r \exp(-s\theta) \quad \text{by Afanasiev-Damaskin.} \quad (5)$$

In these equations  $\Delta U$  - is an additional latent barrier causing difficulties in cations' penetration through the thick adsorptional layer, while  $\theta$  - is the degree of electrode surface coverage by adsorbate molecules, and  $b$ ,  $r$ ,  $s$  - are inhibition parameters.

However, from the theoretical point of view the derivation of equations (1)-(5) is not strict enough, since in this case the organic surfactants' specific adsorption is not taken into consideration.

The derivation of kinetic equations made on the basis of statistical and wave mechanics gives an opportunity to take into account the organic surfactants' specific adsorption.

In the present article the solution of this problem is grounded on the ideas of ref.1, in which the following equation has been derived:

$$i = \exp[-E_{K^+}(H_2O)/RT] \exp(F\varphi/RT) \exp(F\varphi_1/RT) n_{K^+}(H_2O) n^0 \quad (6)$$

concerning the case when the system lacks organic surfactants. The organic surfactants' adsorption taking place, the equation acquires the following form:

$$i = \exp[-E_{K^+}(H_2O)/RT] n^0 n'_{K^+}(H_2O) \exp[F\varphi_{K^+}(H_2O)/RT] / \left\{ 1 + n'_{K^+}(H_2O) \exp[F\varphi_{K^+}(H_2O)/RT] + n'_M \exp(F\varphi_M/RT) \right\} \quad (7)$$

when both metal cations and organic molecules are acceptors, and

$$i = \exp[-E_{K^+}(H_2O)/RT] n^0 / \{1 + 1/n_{K^+}(H_2O) \exp[-F\psi_{K^+}(H_2O)/RT]\} \quad (8)$$

concerning the case when metal cations are acceptors, while organic molecules are donors. In these formulas  $\psi_{K^+}(H_2O)$  - is a potential caused by specific adsorption while  $E_{K^+}(H_2O)$  - activation energy,  $n_{K^+}(H_2O)$  - volume concentration of metal cations,  $n^0$  - the number of active centres,  $n_{K^+}(H_2O)$  - surface concentration of metal cations, and  $n_M^1$  - surface concentration of organic molecules.

The suggested equations allow to explain qualitatively the following experimental facts:

- a) the inhibition of cations' reduction rate as a result of the introduction of surface-active organic cations;
- b) the increase in cations' reduction rate as a result of the introduction of surface active organic anions;
- c) the effect of neutral organic surfactants on cations reduction kinetics.

#### Reference

1. N.K. Altayev, Quantum-statistical approach to the description of chemical kinetics' problems. Dep. in VINITI, 1981, N 5697 - 81.

#### ADSORPTION OF ORGANIC COMPOUNDS ON A BISMUTH ELECTRODE FROM ETHYLENE GLYCOL

A. Alumaa

Tartu University, Tartu

Adsorption of organic compounds from non-aqueous medium is associated with many peculiarities, first of all must be



mentioned the more non-equilibric feature of adsorption process /1/, as well as the desolvation or the resolution of the double layer ions and the change of effective dimension of adsorption layer at high bulk concentrations /2,3/. The present report is devoted to the study of adsorption of some aliphatic and aromatic compounds from ethylene glycol (EG) in order to develop the points of view on their adsorption from alcoholic media /2,3/.

By measuring the dependence of the differential capacity  $C$  on the solid drop Bi electrode potential  $E$  /1-3/ the adsorption of 1-decanol, naphthalene, aniline and thiocarbamide has been studied.

Alkanes being practically insoluble in EG and having negligible adsorption effects drop out of the representatives of different classes of organic compounds studied in the non-aqueous media.

The adsorption process of 1-decanol from EG on Bi has a considerably non-equilibric feature, which has been indicated by lowered maximums on  $C, E$ -curves. So, the area of the negative maximum on the  $C, E$ -curve in 0.1 M solution of 1-decanol is by 45 % smaller than the equilibric one. As in the case of the adsorption of organic compounds from dimethylformamide /1/, it is the result of a strong interaction between solvent molecules and the Bi surface, which also followed from the comparison of the adsorption data on the Bi/solution and the Hg/solution /4/ interface (Table 1). The surface activity of 1-decanol increases in the sequence  $Bi < Hg < air$ , at which on bismuth it is considerably lowered.

The shape of the  $C, E$ -curves of Bi and Hg /4/ in the saturated solution of 1-decanol indicates the formation of polylayer in the adsorption region, considerably complicating the calculation of the adsorption characteristics and their comparison on different interfaces. Nevertheless, it can be concluded that the value of  $a$  in the case of the adsorption from EG as a strongly associated solvent, is noticeably higher than that in the case of the adsorption from alcohol. Differently from the adsorption of alkanes from alcohol /2,3/ in this case the energetic heterogeneity of the bismuth solid

drop electrode is expressed very weakly both in the shape of C,E-curves and in the isotherm.

Table 1

Adsorption characteristics of 1-decanol on Bi and Hg in 0.5 M LiClO<sub>4</sub> solution /4/<sup>⊗</sup>

Elec-trode	a	C', μF·cm <sup>-2</sup>	E <sub>N</sub> , V	10 <sup>10</sup> ·Γ <sub>m</sub> , mol·cm <sup>-2</sup>	B <sub>0</sub> , l·mol <sup>-1</sup>	-ΔG <sub>A</sub> <sup>⊗</sup> , kJ·mol <sup>-1</sup>	Δ(-ΔG <sub>A</sub> ) <sub>0</sub> , kJ·mol <sup>-1</sup>
Bi	1.4	3.3	0.10	2.6	10.2	93.9	-2.8
Hg	1.2	4.3	0.14	2.6	23.2	95.7	-0.6

<sup>⊗</sup> In Tables a - attraction constant in the Frumkin isotherm; C' - the limiting value of the differential capacity; ΔC<sub>m</sub> - maximum value of the differential capacity depression; E<sub>N</sub> - maximum adsorption potential at q=0; Γ<sub>m</sub> - maximum adsorption; B<sub>0</sub> - adsorption equilibrium constant at E<sub>q=0</sub>; -ΔG<sub>A</sub><sup>⊗</sup> - standard free energy of adsorption at E<sub>q=0</sub> and Γ=1 molecule·cm<sup>-2</sup> in the rational scale considering the saturation of the surface layer with adsorbate molecules /5/; Δ(-ΔG<sub>A</sub>)<sub>0</sub> - profit in the free adsorption energy at transition from Bi/solution to air/solution.

Adsorption of aromatic compounds on Bi from EG is principally determined by the π-orbital interaction between the adsorbate and electrode surface, being essentially weaker than that with Hg. In the case of aniline, the difference between the adsorption energy on Bi and Hg at charge q=0 is 14 kJ·mol<sup>-1</sup>, a great part of which is caused by the difference in the π-orbital interaction. Such a great difference in the adsorption activity also leads to qualitatively different C,E-curves of Bi and Hg in the solution of aniline.

Tables 2 and 3 show that the transition from butanol to methanol increases the adsorption effect in the adsorption region at q=0. It is caused by strengthening of the structural squeezing out of aromatic hydrocarbon from the bulk solution by increasing of solvent polarity, as well as

by decreasing of displacement work  $W$  of solvent molecule from the electrode surface. At the same time, in the case of transition from methanol to EG (close constants of the dielectric permeability) the adsorption effect decreases in the adsorption region near  $E_{q=0}$  as a result of the increase in  $W$ . The adsorption activity of thiocarbamide also decreases essentially at transition from alcohols to EG. The values of  $-\Delta G_A^{\ddagger}$  in the case of adsorption of thiocarbamide from methanol, ethanol, n-propanol and EG are 93.8; 93.7; 92.6 and 89.6  $\text{kJ}\cdot\text{mol}^{-1}$ , respectively.

Table 2

Adsorption characteristics of naphthalene on Bi in the adsorption region near  $E_{q=0}$  ( $q_m \sim -1 \div -2 \mu\text{C}\cdot\text{cm}^{-2}$ ;  $E_m \sim -0.05 \div -0.15$  V in reference  $E_{q=0}$ )

Solvent	$\Delta C_m$ , $\mu\text{F}\cdot\text{cm}^{-2}$	$10^{10} \cdot \Gamma_m$ , $\text{mol}\cdot\text{cm}^{-2}$	$E_N$ , V	$-\Delta G_A^{\ddagger}$ , $\text{kJ}\cdot\text{mol}^{-1}$	$\Delta(-\Delta G_A)$ , $\text{kJ}\cdot\text{mol}^{-1}$
EG	2.8	1.1	-0.065	93.3	7.0
Methanol	4.3	2.4	-0.06	95.1	-
Ethanol	2.5	1.8	-0.085	92.2	-
Butanol	1.1	0.4	-0.05	90.9	-

Table 3

Adsorption characteristics of naphthalene on Bi at High positive charges ( $q_m \sim 12-13 \mu\text{C}\cdot\text{cm}^{-2}$ ;  $E_m \sim 0.5$  V in reference  $E_{q=0}$ )

Solvent	$\Delta C_m$ , $\mu\text{F}\cdot\text{cm}^{-2}$	$a$	$10^{10} \cdot \Gamma_m$ , $\text{mol}\cdot\text{cm}^{-2}$	$-\Delta G_A^{\ddagger}$ , $\text{kJ}\cdot\text{mol}^{-1}$
EG	5.1	0	2.0	97.2
Methanol	7.1	-0.25	2.0	98.6
Ethanol	9.8	-0.15	1.8	96.7
Butanol	10.7	-1.0	1.0	96.1

As it appears from Table 3, the change in the dielectric

properties of aromatic hydrocarbon connected by its  $\pi$ -orbital interaction with electrode surface at high positive charges strongly depends on the polarity of the solvent. According to the specific depression of capacity  $\Delta C_m/\Gamma_m$  and the repulsional interaction between adsorbed molecules in the adsorption layer, the solvents studied are in the following sequence water < EG < methanol < ethanol < butanol.

Thus, on the one hand, EG reveals itself to be a solvent relatively strongly interacting with the Bi surface, and on the other hand, a solvent, the molecules of which are essentially associated.

#### References

1. A.R.Alumaa, U.V.Palm, *Elektrokhimiya*, 13 (1977) 1216.
2. U.Palm, A.Alumaa and U.Past, *J.Electroanal.Chem.*, 239 (1988) 333.
3. A.Alumaa, U.Past, U.Palm, *Trans. Tartu State Univ.*, 757 (1986) 56.
4. J.I.Japaridze, N.A.Abuladze, Sh.S.Japaridze, A.de Battisti, S.Trasatti, *Electrochim.Acta*, 31 (1986) 621.
5. U.E.Past, A.R.Alumaa, U.V.Palm, *Elektrokhimiya*, 23 (1987) 568.

#### VOLTAMMETRY OF ORGANIC COMPOUNDS ON THE GLASSY CARBON ELECTRODE IN THE PRESENCE OF LEAD IONS

I.A.Avrutskaya, S.S.Kucherov, A.N.Zhuravlev,  
G.V.Itov, N.A.Vishnyakova

Moscow D.I.Mendeleev Chemical and Technological Institute,  
Moscow

Possibilities of the voltammetry in the study of electrochemical behaviour of organic compounds on the glassy

carbon electrode can be essentially enlarged by adding to the solution metal ions, depositing at less negative potentials than the organic substrate discharge during linear potential sweep /1/. Good reproducibility of the results obtained on the glassy carbon electrode with electrodeposited metals on its surface enable us to use this method for the investigation of electrochemical behaviour of organic compounds on electrodes applied in preparative electro-synthesis.

Electrochemical behaviour of dichloro- and monochloroacetic acids (DCAA and MCAA), 2,2-dichloro- and 2,2-monochloropropionic acids (DCPA and MCPA) was studied on the glassy carbon electrode in the presence of lead ions. Primarily it was found that all the above mentioned acids did not influence the shape of the background curve on the glassy carbon electrode in 0.1 M HCl solution, or in cathodic and anodic potential regions.

Addition of lead ions into 0.1 M HCl solution leads to the appearance of the peak ( $E_p = -0.6$  V) and the background discharge is removed to the cathodic region up to the potentials of hydrogen evolution on the lead microelectrode. This indicates the presence of lead on the glassy carbon electrode surface. The reverse course of the potential sweep gives the peak of anodic lead dissolution ( $E_p = -0.5$  V). The height of the cathodic peak is proportional to the lead ions' concentration in the solution and linear to the square root of the potential sweep velocity. The lead deposit has a local distribution.

Addition of DCAA or DCPA to the solution containing metal ions in  $10^{-4}$  -  $10^{-3}$  M leads to the appearance of another cathodic peak due to the reduction of dichloroacids to the monochlorocarboxylic acids with potentials -1.2 and -1.0 V, respectively. Increase in lead ions' concentration removes these peaks into the region of less negative potentials. That, probably, deals with the change in the deposit structure. The clearest peaks are observed in the region of lead ions' concentrations  $(2,5 - 5) \cdot 10^{-4}$  M.

Limiting currents of DCAA and MCAA reduction are in

directly proportional relationship with their concentrations in the solution and with the square root of the potential sweep velocity. The latter indicates the diffusion nature of the limiting current of dicarboxylic acids' reduction.

The electrochemical behaviour of methyl ester of cyano-benzoic acid and monomethyl ester of terephthalic acid amide used in the synthesis of radioprotective preparation - para-aminomethylbenzoic acid, was studied in the same route. The peaks of these compounds' reduction to the corresponding am-  
noderivates in a strongly acidic medium were observed on the glassy carbon electrode in the presence of lead ions at potentials more negative than lead ions' reduction. Peak potentials are similar to those obtained on the lead micro-electrode.

On a dropping mercury electrode, in the same conditions all compounds discussed do not give clear waves, especially in strongly acidic media. Keeping in mind that lead is a cathode in the preparative reduction of these compounds, the application of this method allows us to study the electrochemical behaviour of organic compounds in conditions close to the preparative electrosynthesis.

The renewing in every cycle and well-reproduced lead deposit that formed during the linear potential sweep on the glassy carbon electrode in the solution containing lead ions can be used for the investigation of electrochemical behaviour and analytical detection of the compounds reducing on lead electrode under potentials more negative than metal ions' discharge.

#### Reference

1. A. N. Zhuravlev, I. A. Avrutskaya, *Elektrokhimiya*, 25 (1989) 563.

## PARAMETERS OF DOUBLE LAYER CHARGING

E.A.Babak, V.S.Kublanovskii

Institute of General and Inorganic Chemistry  
Ukr.SSR Acad. Sci., Kiev

The time constant of electrode charging-discharging process, that is the product of interphase resistance and its capacity, is one of important parameters in electrochemical kinetics. At present this parameter is not used as an independent characteristic of electrode. It is related to the fact that the resistance and capacity of the electrode depend on the supplied potential as well as on the frequency and shape of supplied pulses (sinusoidal and non-sinusoidal). But the time constant is used as a real physical value in such experimental electrochemical methods as commutator and current double pulse methods, square-wave polarography etc.

If the action of supplied pulses does not accumulate on electrode as it occurs in cyclic methods and each pulse corresponds to a standard initial electrode state then a single pulse can be considered. For such a single pulse the Fourier series expansion shows a maximum contribution of low-frequency sinusoidal components. Thus, for single pulses the time constant of electrode charging can be determined either from the direct measuring of resistance and capacity under pulse supply or from the frequency spectrum of electrode impedance when extrapolating it to zero frequency.

The study of electrode behaviour in pulse regime and frequency characteristics of impedance allows the time constant to be introduced as an electrode process parameter and makes it possible to determine the order of magnitude of this value for different reactions.

THE INFLUENCE OF METAL NATURE ON THE STRUCTURE OF THE ELECTRIC DOUBLE LAYER IN N-METHYLFORMAMIDE IN THE SOLUTION OF INACTIVE ELECTROLYTE.

I.A. Bagotskaya, V.V. Yemets, V.G. Boytsov, V.E. Kazarinov  
Frumkin Institute of Electrochemistry, USSR Acad. Sci., Moscow

In N-methylformamide (a proton solvent, dielectrical constant of 182,4 at 25°C, dipole moment of 3,82D) the structure of the electric double layer (EDL) was studied in metals of the Ga-subgroup. Those were Ga, the Jn-Ga eutectic alloy (16,4 at.% Jn) and the Tl-Ga alloy (0,02 at.% Tl). Combined with Ga, Jn and Tl are surface active components and the above alloys are close to pure Jn and Tl in their electrochemical properties. The investigation was performed on dropping electrodes by measuring differential capacity with AC bridge at 32°C. Potentials of zero charge on metals were determined with an open streaming electrode placed in the same solution. To compare, measurements were taken under the same conditions using a dropping and streaming Hg electrodes.

It was established that it is alkali metal perchlorates that function as surface inactive electrolytes in the Ga-subgroup metals in N-methylformamide. It was shown that on C,E-curves for Ga electrodes (where C is differential capacity and E is potential) in dilute  $\text{ClO}_4^-$  solutions there appears a minimum whose depth increases as the solution is diluted and the minimum potential does not depend on  $\text{ClO}_4^-$  concentration and is similar to that of the open streaming electrode. In Jn-Ga and in Tl-Ga as well as in Hg the minimum potential on the C,E-curves depends on  $\text{ClO}_4^-$  concentration. With further dilution it deepens, shifts in the positive direction and has no correspondence to potential of zero charge, which results from the inner layer capacity ( $C_1$ ) passing through the minimum at insignificant negative charges ( $\sigma$ ), low  $C_1$  values and a negligible contribution of the



diffuse layer capacity ( $C_d$ ) to the magnitude of  $C$  due to the high value of N-methylformamide (N-MF) dielectrical constant

It was shown that in Ga and Tl-Ga as well as Hg the Gouy-Chapman-Graham theory is valid over the investigated charge range. For Jn-Ga, it is valid under  $\sigma > 0$ , and  $\sigma < -5 \cdot 10^{-2} \text{C/m}^2$ .

As can be seen in the figure, the shape of  $C, \sigma$ -curves in N-MF is strongly affected by the nature of the metal. Tl-Ga as well as Hg, reveals a hump in the negative range, whose presence is related to the EDL dense part being half filled with associates and free dipoles N-MF oriented along the field [1]. In Jn-Ga the hump is less pronounced, in Ga it disappears completely degenerating into a bend. Under considerable negative charges  $\sigma < -13 \cdot 10^{-2} \text{C/m}^2$  the value of differential capacity is practically independent of the me-

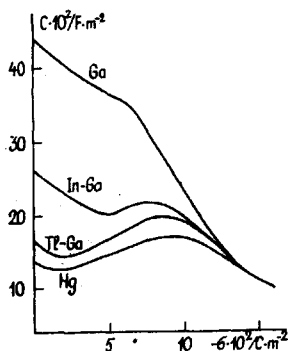


Fig. Plots of differential capacity  $C$  against electrode charge density  $\sigma$  in 0,1M solution  $\text{NaClO}_4$  in N-MF for Ga, Jn-Ga, Tl-Ga and Hg electrodes

tals nature, which indicates similar structure of EDL in different metals. With the decrease of the negative charge  $C, \sigma$ -curves diverge; under  $\sigma=0$  their sequence is changed:  $C_{\text{Ga}} > C_{\text{Jn-Ga}} > C_{\text{Tl-Ga}} > C_{\text{Hg}}$  which reveals N-MF species re-orienting with the negative end of the dipole towards the surface of the electrode due to chemisorption resulting from the interaction between the  $-\text{C}=\text{O}$  oxygen and the metal.

Potential difference between Hg and Ga-subgroup metals in N-MF under  $\sigma \ll 0$   $\Delta E_{\sigma \ll 0}^{\text{Hg-M}}$  does not depend on the magnitude

of  $\sigma$  and is close to  $\Delta E_{\sigma \ll 0}^{\text{Hg-M}}$  in other solvents (dimethylformamide, dimethylsulfoxide, acetonitrile, water)/2/ and, consequently, to the difference of work at the output between the metals into the vacuum (see the Table). The values of

Metal	$C_i \cdot 10^2 \text{ F/m}^2$	$\Delta E_{\sigma=0}^{\text{Hg-M}}$	$\Delta E_{\sigma \ll 0}^{\text{Hg-M}}$	$(\Delta E_{\text{N-MF}}^{\text{Hg-M}})_{\sigma=0}$
Ga	68	0,60	0,18	0,42
Jn-Ga	33	0,56	0,34	0,22
Tl-Ga	19,4	0,55	0,47	0,09
Hg	15,5	0	0	0

$\Delta E_{\sigma=0}^{\text{Hg-M}}$  are significantly different from those of  $\Delta E_{\sigma \ll 0}^{\text{Hg-M}}$ . Adsorption N-MF potential jumps in Ga-subgroup metals relative to Hg which under  $\sigma=0$  are equal to  $(\Delta E_{\text{N-MF}}^{\text{Hg-M}})_{\sigma=0} = \Delta E_{\sigma=0}^{\text{Hg-M}} - \Delta E_{\sigma \ll 0}^{\text{Hg-M}}$  in the Tl-Ga < Jn-Ga < Ga series increase with the output work in the same sequence, which confirms the fact that N-MF functional group bearing a negative charge as well as in previously studied solvents /2/ in interaction with the surface of the electrode acts as a donor in relation to the metal.

Thus, from the data cited above it follows that the disappearance of the hump on the C, E-curves from Hg through Tl-Ga and Jn-Ga to Ga is due to chemisorption at the electrodes of the solvent leading to the balance shift in dense layer between the associates and free N-MF dipoles in the direction of the latter.

#### References

1. Z.Borkowska, R.M.Denobriga, W.R.Fawcett, J.Electroanalyt. Chem., 124 (1981) 263.
2. I.A.Bagotskaya, V.V.Yemets, V.G.Boytsov, V.G.Kazarinov Elektrokhimiya, 24 (1988) 1145.

THE EFFECT OF ELECTRO-OXIDATION OF OXIDE-CONTAINING IONS  
ON THE ADSORPTION CAPACITY OF THE CHLORINE GLASS-CARBON  
ELECTRODE AND ON THE CHLORIDE ION CHARGE

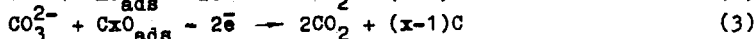
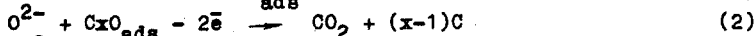
N.M.Barbin, V.N.Nekrasov, L.E.Ivanovsky

Institute of Electrochemistry, Ural Department of the USSR  
Acad. of Sci., Sverdlovsk

The suggested in literature /1/ scheme of electrolytic hydrogen extraction including charge transfer reaction followed by a recombination reaction and/or electrochemical desorption was successfully used for the analysis of extraction processes of other diatomic gases (halogen, oxygen) in aqueous solutions and salt melts. The development of gas electrode theory is connected with studying the adsorption effect on electrode processes.

In the oxide-chloride electrolyte chlorine extraction is preceded by a discharge of oxide ions. Discharge products being adsorbed on the electrode surface will influence the process of chlorine extraction which will affect the adsorption characteristics of chlorine and the nature of the electrode process.

In Figure 1 are given chronopotentiograms of switching on (a) and switching off (b) the anode current for the glass-carbon electrode in the melt  $\text{CaCl}_2\text{-KCl-CaO}$  (1 mole %) at  $750^\circ\text{C}$ . The oxidation of oxide ions is represented in sections including /2/ stages of electrochemical adsorption (AB)(1) followed by a discharge of oxide (BC) and carbonate (CD) ions via electrochemical desorption mechanism (2,3)



The quantity of electricity  $Q$  necessary for the electrooxidation of oxide-containing ions is determined by the chronopotentiograms of switching on. Chlorine extraction is represented in reaction (DE).

The mechanism of the process proceeds as follows /3/ -

fast at high temperatures (above 600°C) reaction of electron transfer (4) is accompanied by a slow recombination reaction (5) which mainly contributes to overvoltage.



For the Frumkin isotherm the adsorption capacity  $C$  in the potential region controlled by adsorption process kinetics is determined by the formula

$$C = (F^2 r^{\frac{2}{3}} / RT) \{ \theta(1-\theta) / [1 + g\theta(1-\theta)] \} \quad (6)$$

According to the chlorine extraction model considered the polarization curve after switching off the current will be determined by the formulas

$$i = -C d\eta/dt, \quad i = i_0 \exp(2\eta F/RT) \quad (7)$$

Integration gives the relation

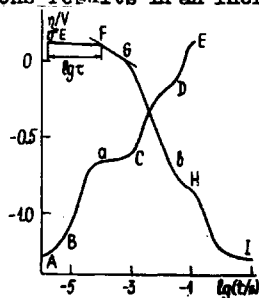
$$-\eta = b \ln [(i_0/bC)(t + \tau)], \quad b = RT/2F. \quad (8)$$

The constant  $\tau = bC/i$  determines the potential delay after switching off the current and includes the parameter  $C$ . Numerically its value can be taken as equal to the part (EF) on the curve of switching off cut by a second with the slope  $b$  formed by extrapolation in the region  $\eta^* < \eta < 0$  of the section (FG) (Fig.1).

The results are given in Table 1. The values of the adsorption capacity of the chlorine glass-carbon electrode decrease while the oxide concentration and temperature increase. A decrease in the supply of electricity for the electro-oxidation of oxide-containing ions results in an increase in

Fig.1

Chronopotentiograms of anode current switching on (a) and switching off (b).



the adsorption capacity. The electrode process proceeds as

follows: at relatively low oxide concentrations (0.1-1.0 mol %) oxide and chloride ions discharge mainly on "their own" adsorption sites and their mutual influence is insignificant. The number of surface adsorption sites for chlorine is large enough and the mechanism of the process is not changed substantially as compared to a purely chloride system. At higher concentrations and temperatures is observed a progressive filling in of the adsorption sites available for chlorine with a discharging oxygen. The degree of filling in the sites increases, the chlorine adsorption capacity drops. Certain changes are observed in the mechanism of chloride ion

#### Table 1 Experimental results

T, K	CaO, mol.%	i, A·cm <sup>-2</sup>	Q, C·cm <sup>-2</sup>	C, μF·cm <sup>-2</sup>
1023	0.1	0.043	9.6·10 <sup>-4</sup>	980
1023	0.1	0.071	6.3·10 <sup>-4</sup>	1000
1023	0.1	0.114	7.2·10 <sup>-4</sup>	1030
1023	1.0	0.441	2.5·10 <sup>-2</sup>	790
1023	1.0	0.882	6.2·10 <sup>-3</sup>	900
1023	1.0	1.470	6.6·10 <sup>-3</sup>	1000
973	5.0	2.597	4.6·10 <sup>-2</sup>	620
973	5.0	3.896	2.2·10 <sup>-2</sup>	830
973	5.0	5.196	1.1·10 <sup>-2</sup>	990
1023	5.0	2.703	6.8·10 <sup>-2</sup>	280
1023	5.0	4.054	4.5·10 <sup>-2</sup>	320
1023	5.0	5.405	2.1·10 <sup>-2</sup>	370
1073	5.0	2.817	8.9·10 <sup>-2</sup>	150
1073	5.0	4.225	4.2·10 <sup>-2</sup>	180
1073	5.0	5.633	1.2·10 <sup>-2</sup>	220

discharge. This manifests itself in a higher overvoltage and in the Tafel slope of the polarization curve. The surface concentration corresponding to the chlorine monolayer appears to be changed.

#### References

1. A.N.Frumkin, Hydrogen Overvoltage, M.: Nauka, 1988, 240.
2. V.N.Nekrasov, N.M.Barbin, L.E.Ivanovsky, Melts, 6 (1989) 55.
3. L.E.Ivanovsky, B.A.Lebedev, V.N.Nekrasov. Anode Processes in Melten Halogenides. M.: Nauka, 1983. 268.

ON THE ROLE OF ADSORPTION PROCESS IN INHIBITION  
OF ANODIC DISSOLVING OF ALLOYS NiZn AND SnIn

A.G.Berezhnaya, V.V.Ekilik, V.A.Fevraleva

Rostov State University, Rostov-on-Don

Inhibition regularities of alloys dissolving differ from those of metals. Here it may be related with violation of the principle of electrode reaction independence, increased structural heterogeneity of alloys, the existence of periods of selective and proportional dissolving of alloys, the transition between which is accompanied by the essential change in the state of surface, kinetics and technique of the process.

In the present paper, the peculiarities of anodic dissolving of alloy NiZn ( $[Ni] = 50, 58, 72$  at %) and Sn5In ( $[In] = 5$  at %) in chloride and perchlorate media with surface-active substances (SAS) have been investigated. As the inhibitors, the organic compounds of tellurium, hydrocinnamic acid, benzotriazole, 9-hydroxyphenalenon, and derivatives of benzimidazole are used. Nonstationary electrochemical measurements have been conducted on a potentiostat PI-1, P5827M in a complex with an oscillograph and recorder "endim-620.02". The degree of the surface coverage with SAS ( $\theta$ ) has been determined from the capacity data.

Theoretical chronoamperograms of a binary solid solution by the stable electropositive component (EPC) is characterized by the successive changing in time ( $\tau$ ) of the slowed-down stages of charge transmission by the diffusion of the electronegative component (ENC), stationary and nonstationary diffusion in solution by nonstationary diffusion of ENC in alloy, between which there are fields of mixed kinetics /1/. Naturally, the inhibition mechanism of the alloy dissolving should be determined by the characteristics of the slowed-down stage of the process. Slowness of electrochemical stage is less characteristic for selective dissolving of alloys in comparison with uniform dissolving. It can be connected with a small  $\tau$  values of the slowed-down stage of charge transmission and high velocity of alloys dissolving

at the beginning of the process.

At the beginning ( $\tau = 0.01-0.1$  s) the dissolving of alloy Sn5In is controlled by electrochemical stage and the inhibitors do not influence it. That may be connected with the slowed-down adsorption process. Later on the dissolving of Sn5In is characterized by a successive change in the  $\tau$  of the slowed-down stages of the ions' diffusion in electrolyte to nonstationary solid diffusion of In. In the former case inhibitors change the velocity by creating a thick protective film on the surface of the alloy or decreasing the diffusion coefficient of the solution product. In the latter case the inhibitors' effect is connected with decreasing the concentration of vacancies because of SAS adsorption. The protective effect of inhibitors is determined by changing solid diffusion coefficient  $D_{ENC}$ . Hence, inhibitors stimulated pure Zn dissolution but inhibited Ni ionization, and adsorbing on the surface of alloys this may inhibit the dissolving of Zn as a component of the alloy. Thus, the organic compounds of tellurium inhibited dissolving of the alloy and Zn as its component, but it stimulated pure Zn ionization ( $K'_{Zn} = 0.7-0.8$ ) and inhibited pure Ni dissolving ( $K'_{Ni} = 10-60$ ).

Under stationary conditions, the ENC and alloy dissolve in keeping with the regularities characteristic of the electropositive component. The influence of inhibitors onto the nature of component is nonspecific. The value of SAS protection effect ( $K$ ) is higher than that ( $K'$ ) for pure metals. It may be presumed that the higher surface activity of EPC in alloy in comparison with a pure metal promotes the increase in adsorption and protecting activity of inhibitors, or in energy heterogeneity of the alloys surface. The analysis of concentration dependences of the filling rate of surface by the addition has shown that when using the Temkin's adsorption isothermes the higher value of the heterogeneity factor of the surface is characteristic for the NiZn than in the case of zinc and nickel. According to that the share of the activation factor of the inhibition process for the alloy was higher in comparison with the blocking and activation factor for pure metals (see Table 1).

Table 1

Value of  $f$ ,  $z$ ,  $z_0$  and  $z_A$  for alloy NiZn, Ni and Zn in perchlorate media. SAS - hydrocinnamic acid

[Ni] at %	-E, B	f	Design- nation of z	Concentration of SAS, mol·l <sup>-1</sup>			
				2·10 <sup>-3</sup>	10 <sup>-3</sup>	7·10 <sup>-4</sup>	5·10 <sup>-4</sup>
0	0.8	0.018	z	83.4	69	50	23
			z <sub>0</sub>	83	42	30	22,7
			z <sub>A</sub>	-	46	29	0.5
50	0.15	0.03	z	99.9	99.4	98	90
			z <sub>0</sub>	96	88	50	35
			z <sub>A</sub>	98	95	96	85
58	0.15	0.036	z	99.9	99.8	98	76
			z <sub>0</sub>	82	48	36	34
			z <sub>A</sub>	99.9	99.6	97	64
72	0.05	0.03	z	99	97	90	69
			z <sub>0</sub>	80	80	66	11
			z <sub>A</sub>	95	85	80	65
100	0.0	0.014	z	98	87	81	44
			z <sub>0</sub>	96	79	65	35
			z <sub>A</sub>	50	38	46	15

Note: z - degree of metal's or alloy's protection,  
 $z_A$  - share of activation factor of inhibition,  
 $z_0$  - degree of protection, when inhibitor effects on  
 block mechanism.

## Reference

1. I.K.Marshakov, A.V.Vvedensky, V.U.Kondrashin, U.A.Bokov, Anodic dissolution and selective corrosion of alloys. Voronezh, 1988, 208.



INFLUENCE OF THE SURFACTANTS' ADSORPTION ON THE PROPAGATION RATE OF MONOATOMIC LAYERS DURING ELECTROCRYSTALLIZATION OF SILVER

V. Bostanov, A.I. Maslii \*, W. Obretenov  
Central Laboratory of Electrochemical Power Sources,  
Bulgarian Academy of Sciences, Sofia  
\* Institute of Solid State Chemistry, Siberian Department of  
the USSR Academy of Sciences, Novosibirsk

The experimental data for the influence of surfactants (impurities) on the process of electrocrystallization, obtained on polycrystalline substrates, can hardly be interpreted reliably by the simplified theoretical models considering the growth of the monoatomic step on a crystal face. The growth shape and propagation rate of monoatomic layers in pure solution have been investigated during electrocrystallization of silver on screw dislocation free faces of silver single crystals [1-3]. The present communication reports the first results on the influence of surfactants on the growth rate of monoatomic steps in this case of electrocrystallization.

**EXPERIMENTAL.** Screw dislocation free (100) face of silver single crystal was obtained by the method described in [4]. Monoatomic layers were successfully deposited on the face by pulse formation at high overvoltage of a single 2D nucleus which subsequently propagated at overvoltages lower than the critical one for 2D nucleation ( $\eta_{or} = -6.5$  mV). The shape and growth rate of each layer was determined by analysis of the current transient recorded during its deposition. The inhibiting effect of the surfactant on the growth of the monoatomic steps was investigated by adding tartaric acid in the electrolyte solution (6N  $AgNO_3$  at pH = 1 and temperature of 45°C). Incidentally, it was found that the propagation rate of the monolayers increase significantly in the presence of carbon tetrachloride in the solution.

**RESULTS.** 1. Tartaric acid with very low concentrations inhibits the growth of the steps. For example, at  $10^{-6}$  mol/l

tartaric acid in the solution, the propagation rate of the monoatomic layers at  $\eta = -4$  mV is more than twice lower than that in pure solutions. It is important to note that in presence of the impurity the character of the overvoltage dependence on the monolayer propagation rate is modified. In pure solutions it is a linear one:  $V_0 = k_V \eta$ . In the presence of the impurity ( $10^{-6}$  mol/l) a linear dependence with a slope virtually equal to that in pure solution is observed at overvoltages higher than 2.5 mV. Below this value the dependence curves towards the origin of the coordinate system. The growth shape, however, does not change remaining round.

The theory discusses the inhibiting effect of impurities on the growth of monoatomic steps on the basis of several models [5-7]. It was established that the best description of the overvoltage dependence of the step propagation rate, obtained in this study, is provided by the model of Albon and Dunning. According to this model the impurity species are adsorbed on the step. At a concentration of the impurity at which the free step lengths are equal to, or less than, the diameter of the critical nucleus, the step can no longer progress. The resulting relationship between  $V$  and  $V_0$ , the step propagation rate in impure and pure solutions respectively,  $c$ , the adsorbed concentration of impurity species (number per atom of the step) and  $r^*$ , the radius of the critical 2D nucleus (atomic diameters) is:

$$V = V_0 [2r^* - (1-c)2r^* + (1-c)] (1-c)^{2r^*} \quad (1)$$

Taking into account that  $V_0 = k_V \eta$  and  $r^* = \epsilon / q_m a \eta$ ,  $\epsilon$  (J/cm),  $q_m$  (C/cm) and  $a$  (cm) being the specific periphery energy of the nucleus, the amount of electricity required for the deposition of one monolayer on a unit surface, and the atomic diameter in the crystal lattice, respectively, the  $V/\eta$  dependence follows from eq. (1):

$$V = k_V \eta [2\epsilon / (q_m a \eta) - (1-c)2\epsilon / (q_m a \eta) + (1-c)] (1-c)^{2\epsilon / q_m a \eta} \quad (2)$$

This dependence agrees well with the experimental data when  $c = 0.1$ . For  $k_v$  the value  $k_v = 2 \text{ cm/sV}$  was obtained and for  $\epsilon$  the value  $\epsilon = 2 \cdot 10^{-13} \text{ J/cm}$  was used [8].

2. If carbon tetrachloride vapours are introduced in the atmosphere of the electrolytic cell, the monolayer propagation rate increases gradually and in about 3 hours reaches a steady state value which is 10-12 times higher than the rate measured in pure solution. Obviously the increase in the propagation rate of the layer is proportional to the  $\text{CCl}_4$  in the electrolyte solution, since this effect occurs immediately when preliminary saturated aqueous  $\text{CCl}_4$  solution is added to the electrolyte. The high growth rate of the monolayers is retained for 10-15 days, i.e. the maximum measurement time for an investigated crystal. This strong catalytic effect of  $\text{CCl}_4$  (or its dissolution products) on the growth rate of the monoatomic steps still remains unclear.

#### REFERENCES

1. V. Bostanov, G. Staikov and D.K. Roe, *J. Electrochem. Soc.*, 122 (1975) 1301.
2. W. Obretenov, V. Bostanov and E. Budevski, *J. Electroanal. Chem.*, 170 (1984) 51.
3. V. Bostanov and W. Obretenov, *Electrochim. Acta*, 34 (1989) 1193.
4. V. Bostanov, A. Kotzeva and E. Budevski, *Bull. Inst. Chim. Phys., Acad. Bulg. Sci.*, 6 (1967) 33.
5. G. W. Sears, *J. Chem. Phys.*, 29 (1958) 1045.
6. N. Cabrera and D.A. Vermilyea, in: *Growth and Perfection of Crystals*, Eds. R.H. Doremus, B. W. Roberts and D. Turnbull, Wiley, New York, 1958, p.441.
7. N. Albon and W. J. Dunning, *Acta Cryst.*, 15 (1962) 474.
8. V. Bostanov, W. Obretenov, G. Staikov, D.K. Roe and E. Budevski, *J. Cryst. Growth*, 52 (1971) 761.

## ELECTRODE POTENTIALS AND WORK FUNCTIONS

N. G. Bukun

New Chemical Problems Institute, Academy of Sciences of the USSR, Chernogolovka

It has been shown by Ukshe [1] that electrode potentials in condensed ionic media (i.e. solid electrolytes or molten salts) can be calculated in "electronic" scale when zero line is the energy level of the rest electron in vacuum. In this case potential of the Ag electrode in solid or liquid AgI equals to work function of silver iodide which is equilibrated with metallic silver

$$E_{\text{Ag}/\text{AgI}} = W_{\text{AgI}(\text{Ag})}^e / e \quad (1)$$

The work function measurements for several solid salts have been made by the contact potential difference method in [2-5]. It has been discovered that values of  $W^e$  depend not only on salt nature but also on the nature and composition of the electrode which is equilibrated with the salt. The value of the contact potential difference between Ag and AgI equilibrated with Ag is [2]:

$$W_{\text{AgI}(\text{Ag})}^e = W_{\text{AgI}(\text{Ag})}^e - W_{\text{Ag}}^e = W_{\text{Ag}}^{\text{Ag}^+} - W_{\text{AgI}(\text{Ag})}^{\text{Ag}^+} \quad (2)$$

where  $W_{\text{Ag}}^{\text{Ag}^+}$  is  $\text{Ag}^+$ -ion work functions. With the help of the Eqs. (1) and (2) and well-knowing data of EMF of the chemical circuits we calculated electrode potentials for several metallic and gas electrodes in solid electrolytes at room temperature. The results of these calculations are given in Table 1 together with electrode potentials in aqueous solutions  $E^*$  [6].

It can be seen that potentials in solid salts depend on their composition and can change in wide limits because of complex formation. In particular in aqueous solutions the silver electrode potential is more positive than iodine po-

Table 1

Electrode potentials for metallic and gas electrodes

electrode	solid salt	E, V	aq. solution	E*, V
Ag	AgCl	4,29	Ag/Ag <sup>+</sup>	0,80
Cl <sub>2</sub>	AgCl	5,35	Cl <sub>2</sub> /Cl <sup>-</sup>	1,36
Ag	AgI	4,09	Ag/Ag <sup>+</sup>	0,80
I <sub>2</sub>	AgI	4,78	I <sub>2</sub> (s)/I <sup>-</sup>	0,54
Ag	Ag <sub>4</sub> KI <sub>5</sub>	4,15		
Ag	Ag <sub>4</sub> RbI <sub>5</sub>	4,24		
I <sub>2</sub>	Ag <sub>4</sub> RbI <sub>5</sub>	4,58		
Ag	Ag <sub>5</sub> PyI <sub>6</sub>	4,27		
Ag	Ag <sub>7</sub> Et <sub>4</sub> Ni <sub>8</sub>	4,29		
Ag	Ag <sub>3</sub> SI	4,75		
Ag	Ag <sub>6</sub> WO <sub>4</sub> I <sub>4</sub>	4,82		
Cd	CdCl <sub>2</sub>	3,52	Cd/Cd <sup>2+</sup>	-0,40
Cl <sub>2</sub>	CdCl <sub>2</sub>	5,30	Cl <sub>2</sub> /Cl <sup>-</sup>	1,36
Cd	CdI <sub>2</sub>	3,30	Cd/Cd <sup>2+</sup>	-0,40
I <sub>2</sub>	CdI <sub>2</sub>	4,34	I <sub>2</sub> (s)/I <sup>-</sup>	0,54
Na	Na <sub>2</sub> O.11Al <sub>2</sub> O <sub>3</sub>	1,54	Na/Na <sup>+</sup>	-2,71
Na	Na <sub>2</sub> O.7Al <sub>2</sub> O <sub>3</sub> .0,2Mn <sub>3</sub> O <sub>4</sub>	1,46		
Na	Na <sub>5</sub> YSi <sub>4</sub> O <sub>12</sub>	1,91		
Na	Na <sub>5</sub> EuSi <sub>4</sub> O <sub>12</sub>	1,81		
Na	Na <sub>5</sub> GdSi <sub>4</sub> O <sub>12</sub>	1,77		
Na	Na <sub>5</sub> YbSi <sub>4</sub> O <sub>12</sub>	1,58		
Na	Na <sub>5</sub> Gd <sub>0,9</sub> Zr <sub>0,1</sub> Si <sub>4</sub> O <sub>12</sub>	1,43		
Li	LiAlSiO <sub>4</sub>	1,02	Li/Li <sup>+</sup>	-3,04

tential,  $E^* = 0.26$  V, but in solid AgI their difference is  $E = -0.69$  V. For silver chloride such inversion of potential for transition from aqueous solution to solid salt does not occur but respective potential differences nevertheless are not the same:  $E^* = -0.56$  and  $E = -1.06$  V. For the systems Cd-Cl<sub>2</sub> and Cd-I<sub>2</sub> such potential differences are  $E^* = 1.76$  and  $0.94$  V,  $E = 1.78$  and  $1.04$  V, respectively. The differences between potentials of sodium in complex silicate Na<sub>5</sub>Gd<sub>0.9</sub>Zr<sub>0.1</sub>Si<sub>4</sub>O<sub>12</sub> and chlorine and iodine in silver halides are ...  $E = 3.92$  and  $3.35$  V when for aqueous solutions  $E^* = 4.07$  and  $3.25$  V. The observed differences for aqueous solutions and condensed ionic phases can not be explained by the differences between hydration energies of different ions [6] because they cannot give the inversion of potentials. Obviously the main cause of aforementioned phenomena is in non-electrochemical electronic exchange between metal electrode and condensed ionic phase [1]. Such exchange is impossible for aqueous solutions. The influence of the electronic equilibria on the formation of double electrical layer probably may be discovered in course of investigations of the solid electrodes of the second kind.

#### References

1. E. A. Ukshe, *Elektrokhimiya*, 25(1989)98.
2. E. A. Ukshe, Yu. I. Malov, N. G. Bukun, A. M. Mikhailova, *Elektrokhimiya*, 24(1988)723.
3. N. G. Bukun, Yu. I. Malov, E. A. Ukshe, *Elektrokhimiya*, 16(1980)112.
4. Yu. I. Malov, L. S. Leonova, S. E. Nadkhina, N. G. Bukun, E. A. Ukshe, *Journal of physical chemistry (Russian)*, 56(1982)1879.
5. I. Zagorska, Z. Koczorowski, *J. Electroanalyt. Chem.* 101(1979)317.
6. G. A. Krestov, *Thermodynamics of ionic processes in solutions (Russian)*. Leningrad: Khimiya, 1984, p. 272.

ON THE MECHANISM OF ELECTROREDUCTION OF ACRYLONITRILE  
ON MERCURY, CADMIUM AND LEAD

I.V.Chumakov, A.V.Tikhomirov

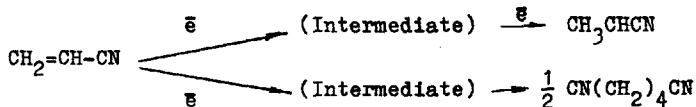
Nizhny Novgorod Polytechnical Institute, Nizhny Novgorod

The cathodic hydrodimerization reaction of acrylonitrile (ACN) forms the basis of the electrochemical method for obtaining adiponitrile (ADN), which is a semiprocessed product in production of nylon. In spite of industrial application, the mechanism of the process remains to be uncertain, mainly due to the fact the interrelated data on electroreduction and acrylonitrile adsorption are not available. In the earlier work /1/ we studied acrylonitrile adsorption on mercury and cadmium with the  $K_2HPO_4$  background.

Adsorption parameters of ACN ( $\beta$ ,  $\theta$ ,  $\alpha$ ) in the wide range of potentials, including electroreduction potentials were estimated.

In this communication the kinetics of acrylonitrile electroreduction on mercury, cadmium and lead in the solutions of potassium hydrophosphate and quaternary ammonium salts were studied. Some kinetics parameters ( $\alpha_{n_a}$ ,  $n$ ,  $K_{FH}^0$ ) with consideration of /1/ were estimated and analysed.

It was found, that independently of the electrode nature and the background electroreduction of acrylonitrile on mercury, cadmium and lead proceeds irreversibly and is controlled by the mass transfer and by the first electron transfer. There were observed two regions of the constant diffusion criteria  $[I_p / (c_{ACN} \cdot \sqrt{v})] I(\bar{c} / c_{ACN})$  with  $c_{ACN} \lesssim 0.1 \approx c_{ACN}$  mole.l<sup>-1</sup> and  $[(I_p / c_{ACN} \sqrt{v})]_{c < 0.1} / [(I_p / c_{ACN} \sqrt{v})]_{c > 0.1} \approx \approx [(I\bar{c} / c_{ACN})]_{c < 0.1} / [(I_p / c_{ACN})]_{c > 0.1} \approx 2$ . From the criteria values the total number of electrons accounted for 1 mole of acrylonitrile, which changes from 2 to 1 within 0.1 mole/l range. Conversion from the two-electrons process to the mono-electron one is associated with a change in the reaction direction. In the range of  $c_{ACN} \lesssim 0.1$  mole/l the main reduction product is propionitrile and with  $c_{ACN} \gtrsim 0.1$  mole/l it is adiponitrile. The probable mechanism of the reaction can be presented by following scheme:



It was found that the range from the propionitrile synthesis to the synthesis of adiponitrile entails retardation of the reaction ( $\Delta E \approx 0.1$  V). From the data obtained from the propionitrile synthesis range, where the peak potential in the first approximation is independent of  $c_{\text{ACN}}$ , we estimated the values of the heterogeneous transfer rate constants at  $E = 0$  V.

Table 1

Apparent rate constants for electroreduction of cyclonitrile with  $E=0$  V and the zero charge potential values on cadmium, lead and mercury

Electrode	Background	$k_{\text{fh}}^0 \cdot 10^{16}, \text{cm} \cdot \text{s}^{-1}$	Zero charge potential, V
Mercury	0.2 M $(\text{C}_4\text{H}_9)_4\text{NI}$	0.15	-0.19
Mercury	1 M $\text{Na}_2\text{HPO}_4$	1.25	
Lead	0.55 M $\text{K}_2\text{HPO}_4$	3.0	-0.59
Lead	0.05 M $\text{K}_2\text{HPO}_4 + 0.02$ M $(\text{C}_4\text{H}_9)_4\text{N}^+$	3.0	
Cadmium	0.05 M $\text{K}_2\text{HPO}_4 + 0.02$ M $(\text{C}_4\text{H}_9)_4\text{N}^+$	9.90	
Cadmium	0.05 M $\text{K}_2\text{HPO}_4$	17.00	-0.82

It can be seen that with  $E=\text{const}$  the reaction rate increases in the electrodes' series  $\text{Hg} < \text{Pb} < \text{Cd}$ . According to /1/ with  $c_{\text{ACN}} \approx 0.1$  mole/l the acrylonitrile electroreduction on cadmium proceeds in the desorption peaks zone of the depolarizer, while on mercury it proceeds cathode wise. The rate constants given in the Table 1 calculated without regard the adsorption are most likely to be apparent values. According to the theory of electroreduction of organic substances from the adsorbed state /2/ they should involve adsorption parameters of initial, intermediate and final states.



With regard to /1/ on the  $K_2HPO_4$  background, the rate constants ratio on cadmium and mercury are also close to the occupations ratio for these electrodes within the electroreduction range  $(K_{fh}^O)_{Cd}^{app}/(K_{fh}^O)_{Hg}^{app} \approx \theta_{Cd}/\theta_{Hg} \approx 14$ . On the one hand, it points to the prevailing contribution of the initial states, which to our opinion is caused by the closeness of the adsorption parameters and by the small surface concentrations of the intermediates that are initial discharge products of acrylonitrile. On the other hand, it seems that it is sufficient to consider differences in adsorption properties to explain the differences in the electroreduction rate of ACN on cadmium and mercury.

In the final analysis the difference of  $(K_{fh}^O)_{app}$  on cadmium and mercury in the range of propionitrile synthesis is attributed basically to the fact that the degree of the cadmium occupation by the depolarizer is by one order higher, compared with mercury. The latter, in turn, is defined by the difference in the zero charge potential and in the electrodes hydrophility. It is believed that occupation degree of the lead electrode in conformity with its zero charge potential holds the intermediate position between cadmium and mercury.

In the range of  $c_{ACN} \geq 0.1$  mole/l the potential of the peaks of the electroreduction shifts to the negative side and as a result of that, acrylonitrile synthesis on the phosphates' background, at least on cadmium and mercury proceeds in the area of depolarizer desorption.

Tetraalkylammonium cations extend the range of acrylonitrile desorption and, depending on concentration and length of the hydrocarbon group, these can both retard and accelerate the process. The possible mechanism of their action is discussed.

#### References

1. J.M.Tjurin, I.V.Chumakov, A.V.Tikhomirov et al, Elektrokhimiya, 27 (1991) 448.
2. A.B.Ershler, Itogi nauki i tekhniki. Elektrokimiya, 19 (1983) 119.

## THE THEORY OF THE PROTONIC ACID DOPING OF POLYANILINE WITH CHANGEABLE LEVEL OF OXIDATION

L.I.Daikhin

A.N.Frumkin Institute of Electrochemistry USSR Acad Sci  
Moscow

H.Reiss put forward the one-dimensional lattice model /1,2/ of the protonic acid doping of the emeraldine. This model is limited by the situation in which the average state of oxidation  $(1-y)$  is firmly restricted to 0.5. It allowed to consider, that all nitrogen atoms are equivalent with respect to adsorption of protons. In ref. /1,2/ the pH dependence of the proton doping of emeraldine was obtained.

But in the electrochemical system the change of the potential drop (E) results in the change of oxidation level and, hence, it influences on protonation. Therefore, it is interesting to consider the process of protonation with the changeable level of oxidation. Here a particular case of that problem will be considered.

Let's assume, that the initial structure is a one-dimensional chain of the completely reduced polyaniline (structure 1A). All of the nitrogen atoms are equivalent with respect to adsorption of protons. As well as in ref. /1,2/, repulsion between protons on adjacent nitrogen along the chain is assumed. The oxidation process is considered as the escape of one electron from the benzenoid ring to the metal (adsorption of the positively charged hole). Let's suppose that two holes on nearest rings repulse with the infinitely large energy. In addition, it is clear, that proton can not adsorb on the nitrogen, being near the charged ring. Therefore, proton and hole, being on the nearest elements of structure, repulse with infinite energy. For simplicity, we shall consider, that the energy of repulsion of two protons on adjacent nitrogens is infinitely large and the other interactions /1/ do not take place.

Thus the model is as follows. There are the sites of two types on one-dimensional chain - nitrogen atoms and benzenoid rings; protons adsorb on nitrogen atoms and holes adsorb on the rings. All particles, being the nearest neighbors, repulse with the infinite energy. This system is in equilibrium with the strong acid solution and the metal. For given E and pH, it is necessary to find the coverage of protons ( $\theta_1$ ) and holes ( $\theta_2$ ). The problem is treated the best in the grand ensemble, and the relevant partition function can be evaluated with the aid of an appropriate transfer matrix. The free energy on one pair of sites (nitrogen atom and ring) of the chain is given by

$$f(z_1, z_2) = 1/3 + \left[ -q(z_1, z_2)/2 + [Q(z_1, z_2)]^{1/2} \right]^{1/3} + \left[ -q(z_1, z_2)/2 - [Q(z_1, z_2)]^{1/2} \right]^{1/3} \quad (1)$$

$$\text{Here } q(z_1, z_2) = -2/27 - (z_1 + z_2)/3 - z_1 z_2 ;$$

$$p(z_1, z_2) = -1/3 - z_1 - z_2 ;$$

$$Q(z_1, z_2) = \left[ p(z_1, z_2)/3 \right]^3 + \left[ q(z_1, z_2)/2 \right]^2 ;$$

$$z_1 = \exp(\mu_1/kT); \quad z_2 = \exp(\mu_2/kT)$$

Here  $\mu_1$  -chemical potential of the proton in the polymer, and  $\mu_2$  -electrochemical potential of the hole in polymer.

As the system is in equilibrium, activities  $z_1$  and  $z_2$  have the form:  $z_1 = K_1 \exp(-2.3 \text{ pH})$  and  $z_2 = K_2 \exp(eE/kT)$ . Here e is the modulus of the electron charge,  $K_1, K_2$  are constants.

From eqn.(1), the expressions for  $\theta_1$  and  $\theta_2$  can be obtained. The coverages  $\theta_1$  and  $\theta_2$  show with little activities  $z_1$  and  $z_2$  ( $z_1 \ll 1, z_2 \ll 1$ ) the following behavior

$$\theta_1 \sim z_1 \left[ 1 - 3z_1 - 2z_2 + 3z_1^2 + 4z_1 z_2 + 2z_2^2 \right]$$

$$\theta_2 \sim z_2 \left[ 1 - 2z_1 - 3z_2 + 2z_1^2 + 4z_1 z_2 + 3z_2^2 \right] \quad (2)$$

## TEMPERATURE EFFECT ON THE ADSORPTION OF THE HOMOLOGUES OF ALIPHATIC ALCOHOLS AND ACIDS

F.I. Danilov, V.B. Obraztsov, Yu.A. Parfjonov  
Dnepropetrovsk Chemical Engineering Institute

The temperature-adsorption method was used to study the adsorption of aliphatic alcohols and acids having a linear structures on the polycrystalline zinc (ZBE) and cadmium (CBE) blade-cutted electrodes. It is shown that at various temperatures the free energy of adsorption of acids and alcohols on ZBE and CBE depends linearly on the methyl group number

$$\Delta G_{\text{a}}^{\circ} = \Delta(\Delta G_{\text{a}}^{\circ})_{\text{f}} + n \cdot \Delta(\Delta G_{\text{a}}^{\circ})_{\text{i}} \quad (1)$$

where  $n$ ,  $\Delta(\Delta G_{\text{a}}^{\circ})_{\text{f}}$ , and  $\Delta(\Delta G_{\text{a}}^{\circ})_{\text{i}}$  are the number of methyl groups, the contributions of the functional and methyl groups respectively. Independently of the electrode and of the functional group nature the values of  $\Delta(\Delta G_{\text{a}}^{\circ})_{\text{i}}$  were approximately the same and that of  $\Delta(\Delta G_{\text{a}}^{\circ})_{\text{f}}$  increased in Hg, Zn, Cd series going from aliphatic alcohols to acids.

The adsorption free energy change resulting from the various types of the interactions in a surface layer

$$\lambda = a \cdot R \cdot T \quad (2)$$

practically remains constant with the temperature varying while the adsorption of alcohols on ZBE and CBE that is  $\partial \lambda / \partial T \approx 0$ . In the case of the carboxylic acids (Fig.1)  $\partial \lambda_{\text{f}} / \partial T < 0$ , and  $\partial \lambda_{\text{i}} / \partial T > 0$ . As  $|\partial \lambda_{\text{f}} / \partial T| \gg |\partial \lambda_{\text{i}} / \partial T|$  the whole effect of the change of  $\lambda$  with temperature is practically related to the specific interaction of the carboxylic group with ZBE on CBE surface. With increasing of the chain length of acids the slope of the  $\lambda, T$ -relation reduces (Fig.1) due to removal of the functional group from the electrode surface and weakening of its interaction with the electrode.

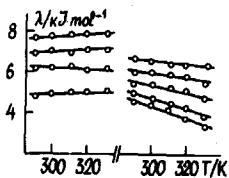


Fig.1.  $\lambda$  Dependence on temperature under the adsorption of alcohols (a) and acids (b) on CBE: 1-propyl alcohol, butyric acid; 2-butyl, valeric acid; 3-amyl alcohol, caproic acid; 4-hexyl alcohol, enanthic acid; 5-caprylic acids acid; 5-caprylic acid.

The data received and presented in Table 1 show the adsorptions of alcohols and acids on ZBE and CBE to be exothermic processes accompanied by entropy increase. The dependence of the thermodynamic parameters of  $\Delta H_{\theta}^{\circ}$ ,  $\Delta G_{\theta}^{\circ}$  and  $T \cdot \Delta S_{\theta}^{\circ}$  on the degree of covering is linear and, unlike alcohols, where  $T \cdot \Delta S_{\theta}^{\circ}$  doesn't depend on  $\theta$ , in the case of the carboxylic acids the entropy reduces with the increase in the degree of covering.

Table 1.

Thermodynamic parameters for alcohols and acids on CBE

Surfactants	$-\Delta(\Delta G_{\theta}^{\circ})_f^*$ kJ/mol	$-\Delta(\Delta G_{\theta}^{\circ})_i^*$ kJ/mol	$-\Delta(\Delta H_{\theta}^{\circ})_f$ kJ/mol	$-\Delta(\Delta H_{\theta}^{\circ})_i$ kJ/mol	$T\Delta(\Delta S_{\theta}^{\circ})_f^*$ kJ/mol	$T\Delta(\Delta S_{\theta}^{\circ})_i^*$ kJ/mol
Alcohols	0.6	3.3	2.2	0.6	3.6	3.2
Acids	5.6	3.1	9.1	1.5	9.7	3.2

\*All the values were received at 296K.

The enthalpy of the adsorption increases when going from alcohols to acids and to a lesser degree on the chain length. The role of the entropy factor of the adsorption becomes greater with the increase in the homologues' chain length and in the case of alcohols at  $n > 3$  this factor makes the main contribution into decreasing of the adsorption free energy value. For acids the exothermicity of the adsorption is considerably higher and that's why the contribution of the entropy term becomes appreciable only at  $n=6$ .

The effects observed are accountable within the scope of the statistic-thermodynamic theory of the hydrophobic hydration of organic compounds in aqueous solutions in combination with the theory on the double electric layer.

When  $z_1$  and  $z_2$  are large ( $z_1 \gg 1$ ;  $z_2 \gg 1$ ) and  $z_1 \approx z_2$  we have

$$\theta_1 \approx \left[ 1 + (2z_1 - z_2) / 3(z_1 z_2)^{2/3} \right]^{1/3} \left[ 1 + (z_1 + z_2) / 3(z_1 z_2)^{2/3} \right];$$

$$\theta_2 \approx \left[ 1 + (2z_2 - z_1) / 3(z_1 z_2)^{2/3} \right]^{1/3} \left[ 1 + (z_1 + z_2) / 3(z_1 z_2)^{2/3} \right] \quad (3)$$

There are polarons and elements of the 1S' structure in the system in second case. From eqn.3, it can be seen that the coverages  $\theta_1$  and  $\theta_2$  are near 1/3.

When activities are large, but  $z_1 \ll z_2$ , we find that  $\theta_1 \rightarrow 0$  and  $\theta_2 \rightarrow 1/2$ . Appeared in the last case structure can be considered as polaron lattice.

### References

1. H. Reiss, J. Phys. Chem., 92 (1988) 3657.
2. H. Reiss, Synth. Met., 30 (1989) 257

### THEORY OF NONLINEAR OPTICAL RESPONSE OF THE ELECTROCHEMICAL INTERFACE: SECOND HARMONIC GENERATION

P.G. Dzavakhidze, A.A. Kornyshev, A. Liesch, M.I. Urbakh

Georgian Technical University, Tbilisi

A.N. Frumkin Institute of Electrochemistry, USSR Acad. Sci., Moscow

Institute of Solid State of Research Centre in Jülich, Jülich, Germany

Tel Aviv University, Tel Aviv, Israel

The dominating contribution to the optical second harmonic generation (SHG) from the metal/electrolyte interface is given by the electronic subsystem of the metal.

The study of electromodulated signals outlines the contribution of the narrow interfacial region. Thus, SHG is regarded as an ideal probe of the surface electronic properties; other degrees of freedom are "seen" in SHG only via their influence on the metallic electrons.

We present and discuss the results of new theory /1/ of (SHG) at the metal electrodes developed on the basis of a Jellium model for the metal in contact with the electrolyte /2/. A continuous picture of the interface in the lateral plane is employed. Thus, the theory gives a description of the background signal and it is not related to "azimuthal flowers" observed in connection with adsorbate superlattices of different symmetry /3/: only the case of delocalized adsorption is studied when we invoke the adsorption into consideration .

The theory predicts the observed asymmetry of SHG potential dependence: weak dependence in the anodic range and rapid rise in the cathodic range /4/. The rise is shown to become steeper with the field induced adsorption of anions /2/.

#### References

1. P.G.Dzhavakhidze, A.A.Kornyshev, A.Liebsch and M.I.Urbakh, *Electrochim.Acta*, 1991 (in Press), *Phys.Rev.B*, 1991 (in Press).
2. For review see:  
A.A.Kornyshev, *Electrochim.Acta*, 34 (1989) 1829.
3. L.J.Simpson, Y.Tang and T.Furtak, *Electrochim.Acta*, 1991 (in Press).
4. G.M.Robinson and G.Richmond, *Electrochim.Acta*, 34 (1989) 1639.

## THE ELECTROREDUCTION OF NITRATE-ANION ON SINGLE CRYSTALLINE SILVER ELECTRODES

N.V.Fedorovich, S.V.Tkachenko

Moscow State University, Moscow

In the few last years some kinetic regularities of the reduction of nitrate-anion /1,2/ were considered in the view of the theory of electrochemical reactions, the kinetics of which is determined by the slowness of the stage of the simultaneous transfer of electron and proton of different nature /3-5/. As donors of protons in the elementary act of discharge can take part the adsorbed molecules of protonic solvents, ammonium and hydronium cations, and the molecules of water, which are a part of the primary hydrate sphere of polyvalency cations. On the example of the reduction of perbromate and bromate anions it was shown, that in the case of participation of adsorbed water in the limiting step of discharge, the rate of the reaction of the reduction of anions increase with the growth of the hydrophilicity of metals /2-5/. In accordance with that, it is possible to draw a conclusion about a stronger or weaker hydrophilicity of the electrode, when comparing the rates of electroreduction of anions, the elementary act of reaction consists in the simultaneous transfer of an electron and a proton from the molecules of water, which are adsorbed on the surface of the electrode. However, at present time there are no simple data on the hydrophilic properties of polycrystalline silver, as well as on its single crystal faces /6/.

The kinetics of the reaction of the nitrate-anion electroreduction was investigated using the method of a disk rotating electrode on crystallographic faces (100) and (111) of single crystalline silver in supposition of the slowness of the stage of the simultaneous transfer of an electron and a proton from proton donors of different nature. In accordance with the theory of the electroreduction of anions, in the limiting stage of discharge of which take part proton donors,



the following regularities of the reduction reaction were determined.

1. The dependence of the discharge rate of nitrate-anion to nitrite-anion on the potential of electrode face (100) has a maximum of the current at positive charges of the surface of the silver electrode, and a minimum at the negative charges, at the same time it was observed that with the increase in the indifferent electrolyte concentration there took place a decrease in the discharge current in the field of positive charges and an increase at the negative charges of the electrode. At the potential of zero-charge the rate of the reaction does not depend on the indifferent electrolyte concentration (Fig.1). On the face (111) of silver electrode the reduction of nitrate-anion proceeds only at high cathode potentials.

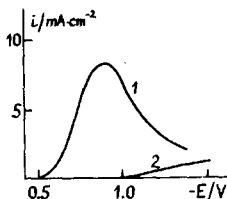


Fig.1.

Dependence of rate of electroreduction of nitrate-anion on the Ag(111) and Ag(100).

2. Total charge of the anion and the proton donor - the adsorbed water molecules, determined from the experimental data is  $0.85 \pm 0.05$ .

3. The rate of the reaction increases with the growth of proton-donor properties of different donors of proton, for example, at the transition from water to cations of ammonium and hydronium-ions.

4. On the grounds of the difference in the rate of the reduction of nitrate-anion on silver faces (100) and (111), when the adsorbed molecules of water act as the donors of proton in limited stage of discharge, it is possibly to make a conclusion about a greater hydrophylity of face (100) in comparison with face (111).

## References

1. N.V.Fedorovich, G.N.Botuhova, ISE 37-th Meeting, Ext.Abs. III, Vilnius, 1986, p.430.
2. N.V.Fedorovich, G.N.Botuhova, IX All-Union Conf. of the Polarography, Ext.Abs., 1987, p.108.
3. N.V.Fedorovich, F.S.Sarbash, Dokl. Akad. Nauk SSSR, 243 (1978) 1231; 255 (1980) 923.
4. N.V.Fedorovich, Itogi Nauki. Elektrokimiya, 14 (1979) 5.
5. N.V.Fedorovich, F.S.Sarbash, G.N.Botunova, Voltamperometry of Organic and Inorganic Substances, M., Nauka, 1986, 25.
6. I.A.Bagotskaya, Itogi Nauki, Elektrokimiya, 23 (1986) 60.

## ON THE EXISTANCE OF ADSORPTION IN HALOGENOUS MOLTEN SYSTEMS

G.A.Gelovani

Institute of Inorganic Chemistry and Electrochemistry of  
the Academy of Sciences of the Republic of Georgia, Tbilisi

In the course of investigation of anodic processes, which take place in boron containing halogenous molten systems an interesting experimental fact was discovered. Particularly, on the chronovoltamperograms two maximums can be seen (anode: carbon-glass  $\phi = 1-2$  mm, the melt consists of KCl-NaCl and  $\text{KBF}_4$ ). The potential of the first maximum depends strongly on the rate of anode potential scanning and varies in the ranges: from +0.350 V (at  $v=100$  V/s) to +0.055 V (at  $v=0.001$  V/s). The potential of the second maximum lies in ranges from +0.900 V to 1.000 V at the same anode potential scanning rate (Fig.1).

Similar investigations have been carried out for the equimolar KCl - NaCl melt with  $\text{NaF}$  additions. The amount of

$F^-$  in added NaF was the same as that of  $F^-$  in potassium tetrafluoroborate, added in the previous experiments. The potential of the maximum for KCl - NaCl + NaF melt, coincides with the potential of the maximum for KCl - NaCl +  $KBF_4$  melt.

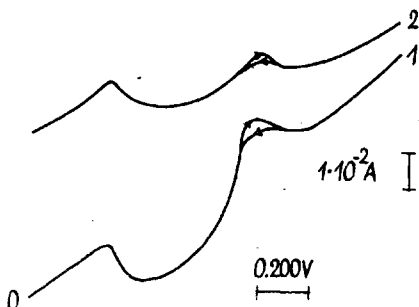


Fig. 1. Cyclic chronovoltamperometrical dependences for anodic processes in systems: 1 - KCl - NaCl +  $KBF_4$ ; 2 - KCl - NaCl + NaF. Anode: carbon-glass;  $v = 4.0 V/s$ ;  $T = 973 K$  reference electrode: Pb/Pb $^{2+}$ ; helium atm.

Analysis of the first maximum in  $i_p/V-V$  plots yield a straight line at  $v \geq 1 V/s$ . It was determined, that its height remains constant through all the investigated  $KBF_4$  concentration ranges.

A further investigation of the second maximum (electrolysis with anode gas accumulation, IR spectroscopy analysis) shows that at the potentials corresponding to the second maximum, fluorine anions oxidization takes place.

As for the first maximum, from the described above we can conclude, that it is of adsorptive origin.

In this case, the  $i_p/v$  value will characterize the adsorption capacity of the electrode surface at the potential of the first maximum, which can be evaluated as  $8 \cdot 10^{-3} F$ .

We also want to report the conditions of the experiments. The experiments took place in quartz air-tight cell, in helium. The melts' container - a carbon-glass melting pot, served also as a cathode. The carbon-glass bar was used as an anode. The experiments took place at 973 K.

THE ADSORPTION OF TIROZINE CATIONS ON THE BISMUTH  
(PLANE 111) AND MERCURY ELECTRODES

S.I.Gilmanshina, G.D.Shilotkach, G.A.Dobrenkov

S.M.Kirov Kazan Institute of Chemical Technology, Kazan

The adsorption behaviour of tirozine aromatic aminoacid ( $pK_1 = 2.2$  (COOH),  $pK_2 = 9.11$  ( $NH_3^+$ )) has been studied in the wide range of potentials in the acid medium  $pH=1.3$  on the background of potassium sulphate by the method of differential capacity and radioactive indicators (RI) according to Kazarinov's method /1/. (The radioactive sample marked by isotope  $^{14}C$  has been used.) The tirozine under investigation is present as cations.

According to the RI method data two adsorption regions are characteristic of the adsorption of tirozine cations (T) on the bismuth electrodes (BE):  $\Gamma_m = 1.9 \cdot 10^{-10}$  (the p.z.c. region where  $q > 0$ ) and  $\Gamma_m = 3.2 \cdot 10^{-10}$  mole/cm<sup>2</sup> (where  $q < 0$ ), the second adsorption region being considerably transferred to the cathode region. The independence of the adsorption on the electrode potential has been fixed in the anode region. The depression of capacity takes place on the C,E-curves of BE:  $C^I = 14.08 \mu F/cm^2$  where  $E = -0.1$  V (p.z.c.). The capacity curves at all concentrations of additives remain lower than the background curve in the anode region. The process of hydrogen evolution takes place in the acid medium at the cathode polarization of BE, which makes it impossible to obtain the differential capacity curves in this region of potentials. The total curve of the differential capacity has been obtained on the mercury electrode (ME). In this case two minimums appear on C,E-curves:  $C^I = 14.28$ , where  $E = -0.1$  V, and  $C^I = 11.90 \mu F/cm^2$ , where  $E = -0.5$  V (p.z.c.). According to the RI method data, the second minimum is situated at the same potentials, relative to the p.z.c. of the electrode as the second adsorption region on BE. Both anode and cathode peaks of desorption are absent. With sufficient cathode potentials C,E the curves with additives coincide with the back-

ground one. In the presence of the positive charges of the surface the capacity curves with SAS remain lower than the background curve, not coinciding with the latter.

On the basis of the calculation of ionic adsorption, taking into consideration the data of the RI method, the supposition of availability of reorientation changes in the adsorption monolayer, dependent upon potential of electrode has been made. The cathode branch of experimental curve of differential capacity has been described using Damaskin's isotherm, taking into consideration the charge of organic adsorbate /2,3/. Frumkin's isotherm has been used for the description of anode branch C,E the curve and the region p.z.c. A good agreement of experimental and calculated curves of differential capacity ME has been obtained for the maximum concentration of additive. At the same time the region of the second minimum on the calculated curve is somewhat transferred towards higher cathode potentials. It is supposed that the process of cathode discharge of hydrogen narrows the region of adsorption on the experimental curves with these potentials. For the EE the calculated C,E-curve has also been obtained. The degree of filling has been determined upon the data of the RI method, according to /4/. There is a second minimum on the calculated curve EE that has not been experimentally fixed. The parameters of adsorption have been obtained.

#### References

1. V.E.Kazarinov, *Elektrokhimiya*, 2 (1966) 1170.
2. B.B.Damaskin, S.I.Karpov, *Elektrokhimiya*, 28 (1982) 3.
3. B.B.Damaskin, S.I.Karpov, S.L.Dyatkina, *Elektrokhimiya*, 28 (1982) 281.
4. U.M.Vyszimov, G.D.Shilotkatch, G.A.Dobrenkov, Dep. N 1155x H-84. Dep. M.: VINITI, (1985) 140.

ON POSSIBLE RELATIONSHIP BETWEEN THE POTENTIALS OF START  
OF PASSIVATION AND ZERO CHARGE OF TRANSITION METALS

V.P.Grigoryev, O.N.Nechaeva, V.E.Gorelik, A.A.Popova

Institute of Physical and Organic Chemistry, Rostov State  
University, Rostov-on-Don

The existence of a possible relationship between the potentials of the initial stage of passivation ( $E_{ps}$ ) and those of the zero charge ( $E_{q=0}$ ) of transition metals has been discussed. Some ideas have been suggested as to the conditions favorable for the appearance of active particles in a given solution whose adsorption on the metal surface leads to its transition into a passive state. The emergence of such particles is possible when there is a certain shift of the metal potential relative to  $E_{q=0}$ . In this case, a quantitative characteristic of the surface charge can be represented by the potential of the passivation start  $\varphi_{ps}$  in the Antropov scale

$$\varphi_{ps} = E_{ps} - E_{q=0} \quad (1)$$

For transition metals, in case there is no significant specific adsorption, one may, with a certain approximation, expect the above-mentioned shift to be independent of the nature of the metal for a given solvent, while the presence of the specific adsorption should lead to more complex relationships. Some equations have been obtained and verified experimentally that relate the potentials of the initial passivation of metals with those of the zero charge. Two cases have been considered.

1. The nature of the solvent L is constant while that of the metal M changes. In this case

$$E_{ps}^L = M_1 E_{ps}^L + \text{const}_{M_2 M_1} + \Delta_{M_2 M_1}^L, \quad (2)$$

where  $\text{const}_{M_2 M_1} \neq f(L)$  and  $\Delta_{M_2 M_1}^L$  represent the specific interaction between metal and solvent. When the effects of

such an interaction are equal or close but their signs are opposite, we have particular case of  $\Delta_{M_2M_1}^L = 0$ . In this case, the potential difference for the passivation start of two metals equals that obtained for the zero charge of these metals. The validity of this statement has been exemplified using both literature data and our results for aqueous, organo-aqueous and organic (both aprotic and protic) media by a number of systems for the following metal pairs: Ni-Ti, Fe-Ni, Ta-Nb, W-Ta, Ti-Nb, Ta-Ti, Mo-W, W-V, Zr-Mo, W-Mo. The data listed in Table 1 partially illustrate this situation. In calculations, the reference-book values of  $E_{q=0}$  were used.

Table 1

Values of  $E_{ps}$ ,  $M_2M_1\Delta E_{ps}$  and  $M_2M_1\Delta E_{q=0}$  for various systems

Conditions, medium	$E_{ps}$		$M_2M_1\Delta E_{ps}, V$	$M_2M_1\Delta E_{q=0}, V$
	$M_1$	$M_2$		
$M_1$ -Ni, $M_2$ -Ti 2M H <sub>2</sub> SO <sub>4</sub> +X % organic solvent (OS) X=0	+0.20	-0.20	-0.40	-0.45
X=12 % dimethylfor- mamide (DMF)	+0.40	-0.05	-0.45	
X=40 % DMF	+0.52	+0.10	-0.42	
X=55 % DMF	+0.56	+0.15	-0.41	
X=40 % acetone (Ac)	+0.20	-0.22	-0.42	
X=90 % Ac	+0.35	-0.10	-0.45	
X=55 % Ac	+0.35	-0.12	-0.47	
$M_1$ -Ta, $M_2$ -Nb 0.1 M LiClO <sub>4</sub> +OS acetonitrile (AN) propylenecarbonate (PC)	+0.45	+0.52	+0.07	+0.10
DMF	+0.45	+0.50	+0.05	
	+0.25	+0.30	+0.05	

2. The nature of the metal is constant while that of the solvent varies. The relationship between the potentials of the passivation start of a given metal M for two solvents L and P is given by

$$M_{ps}^{E,L} = M_{ps}^{E,P} + \text{const}^{L,P} + \Delta_M^{L,P}, \quad (3)$$

where  $\text{const}^{L,P} \neq f(M)$  and  $\Delta_M^{L,P}$  characterizes the interaction of solvents L and P with the metal.

Clearly, in a general case, there must exist a rather complex relationship between the  $E_{ps}$  values of the given metal in solvents L and P. However, if the total effect of the specific reaction of L and P with M is zero or close to it, then the difference between the potentials of the start of metal passivation in the two solvents is determined by the nature of these solvents and it does not depend on the nature of the metal, see Table 2.

Table 2

$E_{ps}^{P,L}$  values for some metals with different solvent pairs

L - P	M	$\Delta E_{ps}^{P,L}, V$	L - P	M	$\Delta E_{ps}, V$
2 M H <sub>2</sub> SO <sub>4</sub>			0.1 M LiClO <sub>4</sub>		
H <sub>2</sub> O-55 % DMF	Ti	+0.35	Et-Met	Ti	0.25
	Ni	+0.35		Nb	0.23
H <sub>2</sub> O-40 % AN	Ti	0.00	Pr-Met	Zr	0.23
	Ni	+0.05		Mo	0.25
55 % DMF- -55 % AN	Ti	-0.27		Ti	0.35
	Ni	-0.21		Nb	0.34
0.1 M LiClO <sub>4</sub>					
AN-PC	Ta	0.00	But-Met	Zr	0.31
	Nb	-0.02		Mo	0.34
AN-Ac	Ta	-0.05	Ti	0.51	
	Nb	-0.06	Nb	0.44	
AN-DMF	Ta	-0.20	Zr	0.46	
	Nb	-0.22	Mo	0.51	

The approach proposed rests on the notion of the adsorptional chemical interaction between the solvent and me-



tal surface, and, clearly, its applicability is limited. Primarily, it is valid in case of the transition metals in the absence of phase films and only in the initial stage of the passivity when the first-order chemisorption takes place, which is mainly determined by electrostatic nonspecific forces. A stable passive state is associated with deep transformations on the metal surface and with the second-order chemisorption.

In this case, the dominant role belongs to the specific forces of the M-L interaction and, accordingly, the above-described systems will be described by more complex relationships.

#### MODELLING OF ADSORPTION LAYERS OF ORGANIC COMPOUNDS ON BISMUTH AND MERCURY ELECTRODES

L.T.Guseva, Y.M.Vyzhimov, G.A.Dobrenkov

Kazan Institute of Chemical Engineering and Technology,  
Kazan

Identification of adsorption parameters of organic molecules and ions on electrodes is closely connected with the usage of physical and molecular models of adsorption layers. One of the possible ways of the approach given in this work /1/ for monomolecular layers was used to characterize a number of molecules at potentials of maximum adsorption of substances /2-4/.

In the present work, the method discussed was applied to the cases of adsorption of combinations characterized by different hydrophobic properties and by the presence of aromatic fragments in molecular chain in the case of filling the electrode surfaces  $\theta = 1$  and  $\theta = 0.6$ . The characteristic potentials of differential capacity curves  $E_m$  and  $E^m$  (cathode) have determined the experimental values of the electrode charges, the corresponding values of surface filling were obtained by capacitance and radioisotopic methods /3,4/.

The results of the coordinating experimental data (experiment) and theoretical calculations (models) are given in the table for bismuth (monocrystal, plane (111)) and mercury electrode.

Table 1

Values of total capacitance in aqueous solution of 0.1 N  $\text{Na}_2\text{SO}_4$ .  $D_1=13.2$  ( $\epsilon=-2.0 \mu\text{C}\cdot\text{cm}^{-2}$ );  $8.8$  ( $\zeta=13.0$ );  $d_1=3.5$  (A),  $D_N=2.2$ ,  $B_P(\text{OH})=23.4$  (B),  $11.8$  (A);  $D_P(\text{COOH})=12.4$  (A)

N combination	Bi (type of model)						Notes
	$E_m$			$E^m$			
	$\theta$	$K_{ex}$	$K_m$	$\theta$	$K_{ex}$	$K_m$	
1 $\text{C}_5\text{H}_{11}\text{OH}(\text{AS})$	0.98	7.0	7.5	0.4	12.2	11.8	
2 $\text{C}_8\text{H}_{17}\text{OH}(\text{OS})$	0.99	7.0	6.4	0.6	13.7	13.7	
3 $\text{C}_6\text{H}_4(\text{OH})\text{COOH}$	0.90	11.8	11.1	0.6	13.5	13.5	$D_P=30$
-----							
	Hg (type of model)						
1 $\text{C}_5\text{H}_{11}\text{OH}$	0.90	6.4	5.1(B)	0.4	12.0	11.9	
3 $\text{C}_6\text{H}_4(\text{OH})\text{COOH}$	0.61	12.7	12.0	0.5	18.6	18.6	$D_N=7.4$
4 $(\text{CH}_2)_4(\text{COOH})_2$	0.78	9.1	9.8	0.2	13.8	13.9	
5 $(\text{CH}_2)_6(\text{OH})_2$	0.99	7.0	7.4	0.4	11.8	11.6	

As in work /1/, two models of adsorption layer were considered for plane - oriented molecules:

$$K = K_1(1 - \theta) + K_P \theta_P + K_N(1 - \theta_P)\theta \quad (\text{model A})$$

and for vertical - oriented molecules:

$$K = K_1(1 - \theta) + \theta K_P K_N / (K_N + K_P) \quad , \quad (\text{model B})$$

where the experimental and model total capacitance are connected with the values  $K = / E_a - \gamma_1$  (experiment) and  $K_1 = - D_1 / 0.113 d_1$  (for water interlayer), but  $K_P$  and  $K_N$  are analogous values for polar and nonpolar fragments of the adsorbate being modelled with the corresponding contributions of surface parts occupied by their  $\theta_P$  and  $\theta_N$ .

The results contained in the Table 1 pay our attention

to the arrangement of polar and nonpolar groups in adsorption layer and to the character of their interaction with the charged surface in conditions of various degrees of filling of the surface  $\Theta$  by water and adsorbate molecules.

In most cases given (carbon composition  $C_5-C_8$ ), the plane orientation of molecular chains on the surfaces of both electrodes in a wide range of potentials ( $E_m - E^m$ ) predominates. It should be emphasized that such an orientation is revealed also for the molecules with one polar group (AS, OS) and two polar groups.

In case of adsorption of salicylic acid, the presence of benzoic radicals leads to specific effects in orientation of polarization of molecule fragments (experiments 3). While the arrangement of all groups of atoms on one layer is being observed on the mercury surface, on bismuth model (B) is being used, according to which the dense layer appears to be a total combination of two parallel capacities, with separators as groups of benzene radical  $K_N$  turned to its edge, and hydrated polar groups  $K_p$ . Polarization of both atom groups can be observed simultaneously in the region of negative charges of electrodes (see notes).

During adsorption of molecules of octyl (exp.2) on bismuth there seems to be no tendency to formation of condensed adsorption layers on fillings  $\Theta \sim 1$ , as is it stated for the mercury electrode /3/.

#### References

1. G.A.Dobrenkov, L.T.Guseva, *Elektrokimiya*, 11(1975) 1721.
2. G.A.Dobrenkov, A.F.Dobrynina, *Proc. 6th Symp. on Double Layer and Adsorption on Solid Electrodes*, Tartu, 1981, p. 125.
3. Y.M.Vyzhimov, G.D.Shilotkatch, G.A.Dobrenkov, *Proc. 7th Symp. on Double Layer and Adsorption on Solid Electrodes*, Tartu, 1985, p. 378.
4. G.D.Shilotkatch, G.I.Ghilmanshina, G.A.Dobrenkov, *Elektrokimiya*, 26 (1990) 1265.

FORMATION AND PROPERTIES OF POLYPYRROLE AND  
POLYTHIOPHENE FILMS ON Pt AND Au

A.Hallik, N.A.Nekrassova, A.Alumas, J.Tamm

Tartu University, Tartu

Electrochemically polymerized conducting polymers have aroused a considerable interest /1/. The electrochemical properties of polymer films obtained anodically are strongly affected by many factors such as the nature of the electrolyte species, solvent and the anode material, temperature, applied potential and so on./1/. To either functionalize or improve their physical properties, various derivatives of simple heterocyclic monomers and inorganic and organic anions as dopants are used /1,2/. In the present work we studied the properties of polypyrrole and polythiophene films synthesized on Pt and Au from acetonitrile and aqueous solutions paying attention to the influence of the nature of the counter-ions.

Polypyrrole and polythiophene films (0.1-1  $\mu\text{m}$ ) were deposited onto a Pt and Au wire and disc. The following electrolytes as dopants were used:  $\text{NaClO}_4$ , sodium dodecylsulfate (DDS), disodium dihydrogen ethylenediaminetetraacetate (EDTA). We used cyclic voltammetry, AC conductivity jump estimation in solution at high frequency (12 kHz) for characterization of the relative quality of deposited films and conductivity measuring on the thick free standing films ( $>10 \mu\text{m}$ ). It was estimated that the location and depth of the conductivity jump depend on various factors and in general the potential region where the jump takes place does not coincide with the maximum potential on voltammograms.

The cyclic voltammetric and conductivity study show a peculiar electrochemical behaviour of deposited films doped with big anions. There is a ground to propose that upon reduction, instead of counteranion removal from the film, cations are incorporated in order to preserve electrical neu-

trality in the resulting uncharged polymer /3/. Thus, the parameters of voltammograms obtained in various electrolytes strongly depend on the nature of the cation. Hereby, in the case of the films doped with EDTA the capability of the cation to form a complex with EDTA is an important factor that determines the electrochemical film properties.

In general, the incorporation of cations in the film is connected with high kinetic resistance and determined by their hydrated radii. So, the reduction of polypyrrole film doped with dodecylsulfate in the solution of  $(C_4H_9)_4NBr$  is possible only by prolonged polarization at high negative potential ( $-0.8$  V vs Ag/AgCl in water). Likewise is impeded the removal of  $(C_4H_9)_4N^+$ -cation from the film during its oxidation. It takes place at potential values  $0.7$  V more positive than in the case of the  $Na^+$ -cation. DDS as a dopant with a long hydrocarbon chain is very strongly bound with polymer films and obviously cannot be removed in the course of the reduction process.

The conductivity measurements of the film, both in the solution, and in the free standing state show that conductivity remains relatively high after reduction and incorporation of cations.

The incorporation of a cation, in particular during the first reduction cycle of the synthesized film, brings about essential changes in the film morphology. Obviously, they are larger than in the case of the reduction connected with the anion removing. For example, the potential of the reduction current maximum on the first voltammogram for polypyrrole film doped with DDS in  $(C_2H_5)_4NClO_4$  solution is shifted in respect of the second cycle  $0.4$  V in negative direction. It is worth mentioning that there is a big difference in capacitive current of oxidized film before and after the first cycle, respectively. Probably, this is connected with a difference in working surface. In all likelihood, in the first cycle does not work the the total volume of the film, but only its external surface layer. By a proper choice of a cation in solution it is possible to separate the capacitive and non-capacitive current and to deter-

mine the capacity of the oxydized film. For polypyrrole films doped with DDS its value in  $\text{NaClO}_4$  solution after the first cycle is  $110 \text{ F}\cdot\text{cm}^{-2}$ , independently of its thickness. Thus, the whole thickness of the film participates in the recharging process.

#### References

1. A.F.Diaz, J.C.Lacroix, *New J. Chem.*, 12 (1988) 171.
2. L.F.Warren, D.P.Anderson, *J. Electrochem. Soc.*, 134 (1987) 101.
3. Qin-Xin Zhou, C.J.Kolaskie, L.L.Miller, *J. Electroanal. Chem.*, 223 (1987) 283.

#### ADSORPTION OF CYCLOHEXANOL ON THE (111) AND (001) FACES OF ANTIMONY

A.Jänes, E.Lust, R.Pullerits  
Tartu University, Tartu

According to the experimental results /1-3/, the electrochemical properties of a solid metal surface do not significantly depend only on the chemical composition but also on the crystallographic structure and electronic properties of the surface of a metal studied /1-3/. The bismuth and antimony are the full electronanalogues, considered as a semi-metals which crystallize in the same rhombohedral system with the electronic structure of  $s^2p^3$ .

Differently from the bismuth single crystal electrodes, in the electrochemical literature there is no quantitative information about the structure of the electrical double layer (edl) and adsorption of ions and organic compounds on the antimony single crystal planes, except our previous data /4/. This is the second paper in a series devoted to the study of the influence of the crystallographic orientation

of antimony on the electrochemical properties of the Sb/solution interface. We began this project investigating the edl structure and parameters in the surface-inactive electrolyte solutions /4/. It was established that the difference of zero charge values  $\Delta E_{\sigma=0} \geq 90$  mV for the (001) and (111) single crystal planes are somewhat higher than for the (001) and (111) planes of bismuth ( $\Delta E_{\sigma=0} \leq 70$  mV). The values of inner layer capacities of the (111) and (001) planes at the surface charge  $\sigma=0$  are 23.6 and  $26.2 \mu\text{F}\cdot\text{cm}^{-2}$ , respectively. These values are somewhat lower than for the (111) and (001) bismuth planes and can be explained by the weaker hydrophility of antimony electrodes or by the higher contribution of the metal phase to the differential capacity of single crystal plane/surface-inactive electrolyte than to the Bi/electrolyte interface /5/. The present paper is devoted to a comprehensive study of the adsorption of cyclohexanol (CH) on the antimony and bismuth single crystal electrodes and polycrystalline (PC) antimony and bismuth solid drop electrodes. The investigation of the adsorption of CH on the (111) and (001) faces and PC Sb electrodes was carried out by means of the differential capacity C (impedance) measurements. The main adsorption parameters of CH, calculated by the Frumkin-Damaskin theory /6/ are given in Table 1, where the symbols have their usual meaning. Fabrication of the Sb single crystal and surface preparation of the electrodes have already been described, as well as the capacity measurement technique and preparation of the solutions /2-4/.

The  $C(E)$  and  $E^{\text{max}} - E_{\sigma=0}(\text{lgc})$  curves, given in Fig. 1, and data in the Table 1 show a significant difference in the adsorption properties of single crystal and PC Sb electrodes. As for single crystal planes of Bi /3/, at high bulk concentration of CH ( $c_{\text{CH}} \geq 0.02$  M) in the region of high negative charge, a sharp maximum is observed for the (001) and (111) planes of Sb. The relative potential ( $E^{\text{max}} - E_{\sigma=0}$ ) of this maximum moves towards the more negative values of E in the sequence:  $\text{Bi}(001) < \text{Bi}(111) < \text{Sb}(001) < \text{Sb}(111)$  and can be explained by the decreasing the hydrophility of electrodes

in the same order. The height of this maximum (at  $c_{CH} = \text{const}$ ) increases in the sequence:  $\text{Sb}(001) < \text{Sb}(111) < \text{Bi}(001) < \text{Bi}(111)$  and it means that the attractive interaction between the adsorbed CH molecules clearly increases by transition from  $\text{Sb}(001)$  to  $\text{Bi}(111)$ . As shown in Table 1, the adsorption activity of CH is somewhat higher on the  $\text{Sb}/\text{solution}$  interface, than on the  $\text{Bi}/\text{solution}$  interface, which can be explained by weaker hydrophilicity of antimony electrodes, compared to that of bismuth electrodes /5/. The values of the concentration of the organic substance corresponding  $\theta = 0.5$ , adsorption equilibrium constant  $B_0$  and standard free energy of adsorption  $-\Delta G_A^0$  of CH are higher on the  $\text{Sb}(001)/\text{solution}$  interface, than on the  $\text{Sb}(111)/\text{solution}$  interface. According to

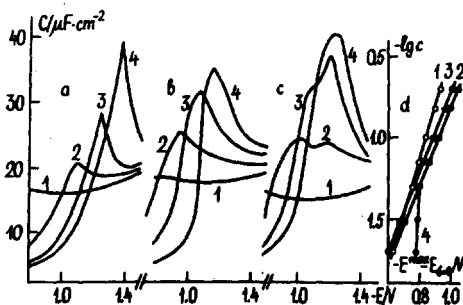


Fig. 1.  $C(E)$  curves for  $\text{Sb}(111)$  - a;  $\text{Sb}(001)$  - b and PC Sb - c electrodes in the 0.1 M aqueous solution of NaF (1) and with additions of CH in concentrations, M: 2 - 0.02; 3 - 0.05 and 4 - 0.1. Dependence of the relative potential  $E^{\max} - E_{\sigma=0}$  of the desorption maximum on the  $\lg c$  of CH (d): 1 -  $\text{Sb}(001)$ ; 2 -  $\text{Sb}(111)$ ; 3 - the first peak and 4 - the second peak for the bifurcated desorption maximum for the PC Sb electrode.



the criterions of /8/, the experimentally determined adsorption energy is the difference between the adsorption energies of organic compound and water. Respectively, the metal/water interaction increases from Sb(111) to Sb(001) or from

Table 1

Adsorption parameters of cyclohexanol on different Sb and Bi electrodes

Electrode	$a_0$	$C'$ ,	$c_{\theta=0.5}$ ,	$B_0$ ,	$-AG_A^0$ ,	$E_{\sigma=0}^{\max} - E$
		$\mu F \cdot cm^{-2}$	M	$dm^3 \cdot mole^{-1}$	$KJ \cdot mole^{-1}$	V (0.1 M CH)
Sb(111)	1.10	3.9	0.0071	41	18.9	0.935
Sb(001)	0.95	4.4	0.0051	68	20.1	0.840
PC Sb	0.65	5.4	0.0090	56	19.7	0.890
Bi(111)	1.83	4.0	0.0091	20	17.1	0.830
Bi(001)	1.49	3.8	0.0084	34	18.5	0.725
PC Bi/7/	1.65	3.7	0.0089	23	17.4	-

Bi(111) to Bi(001). But this conclusion is valid, provided the adsorption of CH does not depend on the metal and on crystallographic orientation. According to our previous data /2,3/ the higher adsorption activities of the planes Sb(001) and Bi(001) than for Sb(111) and Bi(111) are mainly determined by strong interaction between adsorbed CH molecules and the surface atoms of Sb(001) and Bi(001), having unsaturated covalent bonds /2,3/. The surface atoms of the Sb(111) and Bi(111) planes are chemically saturated and the adsorption of CH on these planes is purely physical.

As follows from Fig.1, the cathodic adsorption-desorption maxima at bulk concentrations of CH  $0.01 < c_{CH} < 0.05$  M on the PC Sb can split into two clearly distinct independent maxima with certain electrochemical characteristics. The potential of the first peak of the bifurcated maximum  $E_I^{\max}$  is in sufficiently good agreement with the  $E^{\max}$  of the plane Sb(001).

The potential of the second peak  $E_{II}^{max}$  is more negative, than  $E^{max}$  for the Sb(111) plane. Differently from the PC Bi electrode [3], at high bulk concentrations of CH ( $c_{CH} \leq 0.05$  M), only one peak on the C(E) curve for the PC Sb can be observed. The potential of this maximum is different from the  $E^{max}$  of the planes Sb(111) and Sb(001) and the lower and broader maximum of the PC Sb lies between the peaks of the planes (001) and (111). In the adsorption isotherms, calculated at the maximum adsorption potentials, the typical characteristic bents for the PC electrodes were observed.

On the basis of the C(E) curves and corresponding adsorption isotherms it can be suggested that on the surface of PCSb drop electrode mainly two energetically relatively homogeneous regions with essentially different energies are distinguished.

#### References

1. A.Hamelin, T.Vitanov, E.Sevastyanov, A.Popov, J. Electroanal.Chem., 145 (1983) 225.
2. E.Lust, U.Palm, Elektrokimiya, 21 (1985) 1381; 22 (1986) 1381; 22 (1986) 411; 22 (1986) 696.
3. E.Lust, U.Palm, Trans. Tartu State Univ., 757 (1986) 105.
4. E.Lust, A.Jänes, Elektrokimiya, 27 (1991) in press.
5. V.Past, R.Pullerits, M.Moldau, Trans. Tartu State Univ., 757 (1986) 140.
6. B.B.Damaskin, O.A.Petrij, V.V.Batnikov, Adsorption of Organic Compounds on Electrodes, Plenum Press, New-York-London, 1971.
7. A.R.Alumaa, U.V.Palm, Elektrokimiya, 8 (1972) 790.
8. A.N.Frumkin, Potentials of Zero Charge, Nauka, Moscow, 1979, 153.

THE FORMATION OF THE QUASI-METALLIC LAYER  
ON THE METAL-MOLTEN SALT INTERFACE

A.I.Karasevskii, R.E.Kris, E.V.Panov

Institute of General and Inorganic Chemistry,  
Ukr.SSR Acad. Sci., Kiev

The interaction of electrons nonhomogeneously distributed on the boundary between a metal and a molten salt forms the surface and effects a number of physico-chemical processes on this interface. In the present work it is shown that a quasi-metallic layer of the thickness of 3-5 Å may be formed on the interface. The Thomas-Fermi-Dirac equation determines the electron density distribution in the molten salt:

$$n(z) = \frac{2\sqrt{2}}{3}(\tau_0 + \sqrt{\tau_0^2 + Y})^3, \quad Y = y_0 - y(z), \quad (1)$$

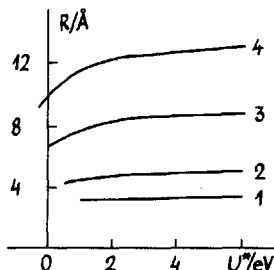
where  $\tau_0^{-1} = \sqrt{2\pi}\epsilon^{\frac{2}{3}}$ ,  $y(z)$  is the potential is determined by the Poisson equation,  $y_0$  is the potential on the medium boundary,  $\epsilon^{\frac{2}{3}}$  is the static dielectric permeability of the molten salt in the near-to-electrode region. The evident form of the thickness of the quasi-metallic layer is

$$R = \frac{\sqrt{5}\beta_{TF}}{\tau_0^{1/2}} \left\{ 1.44 - 2\left(\frac{\tau_0^2}{y_0}\right)^{1/4} \left[ 1 - 0.62\left(\frac{\tau_0^2}{y_0}\right)^{1/2} \right] \right\} \quad (2)$$

The quasi-metal layer with a thickness of ~3-5 Å formed in the medium near the metal surface is extremely interesting in our view. It should be noted that this layer is considerably different from the macroscopic double layer which formed at the metal-semiconductor boundary. A considerable additional contribution to the decrease in the potential energy of the electrons occurs due to partial penetration of the inhomogeneous metal electron gas into the molten salt [1]. In this case, the Thomas-Fermi radius of screening increases in the polar medium, which results in the formation of the macroscopic quasi-metal layer. The thickness of the layer is weakly dependent on  $U^{\frac{2}{3}}$ , the bottom of the conduction band, and strongly dependent on the dielec-

tric permeability  $\epsilon^{\#}$  of the near-to-electrode region (Fig.1).

Fig.1.  
Quasimetallic layer thickness vs  $U^{\#}$  dependence at different  $\epsilon^{\#}$ : 1 -  $\epsilon^{\#}=3$ ; 2 -  $\epsilon^{\#}=4$ ; 3 -  $\epsilon^{\#}=6$ ; 4 -  $\epsilon^{\#}=8$ .



The existence of a quasi-metallic layer in the near-to-electrode region gives a new approach to the explanation of the large width (3-5 Å) of the area of adiabatic reactions in the near-to-electrode region /2/, and the independence of the constant of the reaction rate of the nature of the metal /3/.

#### References

1. A.I.Karasevskii, R.E.Kris, E.V.Panov, J.Electroanal.Chem. (to be submitted).
2. J.T.Hupp, M.J.Werver, J.Phys.Chem. 88 (1984) 1463.
3. T.Iwasita, W.Shmicler and J.W.Shultze, J. Electroanal. Chem., 194 (1985) 355.

#### STUDY OF THE CHEMISORBED SURFACE LAYERS FORMED AT HIGH ANODIC POTENTIALS ON THE FACES OF PLATINUM MONOCRYSTAL

E.V.Kasatkin, E.B.Neburchilova, G.I.Kaplan

Karpov Institute of Physical Chemistry, Moscow

As we have shown earlier, the electrocatalytic activity and selectivity on the faces of Pt monocrystal in ammonium peroxodisulphate (PDSA) and peroxodisulphuric acid electro-synthesis are considerably higher than on the untextured polycrystal (PC) /1/. The correlation between the current ef-

iciency for PDSA formation and coverage by the labile oxygen chemisorbed on the surfaces with different structure was found. It was interesting to study the influence of chemisorption of sulphate particles the intermediately formed on the monocrystalline and polycrystalline electrodes on the kinetics of the peroxodisulphuric acid formation.

Using X-ray photoelectron spectroscopy we studied the electronic structure and chemical composition of the polycrystalline and monocrystalline Pt-surfaces (111), (110), (100), (311) after anodic polarization at high anodic potentials in 12 N  $H_2SO_4$ . It was found that on the surface there were present sulphur containing adsorbed particles which were the intermediates of the peroxodisulphate ion formation. Analysis of Pt 4f core level spectra showed that the increase in the atomic density in the order of electrodes PC < reconstructed (111) < (110) < (311) < (100) correlated with the growth of the Pt oxidation degree. This is in a good agreement with the potentiodynamic data of the oxygen chemisorption in 12 N  $H_2SO_4$  (Table 1). So, we have a considerable cathodic shift of the desorption potentials ( $E_{des}$ ) of the first and third chemisorbed oxygen forms (accordingly CO-1 and CO-3) in the above-mentioned order of electrodes. It, testifying the binding energies increase of these charged forms on the Pt surface, causes the decrease in the oxidated surface effective positive charge in the mentioned order of electrodes.

Analysis of O1s and S2p core level spectra showed that the surface oxygen coverage increased in the order of electrodes (100) < (311) < (111) < PC corresponded to the sulphur particles containing decrease on the Pt surface. This is in good agreement with the fact of the competitive adsorption of intermediate oxygen and sulphate particles, that influenced the partial current densities for peroxodisulphuric acid formation and oxygen evolution. Thus, the increase in the surface coverage by sulphate particles in the order of electrodes PC < (111) < (311) < (100) in electrosynthesis correlates with the growth of electrocatalytic activity for the peroxodisulphuric acid formation.

Table 1

12 N H<sub>2</sub>SO<sub>4</sub>, t = 10°C, E = 3.7 V, i = 0.34-0.56 A·cm<sup>-2</sup>

Characteristics	Pt anods structure				
	PC	(111)	(110)	(311)	(100)
Current efficiency for H <sub>2</sub> S <sub>2</sub> O <sub>8</sub> , %	42	48	51	54	60
i <sub>H<sub>2</sub>S<sub>2</sub>O<sub>8</sub></sub> , A/cm <sup>2</sup>	0.18	0.16	0.22	0.28	0.33
S2p binding energies, eV	169.3	168.7	168.6	168.5	167.1
Stoichiometry S-to-Pt	0.03	0.04	0.08	0.06	0.11
E <sub>des</sub> CO-1, mV	537	487	463	380	250
E <sub>des</sub> CO-3, mV	620	588	570	532	474

It was found that the observed increase in the oxidated surface effective positive charge correlates with a considerable decrease in the S2p electron binding energies in the order of electrodes PC < (111) < (110) < (311) < (100) (Table 1). This corresponds to the decrease of the binding strength of the intermediate sulphate particles with the Pt surface and causes the acceleration of their recombination, that forms S<sub>2</sub>O<sub>8</sub><sup>-</sup> ions.

Thus, the increase of the electrocatalytic activity for the H<sub>2</sub>S<sub>2</sub>O<sub>8</sub> formation reaction in the order of electrodes PC < (111) < (110) < (311) < (100) is related, on the one hand, to the decrease of the binding strength of the intermediate sulphate species with the Pt surface in accordance with the increase in its atomic density, caused by the properties of the surface oxidation layers, and on the other hand, to the increase in the reactive sulphate particles coverage of the electrocatalyst's surface.

#### Reference

1. E.B.Bezlepkina, E.V.Kasatkin, *Elektrokhimiya*, 24 (1988) 223.

## THE IMPEDANCE OF THE CATHODIC HYDROGEN EVOLUTION ON COPPER IN ACIDIC SULPHATE SOLUTIONS

N.I.Kavardakov, V.I.Kichigin

Perm State University, Perm

The conclusions about mechanism of the hydrogen evolution reaction (HER) on copper made by some authors /1-4/ are contradictory. The amount of the hydrogen adsorbed on copper in electrolytes is also controversial /5-6/. In the present work, HER on copper in acidic solutions has been investigated using ac impedance and galvanostatic polarization measurements. Some data on frequency dispersion of the real component of Cu electrode admittance were reported previously /1/, however, they are very incomplete.

The measurements were carried out on polycrystalline copper (99.99 %) in deaerated solutions  $x$  M  $H_2SO_4$  +  $(1-x)$  M  $Na_2SO_4$ , with  $x = 0.1 - 1.0$ , at room temperature. The surface of the copper electrode was electrolytically polished in concentrated  $H_3PO_4$ . Before measurements, the electrode was reduced in 1 M  $H_2SO_4$  at the overvoltage  $\eta = 0.4$  V for 2 h. The impedance was measured in the frequency range from 20 Hz to 20 kHz.

The steady-state cathodic polarization curves of Cu electrode in all solutions examined here have the Tafel slope of 105 mV/decade, the constant  $a$  of the Tafel equation for 1 M  $H_2SO_4$  is equal to 760 mV; these coefficients are in agreement with reported data /2, 4/.

Four probable equivalent circuits (Fig.) were taken into account in processing of the impedance data. The equivalent circuit A corresponds to the two step electrode process like the HER /7/. Model B is used quite widely /8, 9/ in describing the hydrogen electrode impedance. The models C and D were employed in the study of the hydrogen evolution impedance on Ib-group metals, viz. silver (model C) /10/ and gold (model D) /11/. CPE in the equivalent circuit D is a constant phase element. The Warburg impedance in models B and C is attributed to the surface diffusion of hydrogen /8-10/.

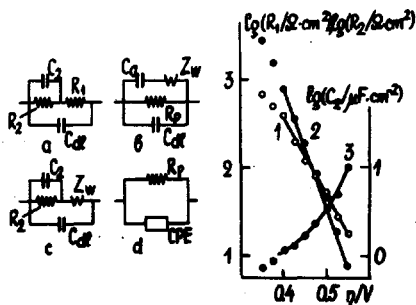


Fig. The examined equivalent circuits and the parameters of the equivalent circuit A as a function of the overvoltage of copper electrode in 1 M  $H_2SO_4$ : (1)  $R_1$ ; (2)  $R_2$ ; (3)  $C_2$ .

The selection of the circuit which is in the best agreement with the experimental data was carried out using F test and residual analysis /12/. As a result of computations the equivalent circuits B and C should be rejected as they describe the impedance spectra unsatisfactorily. The models A and D fit nearly equally well the experimental data in the range of the overvoltages  $0.4 < \eta < 0.6$  V. Since the circuit A has a more clear physical meaning, we accept it as the best model. Only at  $\eta < 0.4$  V the model D is more preferable than the circuit A.

The relation between the parameters of the equivalent circuit A and overvoltage for the Cu/1 M  $H_2SO_4$  interface is shown in Fig. It was found that when the solution pH at a constant overvoltage increases, the capacitance of  $C_2$  decreases, while resistances  $R_1$  and  $R_2$  increase, and  $R_2$  increases more rapidly than  $R_1$ . This result shows that proceeding from the HER on Cu electrode via the Volmer-Heyrovsky route is more probable than via the Volmer-Tafel mechanism /13/. The calculation of the surface coverage of the Cu electrode with adsorbed electroactive hydrogen by the procedure /14/ shows that increases from  $4 \cdot 10^{-4}$  to  $2 \cdot 10^{-3}$  while  $\eta$  rises from 0.35 to 0.55 V. The obtained values of  $\theta$  are significantly smaller than those estimated in /15/ being very similar to those found for Au electrode /16/.

Iodide adsorption on the electrode surface in 1M



H<sub>2</sub>SO<sub>4</sub> (when adding 10<sup>-5</sup> - 10<sup>-2</sup> M KI) at  $\eta = 0.55$  V causes the inhibition of the hydrogen evolution reaction and raising of R<sub>1</sub> and R<sub>2</sub>. In this case the ratio R<sub>1</sub>/R<sub>2</sub> and capacitance C<sub>2</sub> pass through a maximum when the iodide concentration increases.

#### References

1. H. Gerischer, W. Mehl, Z. Elektrochem., 59(1955)1049.
2. M. Mägi, U. Palm, V. Past, Trans. Tartu University, 193 (1966)96.
3. K. Gossner, F. Mansfeld, Z. phys. Chem., 58(1968)19.
4. S. Ya. Lanina, Z. A. Iofa, Elektrokimiya, 5(1969)359.
5. A. K. Vijh, J. Electrochem. Soc., 118(1971)263, 1963.
6. S. Trasatti, J. Electrochem. Soc., 118(1971)1961.
7. D. A. Harrington, B. E. Conway, Electrochim. Acta, 32(1987)1703.
8. S. P. Shavkunov, I. N. Sherstobitova, V. V. Kuznetsov, Elektrokimiya, 19(1983)706.
9. A. A. Kuznetsov, Elektrokimiya, 22(1986)1361.
10. D. I. Leikis, D. P. Aleksandrova, Elektrokimiya, 3(1967)865.
11. G. J. Brug, A. L. G. van den Eeden, M. Sluyters-Rehbach, J. H. Sluyters, J. electroanal. Chem., 176(1984)275.
12. E. D. Sprague, C. E. Larrabee, J. Chem. Educ., 65(1988)238.
13. V. I. Kichigin, I. N. Sherstobitova, V. V. Kuznetsov, Elektrokimiya, 12(1976)249.
14. V. I. Kichigin, Elektrokimiya, 23(1987)1689.
15. U. Palm, M. Pärnoja, Trans. Tartu University, 265(1970)34.
16. B. E. Conway, L. Bai, Electrochim. Acta, 31(1986)1013.

## ELECTRIC DOUBLE STRUCTURE AND ADSORPTION AT ELECTRODES MODIFIED BY ELECTRON-CONDUCTING POLYMER FILMS

V.E.Kazarinov

A.N.Frumkin Institute of Electrochemistry, USSR Acad. Sci.,  
Moscow

Electron-conducting polymers synthesized in the form of free-standing films or covering a metal or a semiconductor electrode surface have been attracting an ever growing attention in view of combination of their unique properties making them highly perspective for numerous applications: in chemical and biochemical sensors and microelectronics, fuel cells and electrocatalysis, batteries, capacitors, solar energy conversion, for protection of inorganic semiconductors at photo corrosion, as ion-selective membranes for a gas separation. On the other hand, practical realization of these perspectives is appreciably retarded because of an insufficient stability of these materials. This shortcoming is greatly due to the lack of adequate information on redox reactions in these systems as well as accompanied physical and chemical phenomena.

Though numerous experimental studies of electrochemical behaviour of conducting polymer films have been carried out, the theoretical description of these phenomena is still based, to a considerable extent, on an immediate application of corresponding concepts derived for the traditional interfaces, a metal/solution or a semiconductor/ solution one.

Intensive experimental and theoretical studies of polymers' electrochemical properties have been carried out in A.N.Frumkin Institute of Electrochemistry, including their doping, the electric double layer structure and kinetics of redox reactions, with a proper account of the specificity of this system consisting of three phases and two interfaces [1-4]. Application of thermodynamic relations has enabled us to avoid the necessity to introduce a detailed model of the interfacial structure in the process of determining the equilibrium potential drops and concentrations of mobile

charge carriers inside the film. A generalization of the slow-discharge theory has been proposed for kinetics of redox reactions of solute species at the film surface which has enabled us to give an interpretation of experimental data for several electrochemical reactions at electrodes covered with the polythiophene, polyparaphenylene and polyaniline films.

The role of anions in the process of electrochemical doping of polyaniline has also been studied by the radioactive traces technique. Anionic sorption inside the film from acidized solutions was shown to be determined mostly by the two processes, protonation and doping. The steady-state sorption due to the former process is a function of bulk solution pH, whereas that due to the latter is determined by the polymer potential and direction of its variation as well. An irreversible oxidation of the polymer resulted in a diminution of the "doping" component of sulfuric acid anion sorption only. At the same time, even practically complete loss of the polymer ability to be doped, after its irreversible oxidation, does not effect its protonation process.

Differential reflectance and electroreflectance light spectroscopy has enabled us to study initial stages of the polymer film formation. Their absorption spectra have been obtained at various degrees of doping. Moreover, a conclusion on polymer chains' orientation in the film and its structural ordering has been made with use of the polarization selectivity of some optical transitions.

## References

1. V.E.Kazarinov, M.D.Levi, A.M.Skundin, M.A.Vorotyntsev, *J.Electroanal.Chem.*, 271(1989)193.
2. M.D.Levi, M.A.Vorotyntsev, V.E.Kazarinov, *Synth.Met.* (in press)
3. M.D.Levi, *Mat.Sci.Forum*, 42(1989)101.
4. V.E.Kazarinov, V.N.Andreev, M.A.Spitsyn, A.V.Shlepakov, *Electrochimica Acta*, 35(1990)899.

GENERATION OF VARIABLE SIGN SPACE CHARGE IN A DIFFUSION LAYER FOR ELECTRODE PROCESS WITH SUBSEQUENT HOMOGENEOUS REACTION

Yu.I.Kharkats, A.V.Sokirko

A.N.Frumkin Institute of Electrochemistry, USSR Acad.Sci.,  
Moscow

It is known that during electric current passing, a space charge region arises in diffusion layer, whose distribution density does not decrease exponentially as it was in diffuse layer, but gradually  $/1/$ . When the current density tends to its limiting value, the space charge density in the vicinity of the electrode increases abruptly, coinciding in sign with that for electroactive ions.

Here we present the results of investigation of space charge distribution in diffusion layer for reduction of cations  $A^{z+} + 2e^- \rightarrow A^0$ , and parallel oxygen reduction  $O_2 + 2H_2O + 4e^- \rightarrow 4OH^-$  with subsequent recombination reaction of  $OH^-$  and  $H^+$  ions in diffusion layer:  $OH^- + H^+ \rightarrow H_2O$ . This reaction scheme was analyzed in detail in ref. /2/, in which the mechanism of migration current exaltation effect in acidic solution was theoretically investigated.

The set of electrodiffusion equations describing the distributions of components' concentrations and the potential in diffusion layer may be written as

$$\frac{dc_1}{dx} + c_1 \frac{d\psi}{dx} = \frac{i_1 L}{FD_1 c_0}, \quad \frac{dc_2}{dx} - c_2 \frac{d\psi}{dx} = 0, \quad (1)$$

$$D_3 \frac{dc_3}{dx} - c_3 \frac{d\psi}{dx} - D_4 \frac{dc_4}{dx} + c_4 \frac{d\psi}{dx} = -\frac{i_2 L}{Fc_0} = -D_3 j_2, \quad (2)$$

$$c_3 c_4 = K_0, \quad c_z + c_3 = c_1 + c_4. \quad (3)$$

Here  $c_1, c_2, c_3$  and  $c_4$  - are dimensionless concentrations of cations  $A^+$ , anions,  $OH^-$  ions and  $H^+$  ions,  $c_0$  is the dimensional concentration of  $A^+$  ions in the solution bulk,  $\psi = F\phi/RT$  is the dimensionless electric potential,  $x$  is di-

dimensionless coordinate ( $0 \leq x \leq 1$ ),  $L$  is the thickness of the Nernst diffusion layer,  $i_1$  and  $i_2$  are current densities for cation's discharge and oxygen reduction,  $K_0$  - the ionic product for water, the boundary conditions at  $x = 1$  can be written as  $c_1(1) = 1$ ,  $c_2(1) = 1 + k$ ,  $c_3(1) = 0$ ,  $c_4(1) = k$ ,  $\psi(1) = 0$ .

Taking into account that the recombination reaction for water is very fast and the equilibrium constant satisfies inequality  $K_0 \ll 1$ , we can suppose that in the diffusion layer either ions  $\text{OH}^-$  or  $\text{H}^+$  ions can exist simultaneously. Correspondingly, the recombination of reaction plane  $x=0$  splits the diffusion layer into two regions,  $0 \leq x \leq \theta$  and  $\theta \leq x \leq 1$ . We can put  $c_4 > 0$  and  $c_3 \approx 0$  in the region spaced to the right of the point  $x = \theta$  and  $c_3 > 0$  and  $c_4 \approx 0$  in the region spaced to the left of the point  $x = 0$ . These approximations make it possible to determine the potential distribution  $\psi(x)$  and then using the Poisson equation, to find space charge distribution  $\rho = -\epsilon RT\psi''/F$ .

Calculated  $\rho(x)$  distributions for series of parameters  $j_1$ , and fixed  $j_2$  and  $k$  values are shown in Figure 1.

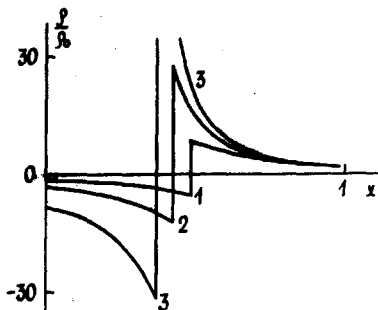


Fig. 1. Space charge distribution for  $D_3/D_4 = 0.56$ ;  $k = 0.8$ ;  $j_2 = 4$ , and  $j_1$ : 1 - 2; 2 - 2.5; 3 - 2.7;  $\phi_0 = 2\text{ec}^\circ$ .  $\cdot (l_D/L)^2$ ;  $l_D$  is the Debye length.

The analysis shows that as a result of recombination

reaction inside the diffusion layer some interesting peculiarities in space charge distribution arise. At the point of homogeneous reaction localization  $x = \theta$  and under the condition  $D_3 J_2 \ll k D_4 J_1$  an abrupt change of the sign and absolute value of  $\rho(x)$  takes place. In the discussed model due to high value of rate constant of recombination reaction its reaction layer had practically zero thickness. In a more general case of moderate reaction rates there must exist some transition region in which space charge varies from positive to negative values. Qualitatively the obtained result can be explained as follows. We can present the plane of recombination reaction localization as some electrode plane at  $x = \theta$ , which is on the one hand brought into contact with  $H^+$  ions, and on the other hand with  $OH^-$  ions. Then in the region  $\theta \leq x \leq 1$  where  $H^+$  ions exist we have positive space charge distribution as usual in electrolyte. And in the region  $0 \leq x \leq \theta$  where  $OH^-$  exists we have correspondingly negative space charge distribution.

We note in conclusion that the peak in space charge distributions including also a change in the sign of charge was earlier predicted in refs. /3,4/ for the systems in which besides movable carriers of charge also fixed charges exist.

#### References

1. V.G.Levich. Physico-chemical Hydrodynamics. M., 1959.
2. A.V.Sokirko, Yu.I.Kharkats, *Elektrokhimiya*, 25 (1989) 232.
3. Yu.I.Kharkats, *Elektrokhimiya*, 20 (1984) 248.
4. Yu.Ya.Gurevich, A.V.Noskov, Yu.I.Kharkats, *Elektrokhimiya*, Proc. Acad. Sci USSR, 298 (1988) 383.

INTENSIFICATION OF HYDROGEN TRANSPORT ACROSS A Pd MEMBRANE  
BY MODIFICATION OF THE ELECTRODE/ELECTROLYTE INTERFACE

I.I. Kolesnichenko, A.G. Pshenichnikov

A.N. Frumkin Institute of Electrochemistry, USSR Acad. Sci.,  
Moscow

Hydrogen transfer across a palladium membrane was investigated in the presence of coupled electrochemical processes of hydrogen injection on the contact side and its extraction on the diffusion side. Experiments were carried out in a two-compartment cell with the membrane fixed between the compartments in 0.1 or 1.0 M  $H_2SO_4$  solutions at room temperature. An electric circuit permitted independent polarization of the input and output sides of the membrane.

The dependence of the exchange current  $i_0$  of the formation and ionization processes of adsorbed hydrogen on potential was studied by the polarization curves method. It was found that in the range of the existence of the  $\alpha$ -phase of  $PdH_x$ ,  $i_0$  varies little and its value is 0.4 mA/cm<sup>2</sup>; in the range of  $\beta$ -phase  $i_0$  increases when potential shifts in the cathodic direction, reaching 1.6 mA/cm<sup>2</sup> at potential of 0.0 (RHE) in the same solution.

Analysis of the curves of switching on and off polarization under galvanostatic conditions showed that the slow steps of the overall process of hydrogen transfer across a thin membrane are the electrochemical processes at the membrane/electrolyte interfaces. Decrease in the limiting step overvoltage can be achieved either by decreasing the current density by increasing the true surface of the membrane/electrolyte interface (by creating on the surface a porous palladium layer for example), or by increasing the effective value of  $i_0$  (say, by surface modification with metals for which the value of  $i_0$  is greater than  $i_0$  on palladium), or by combination of the two methods used.

The influence of various methods of membrane surface treatment on the hydrogen transfer rate in the  $H_2$  (1 atm)/membrane/electrolyte system was investigated. It was shown by special experiments that in the absence of electrolyte film

on the contact side of the membrane, hydrogen absorption process occurs under nearly equilibrium conditions (effective overvoltage on the contact side is small) and the change in the membrane permeability to hydrogen is due to that in the characteristics of its output side. It is clear from Fig.1 that both increases surface roughness factor (curve 2) and modification of the surface with rhodium (curve 5) lead to activation of hydrogen transfer across the membrane. It can be assumed that in the presence of rhodium atoms on the surface, the step of hydrogen transfer from absorbed to adsorbed state and the steps of electrochemical hydrogen oxidation on the diffusion side prove to be separated in space: the step of absorbed hydrogen transfer to adsorbed state occurs on palladium atoms, and  $H_{ads}$  electrooxidation occurs on rhodium atoms; exchange of adsorbed hydrogen between the above-mentioned sites occurs by surface diffusion (spill-over mechanism). A method of creating a strong adhesion layer of palladium on membrane surface was developed.

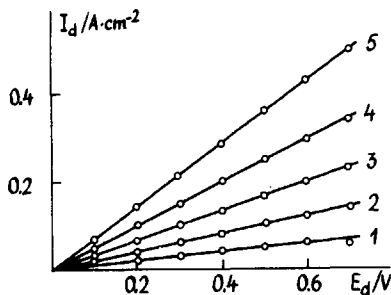


Fig.1. Steady-state polarization curves for hydrogen oxidation on a palladium membrane electrode in the case of contact between the diffusion side of the membrane and electrolyte (0.1 N  $H_2SO_4$  at  $20^\circ C$ ) and between the contact side and gas. 1 - membrane after stepwise polarization; 2 - membrane after heating in air ( $t=780^\circ C$ ); 3 - membrane after application of dispersed palladium; 4 - membrane after application and sintering of dispersed palladium; 5 - membrane with sintered dispersed palladium after application of Rh.



INVESTIGATION OF DOUBLE ELECTRIC LAYER ON GLASSY  
CARBON ELECTRODE BY ELECTROREFLECTANCE METHOD

G.V.Korshin, I.R.Manyurov, A.A.Petukhov

Kazan Chemical Technological Institute, Kazan

Electric double layer and adsorption on glassy carbon (GC) electrode were investigated by electroreflectance (ER) method. It was shown that for quantum energy values less than 4 eV, ER spectra may be described in terms of the Drude theory. The value of plasma frequency of oscillations of free charge carriers depends on the potential; dependence of relaxation time of free charge carriers on the potential gives by some orders of magnitude weaker optical effect. Since GC is a semi-metal and the concentration of charge carriers increases both in the case of cathodic polarization due to injection of electrons into conduction band and in the case of anodic one due to injection of holes into valence band, the minimal value of plasma frequency  $\omega_p$  must be observed at the potential of zero charge (p.z.c.). This corresponds to the condition of zero value of ER signal at the p.z.c. in the case of registration of  $dR/(RdE)$ , E-curves. The integration of the  $dR/(RdE)$ , E-curve allows to obtain the two-dimensional conductivity in the region of space charge as a function of electrode potential. Thus, fundamental parameters of double electric layer on GC electrode (and other carbon materials) may be obtained directly from ER data for solutions of any composition and concentration.

The features of the ER spectrum of GC electrode for  $\hbar\omega > 4$  eV arise as a result of  $\pi \rightarrow \pi^*$  interband optical transitions. In this region of  $\hbar\omega$  values the intensity of ER signal is proportional to the density of electronic states in valence and conduction bands of the carbon material.

The semi-metallic nature of GC provides a thickness of space charge region which is about an order of magnitude greater than that of typical metals, this leading to the rather low sensitivity of ER spectra of GC electrode to the

adsorption, unless the adsorbate does penetrate into the near-surface region of the electrode or forms surface compounds. Formation of intercalates in transient layer in the case of penetration of  $\text{HSO}_4^-$  and  $\text{ClO}_4^-$  anions into GC bulk is accompanied by the appearance of a very intense light absorption band in the region of  $h\nu < 2.5$  eV, the existence of this band may hardly be explained in frames of the free charge carriers approximation. It was supposed that the band existed due to the formation of surface electronic levels located in the transient layer of carbon material. In the conditions where there is no intercalation, the polarization of GC electrode is accompanied by a shift of maximum in ER spectrum, this feature cannot either be adequately described in terms of the Drude model. It was suggested that the uptake of solution components by the space charge region takes place for the potentials which are not equal to p.z.c., this process leading to the light adsorption band formation, though its intensity is small in comparison with that for case of intercalation. Therefore the region of interaction of solution components with an electrode cannot be associated only with the local phase boundary "the first layer of carbon atoms the first layer of adsorbed particles", rather this region is spread towards the electrode bulk even in the absence of intercalation. The transition metal ions, in particular  $\text{Cu}^{2+}$  ion, interact with the GC surface in a special way. In such a case the electronic structure of the transient layer undergoes sharp a change, in some conditions the appearance of energetic gap between the valence and conduction bands and the formation of inverse layer are possible. Copper ions form a strong chemisorption bond with surface atoms and they can be removed only at high anodic potentials. Copper atoms which are bonded on the GC surface influence in a crucial way the mechanism and kinetics of the formation and growth of copper deposit on the GC surface.

## KINETICS AND MECHANISM OF MONOLAYER SILVER ELECTRODEPOSITION FROM RHODANIDE SOLUTION

I.N.Kosenko, V.V.Trofimenko

Chemical Faculty, Dniepropetrovsk State University,  
Dniepropetrovsk

Silver electrocrystallization from the rhodanide solutions is characterized by a high reversibility of the discharge stage [1] and by a considerable adsorption of the electrolyte components [2]. The incorporation of the adatoms (adions) into the growth sites of the silver lattice may be a probable slow stage of the cathodic process due to the peculiarities mentioned. This assumption check-up is of principle importance, as a experimental confirmation of such a metal electrocrystallization mechanism has not been reported in literature yet.

Galvanostatic silver monolayer formation from the solution containing 0.24 mol/l  $\text{Ag}^+$  and 2.57 mol/l KSCN was studied. The platinum end-wire electrode with the surface area of  $0.002 \text{ cm}^2$  was used. It has been preliminarily plated by silver of  $1\mu$  thickness at the current of  $10\mu\text{A}$ . The parameters of the discharge and crystallization stages (exchange current,  $j_0$ , crystallization exchange flow,  $v_0$ , adatom concentration at the equilibrium potential,  $c_0$ ) were determined from the transient curves of total overpotential  $\eta$  by using Bockris-Mehl model [3]. It has preliminarily been found that the contributions of the diffusion and reaction overpotentials to  $\eta$  quantity may be neglected. This method [3] permits to determine the overpotentials of the transition,  $\eta_n$ , and the crystallization are  $\eta_k$ , and the accepted value of the diffusion coefficient of  $10^{-8} \text{ cm}^2 \text{ s}^{-1}$  - to calculate the growth step density,  $N_s$  [4]. The dependence of the quantities of  $j_0$ ,  $c_0$  and  $v_0$  on  $j$  (Fig.) shows their pseudoequilibrium character being probably stipulated by the participation in exchange process of that part of the growth steps activated by the current pulse at the initial period.

The comparison of  $j_0$  and  $v_0$  quantities evidences a con-

siderable inhibition of the crystallization stage which due to the antibiotic character of the  $j_0$  and  $c_0$  dependences on  $j$  may not be related to the deposit growth proceeding by adatoms diffusion: such a kinetic scheme implies the direct participation of the adatoms in the discharge stage and, hence, the proportionality of  $j_0$  and  $c_0$  quantities. All the experimental data are satisfactorily interpreted in case the silver ions are assumed to mainly discharge into the region of the growth centres followed by a slow incorporation stage of the adatoms into the semicrystalline sites. In this case  $\eta_k$  also arises and  $j_0$  currents become proportional to  $N_s$  value (Fig.).

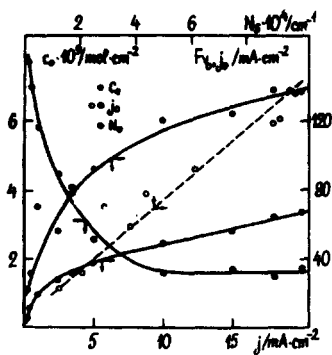


Fig. See the text.

The adatom surface diffusion don't noticeably contribute into the electrocrystallization rate due to  $\text{SCN}^-$  and  $\text{AgSCN}$  adsorbed particles, deeply inhibiting the process discussed. The limited mobility of the silver adatoms leads to surface blocking and to discharge transfer into the region of the growth steps. The behaviour of  $j_0$  dependence on  $N_s$  shows not only the discharge centres to be slightly changed under the step length increasing. This dependence extrapolation to  $N_s=0$  leads to a low exchange current at the plane part of the deposit surface ( $j_{0,\text{ad}} < 0.01 \text{ A}/\text{cm}^2$ ). Assuming the surface limited to the width of one row of the atoms to participate in the electrone exchange at the step according to ref.[4], the exchange current at the deposit growth front has a mean value  $j_{0,s} \approx 50 \text{ A}/\text{cm}^2$ . It is expected the high local supersaturations causing the activation

of new crystallization sites to arise at the steps.

The data obtained by the analysis of the temperature dependences of  $c_0$  and  $v_0$  (4+40°C) allows to determine the thermal effect  $\Delta H \approx -42$  kJ/mol, the entropy change  $\Delta S \approx 21$  J/(mol·K) and real activation energy  $\Delta H^* \approx 0$  for the crystallization stage at the equilibrium potential [5]. The absence of the energy barrier for the incorporation stage means that at the equilibrium the growth sites interexchange together with the adatoms (adions) adsorbed at them. The conclusion drawn confirms also a slight entropy change during the incorporation process: the degree of order for the system does not practically change. In contrast to this the silver monolayer formation is related to overcoming of a high energy barrier,  $\Delta H_j^* \approx 63$  kJ/mol for the stage of the adatom incorporation ( $\Delta H_j^*$  value is determined by the analysis of the corresponding  $\eta_{k,j}$ -curves). Thus, the incorporation stages of the silver adatoms at the equilibrium and during electrodeposition process proceed by the different mechanisms.

#### References

1. R.Yu.Bek, V.N.Pautov, Izv. SO AN SSSR, ser. him. nauk, 6(1971)121.
2. V.N.Pautov, Double Layer and Adsorption at Solid Electrodes. VII. Proc. Tartu University, (1988)310.
3. W.Mehl, J.O'M.Bockris, Can. J. Chem., 37(1959)190.
4. Ye.Budevski, V.Bostanov, T.Vitanov, The growth of crystals, M.:Science, 10(1974)230.
5. H.Gerischer, Z. Elektrochem., 62(1958)256.

## INFLUENCE OF PULSE POLARIZATION ON SURFACE-ACTIVE SUBSTANCES ADSORPTION IN METAL ELECTROPLATING

N.A.Kostin

Dnepropetrovsk Institute of Transport Engineering,  
Dnepropetrovsk

There are two directions of development in applied electrochemistry today: classical - creation of new surface-active substances (SAS) and pulsed electrolysis. These ways are worked out independently by different schools of scientists. The SAS-based direction uses direct current only for electrolysis, while the new SAS, on the opposite-pulsed electrolysis uses the same content solution but different types of non-direct current as a subject of variation. Our opinion is that the joint development of these two, still separate, ways of electrolysis can open wide range of possibilities for influence on the electrode processes. The opportunities for such influence are based on SAS adsorption-desorption control by means of  $E$  (cathode potential) variation from  $E_{zc}$  (zero charge) potential (during pulse-time or all the time of plating). Necessary cathode potential ( $E$ ) variation is made by use of pulse current (the form and parameters of pulse current can be varied by special programme). Second, the SAS diffusion during off-time and hydrodynamic conditions variation during pulse-time are not less important factors which determine the filling up of the cathode surface by adsorbate and the adsorption layer density. The report deals with the influence of pulse current parameters ( $I_p$  - pulsed current density, off-time, current frequency, etc) on the main features of processes mentioned.

For example, for the metals with  $E_{st}$  (stationary cathode potential) more positive, than  $E_{zc}$ , densed adsorption layer is formed only for high  $I_p$  and long pulses which ensure achieving  $E_{zc}$ . With short pulses cathode potential cannot reach the necessary value even for very high  $I_p$ , so adsorption film may have not enough time to be formed (see example in report).

During the off-time, cathode potential is decreasing and it can be lower than the adsorption potential, so it can be out of this value range. This is determined by cathode potential (E) decline velocity and by the off-time. The E-decline speed is different for different metals and electrolytes. For diffusion stage-limited processes E(t) has the same shape as the current and it decreases very quickly to its stationary value. So, for these processes and if  $E_{st}$  is positive and very different from  $E_{zc}$ , SAS desorption is possible during the off-time (the report has an example on tin electroplating).

Cathode potential is essentially distorted for the inhibited discharge stage processes, especially in many component electrolytes, and it has a more negative value during the off-time (the report has an example on nickel sulphate-plating in brightness additive electrolyte).

There is a possibility to control cathode potential by reverse pulses (for processes where E has the same value during  $I=0$ ). The time of cathode potential reset to the value of  $E_{st}$  and more is determined by the quantity of electricity and the rate of reverse pulse rise. With increasing of these parameters the time of E reset to  $E_{zc}$  and than to  $E_{st}$  is reduced.

For metals with  $E_{st}$  more negative than  $E_{zc}$  direct pulses, the amplitude does not influence adsorption processes. In this case, frequency is the most influential control parameter of pulse current (the process of ammoniate zinc plating is considered in detail in report).

Pulse polarization shows its influence not only on additives put onto solution before electrolysis begins but also the additives formed during pulse electrolysis. For example, superhigh  $I_p$  ( $25-50 \text{ A/dm}^2$ ) pulse current with the use of 50-70 Hz frequency promotes forming and adsorption of nickel hydroxide with special structure, which serves as the first grade brightness-forming additive.

Except mentioned influence pulsed current gives the opportunity to use solutions with smaller numbers of components (as compared with direct current) or to decrease the concentration of rare additives (the report has the results of chloride ammonite zinc and copper sulphate plating research).

ON THE INFLUENCE OF SUPPORTING ELECTROLYTE CONCENTRATION ON  
THE ELECTROREDUCTION RATE OF DIPYROPHOSPHATE METAL COMPLEXES

V.I.Kravtsov, V.V.Kondratiev  
Leningrad State University, Leningrad

By dipyrophosphate complexes of lead(II) and tin(II) electroreduction at a dropping mercury electrode (d.m.e.) a reversible preceding chemical step takes place, as a result of which electroactive monopyrophosphate complexes are formed participating in a slow two-electron electrochemical step. Alkali metal cations of supporting electrolyte participate in the preceding chemical step the equilibrium and double layer structure of which depend on the supporting electrolyte concentration. To elucidate the degree of influence of both factors on the rate of dipyrophosphate complexes' electroreduction, the influence of sodium perchlorate concentration (0.05-1.0 M) on the half wave potential of corresponding irreversible cathodic wave was investigated. Calculations carried out with stability constant of  $\text{NaP}_2\text{O}_7^{3-}$  ( $12.6 \text{ M}^{-1}$ ) and Tafel slope  $b_c = 50 \text{ mV}$  have shown that half-wave potential shift to the positive direction obtained at the sodium perchlorate concentration increase is determined by the shift of the preceding chemical step equilibrium. Insensitivity of complexes  $\text{Pb}(\text{P}_2\text{O}_7)_2^{6-}$  electroreduction rate, to the potential drop in a diffuse part of the double layer is explained by specific adsorption of electroactive complexes whose metal ions are bound with the surface atoms of metal electrode.

At electroreduction of complexes  $\text{Sn}(\text{P}_2\text{O}_7)_2^{6-}$  from solutions containing  $\approx 10^{-2} \text{ M}$   $\text{Na}_4\text{P}_2\text{O}_7$  (pH=8, 1 M  $\text{NaClO}_4$ ) irreversible cathodic polarographic wave is observed with the Tafel slope  $b_c = 50 \text{ mV}$ . The shift of  $E_{1/2}$  observed at sodium perchlorate concentration increase from 0.05 M to 1.0 M is equal to 74 mV and exceeds more than twice the shift of  $E_{1/2}$  obtained in the case of  $\text{Pb}(\text{P}_2\text{O}_7)_2^{6-}$  electroreduction (30 mV). The results obtained may be explained supposing that the sodium perchlorate concentration increase is followed by displacement of equilibrium of preceding chemical step leading to the formation of adsorbed electroactive complexes  $\text{SnP}_2\text{O}_7^{3-}$  and probably of  $\text{NaSnP}_2\text{O}_7^-$ . The conclusion about cesium and possibly



about some other alkali metal cations presence in electroactive monoproposphate complexes of tin was drawn earlier /1/ based upon the increase in electroreduction rate of complexes  $\text{Sn}(\text{P}_2\text{O}_7)_2^{6-}$  in the sequence of  $\text{Rb}^+ \approx \text{K}^+ < \text{Cs}^+ < \text{Na}^+ < \text{Li}^+$ . This order differs from order  $\text{Cs}^+ < \text{K}^+ < \text{Na}^+ < \text{Li}^+$  obtained by complexes  $\text{Pb}(\text{P}_2\text{O}_7)_2^{6-}$  electroreduction /2/ which coincides with  $\text{MP}_2\text{O}_7^{3-}$  complexes stability row ( $\text{M}^+$  - alkali metal ion). The absence of alkali metal ions in electroactive lead(II) complexes is probably connected with electroreduction of complexes  $\text{Pb}(\text{P}_2\text{O}_7)_2^{6-}$  at more positive potential values in comparison to complexes  $\text{Sn}(\text{P}_2\text{O}_7)_2^{6-}$  (about 0.3 V).

In the case of  $\text{Cu}(\text{P}_2\text{O}_7)_2^{6-}$  electroreduction, an irreversible wave is observed with  $E_{1/2} \approx -1.1$  V (SCE) and Tafel slope  $b_c$  128 mV and 146 mV corresponding to pyrophosphate ions concentrations 0.07 M and 0.02 M (pH 8, 1 M  $\text{NaClO}_4$ ). These  $b_c$  values are more than twice higher than the slope  $b_c = 50$  mV obtained for dipyrophosphate complexes of lead and tin, but they are much smaller than slope  $b_c = 500$  mV obtained for complexes  $\text{Cu}(\text{P}_2\text{O}_7)_2^{6-}$  electroreduction on copper electrode /3/. Unfortunately, the authors /3/ who used a rotating disk electrode have taken into account the diffusion processes of one kind of particles only though it was necessary to take into account the diffusion processes at both copper complexes and pyrophosphate ions. Therefore, the overestimated values of  $b_c$  were given in the paper /3/.

We have obtained the order of  $\text{Cu}(\text{P}_2\text{O}_7)_2^{6-}$  electroreduction on d.m.e. in respect to pyrophosphate ions being equal to -0.4. This order is determined probably by the course of parallel electrode reactions with different mechanisms (CECE, ECE). The slope  $b_c$  obtained testifies to a slow transfer of the first electron. The shift of  $E_{1/2}$  to the more positive potentials obtained for  $\text{Cu}(\text{P}_2\text{O}_7)_2^{6-}$  electroreduction of sodium perchlorate concentration increase is higher than in the case of  $\text{Sn}(\text{P}_2\text{O}_7)_2^{6-}$  electroreduction.

#### References

1. I.Ya.Tur'yan, V.I.Kravtsov, V.V.Kondratiev, *Elektrokhimiya*, 23 (1987) 847.
2. V.V.Kondratiev, V.I.Kravtsov, *Elektrokhimiya*, 23 (1987) 1118.
3. H.Konno, N.Nagayama, *Electrochim. Acta*, 22 (1977) 353.

INFLUENCE OF DOUBLE LAYER STRUCTURE ON THE HYDROGEN  
EVOLUTION REACTION AT HIGH TEMPERATURES

L.B.Kriksunov

A.N.Frumkin Institute of Electrochemistry, USSR Acad.Sci.,  
Moscow

The influence of high temperatures (above  $100^{\circ}\text{C}$ ) on the double layer effects in kinetics has not been investigated until recently. The investigation of this problem is necessary to begin with non-complicated systems studied at room temperatures, such as mercury electrode in aqueous solutions. The technique of high temperature electrochemical experiment /1/ developed by us gives an opportunity to investigate the electrochemical kinetics as well as the structure of double layer. With this technique the data has been obtained on the kinetics of cathodic hydrogen evolution reaction on mercury from diluted acid solutions at temperatures up to  $300^{\circ}\text{C}$  and on the influence of  $\Psi_1$ -potential on kinetics. The influence of  $\Psi_1$ -potential on kinetics is known to be expressed first of all in change of overpotential. Besides that, the slopes of polarization curves are also dependent on the  $\Psi$ -potential if the latter is dependent on electrode potential.

Experimental data on the temperature dependence of slopes of polarization curves in solution without specific adsorption show the slopes to be lower than the "theoretical" value  $b_T = 2.3RT/0.5F$ . Calculations on the basis of the Gouy-Chapman model (with the assumption that  $\Psi_1 = \Psi_0$ ) pointed out that experimental data in alcohols ( $-70$  to  $+50^{\circ}\text{C}$ ) as well as in diluted aqueous solutions ( $0$  to  $+200^{\circ}\text{C}$ ) can be explained by an effect of  $\Psi_1$ -potential only /2/.

In the case of specific adsorption the picture is more complex. In very diluted solutions of HCl, the slopes of polarization curves coincide with those in solutions of  $\text{H}_2\text{SO}_4$  of the same concentration. In  $0.3-1$  M HCl the slope is higher than  $b_T$  and the difference increases with temperature. That follows both from our (to  $+200^{\circ}\text{C}$ ) as well as from literature ( $0$  to  $+80^{\circ}\text{C}$ ) data. It is an evidence for an increase in specific adsorption of  $\text{Cl}^-$  with temperature increase.

The dependence of the overpotential on the concentration of  $\text{Cl}^-$  has been studied. Of special interest is the dependence of specific adsorption from temperature. As a measure of specific adsorption we can adopt the change of overpotential relative to solutions without specific adsorption. One can see from the figure 1 that with increasing temperature the specific adsorption of  $\text{Cl}^-$  rises. This result is in accordance with the conclusions obtained from the temperature dependence of slopes of polarization curves. In the case of specific adsorption of tetrabutylammonium cation we have observed an opposite effect: the increase in temperature results in a strong decrease in specific adsorption. This result still needs discussion and further investigation.

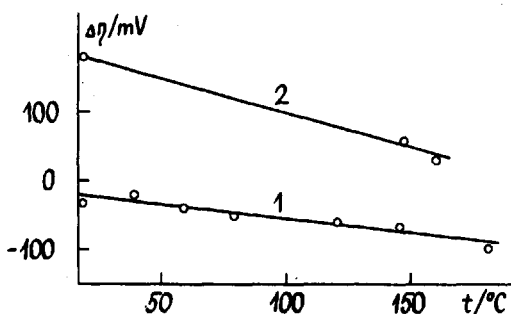


Fig. 1. The change in overvoltage of reaction under influence of specific adsorption as a function of temperature. Current density  $|g_i| = -3.3 \text{ A/cm}^2$ . 1 - 0.5-1.0 M HCl; 2 - 0.5 M HCl + 0.005 M tetrabutylammonium bromide.

#### References

1. V.M. Tsionskii, L.B. Kriksunov, J. Electroanal. Chem., 204 (1986) 131.
2. V.M. Tsionskii, L.B. Kriksunov, Pribory i tehnika eksperimenta, 1 (1988) 224.
2. V.M. Tsionskii, L.I. Krishtalik, L.B. Kriksunov, Electrochim. Acta, 33 (1988) 623.

## ELECTROSTATIC INTERACTION OF IONS WITH A SOLVENT

L.I.Krishtalik, N.M.Alpatova, E.V.Ovsyannikova

A.N.Frumkin Institute of Electrochemistry, USSR Acad. Sci.,  
Moscow

A new method has been proposed for the experimental determination of the electrostatic part of the transfer free energy for large compact ions. It is based on the differences of standard potentials  $\Delta E$  for two subsequent one-electron redox steps. The  $\Delta E$  values for redox couples of cobaltocene  $\text{Cp}_2\text{Co}^{+/0/-}$  and nickel(bis)dicarbollyl  $\text{Cb}_2\text{Ni}^{0/-/2-}$  were measured. For several aprotic solvents with feeble donor-acceptor properties (and their mixtures), the electrostatic part of the transfer energy obeys quantitatively Born equation (see Fig., curves 1 and 2). This qualitatively contradicts the conclusions of nonlocal electrostatics employing the model of monotonously decaying correlation of orientational polarization.

In the presence of strong specific interactions (e.g. hydrogen bonds water-anion, donor-acceptor interaction DMSO-Lewis acid), the transfer energy deviates substantially from the Bornian one (Fig.). The hypothesis on the role of hydrogen bonding with anion is substantiated by the Bornian behaviour both aprotic solvents and their mixtures with water in a purely cationic system of ruthenium(tris)bipyridil  $\text{Ru}(\text{bpy})_3^{0/+ /2+}$  (Fig., curve 3).

For the comparison of electrode potentials in different solvents, the couples  $\text{Cp}_2\text{Co}^{+/0}$  and  $\text{Cp}_2\text{Co}^{-/0}$  were proposed. In aprotic solvent not prone to specific interactions, any of these couples can be used taking into account a correction for transfer energy. The latter can be calculated after Born or found experimentally as  $1/2 (\Delta E_1 - \Delta E_2)$ . For water and other acceptor solvents, the corrected potential of  $\text{Cp}_2\text{Co}^{+/0}$  couple is to be used, the couple  $\text{Cp}_2\text{Co}^{-/0}$  is recommended for donor solvents. It was shown that ferrocene-ferrocenium couple may be used as a reference electrode with corrections found for  $\text{Cp}_2\text{Co}^{+/0/-}$ . These reference electrodes can be employed also for evaluation

of interfacial potential drops at the boundaries water/non-aqueous solvent.

The described reference electrode was used for determination of the transfer free energy of single ions. The values obtained for  $K^+$  are close to those obtained by TATB method (difference  $\approx 3$  kJ/mole). However, our method seems to be more justified (due to the open structure of TA and TB, there is a possibility of a rather close contact of solvent molecules with the center of these ions resulting in a marked asymmetry of solvent interaction with cation and anion).

The applicability of Born equation was used to calculate the electrostatic part of chemical solvation energy of ferricenium cation. The same for real solvation energy was found from Volta potential metal/solution at the standard  $Cp_2Fe^{+/0}$  potential and other thermodynamic data available. The difference of real and chemical energies gives the value of surface potential drop.

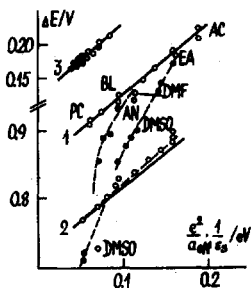


Fig. Dependence of  $\Delta E(V)$  on the parameter  $z^2/a_{eff}^3(eV)$ . Redox systems: 1 -  $Cp_2Co^{+/0/-}$ ; 2 -  $Cb_2Ni^{0/-/2/-}$ ; 3 -  $Ru(bpy)_3^{0/+ /2/+}$  PC - propylencarbonate; BL - butyrolactone; AN - acetonitrile; DMF - dimethylformamide; EA - ethanol; AC - acetone; DMSO - dimethylsulfoxide; o - aprotic solvents and their mixtures; • - mixtures of water with aprotic solvents; ◐ - mixtures water-ethanol. Dashed straight line (curve 2) includes a small correction due to a large dipole moment of  $Cb_2Ni^0$  which disappears upon reduction

ADSORPTION AND ELECTROCATALYTIC PROPERTIES OF  
SULFUR-CONTAINING COMPOUNDS OF IRON GROUP METALS

Yu.I.Kryukov, S.F.Chernyshov, L.I.Al'tentaller

A.N.Frumkin Institute of Electrochemistry, USSR Acad.Sci.,  
Moscow

The problem involving investigation of electrocatalytic characteristics of sulfur-containing nickel compounds has recently become again a subject of attention. In the majority of studies, deposition of electrodes of active sulfur-containing compounds is achieved by galvanic methods by introducing soluble thiocompounds /1,2/ and also along with them, dispersed powders of transition metal sulfides /3/ into the nickel plating bath.

We have proposed a simple method for activating the cathodes of hydrogen-oxygen electrolyzers with alkaline electrolyte which permits chemical deposition of coatings to be effected only on the electrode base surface without formation of active coating components in solution bulk. It has been established that such cathodes containing active catalyst mass in the amount of 3-5 mg/cm<sup>2</sup> show sufficient electrochemical activity in hydrogen evolution reaction: at 70°C (7 M KOH) and current density of 0.4 A/cm<sup>2</sup>, hydrogen overvoltage is not higher than 0.1 V. The polarization curves of hydrogen evolution on these electrodes are characterized in the Tafel coordinates by two linear sections with the slopes of 40-45 mV and  $\approx$  100 mV for low and high current densities, respectively.

Analysis of the dependence of current density on the active layer thickness at fixed polarization values at the cathodes with NiS<sub>x</sub> catalyst showed that the characteristic length of hydrogen evolution process at  $\eta = 0.1$  V is 15-20  $\mu$ , which is 5-6 times less than for nickel surface skeleton catalyst (SSC) /4/. The small characteristic length values, as compared to those found for nickel SSC, are caused by two factors: much higher values of the specific elec-

trical resistance of catalyst layer (70-90  $\Omega$  1-cm), and the exchange current of hydrogen reaction, whose value at 70°C in 7 N KOH is  $7 \cdot 10^{-5}$  A/cm<sup>2</sup>. A study was made of the dependence of the apparent exchange current of hydrogen reaction  $i_0^{\text{H}}$ , obtained by extrapolation of the second Tafel section of the E<sub>1</sub>lg*i*-dependence to the zero value of polarization per unit catalyst surface in the active layer, on the amount of catalyst *m* in it. The specific surface of the chemically deposited sulfur-containing nickel catalyst, determined by the BET method, is equal to 14 m<sup>2</sup>/g.

It was established that the  $i_0^{\text{H}}, m$  dependence is of extremal nature and consists of three sections. The first section in the range of catalyst content in the active layer  $0 < m < 0.13$  mg/cm<sup>2</sup> shows a linear increase in exchange current with increasing *m*. Within this section no ohmic or diffusion losses occur in the catalyst layer and the value of  $i_0^{\text{H}}$  on the surface of the first layer of catalyst grains is affected (decreasing it) by the electrode base (nickel electrode), on which the exchange current of electrode reaction is approximately by 1-1.5 orders less than on a sulfur-containing catalyst. At  $0.15 < m < 0.3$  mg/cm<sup>2</sup> (the second section) the exchange current of hydrogen reaction is practically independent of the catalyst amount in the layer. On this section  $i_0^{\text{H}}$  is equal to the true exchange current. With a further increase in *m* (in the region of the third section of the  $i_0^{\text{H}}, m$ -dependence) the apparent exchange current decreases considerably owing to the increased total contact electrocal resistance between catalyst grains in the layer.

It has been revealed by galvanostatic and potentiodynamic methods that at potentials more positive than 0 V (RHE) practically no hydrogen adsorption occurs on chemically deposited NiS<sub>x</sub> catalysts. These data agree with the results of vacuum-adsorption measurements, which showed the absence of hydrogen adsorbed from the gas phase on sulfur-containing nickel and iron compounds. The obtained data explain the absence of the activity of NiS<sub>x</sub> catalysts investigated by us towards the molecular hydro-

gen ionization reaction.

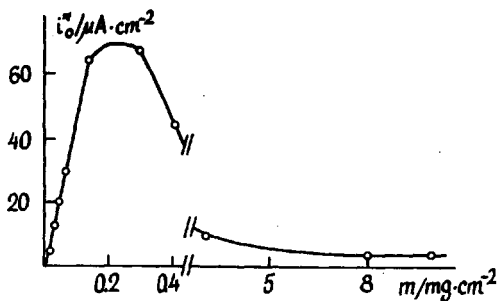


Fig.1. Dependence of the effective exchange current of hydrogen evolution reaction on  $\text{NiS}_x$  catalyst on the amount of catalyst in the active layer.

#### References

1. H.Vandeborre, Ph.Vermeizen, R.Leyzen, *Electrochim. Acta*, 29 (1984) 297.
2. R.Sabela, I.Paseka, *J.Appl.Electrochem.*, 20 (1990) 500.
3. A.Nidola, R.Schira, *Hydrogen Energy Progr.*, Part V, N.Y., Perg. Press, 909.
4. A.G.Oshenichnikov, S.F.Chernyshov, Yu.I.Kryukov et al, *Elektrokhimiya*, 18 (1982) 1011.



## SPECIFIC FEATURES OF THE FORMATION OF SUBSURFACE OXIDES ON NICKEL AND IRIIDIUM ELECTRODES

Z.I.Kudryavtseva, L.A.Burkal'tseva

A.N.Frumkin Institute of Electrochemistry, USSR Acad. Sci.,  
Moscow

Earlier optico-electrochemical studies of the surface state of a nickel electrode showed that upon cycling of a nickel electrode in 0.1 N KOH subsurface oxides are formed /1-3/. In the present study, of the formation processes of subsurface oxides of SSO on nickel and iridium electrodes are compared. It was found that in electrochemical oxidation-reduction of a nickel electrode in the potential range  $E = 0.01-0.5$  V followed by its exposure at  $E = 0.02$  V (surface reduction - SR) the ellipsometric parameters  $\Delta_0$  and  $\psi_0$  measured at  $E = 10$  mV correspond to those of the reduced surface  $\Delta$  and  $\bar{\psi}$ . When the cyclic amplitude was increased to  $E = 1.0$  V, the values of ellipsometric parameters after SR differ from initial values,  $\Delta_0 < \bar{\Delta}$ ,  $\psi_0 > \bar{\psi}$ . Change in ellipsometric parameters  $\delta\Delta$  and  $\delta\psi$  is observed during the first 4-5 cycles, where upon this dependence forms a plateau. In the oxidation cycles the values of  $\delta q$  (amount of electricity derived from potentiodynamic curves) and  $\delta\Delta$  are practically constant, i.e. in all the cases considered each oxidation cycle begins on reduced surface. The maximum changes of  $\delta\Delta$  and  $\delta\psi$  are  $5.5^\circ$  and  $1.5^\circ$ , respectively. Taking into account the depth of light penetration into material ( $\sim 100 \text{ \AA}$ ), it can be apparently assumed on the basis of the obtained data (equivalent thickness of SSO is  $\sim 50 \text{ \AA}$ ) that the SSO layer consists of isolated oxide islets in nickel bulk (approximate SSO/metal ratio 1/3). The following mechanism of SSO formation can be suggested. At  $E > 0.7$  V in 0.1 N KOH /1/ nickel undergoes dissolution. Thus, during exposure of a nickel electrode at  $E = 1.0$  V, along with oxidation, nickel undergoes dissolution. During reduction at  $E = 0$  V, dissolved nickel is deposited on the

electrode surface and owing to this fact the reduction process is always followed by arising an oxide-free surface recorded by the optico-electrochemical method ( $\delta q, \delta \Delta - \text{const}$ ).

The surface state of an iridium electrode was studied under conditions of electrochemical formation and reduction of an oxide layer on its surface in 0.1 N KOH with the electrode subjected to cycling in the potential range 0 - 1.4 V (RHE) at the sweep rate of 100 mV/s. Ellipsometric parameters were measured (checking the cycling results) at the potentials of 0.35 and 1.4 V after exposure under potentiostatic conditions when current close to 0 was reached. When potential varies stepwise from 0.35 to 1.4 V, an oxide layer of stoichiometric composition,  $\text{IrO}_2$ ,  $\sim 5 \text{ \AA}$  thick is reversibly formed (1.4 V) and reduced (0.35 V). In this case ellipsometric parameters vary in the following manner regardless of the number of cycles  $\delta \Delta (E = 0.35 \div 1.4 \text{ V}) \sim 1^\circ$ ,  $\delta \Psi (E = 0.35 \div 1.4 \text{ V}) \sim 10'$ . The maximum change in these parameters is  $\delta \Delta \sim 5^\circ 30'$  and  $\delta \Psi \sim 1^\circ 30'$  (after 170 cycles). Just as in the case of a nickel electrode, each subsequent oxidation cycle starts on reduced surface. These results can be explained by SSO formation.

SSO formation processes were compared on nickel and iridium electrodes. While on a nickel electrode undergoing alternatively oxidation and reduction of its surface, the relative value of  $\delta \Delta_{\text{O}} / \delta \Delta_{\text{OX}}$  characterizing the mass (number of monolayers) of the subsurface oxide no longer depends on the number of oxidation-reduction cycles (treatment time) when 4 monolayers are achieved, on an iridium electrode even after 6 monolayers, the intensity of SSO formation is preserved. These data and also the high corrosion resistance of the iridium electrode suggest a different formation mechanism of the subsurface oxides for these metals.

#### References

1. A.G.Pshenichnikov, Z.I.Kudryavtseva, L.A.Burkal'tseva, *Elektrokhimiya*, 23 (1987) 480.
2. Z.I.Kudryavtseva, A.G.Pshenichnikov, L.A.Burkal'tseva, *Abstr. of papers of the III All-Union Conf. on Ellipsometry*, Novosibirsk, 1987, p.102.
3. Z.I.Kudryavtseva, A.G.Pshenichnikov, L.A.Burkal'tseva, *Elektrokhimiya*, 25 (1989) 857.

ON THE PREDICTION OF THE NON-SPECIFIC ADSORPTION  
IN THE ORGANIC MOLECULE - METAL - WATER SYSTEM

V.P.Kuprin, F.I.Danilov, A.B.Shcherbakov  
Dnepropetrovsk Chemical Engineering Institute, Dnepropetrovsk

The energy of the adsorption of organic compounds from the aqueous solutions on the uncharged metal surface ( $\Delta G_A^0$ ) is known to depend on the energy relation for the metal-adsorbate ( $\Delta G_{M/A}$ ), metal-solvent ( $\Delta G_{M/H_2O}$ ) and adsorbate-solvent ( $\Delta G_{A/H_2O}^0$ ) bonds. The latter, as a rule, quantitatively equals to the energy of the adsorption of the surfactant ( $\Delta G_{A/G}^0$ ) at the solvent-air interface.

The total energy balance contains at least one term ( $\Delta G_{A/G}^0$ ) resulting from the exhibition of the nonspecific intermolecular forces, and the term being described within the scope of the microscopic (the first approximation of the theory on the molecular orbital perturbations) or macroscopic (theory by E.M.Lifshitz) approaches. However it is not always possible to carry out the correct quantum-chemical calculations in the metal-solvent-adsorbate system by the known reasons. In this connection use of various correlation parameters characterizing the intermolecular interactions in the system is vital as usual.

In order to predict the adsorption behaviour of the organic compounds at the interfaces we suggest to use the parameter of the intermolecular interaction intensity ( $\phi$ -factor) first introduced by I.B.Sladkov as the criterion for the inorganic compound polarity [1]:

$$\phi = 0.1 \ln T_b - 0.122 \ln v_b^1 + 0.006.$$

To calculate  $\phi$ -factor for any compound it is enough to know only its boiling point,  $T_b$  and the molar volume of the liquid at this temperature,  $v_b^1$ .

It is found, that dependence of  $\Delta G_{A/G}^0$  on  $\phi$ -factor for the aliphatic alcohols, acids and amines is of a linear character. It is interesting, that a linear correlation is also possible for the aliphatic alcohols on metals (Fig.1a).

Assuming in the first approximation the energy of the metal-amy alcohol interaction to be constant and all the changes of  $\Delta G_A^0$  to be stipulated only by the adsorbate hydrophilicity the energetics of the interaction in the

metal-water system may be evaluated by the difference,  $\Delta\Delta G^{\circ} = \Delta G_A^{\circ} - \Delta G_{A/G}^{\circ}$ . Fig.1b shows a linear correlation between  $\Delta\Delta G^{\circ}$  and  $\psi$ -factor of metals. The data received may be explained if we take into account the existence of the numerical relation between  $\psi$ -factor of the molecule and Lennard-Jones potential.

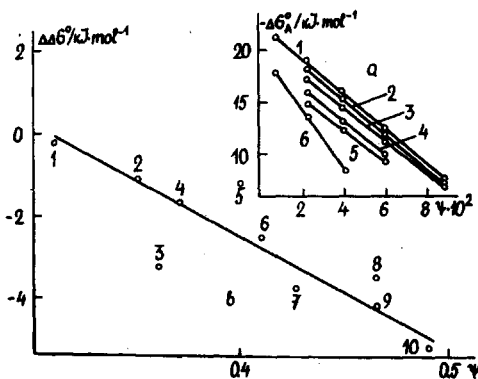


Fig.1a. The dependence of the standard free energy of the aliphatic C2-C6 alcohols adsorption on adsorbate  $\psi$ -factor at the solution-metal interface: 1-Hg [2]; 2-Sn [3]; 3-In-Ga [4]; 4-Cd [5]; 5-Zn [6]; 6-Au [7].

Fig.1b. The dependence of the energy gain of n-amyl alcohol on adsorbent  $\psi$ -factor while passing from solution-air to solution-metal interface in aqueous electrolyte: 1-Hg [2]; 2-Bi [8]; 3-Cd [5]; 4-Pb [9]; 5-Sn [3]; 6-In-Ga [4]; 7-Zn [6]; 8-Ag(100), 9-Ag(111) [10]; 10-Au [7].  $\psi$ -factor for In-Ga is calculated as follows:  $\psi_{\text{In-Ga}} = 0.164 \psi_{\text{In}} + 0.836 \psi_{\text{Ga}}$ .

As to metals the validity of  $\psi$ -factor as the parameter of the intermolecular interaction intensity is confirmed by the direct relation between the surface tension of a liquid metal at the melting point ( $\sigma_{\text{ml}}$ ) and  $\psi$ -factor (for 40 metals the correlation coefficient is 0.938) and as the surface energy of the solid metal may be regarded as  $U_s = f(\sigma_{\text{ml}})$  [11], thus  $U_s = F(\psi)$ .

The usage of  $\psi$ -factor as the metal hydrophility criterion is also valid for the macroscopic theory of the intermolecular forces according to which the interaction energy is described by the dispersion of the substance's

dielectric constant function on the frequency axis and the contribution of any spectral region into a total energy is determined by the optical density at a given range of the wave lengths. As the effects of the specific behaviour and also of the metal interaction exhibit themselves in the water transparency region (3-10 eV) and the main contributions into the dielectric properties and  $\phi$ -factor of water and the metals is made by the frequency region ranging from 0 to IR inclusive, it is possible to assume that intermolecular forces prevail in the water adsorption on an uncharged surface.

It should be noted, that with the account of the limitations introduced the series of increasing metal  $\phi$ -factors is not the series proper of hydrophilicity, it shows only an ability of a metal to enter into a nonspecific interaction. In spite of the fact that silicon has a high  $\phi$ -factor (higher than that of Ga), but because of its transparency in IR-range of frequencies [12], silicon is a rather hydrophobic material.

Thus,  $\phi$ -factor as the polarity and similarity criteria of substances may be used to predict the adsorption phenomena stipulated by the nonspecific intermolecular interaction.

#### References

1. I.B.Sladkov, Zh.Fiz.Khim., 10(1982)2412.
2. B.B.Damaskin, A.A.Survila, L.E.Rybalka., Elektrokimiya, 3(1967)146.
3. N.B.Grigoryev, V.P.Kuprin, Yu.M.Loshkaryev, Elektrokimiya, 9(1973)1842.
4. N.B.Grigoryev, A.M.Kalyuznaya, Elektrokimiya, 10(1974)1287.
5. L.E.Rybalka, B.B.Damaskin, D.I.Leykis, Elektrokimiya, 11(1976)286.
6. Yu.P.Ipatov, V.V.Batrakov, V.V.Shalaginov, Elektrokimiya, 12(1976)286.
7. M.Beltowska-Brzezinska, E.Dutkiewicz, P.Skoluda, J.Electroanal.Chem., 181(1984)235.
8. R.Ya.Pullerits, U.V.Palm, B.E.Past, Elektrokimiya, 5(1969)886.
9. N.B.Grigoryev, D.N.Machavariani, Elektrokimiya, 5(1969)87.
10. R.Holze, M.Beltowska-Brzezinska, Electrochim.Acta, 7(1985)30.
11. E.T.Turkdogan. Physical Chemistry of High Temperature Technology. N.Y.:Acad.Press.1980.P.344.
12. Handbook of Optical Constants of Solids. Ed.E.B.Palik. N.Y.:Acad.Press.1985.P.804.

# A MONTE CARLO SIMULATION OF THE INTERACTION OF HYDRATED IONS WITH THE METAL SURFACE

An. M. Kuznetsov, L. Yu. Man'ko

Kazan Chemical Technological Institute, Kazan

The features of interaction of the hydrated ions in dilute background electrolyte with the electrode surface and also the form of their interionic potential curve are of great interest for the electrical double layer theory. In this connection, we have considered the behaviour of the statistical ensembles  $\text{Na}^+(\text{H}_2\text{O})_n$  and  $\text{Cl}^-(\text{H}_2\text{O})_n$  ( $n=115$ ) contacting with a metal surface. Computations were performed by standard Monte Carlo technique. As a model for a single water molecule the 4-site TIP5P model described in literature was used. The water-water, ion-water and ion-ion interactions were simulated by an atom-atom pair potential in the form 12-6-1 and the interaction of these particles with the metal surface was modelled by their image charges. For the chloride ion in the chemisorption state the partial charge transfer to the metal obtained by means of quantum chemical calculations was taken into account.

The energetic profiles of the interaction of each of ions with the surface, and the water molecule distribution function have been computed. This allowed to analyse a structural "perestroika" of the hydrate shell of ions at their approaching to the surface. Besides that, the potential curve of the interaction between hydrated  $\text{Na}^+$  and  $\text{Cl}^-$  near the surface has been constructed. A barrier on the potential profile at the short distances between ions recently detected by Karim and Mc.Cammon (J. Amer. Chem. Soc., 1986, v.108, p.1762) by using the same approach for the same ions in the bulk of solution was found to decrease under influence of the metal surface.

The computational results are analysed in detail and discussed in the light of electrochemical data.

## ROLE OF ADSORPTION PHENOMENA IN CADMIUM AND CUPRIC IONS DISCHARGE KINETICS IN MIXED SOLVENTS

V.V.Kuznetsov, L.G.Bozhenko, S.S.Kucherenko, O.V.Fedorova

Institute of Physical and Organic Chemistry,  
Rostov State University, Rostov-on-Don

On the basis of systematic investigation of binary mixture of water and non-aqueous solvents  $M-Z$  it was established that the metal ions discharge on the positively charged surface of electrode took place in conditions of competitive adsorption of anions and molecules of organic component (OC) of the mixture. The processes of structure formation and complexing in the mixed solvents having influence on the degree of anion solvation determine the value of its adsorption on electrode and, as a result, the surface concentration of OC.

In perchlorate water-dimethylformamidic electrolytes  $M/$  under "small" concentration of DMF  $C_{DMF}$  (less than 4 M) the discharge of  $Cd^{2+}$  ions through the film of organic solvent molecules adsorbed at the electrode plays a decisive role in the kinetics of the process. Realization of such a mechanism is accompanied by the inhibition of electrode reaction (Fig., curve 1). The effect achieves its maximal dimensions in the area of structural stabilization of the mixed solvent (4 M of DMF) (solution of DMF in water), where the influence of its salting-out action on the solution components leads to a decrease in the reducible ion size. Under "intermediate" DMF concentrations (4-8 M) (complexing zone), the participation of non-aqueous solvent molecules in the cation process oversolvation and of anions in the formation of adsorption layer at Cd-cathode surface exert a decisive influence on electroreduction rate of ions. According to the elementary act theory of electrochemical reactions this fact is accompanied by the acceleration of electrode reaction. Under "large"  $C_{DMF}$  (9-12 M) (solution of water in DMF), the discharge of complex cations with heterogeneous ligands being formed in solution is carried out at adsorbed state.

When surface-inactive non-coordinating perchlorate ani-

ons having disordering action on water structure are replaced by iodine anions being able to form covalent bond with surface metal atoms, to participate in coordination with metal ions in solution and to destroy water structure, the processes in the liquid phase do not change their character (data of thermochemical measurements). While both kinetics and mechanism of  $\text{Cd}^{2+}$  ions discharge change significantly /2/, When

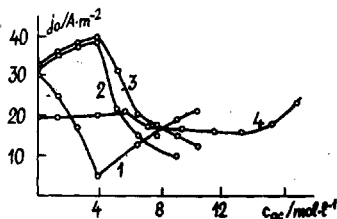


Fig. Dependence of exchange current  $j_0$  of discharge reaction of cadmium (1,2,4) and cupric ions (3) on OC concentration in mixture of water and DMF, containing 0.01 M  $\text{CdSO}_4$  + 0.1 M  $\text{LiClO}_4$  (1); 0.01 M  $\text{CdSO}_4$  + 0.1 M  $\text{LiI}$  (2); 0.01 M  $\text{CuSO}_4$  + 0.5 M  $\text{H}_2\text{SO}_4$  (3); in mixture of water and acetonitrile, containing 0.01 M  $\text{CdSO}_4$  + 0.1 M  $\text{LiI}$  (4) (298 K).

the composition of liquid phase is varied either organic solvent molecules or  $\text{I}^-$  are as ligands in the reducible complex of cadmium ions. Under  $c_{\text{DMF}} \leq 4$  M the formation of  $\text{Cd}^{2+}$  activated complexes with iodine ions in adsorption layer is accompanied by the acceleration of electrode reaction (Fig., curve 2). While under  $c_{\text{DMF}} > 4$  M the complexing in solution bulk and at electrode surface with participation of DMF molecules leads to the inhibition electroreduction of cadmium ions owing to formation of the dense adsorption film. The latter contains cationic complexes with organic ligands, which is promoted by adsorption of surface-active  $\text{I}^-$  anions at the electrode (data of independent measurements).

The study of electroreduction of cupric ions in sulfate water-dimethylformamidic mixtures /3/ again confirms the conclusion about a decisive role of the electrolyte anionic composition in the kinetics of cathodic process. The ability of



sulfate ions to form ionic pairs and polynucleated complexes with cupric ions where  $\text{SO}_4^{2-}$  anions act as bridge ligands has determined the character of exchange current dependence on the composition of the mixture (Fig., curve 3). The latter is analogous to that observed in the case of ions discharge in presence of  $\text{I}^-$  anions. However, the change of acceptor properties of the reducible ions is displayed to some extent in the discharge mechanism. So, under  $c_{\text{DMF}} < 4 \text{ M}$ , the electrode reaction acceleration is connected with formation of the activated complexes of cupric ions with sulfate ions in double layer region. While under DMF concentration 6-8 M the inhibition of  $\text{Cu}^{2+}$  electroreduction is conditioned by the kinetic difficulties which are connected with the proceeding dissociation of mixed complexes of type  $[\text{Cu}(\text{H}_2\text{O})_x(\text{DMF})_y]^{2+}$  in solution bulk. Under  $c_{\text{DMF}} > 8 \text{ M}$  the main cause of the inhibition of the cathodic process is the discharge of complex cations of type  $[\text{Cu}(\text{DMF})]^{2+}$  at adsorbed state.

The replacement of DMF by acetonitrile which is characterized by considerably poorer coordinative and adsorptive properties is accompanied by a sharp decrease in the sensitivity of the  $\text{Cd}^{2+}$  ions discharge rate to changes of solvent composition (Fig., curve 4). As faint a  $j_0$ -composition dependence is also observed when both a depolarizator and an electrode are selectively solvated by particles of the same type. In experimental conditions water is specifically adsorbed at the electrode surface (Cd) and it also forms the ion shale.

#### References

1. V.V.Kuznetsov, L.G.Bozhenko, S.S.Kucherenko, O.V.Fedorova, 37th Meeting of Intern. Electrochem.Soc., Vilnius, 2(1986) 172.
2. V.V.Kuznetsov, L.G.Bozhenko, S.S.Kucherenko, O.V.Fedorova, Elektrokimiya, 24 (1988) 633.
3. V.V.Kuznetsov, O.V.Fedorova, N.V.Komissarova, Proceedings of Higher Educational Establishments (USSR), 33 (1990) 72.

VOLTAMMETRY AND IR SPECTROSCOPY OF NITROGEN (5+) IN HIGH-BASIC MEDIA

R.K.Kvaratskheliya, G.R.Kvaratskheliya, M.G.Zhamierashvili  
Institute of Inorganic Chemistry and Electrochemistry,  
Academy of Sciences of Georgia, Tbilisi

In this paper the results of the study of electroreduction and state of nitrogen (5+) in the  $\text{HNO}_3$  solutions in high-basic solvents - pyridine and formamide are described.

The measurements have been carried out by the methods of voltammetry at the rotating disk electrodes, chronovoltammetry and potentiostatic macroelectrolysis with an accumulation and identification of the reduction products. The high-purity electrodes from Cd, Zn, Sn, Cu, Cu-Hg and Ni have been used. The solvents and salts underwent thorough purification and drying. The anhydrous nitric acid was obtained and used. Together with the electrochemical measurements the IR spectrograms of the  $\text{HNO}_3$  solutions in studied solvents were also registered.

Solvent	Electrode	$-E_{1/2}$ , V (s.c.e.)	$k_0$ , cm/s
Pyri- dine	Cd	0,77	$3,4 \cdot 10^{-8}$
	Zn	1,11	-
	Sn I	0,84	$1,2 \cdot 10^{-11}$
	II	1,34	-
	III	1,56	-
	Cu	0,54	-
	Cu-Hg Ni	0,72 0,67	$2,4 \cdot 10^{-7}$ $1,1 \cdot 10^{-6}$
Form- amide	Cd	1,05	$3,3 \cdot 10^{-9}$
	Zn	1,12	-
	Sn	-	-
	Cu	-	-
	Cu-Hg	-	-
	Ni	-	-

One can see from the table that the electrochemical activity of nitrogen (5+) in pyridine and formamide is different. The waves of nitrogen(5+) reduction in the 0,1M  $\text{LiClO}_4$  pyridine solutions are observed at all used electrodes (in the case of Cd and Cu-

Hg electrodes the clear peaks at the chronovoltammograms are also observed). In the 0,1M  $\text{LiClO}_4$  formamide solutions the well-derived wave is observed in the case of Cd only; the ill-derived wave takes place in the case of Zn. Potentiostatic macroelectrolysis of the  $\text{HNO}_3$  solutions in the studied solvents showed that the main product of reduction

is  $\text{HNO}_2$ .

IR spectroscopic measurements have shown that in the  $\text{HNO}_3$  pyridine solutions in the frequency region 2900 - 3100  $\text{cm}^{-1}$  (where the absorption band of pyridine is observed) two new bands corresponding to the N-H bond vibrations arise (at 2970 and 3040  $\text{cm}^{-1}$ ). This fact testifies to the existence of pyridinium cation  $\text{C}_5\text{H}_5\text{NH}^+$  in solution. The band at 1350  $\text{cm}^{-1}$  corresponds to a  $\nu_3$  vibration of  $\text{NO}_3^-$  ion with  $D_{3h}$  symmetry. IR spectrum of high-structured formamide contains a number of the broad absorption bands hindering the observation of the nitrogen (5+) bands. Therefore only the weak band at 820  $\text{cm}^{-1}$  corresponding to a  $\nu_2$  vibration of  $\text{NO}_3^-$  ion with  $D_{3h}$  symmetry has been registered. Hence the main state of nitrogen (5+) in the studied high-basic media is  $\text{NO}_3^-$  ion.

The existence of nitrogen (5+) in the high-basic solvents in anionic form causes the appreciable influence of medium on the kinetics of its electroreduction. This fact is confirmed by the table data testifying to a high electrochemical activity of  $\text{NO}_3^-$  ion in pyridine and a low activity (absence of the waves at a majority of the electrodes) in formamide. In the latter (which is a protonic solvent) the anions are appreciably solvated. It is clear that reduction of a strongly solvated  $\text{NO}_3^-$  ion is connected with the difficulties; besides, in formamide (owing to its very high dielectric constant) it is hard to form the electrochemically active associates of  $\text{NO}_3^-$  ion with the lyonium cations - proton donors. High electrochemical activity of  $\text{NO}_3^-$  ion in aprotic pyridine is caused by two main reasons: weak solvation of the anion and low dielectric constant (which causes the existence of  $\text{NO}_3^-$  ions in the  $\text{HNO}_3$  pyridine solutions in the form of electrochemically active ionic pairs with the pyridinium cations - proton donors).

One can also see from the table that the kinetic parameters of the process of  $\text{NO}_3^-$  ions electroreduction are noticeably dependent on electrode nature. One of the reasons of this dependence is, in our opinion, a necessity of a structural correspondence between the elements of the crystalline structure of the electrode surface and the above-mentioned electrochemically active associates.

TO THE ISING MODEL APPLICATION FOR ADSORPTION DESCRIPTION  
OF TWO-DIMENSIONAL CONDENSED LAYERS OF ORGANIC SUBSTANCES  
ON ELECTRODE/SOLUTION INTERFACE

S.Laushera, E.V.Stenina

Moscow State University, Moscow

The Frumkin-Damaskin theory of organic compound adsorption is the most ordinary base for explaining of experimental data, concerning adsorption of surface-active organic substances (SAS) on electrodes. This theory is based on middle field approximation that corresponds to taking into consideration the long-range order of molecules in adsorption layer only. At the last time it has been pointed out that from physical point of view for adsorption description of two-dimensional condensed layers of SAS it is necessary to use lattice gas model (Ising model). This model is based on the statistics of the nearest neighbours in the lattice, this means that the interactions of the adsorbed particle are taken into account only with those particles, which are firmly fixed in the nearest to it sites in the lattice of definite configuration.

The problem of choice of adequate model for description of SAS adsorption can be solved on the base of SAS adsorption data in wide temperature range. Recently it was established, that Ising model is applicable for substances with flat molecular structure or to organic ions. Therefore it is interesting to verify different ways of adsorption description for condensed layers of SAS, formed by spatial molecules, particularly with diamondlike framework structure. Such layers are characterized by highest values of attraction constants in Frumkin isotherm (4,5-6). It can be assumed that Ising model considering the short-range order of molecules is most applicable to these two-dimensional systems.

Adsorption of 1-oxyadamantan (1-AdOH), 3-oxyhomoadamantan (3-OGAd) and borneol was investigated in wide tempera-

ture range by way of capacity (C), potential (E) curves on dropping mercury electrode. C,E-curves were measured in 1 M  $\text{Na}_2\text{SO}_4$  and in some experiments in 3.9 M NaCl with addition of 1-AdOH, 3-OGAd and borneol in temperature ranges 6-100.6°, 7,5-85.4°, 19-104,6°C at final times of drop life (8-9 s). The effect of narrowing of adsorption region with temperature increase is observed for all investigated substances. In all studied temperature intervals the form of C,E-curves does not change essentially, it shows absence of new structure of condensed layers at low temperatures. The general peculiarity is also the rise of  $C_c$  values at potential of the cathodic pit edge ( $E_c$ ), corresponding to phase transition of the first kind.

At  $T > 100.5^\circ\text{C}$  for 1-AdOH and  $T > 85.4^\circ\text{C}$  for borneol, condensed layer is destroyed, it is proved by disappearance of jumps on C,E-curves and capacity increasing in the region of maximal adsorption. For 1-OGAd at the highest possible temperature (104.6°C in 3.9 M NaCl) this effect has not been observed. The effect of existence of condensed layers of investigated compounds molecules at such high temperatures is found in the present work for the first time. It is explained by essentially more strong intermolecular interaction in these layers in comparison with other types of firm adsorbed layers.

The values of surface coverage ( $\theta$ ), received from capacity data, were used for calculating attraction constant ( $a$ ) for Frumkin model, quasichemical approximation and Ising model for different lattices: triangular, square and hexagonal. Received  $a, 1/T$ -dependencies are approximately linear, as it follows from theory. However, for Frumkin model and quasichemical approximation there is noticeable change of plots slope at high temperatures. The results of linear regression analysis show, that  $a, 1/T$ -plots are described by linear relations better in the case of Ising model for all investigated compounds. The best conformity to linear law is when relations for hexagonal lattice are used. The values of critical temperature for destruction of condensed layers ( $T_c$ ) were found by extrapolation of  $a, 1/T$ -plots. These va-

lues of  $T_c$  are essentially higher for Frumkin model and quasi-chemical approximation in comparison with experimental and those derived from Ising model values. For borneol and 1-AdOH the values of  $T_c$  are practically identical for different lattices and coincide with experimental values (101 and 85,4°C for 1-AdOH and borneol). For 1-OGAd with  $\text{Na}_2\text{SO}_4$  as indifferent electrolyte, the values of  $T_c$  for different lattices coincide practically also (116.7-117.4°C). When 1 M  $\text{Na}_2\text{SO}_4$  is substituted for 3.9 M NaCl, Ising model shows for different lattices noticeable distinction of  $T_c$  values, which is larger than possible errors (121.7, 123, 125.2°C for triangular, square and hexagonal lattices). There is the increase of a values when 1 M  $\text{Na}_2\text{SO}_4$  is substituted for 3.9 M NaCl. These effects show important role of indifferent electrolyte in forming of two-dimensional condensed layers of SAS.

Evaluated values and relations for different models and lattices were used for calculating  $\Theta_c, T$ -dependencies at large temperature interval up to  $T_c$ . These dependencies were compared with experimental ones. The curves, considering Ising model, differ essentially from the ones, calculated according to Frumkin model and quasichemical approximation. In the case of 1-OGAd accessible for measuring values of temperatures were far enough from  $T_c$ . Therefore experimental data for 1-OGAd are in the region of high values of  $\Theta$ , where results of experiments and calculations coincide practically. For borneol and 1-AdOH experimental  $\Theta_c, T$ -dependencies coincide with results calculated by the Ising model.

EQUILIBRIUM DOUBLE LAYER STRUCTURE AND ELECTRODE KINETICS AT ELECTRON-CONDUCTING POLYMERS.

M.D.Levi

A.N. Frumkin Institute of Electrochemistry of the Academy of Sciences of the USSR, Moscow.

Thermodynamic analysis of electron-ionic equilibriums at the (metal) / (electron-conducting polymer film) / (background electrolyte solution) interfaces shows [1,2] the charge carrier concentration (of polaron type) inside the polymer to be dependent on the Galvani potential across the metal/polymer interface by the equation:

$$\ln[PT^+] = \text{const} + F_m \phi_p / RT \quad (1)$$

On the other hand, assuming a Donnan-type equilibrium (i.e. selectively permeable properties) for anions  $A^-$  at the polymer/solution interface the bulk concentration of these species was found to be

$$\ln[A_p^-] = \text{const}' + F_p \phi_s / RT, \quad (2)$$

where  ${}_p\phi_s$  is Galvanic potential across polymer/solution interface.

Potential drop across a whole cell at equilibrium,  $E$ , is the sum of three interfacial differences:

$$E = {}_m\phi_p + {}_p\phi_s + {}_s\phi_m \quad (3)$$

with  ${}_s\phi_m$  depending on the reference electrode (we consider a reference electrode to be in equilibrium with the cations of electrolyte in the solution).

Due to the local electroneutrality in the polymer bulk the concentration of polarons is counterbalanced by the concentration of anions:

$$[PT^+] = [A_p^-] \quad (4)$$

Now substituting Equation (3) into (1) and (2) with taking into account Equation (4), one obtains

$$[PT^+] = [A_p^-] = K([M_s^+] [A_s^-])^{1/2} \exp(FE/2RT), \quad (5)$$

where K is a combination of standard potentials of the corresponding species,  $[M_s^+]$  is a concentration of cations in the solution.

It is to be noted, that Equation (5) is true for relatively low values of doping ( $\theta \ll 1$ ). Double-value slope for the dependence of the electrode potential E on the logarithmic concentration of polarons  $\lg[PT^+]$  as compared to typical Nernstian behaviour results immediately from this equation.

Analysis of a set of different equilibria during doping of the polymer could in principle be generalized for both intermediate and limiting doping values. In the last case one obtains two alternative potential distributions across Galvanic circuit depending on the particular entropy contribution to a free energy expression for doping reaction. The first one corresponds to potential drop across the polymer/solution interface (quasimetal behaviour of conducting polymers, e.g. polypyrrole, polythiophene, etc) whereas the second one leads to variation of potential across the metal/polymer interface only (conventional redox polymers, e.g. polyvinylferrocene).

Reactions of different solute redox couples at polythiophene will be discussed in details, thus supporting the phenomenological model for the mechanism and kinetics of electrochemical reactions at electrodes, covered with conducting polymers films [3-5].

#### References

1. V.E. Kazarinov, M.D. Levi, A.M. Skundin, M.A. Vorotyntsev, *J. Electroanal. Chem.*, 271 (1989)293.
2. M.D. Levi, *Nat. Sci. Forum*, 42 (1989)101.
3. M.D. Levi, A.M. Skundin, *Elektrokhimiya*, 25 (1989)67.
4. M.D. Levi, A.M. Skundin, V.E. Kazarinov, *ibid.* 25 (1989)471.
5. M.D. Levi, A.M. Skundin, *ibid.*, 25 (1989)620.

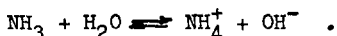


THE EFFECT OF TEMPERATURE ON THE OUTPUT SIGNAL  
OF AMMONIA GAS SENSOR

V. Loodmaa, M. Arulepp, A. Tüür

Tartu University, Tartu

Gas-sensing electrodes consist of an ion-selective electrode in contact with a thin layer of aqueous electrolyte that is confined to the electrode surface by an outer membrane. The latter is chosen to be permeable to the gas. In the case of ammonia microporous membranes are used. Dissolution of the  $\text{NH}_3$  in the thin layer of electrolyte causes a change in pH due to a shift in the equilibrium position of the chemical reaction



The change in the pH sensed by the underlying pH glass-electrode is proportional to  $p_{\text{NH}_3}$  of the sample.

Potentiometric gas sensors are widely used today for water analysis and bioanalysis /1/. As the  $\text{NH}_3$  content of water is of essential significance for fishs, the ammonia sensors are very important in water analysis in fish-breeding /2/. Ammonia gas sensors can be used for continuous monitoring of ambient ammonia in fish-ponds. The main technical problem when using ammonia sensors is a great and sometimes nonlinear dependence of the output signal of the sensor on temperature. Our other investigations of the problem have been published earlier /3/.

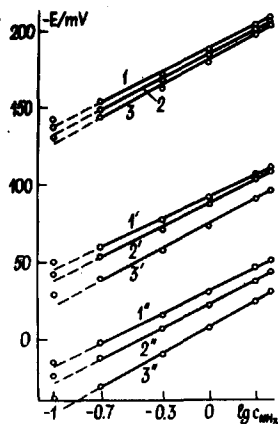
The investigated ammonia sensors have been made in Tartu University. The buffer solutions pH inside glass-electrodes of sensors was equal to 4.01; 5.70 or 6.86. The inner solution of the sensors consists of 0.01 M  $\text{NH}_4\text{Cl}$ +0.1 M KCl. The reference electrode and the one inside glass were silver-silverchloride electrodes. The probe was separated from the sample with the microporous membrane. All investigations have been done at constant temperatures at 15, 25 and 35°C. Before the measurements 1 M NaOH solution was added to the samples to make pH 11.6 and transform all  $\text{NH}_4^+$

into the  $\text{NH}_3$  form.

The main results of measurements are shown in Figure 1. From the results, it is clear that the dependence of the output signal of ammonia sensor on temperature is quite similar in all three cases, although the signals' value itself increases by 55 mV/pH with pH growing inside the glass-electrode. Our calculations show that in the most common case, when the solution under investigation contains 0.2 mg/l  $\text{NH}_3$ , the pH value of the inner solution of the sensor will be 6.42.

Fig.1.

Effect of pH of solutions in glass-electrodes on  $\text{NH}_3$  sensors' calibration curves. pH inside glass-electrodes: 1,2,3 - 4.01; 1',2',3' - 5.70; 1'',2'',3'' - 6.86. Temperature: 1,1',1'' - 15°C; 2,2',2'' - 25°C; 3,3',3'' - 35°C.



It was found [4] that glass-electrode potential slightly depends on temperature, where in the so called isopotential point pH values inside and outside glass-electrode were close. Our results show that the temperature dependence of the sensors' output signals differs from the dependence of glass-electrode's potential. The slopes of curves in Fig.1 are about 50-55 mV and they increase by about 5 mV with rising temperature to 20°C.

#### References

1. C.E.Lunte, W.R.Heinemann, *Electrochemistry II*, 143(1988) 3.
2. *Environmental Health Criteria*, Vol.54, Ammonia, 1986, 210 p.
3. M.Arullepp, A.Tüür, V.Loodmaa, *Trans.Tartu Univ.*, 905(1990) 127.
4. R.G.Megeryan, *Electrochemical Sensors and Environment Protection*, Abstracts, Tartu, 1989, p. 93.

## ADSORPTION OF SURFACTANTS AND METAL ELECTRODEPOSITION KINETICS

Yu.M.Loshkaryov

Dniepropetrovsk State University, Dnieppetrovsk

The effect produced by the adsorption of surfactants on various stages of metal electrodeposition is discussed.

a. The discharge and penetration stages. The effect of a sharp inhibition of cathodic metal electrodeposition at high surface coverage by the adsorbate, the effect being found in 1939 became the basis for the subsequent theoretical and applied investigations. Later on, it has been shown that a low adsorption limiting current ( $i_{1,ads}$ ) arisen by the surfactant adsorption was stipulated by the slowness of the stage of the reacting ion penetrations through the surfactant adsorption layers (M.A.Loshkaryov). Appearing of  $i_{1,ads}$  results from the model according to which at the surfactant presence the electrode reactions always involves the penetration stage of the reacting particles into the surface layer (B.N.Afanas'ev). The effects produced by pH, temperature, the nature and concentration of the anions in the supporting solution, the adsorbed particle orientations on the effectiveness of the surfactant inhibiting action has been studied on the basis of the concepts on the roles of the discharge and penetration stages (Yu.M.Loshkaryov, F.I.Danilov).

b. Chemical stages. The approach accounting chemical interaction between the metal ions and the additives which is used for the discussion of the inhibiting and accelerating actions of the surfactants is presented (Yu.M.Loshkaryov, V.F.Vargalyuk).

The adsorption of the metal ion-surfactant complexes on the hard electrodes and their concentrations ( $\Gamma$ ) are determined by the double layer differential capacity measuring methods, by the chronocoulometry and the cathodic and anodic chronopotentiometries. The values of  $\Gamma$  obtained coincide with  $\Gamma$  that observed at the monolayer adsorpti-

on. The advantages of the anodic chronopotentiometry used for study the adsorption of electroactive complexes of metal ions with surfactants are discussed.

The chemical reaction precedes the electron transfer stage provided that the interaction between the reacting ions and surfactants results in the formation of the electroactive complexes. It has been found by the chronopotentiometry that these reactions occur not in the bulk layer but directly on the electrode surface involving the surfactants observed. Depending on the nature of the surfactants, the presence of the bridge atoms or groups in them and their orientations on the surface, the formation of the complexes adsorbed may lead both to discharge acceleration and to its inhibition and in both cases mentioned the mechanism of the process involving the surface chemical reaction of the metal ions and the surfactants adsorbed preceding the discharge process is realized.

The rate constants of the formation of the corresponding monoligand complexes are determined. The electroinactive complexes of the metal ions and the surfactants produce the same effect on metal electrodeposition as the electrochemically inert surfactants do.

c. The crystallization stages. The effects of the surfactants on the nucleation at a foreign surface and on the following growth of the metal polyatomic layers have been analysed (V.V.Trofimenko, Yu.M.Loshkaryov, T.I.Lezhava, et al.) The two basic mechanisms of the surfactant effect on the nucleation have been found:

1) the surfactant adsorbed at the metal nuclei inhibits their growth and decreases the rate of the development of the nucleation exclusion zones forming around the crystals growing;

2) the surfactant adsorbed at the active centres of a foreign surface excludes the latter from the nucleation.

The inhibition of the copper nucleation at a foreign electrode manifests in a considerable increase in the crystallization overpotentials ( $\eta_k$ ) and in changing of the nucleation work ( $A$ ); there is no correlation between  $\eta_k$  and  $A$ . The comparison of  $A$  values obtained at the presence as well as at the absence of the surfactant permits to evalua-

ie qualitatively the effects of the additives adsorbed at the electrode-solution, nucleus-solution and electrode-nucleus interfaces on the value of the nucleation work.

While studying multilayer electrodeposition the most productive approach is a combined one involving the comparison of the polarization characteristics, the fine structure and the physico-mechanical properties of the coatings. The influence of the additives mostly on the crystallization without a considerable inhibition of other stages of the electrode process is discussed. In such systems a slight increase of the polarization results in a radical change of the morphology and the structure of the platings. The interrelation between the surfactant effect on the crystallization stage and the effects of the chemical interactions of the reacting ions and the additives has been shown.

There are discussed the following unsolved questions being the matter of interest for further investigations: the determination of the relation between the nature of the surfactants, their effects on the kinetics of separate stages of the electrode process, and finally, on the structures and properties of the platings; the elucidation of the penetration mechanism of the metal ions through the surfactant effect on the electrode process kinetics and mechanism in the range of the negative potentials (the incorporation of the alkali metals and hydrogen evolution, the discharge of the electronegative metal ions resulting in alloy plating).

The questions being the matter of interest for the metal electrodeposition have been discussed. They are following: the role played by various components of the total overpotential; the possibility of the additive selection based on E.A.Nechaev's concept on the selective adsorption of surfactants on metals and oxides; the functional application of the components of the surfactant mixtures.

ELECTRICAL DOUBLE LAYER ON THE SINGLE CRYSTAL ANTIMONY  
ELECTRODES IN THE ETHANOLIC SURFACE INACTIVE  
ELECTROLYTE SOLUTIONS

E.Lust, K.Anni

Tartu University, Tartu

The electrical double layer (edl) and adsorption properties of electrodes do not significantly depend only on the chemical composition and crystallographic structure of the surface, but also on the geometric dimensions and composition of solvent molecules /1,2/. But the influence of the crystallographic orientation of single crystal planes on the edl characteristics have been studied mainly in the aqueous solutions and in the electrochemical literature there are only few works /3,4/, devoted to the study of the edl structure the single crystal planes in nonaqueous solutions.

This paper concentrates on a comprehensive study of the influence of the surface structure of Sb and Bi single crystal planes on the edl parameters in the ethanolic surface inactive electrolyte solutions.

Preparation and surface treatment of the Sb and Bi single crystal electrodes have already been described, as well as the impedance measurement technique and preparation of the solutions /3-6/.

The edl differential admittance was measured in the range of 110 to 5100 Hz. As for the single crystal planes of Bi in aqueous and ethanolic solutions /3-5/, and for the single crystal planes of Sb in aqueous solutions /6/, the differential capacity  $C$  dispersion for the contact Sb/EtOH over the whole potential  $E$  range is 8-12 % with a.c. frequency  $\nu$  varying from 710 to 5100 Hz. At  $\nu \leq 510$  Hz, in the region of  $-0.75 < E < -0.55$  V, the maximum of pseudocapacity on the  $C(E)$  curves has been observed. The height of this maximum decreases as the frequency increases and at  $\nu \gg 1100$  Hz, this maximum has not been observed.

The  $C(E)$  curves for the Sb(001) in the ethanolic solu-

tion of  $\text{LiClO}_4$  at  $\nu = 2100$  Hz are represented in Fig.1. As can be seen, the potential of the capacity minimum  $E_{mc}$  is independent of the  $c_{\text{ClO}_4^-}$  with a relative accuracy of  $\pm 10\text{mV}$ , when the  $c_{\text{ClO}_4^-}$  changes  $^4$  from  $5 \cdot 10^{-4}$  to  $5 \cdot 10^{-3}$  M.As for the

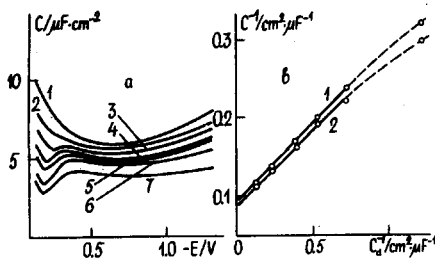


Fig.1.  $C(E)$  curves (a) for the plane (001) of Sb at  $\nu = 2100$  Hz in the ethanolic solutions of  $\text{LiClO}_4$ , M: 1 - 0.1; 2 - 0.03; 3 - 0.01; 4 - 0.005; 5 - 0.003; 6 - 0.001; 7 - 0.0007. The Parsons-Zobel plots (b) at  $\sigma = 0$  for the planes (111) - 1 and (001) - 2.

single crystal planes of Bi in EtOH [3/], it may be assumed that a very slight specific adsorption of  $\text{ClO}_4^-$  anions occurs at the  $E_{mc}$  and for the most dilute  $\text{LiClO}_4$  solution the value of  $E_{mc}$  may be identified with  $E_{\sigma=0}$  for the single crystal planes of Sb in the EtOH (Table 1).

Table 1

Electrical double layer parameters for the single crystal planes of Sb and Bi in EtOH

Electrode	$E_{\sigma=0} \pm 0.01$ , V	$f_{P-Z}$	$C_{\sigma=0}^i$ , $\mu\text{F} \cdot \text{cm}^{-2}$	$C_{\sigma \ll 0}^i$ , $\mu\text{F} \cdot \text{cm}^{-2}$	$C_{\sigma=0}^i / C_{\sigma \ll 0}^i$
Sb(111)	-0.26	1.01	11.5	6.5	1.78
Sb(001)	-0.19	1.04	13.0	7.2	1.80
Bi(111) /3/	-0.45	1.03	15.1	6.9	2.18
Bi(001)	-0.42	1.08	16.4	7.6	2.15

As for the aqueous solutions /5,6/, the dispersion of zero charge potentials  $\Delta E_{\sigma=0}$  for the planes (001) and (111) of Sb in EtOH is higher than  $\Delta E_{\sigma=0}$  for the planes (111) and (001) of Bi (Table 1). The  $\Delta E_{\sigma=0}$  for the planes (001) and (111) of Sb and Bi in ethanol is somewhat lower than in the aqueous surface inactive electrolyte solutions /5,6/.

The Parsons-Zobel plots for the Sb(001) and Sb(111) in EtOH solutions can be considered linear, when the  $c_{LiClO_4}$  decreases from 0.1 to  $3 \cdot 10^{-3}$  M (Fig. 1b). The inverse slope of the Parsons-Zobel plots  $f_{P-Z}$  is equal to 1.01 and 1.04 for the planes (111) and (001) of Sb. These values are somewhat lower, than for the aqueous /5/ or acetonitrilic (AN) solutions /4/ and can be ascribed to weaker dependence of the values of zero charge potential on the crystallographic structure of planes in EtOH, than in the  $H_2O$  or in the AN solutions.

The inner layer capacity charge density,  $C^i(\sigma)$ , curves were calculated according to the Grahame model and the Vallette-Hamelin method. The monotonic  $C^i(\sigma)$  curve was obtained for the value of the fitting coefficient F, which varied from 1.03 to 1.20 for the Sb(111) and from 1.06 to 1.30 for the Sb(001), when the  $c_{LiClO_4}$  decreases from 0.1 to  $10^{-3}$  M. As for the Bi/ $H_2O$ , Bi/AN, Bi/EtOH and Sb/ $H_2O$  interfaces, the values of the inner layer capacity at  $\sigma=0$  and at  $\sigma \ll 0$  for the Sb(001)/EtOH interface are somewhat higher than for the Sb(111)/EtOH system. It follows from Table 1 and data of works /3-6/ that the relation  $C^i_{\sigma=0}/C^i_{\sigma \ll 0}$  is practically independent of the crystallographic structure of the plane and it increases in the sequence of systems Bi/AN < Bi/ $H_2O$  < Sb/ $H_2O$  < Sb/EtOH < Bi/EtOH. Respectively, according to the criterions of /2/, the specific interaction of the solvent molecule dipole with the electrode surface atoms increases in the same order of systems.

#### References

1. A.Hamelin, T.Vitanov, E.Sevastyanov, A.Popov, J. Electroanal. Chem., 145 (1983) 225.
2. M.D.Levi, A.V.Shlepakov, B.B.Damaskin, I.A.Bagotskaya, J.



- Electroanal.Chem., 138 (1982) 1.
3. K.L.Anni, M.G.Väärtnõu, U.V.Palm, Elektrokhiimiya, 22(1986) 992; 24 (1988) 846.
  4. E.J.Lust, Elektrokhiimiya, 27 (1991) 432.
  5. E.J.Lust, U.V.Palm, Elektrokhiimiya, 21 (1985) 1256; 24 (1988) 557.
  6. E.J.Lust, A.A.-J.Jänes, Elektrokhiimiya, 27 (1991) (in press).

ELECTRICAL DOUBLE LAYER AND ADSORPTION OF CYCLOHEXANOL ON THE (0001) AND (11 $\bar{2}$ 0) FACES OF CADMIUM

E.Lust, J.Ehrlich

Tartu University, Tartu

According to the experimental results /1-5/ the electrochemical properties of zinc and cadmium electrodes do not significantly depend only on the chemical composition but also on the crystallographic structure of the surface. The zinc and cadmium are electron-analogues and they are crystallized in the same hexagonal close-packed system. Differently from the zinc single crystal electrodes /1,2/, in the electrochemical literature there is no quantitative information about the structure of the electrical double layer (edl) and adsorption of ions and organic compounds on the cadmium single crystal faces, except the preliminary data of /5/.

The present paper is devoted to a comprehensive study of the edl structure and adsorption properties of the cadmium and zinc single crystal planes in aqueous solutions.

The electrodes are discs of 3-4 mm in diameter and 5 mm in thickness that have been prepared by cutting from the monocrystalline Cd by using the anodic dissolution method in aqueous H<sub>3</sub>PO<sub>4</sub> solutions. The crystallographic orientation is determined by X-ray using a special goniometric head. The pre-

cision on the orientation is  $\pm 0.2^\circ$ . The isolation of the faces has been carried out by a thin polystyrene film (dissolved in toluene) covering the part of no interest, and then the sample was placed into a Teflon holder. The surface has polished to a mirror finish by using standard metallographic procedures. The final surface preparation was obtained by alternative electrochemical polishing in the aqueous  $H_3PO_4$  solutions and cathodic polarization in the working solutions /3/. The basal face (0001) was prepared by cleaving of a single crystal at the temperature of liquid nitrogen. The capacity measurement technique and preparation of the solutions have already been described in /1,5/.

The edl differential admittance was measured from 110 to 11000 Hz. As for the polycrystalline cadmium (PC Cd) /3/, a slight variation ( $< 9\%$ ) as a function of the frequency, in the 0.1 M NaF solution, allows the measured admittance to be identified with the differential capacity C. The potential range extended from -0.9 to -1.7 V vs. SCE. The influence of the diffuse layer to the total capacity of edl is visible for concentration  $c_{NaF} \leq 0.1$  M. The potential of the capacity minimum  $E_{mc}$  is independent of the  $c_{F^-}$  with a relative accuracy of  $\pm 5$  mV, when the  $c_{F^-}$  changes from  $10^{-3}$  to  $10^{-2}$  M. As for the PC Cd /3/, it may be assumed that no significant specific adsorption of  $F^-$  occurs at the  $E_{mc}$  and the value of  $E_{mc}$  may be identified with  $E_{\sigma=0}$  for the single crystal planes of Cd (Table 1). It follows from Table 1, that the dispersion of the  $\Delta E_{\sigma=0}$  for the (0001) and (11 $\bar{2}$ 0) faces of Cd is somewhat lower than for the (0001) and (11 $\bar{2}$ 0) planes of zinc ( $\Delta E_{\sigma=0}$  90 mV) /1,2/. The value of  $E_{\sigma=0}$  for the Cd (11 $\bar{2}$ 0) plane is in good agreement with that given in ref./5/: -0.99 V. The inverse slope of the Parsons-Zobel plots  $f_{p-z}$  is equal to 1.18 for the (0001) and 1.27 for the (11 $\bar{2}$ 0) plane of Cd. The higher values of  $f_{p-z}$  in ref. /5/ can mainly be explained by the geometric roughness and the energetic inhomogeneity of the mechanically cutted Cd (11 $\bar{2}$ 0) electrodes.

The inner layer capacity  $C^1(\sigma)$  curves were calculated according to the Grahame model and the Valette-Hamelin method /6/. The monotonic  $C^1(\sigma)$  curve is obtained for the value of

the fitting coefficient  $F$  which varied from 1.05 to 1.25 for the (0001) plane and from 1.10 to 1.35 for the (11 $\bar{2}$ 0) plane when the  $c_{\text{NaF}}$  decreased from 0.1 to 0.001 M.

Table 1

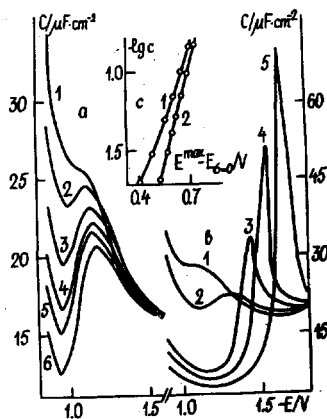
The edl and adsorption parameters of cyclohexanol on the single crystal planes of cadmium

Electrode	$E_{\sigma=0}$ $\pm 0.01$ V	$f_{P-Z}$	$C_{\sigma=0}^i$ F cm $^{-2}$	$C_{\sigma \ll 0}^i$ F cm $^{-2}$	$a_0$	$B_{0,2}$ $\frac{\text{dm}^3}{\text{mol}}$	$D \times 10^{-15}$ , atom.cm $^{-2}$
Cd(0001)	-0.93	1.16	39.3	17.1	1.57	14.2	1.31
Cd(11 $\bar{2}$ 0)	-1.01	1.27	34.6	16.5	1.37	21.3	0.69
PC Cd /3,5,6/	-0.97	1.30	30-35	17-18	1.28	14.0	-

The main adsorption parameters of cyclohexanol (CH), calculated by the Frumkin-Damaskin theory, are given in Table 1, where the symbols have their usual meanings. The  $C(E)$  and  $E^{\text{max}} - E_{\sigma=0}$  (lgc) curves given in Fig.1b and 1c, as data in Table 1, show a significant difference in the adsorption

Fig.1.

$C(E)$  curves (a) for Cd(0001) in aqueous solutions of NaF, M: 1 - 0.1; 2 - 0.05; 3 - 0.02; 4 - 0.01; 5 - 0.007; 6 - 0.0045.  $C(E)$  curves (b) for Cd(0001) in 0.1 M NaF solution (1) and with additions of CH in concentrations, M: 2 - 0.01; 3 - 0.05; 4 - 0.1; 5 - 0.2. Dependence of the relative potential  $E^{\text{max}} - E_{\sigma=0}$  of the adsorption-desorption maximum on the lgc of CH (c) for the (11 $\bar{2}$ 0) - 1 and (0001) - 2 planes of Cd.



properties of single crystal and PC Cd electrodes /4/. As for the zinc electrodes /2/, the height of the adsorption-desorption maximum at  $c_{\text{CH}} = \text{const}$ , increases in the sequence of PC Cd < Cd(11 $\bar{2}$ 0) < Cd(0001), which means, that the attractive interaction between the adsorbed CH molecules increases in the sequence from PC Cd to Cd(0001). As shown in Table 1, the adsorption activity of CH increases in the sequence of PC Cd < Cd(0001) < Cd(11 $\bar{2}$ 0). Consequently, as for the zinc electrodes /1,2/, the adsorption activity of CH increases as the superficial atomic density D of Cd single crystal planes decreases. But the adsorption activity of CH is somewhat higher on the Cd/solution interface than on the Zn/solution interface, which can be explained by increasing the hydrophylity of electrodes in the sequence: Cd(11 $\bar{2}$ 0) < PC Cd < Cd(0001) < Zn(11 $\bar{2}$ 0) < PC-Zn < Zn(0001).

#### References

1. A.Hamelin, T.Vitanov, N.Sevastyanov, A.Popov, J. Electroanalyt. Chem., 145 (1983) 225.
2. V.V.Batrakov, B.B.Damaskin, J. Electroanalyt. Chem., 65 (1975) 361.
3. D.I.Leikis, K.V.Rybalka, E.S.Sevastyanov, Adsorption and Electric Double Layer in Electrochemistry, ed. by A.N.Frumkin and B.B.Damaskin, Nauka, Moscow, 1972, p.5.
4. L.Eu.Rybalka, B.B.Damaskin, Elektrokimiya, 9 (1973) 1562.
5. A.P.Korotkov, E.B.Beslepkina, B.B.Damaskin, Eu.F.Golov. Elektrokimiya, 21 (1985) 1298.
6. M.A.Vorotyntsev, Mod. Aspects of Electrochem. No 17. New-York-London, 1986, p.131.

ADSORPTION OF  $\text{Cl}^-$ ,  $\text{Br}^-$ ,  $\text{I}^-$  and  $\text{SCN}^-$  ANIONS  
ON SINGLE CRYSTAL PLANES OF BISMUTH ELECTRODES

K.Lust, M.Salve, E.Lust  
Tartu University, Tartu

The adsorption of halides and  $\text{SCN}^-$  on the single crystals of various metals has so far been the object of a few quantitative studies /1-3/. In this work the specific adsorption of  $\text{Cl}^-$ ,  $\text{Br}^-$ ,  $\text{I}^-$  and  $\text{SCN}^-$  has been studied on (111), (001), (011), (101) and (211) faces of bismuth. Bismuth as the electrode material is characterized by the existence of two types of bonds (covalent and metallic) between the atoms in the lattice, by the low dispersion of the zero charge potentials  $E_{c=0}$  of various planes, but by the strong dependence of the adsorption parameters for organic compounds on the crystallographic structure of the planes /4/.

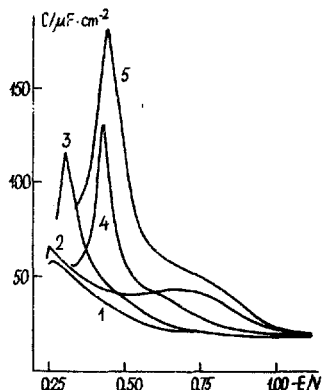
The investigations of the specific adsorption of anions on the single crystal planes of bismuth were carried out in mixed aqueous solutions  $xM \text{KA}^{\bar{x}} + (0.1-x)M \text{KF}$  with constant ionic strength by measuring the dependence of the differential capacity  $C$  of the electrical double layer on the electrode potential  $E$ . According to our previous data  $\text{F}^-$  ions are surface-inactive on bismuth and therefore they were chosen as reference anions. The reference electrode was an aqueous saturated calomel electrode. Fabrication of the single crystals of bismuth and surface treatment of the electrode have been described, as well as the capacitance measurement techniques and preparation of the solutions /1,3,4/.

In the presence of specifically adsorbed anions in solutions a sharp maximum on the  $C, E$ -curves is observed at the potentials  $E \gg -0.55 \text{ V}$  for  $\text{I}^-$ , at  $E \gg -0.5 \text{ V}$  for  $\text{Br}^-$ , at  $E \gg -0.45 \text{ V}$  for  $\text{Cl}^-$  and at  $E \gg -0.3$  for  $\text{SCN}^-$  anions, respectively (Fig.1). This maximum moves towards the more negative potentials, with the fraction of the surfaces active electrolyte  $x$  in the mixture decreasing and the height of this maximum ( $x = \text{const}$ ) increases in the sequence of planes (111)  $\leq$

$\leq (2\bar{1}\bar{1}) < (0\bar{1}\bar{1}) < (\bar{1}0\bar{1}) \leq (001)$  and for the anions range  $\text{Cl}^- < \text{SCN}^- < \text{Br}^- < \text{I}^-$ . This capacity maximum is probably caused by the strengthening of the covalent nature of the adsorptive bond between the halide ions and the surface of bismuth, caused by the charge transfer process. At the potential values  $E > -0.5$  V the capacity dispersion with frequency took place and only the equilibrium C,E-curves at  $E \leq -0.5$  V were used for the quantitative treatment.

Fig. 1.

C(E) curves for the single crystal plane (001) of bismuth in 0.1 M aqueous solutions of various electrolytes: 1 - KF; 2 - KCl; 3 - KBr; 4 - KSCN and 5 - KI.



The charge of specifically adsorbed anions and the other adsorption parameters calculated according to the Hurwitz-Parsons-Dutkiewicz method are reported in Table 1. The symbols in Table 1 have their usual meaning.

On the basis of  $\sigma_1, \sigma'$ -plots the specific adsorption of anions would seem to increase as the superficial atom density increases in the sequence  $(\bar{1}0\bar{1}) < (001) < (111) < (2\bar{1}\bar{1}) < (0\bar{1}\bar{1})$ . For every face the specific adsorption of anions increases from  $\text{F}^-$  to  $\text{I}^-$  as the hydration energy of anions decreases in the sequence  $\text{F}^- > \text{Cl}^- > \text{Br}^- > \text{SCN}^- > \text{I}^-$ . It is very interesting to note that the differences in the surface activities for various single crystal planes of bismuth increase with the growth of the adsorption activity of anions. But it must be mentioned that the adsorption of halides on the single crystal planes of silver is as strong as the adsorption of  $\text{Cl}^-$ ,  $\text{Br}^-$  and  $\text{I}^-$  anions on the single crystal planes of bismuth. According to our previous data /4/ the adsorption of water would be higher for silver and the difference in beha-

viour between these two metals may be considered for a confirmation that the determinative factor of the specific adsorption of anions on Ag is the halide-metal interaction /2/.

Table 1

Adsorption parameters of anions for the bismuth single crystal planes in the aqueous solutions ( $\sigma = 3\mu\text{C}\cdot\text{cm}^{-2}$ )

Anion	Plane	$\ln\beta_{\sigma=0}$	B, nm $\cdot$ ion $^{-1}$	$K_{02}$ , $\mu\text{F}\cdot\text{cm}^{-2}$	$K_{12}$ , $\mu\text{F}\cdot\text{cm}^{-2}$	$\frac{x_2-x_1}{x_2}$
Cl $^{-}$	(111)	3.4	4.5	28.3	115	0.25
	( $\bar{1}0\bar{1}$ )	2.7	0.5	31.6	158	0.20
	(001)	2.8	1.8	32.0	150	0.21
	(01 $\bar{1}$ )	2.9	2.6	30.3	86	0.34
	(2 $\bar{1}\bar{1}$ )	3.4	3.2	29.4	93	0.32
Br $^{-}$	(111)	4.8	1.6	27.5	102	0.27
	( $\bar{1}0\bar{1}$ )	4.7	1.1	28.0	104	0.28
	(001)	5.0	2.4	29.0	94	0.31
	(01 $\bar{1}$ )	6.0	2.6	29.0	81	0.36
	(2 $\bar{1}\bar{1}$ )	5.3	1.1	28.9	81	0.36
I $^{-}$	(111)	7.6	0.7	28.3	96	0.29
	( $\bar{1}0\bar{1}$ )	7.7	0.4	29.4	99	0.30
	(001)	8.4	1.6	28.6	91	0.32
	(01 $\bar{1}$ )	10.8	4.3	21.9	56	0.39
	(2 $\bar{1}\bar{1}$ )	9.6	2.8	23.4	65	0.36
SCN $^{-}$	(111)	7.4	2.2	25.0	125	0.20
	( $\bar{1}0\bar{1}$ )	7.3	0.8	23.0	120	0.19
	(001)	7.7	0.9	25.2	137	0.18
	(01 $\bar{1}$ )	8.3	0.7	25.1	125	0.20
	(2 $\bar{1}\bar{1}$ )	7.9	0.8	25.0	119	0.21

According to the data of Table 1 the values of the equilibrium adsorption constant  $\ln\beta$  relatively weakly depend on

the crystallographic structure of the plane. Lateral interaction coefficient B in the virial isotherm depends to a great extent on the bismuth single crystal plane index. The inner layer parameters for aqueous solutions are less sensitive to the variations of the crystallographic indexes than for ethanolic solutions /5/ due to the change of the solvent molecule orientation on different single crystal planes and to the fact that water molecules are more symmetrical than the ethanolic ones.

#### References

1. M.P.Pärnoya, U.V.Palm, Elektrokimiya, 16 (1980) 1599.
2. G.Valette, J. Electroanal. Chem., 255 (1988) 215; 255 (1988) 225; 269 (1989) 191.
3. K.K.Lust, E.J.Lust, M.A.Salve, U.V.Palm, Elektrokimiya, 25 (1981) 510; 25 (1989) 1381.
4. E.J.Lust, U.V.Palm, Elektrokimiya, 21 (1985) 1256.
5. K.L.Anni, M.G.Väärtnõu, U.V.Palm, Elektrokimiya, 22 (1986) 1673; 24 (1988) 858.

#### STRUCTURE OF DOUBLE ELECTRIC LAYER AND RADIATION OF RADIO WAVES

T.A.Marsagishvili, G.D.Tatishvili

Institute of Inorganic Chemistry and Electrochemistry,  
Georgia Acad.Sci., Tbilisi

Electrode's electronic structure near the surface is rather significant for the development of a double electric layer in electrochemical systems.

Temporal change in the electromagnetic field formed by electrode brings to the irregular movement of electrolyte ions. And it can result in electromagnetic waves radiation. So, during the process of forming or changing of double elec-



tric layer (DEL), one can observe, in principle, the electromagnetic radiation of different frequency ranges. In present, the radiation of electrowaves' range is experimentally registered /1,2/.

To be sure, let's examine a flat electrode. The Fourier-component of electromagnetic field's vector-potential in point  $\vec{r}$ , formed by  $q$  charged particle and moving at  $\vec{v}(t)$  rate looks like:

$$\vec{A}_\omega(\vec{r}) = \frac{q}{c|\vec{r}-\vec{r}'|} \int_{-\infty}^{\infty} dt \vec{v}(\vec{r};t) e^{i(\omega t - k|\vec{r}-\vec{r}'(t)|)} \quad (1)$$

In the frame of linear response theory:

$$V_\alpha(\vec{r}, t) = - \int d\vec{r}' \int_{-\infty}^{\infty} dt' \varepsilon_{\nu\alpha p\beta}(\vec{r}, \vec{r}'; t-t') E_\beta^{\text{ex}}(\vec{r}', t'), \quad (2)$$

where  $E^{\text{ex}}$  - is a field created by electrode and  $\varepsilon_{\nu\alpha p\beta}(\vec{r}, \vec{r}'; t-t')$  is a temporal delay of green function (GF) operators  $\nu$  and medium polarization  $p$ , that could be bound to the GF operators of electrode polarization:

$$i\omega g_{\nu\alpha p\beta}(\vec{r}, \vec{r}'; \omega) = \varepsilon_{\nu\alpha p\beta}(\vec{r}, \vec{r}'; \omega) \quad (3)$$

The coordinate of particle  $\vec{r}(t)$ 's is determined by integration of correlation (3) in corresponding boundary conditions.

In general, calculation for concrete GF  $g_{pp}$  systems is a complicated problem, though one can use correlational ratio between  $\varepsilon_{\nu\alpha p\beta}(\vec{r}, \vec{r}'; \omega)$  and dielectric permeability  $\varepsilon_{\alpha\beta}(\vec{r}, \vec{r}'; \omega)$  /3/ of system and apply different  $\varepsilon_{\alpha\beta}(\vec{r}, \vec{r}'; \omega)$  models to determine  $g_{pp}$ .

When electrode is wet with the solution of electrolyte or a polar liquid, one can observe the electromagnetic radiation of radiowaves' range.

Indeed, in "gelii" model of metal, supposing that electronic density  $n$  is changing perpendicularly to the electrode surface (axes  $z$ ):

$$n(z) = \frac{\bar{n}}{2} e^{-\beta z} \Theta(z) + n(1 - \frac{1}{2} e^{\beta z}) \Theta(-z). \quad (4)$$

For liquid we use a model, where medium is characterized by one characteristic time of fading  $\tau_D$ .

In this case we can write an equation of the movement for a radiating particle:

$$m \frac{dv}{dt} = q \frac{\partial \mu}{\partial t} - \frac{v}{\tau_D} m, \quad (5)$$

where  $m$  - is a mass of particle,  $\mu$  - a chemical potential of the metal.

Expressions for rate and coordinates look like:

$$v(z, t) = \frac{q}{m} \tau_D \frac{\partial \mu}{\partial z} (1 - e^{-t/\tau_D}) \quad (6)$$

$$z(t) = \frac{q}{m} \tau_D \frac{\partial \mu}{\partial z} (t + \tau_D e^{-t/\tau_D}) + z_0$$

where  $z_0$  - is determined from the boundary conditions (depending on the structure of forming DEL).

#### References

1. N.G.Khatiashvili, M.E.Perel'man. Physics of the Earth and Planetary Interiors, 57 (1989) 169.
2. J.I.Japaridse, M.O.Khokhashvili, ISE 40th Meeting, Kyoto, 1989.
3. R.R.Dogonadze, T.A.Marsagishvili, Surf. Sci., 101 (1980) 439.

# INVESTIGATION OF THE ELECTRIC DOUBLE LAYER AT THE ION-EXCHANGE/ELECTRODE INTERFACE AND INSIDE ION-EXCHANGE MEMBRANE

V.M.Mazin, Ju.M.Volkovich, V.D.Sobolev, N.V.Churaev

A.N.Frumkin Institute of Electrochemistry, USSR Acad.Sci.  
Moscow

Investigation of the electrochemical properties of the ion-exchange membranes (IEM) is acquiring great importance due to the ever increasing use of these membranes in various electrochemical devices (electrolyzers, fuel cells).

The impedance spectra of a mercury-contact cell with IEM at different water content in the frequency range of  $10^{-1}$ - $2 \cdot 10^5$  kHz were obtained with the use of a frequency response analyzer Solartron-1255. The spectra were interpreted on the basis of an equivalent circuit consisting of two parts connected in series. The first part corresponds to IEM proper and consists in the ohmic resistance of IEM  $R_1$  and the geometric capacity of IEM  $C_1$  parallel to it. The second part of the circuit corresponds to the IEM/electrode interface. This circuit is used to describe solid electrolyte/electrode interface /1/. It includes electric double layer (EDL) capacity  $C_2$  and the Warburg constant describing the vibration under the action of the electric field of fixed IEM ions. The porous structure of the IEM was examined by the standard porosimetry method /2/. The electrokinetic potential was determined by the streaming potential method.

From the values of  $R_1$  and  $C_1$  the values of the electrical conductivity ( $\kappa$ ) and effective dielectric constant ( $\epsilon$ ) of IEM were calculated. The dependence of  $\kappa$  on moisture content ( $\theta$ ) can be divided into three sections. In the first section, with decreasing  $\theta$ ,  $\kappa$  gradually decreases due to a greater sinuosity of the current path, formation of dead ends, etc. The membrane thickness in this case does not change, which points to unchanged structure. In the general case when IEM is impregnated with the solution of a certain equilibrium concentration  $C_p$ ,  $\kappa$  is equal to a sum of

parallel conductivities - the effective conductivity  $\alpha_v$  of the solution of concentration  $C_p$  present in the pore bulk (excluding the layer near the surface) and the effective surface conductivity  $\alpha_s$ , i.e. the effective longitudinal conductivity of EDL. If IEM is impregnated with water  $\alpha_v=0$ . Because of this fact, by using a power series of the Archie type to describe the dependence of  $\alpha$  on  $\phi$  it is possible to estimate the value of the specific surface conductivity  $K_s$ , that of the longitudinal conductivity of EDL  $\alpha_{EDL}=K_s/2l_{EDL}$  and also the mean bulk concentration of counterions in EDL  $C_{EDL}=Q/2Sl_{EDL}$ , where  $l_{EDL}$  is the Helmholtz layer thickness taken, to be equal to  $4A$  (see Table 1).

Table I.

IEM	$K_s \cdot 10^3$ om <sup>-1</sup>	Mean pore diameter (nm)	Exchange capacity, (mg-eq/g)	Specific surface, (m <sup>2</sup> /g)	Charge surface density, $\sigma$ (KJ/m <sup>2</sup> )	Thickness (mm)
MK-40	3.2	25	2,65	143	1,79	0,5
MA-4I	8.0	25	2,0	110	1,75	0,5

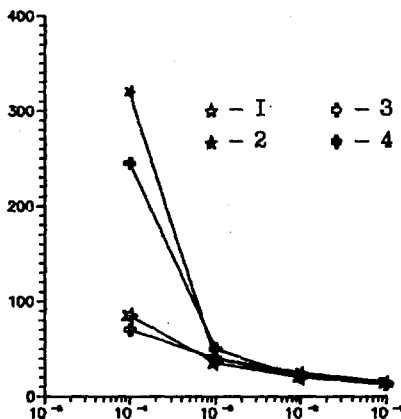
The values of  $\alpha_{EDL}$  are significantly higher than the maximum value of specific electrical conductivity of the solutions of corresponding salts. This can be explained by the absence in IEM of the mutual retardation effects of oppositely charged ions since the conductivity in IEM is practically monopolar due to counterions. The obtained values of  $\epsilon_{IEM}$  at large  $\phi$  are very high, up to  $10^5$ . Possibly, this can be explained by the existence of a peculiar dipole - counterion-fixed ion, whose length, allowing for the hydration shells of both ions, can be quite significant - 10-15 A.

From the values of  $C_2$  the value of the EDL capacity  $C_{EDL}$  at the IEM/mercury electrode interface was calculated.  $C_{EDL}$  proved to be close to that of the EDL capacity at the H<sub>2</sub>SO<sub>4</sub> solution/mercury interface. The correct choice of the equivalent circuit was supported by the results of similar measurements with IEM treated with n-butyl alcohol, in the case of which  $C_{EDL}$  decreased due to alcohol adsorption on mercury.

The streaming potential values obtained were then used to determine the electrokinetic potential of the membrane pore surface.

Fig.1. Results of the calculations of the electrokinetic potential  $\zeta$  of IEM MK-40 (1,2) and MA-41 (3,4) at different concentrations  $C$  of KCl solution.

1 and 3 - calculated as in /3/. 2 and 4 - calculated as in /4/.



The calculations were made according Helmholtz-Smoluchowski equation /3/ and with a correction for the overlapping of EDL in thin pores/4/. Fig 1. shows the results of the calculations of the absolute values of the  $\zeta$ -potential for IEM MK-40 and MA-41. The influence of the overlapping of EDL comes into action at KCl concentrations below  $10^{-2}N$  when  $\alpha r \ll 1$ . Analysis of the obtained data shows that at the KCl concentration of  $10^{-1}$  (if  $\alpha r \approx 10$ ) the water transport in IEM is satisfactorily described by the classical Helmholtz-Smoluchowski's theory. By measuring the outflowing solution concentration, it was possible to study the reverse-osmotic properties of IEM. An appreciable rejection of the KCl solution is observed for MK-40 only at a low concentration (30% - at  $10^{-3}N$  and 80% - at  $10^{-4}N$ ) when EDL are strongly overlapped.

#### References

1. B.M.Grafov, E.A.Ukshe, *Electrokhimiya*, 10(1974)1875.
2. N.P.Kononenko, N.P.Berezina, Yu.M.Vol'fkovich, *Zhurn. prikl.khimii*, 58(1985)1620.
3. S.S.Dukhin, *Electrical conductivity and electrokinetic properties of disperse systems*, Kiev: Naukova Dumka, 1975.
4. N.V.Churaev, B.V.Deryaguin, *DAN SSSR*, 169(1966)396.

THE INFLUENCE OF SUPPORTING ELECTROLYTE COMPOSITION ON  
ELECTROCHEMICAL REACTIONS AND SUBSEQUENT DEGRADATION  
OF SOLID-PHASE POLYMERIC DIELECTRICS

O.E.Mikulina, G.S.Shapoval, A.P.Tomilov, A.A.Pud

Institute of Bioorganic Chemistry and Oil Chemistry, Kiev

Previously it has been established that the electrochemical reactions and subsequent degradation of solid-phase polymeric dielectrics are realized in the dense part of double electric layer (DEL) along three-phase polymer-electrode-solution interface (TI). As a whole, these processes are determined as electrochemical reductive degradation (ECD) /1/.

In present paper the influence of supporting electrolyte composition (various tetraalkylammonium salts) on the peculiarities of these processes for the polytetrafluorethylene (PTFE) and poly(ethyleneterephthalate) (PETF) have been studied.

All experiments were carried out in dimethylformamide (DMF) in the presence of various tetraalkylammonium salts (0.1 M) in a special cell, worked out by authors. This cell secures the creation of a sufficiently big and reproducible TI.

The degree of ECD of the polymers can be calculated from the following formula

$$\alpha = \Delta m / S$$

where  $\Delta m$  - decrease in the mass of the polymer films per unit of its square surface  $S$ .

The essence of research processes consists in the following. With the electrochemical reduction of the polymer along TI occur irreversible changes in its thin surface layer. The changes are connected with the elimination of functional groups and/or with the break of macromolecular chain accompanied with the decrease in the mass of the polymer.

The formed anion-radicals and dianions are accumulated

on the polymer surface in the dense part of DEL along TI as a result of PETF reduction. That leads to redistribution of electron density in macromolecules, to a strong Coulombic repulsion between charged fragments as well as between the latter and the negatively charged electrode surface and then to the break of the bonds least durable in these conditions and to the transition of these fragments into the solution. Here the erosion of PETF polymer surface is observed.

In case of PTFE electron transfer from cathode onto C-F bonds with a subsequent dissociation of the latter and chip off the F<sup>-</sup> anions are realized. And thin surface layer of PTFE is coloured black and it obtains semiconductive properties.

#### Table

The influence of supporting electrolyte nature on the reductive potentials and  $\alpha$  of the PETF and PTFE

Electrolyte	PETF			PTFE	
	$-E_{1/2}$ , V	$-E_{1/2}$ V	$\alpha$ , $g \cdot cm^{-2}$	$-E_{1/2}$ , V	$\alpha$ , $g \cdot cm^{-2}$
$(C_4H_9)_4NI$	1.58	2.30	$0.47 \pm 0.09$	2.15	$0.062 \pm 0.016$
$(C_4H_9)_4NBr$	1.63	2.35	$0.46 \pm 0.02$	2.14	$0.051 \pm 0.010$
$(C_4H_9)_4NBF_4$	1.67	2.38	$0.49 \pm 0.03$	2.14	$0.057 \pm 0.015$
$(C_4H_9)_4NClO_4$	1.70	2.39	$0.50 \pm 0.03$	2.13	$0.050 \pm 0.019$
$(C_2H_5)_4NClO_4$	1.68	2.34	$0.79 \pm 0.06$	2.11	$0.063 \pm 0.021$
$(CH_3)_4NClO_4$	1.63	2.28	$0.82 \pm 0.03$	2.11	$0.009 \pm 0.002$

It is established that the PTFE reductive potentials depend on the nature of anion and on the size of tetraalkylammonium cation (Table 1). The anions can be disposed into the line  $I^- < Br^- < BF_4^- < ClO_4^-$  according to their influence on the PTFE reductive potentials.

At the same time, the nature of the electrolyte anions has practically not influenced the peculiarities of subsequent chemical transformation of PETF. It can be connected with the fact that the decay of reductive molecules and push-

ing of charged fragments out into the solution are realized along TI in dense part of DEL at the cathode. Its structure in aprotic solvent by sufficiently high potentials is determined by the cation composition of electrolyte and it practically does not depend on the nature of anion.

In line of  $(C_4H_9)_4N^+$ ,  $(C_2H_5)_4N^+$ ,  $(CH_3)_4N^+$  the PETF reductive potentials become more positive and the speed of the decay of its reductive macromolecules is growing.

The gain in energy by the formation of ionic pairs of charged products of the reduction with the cations having smaller radii can be another possible reason of the decrease in the PETF reductive potentials.

For PTFE the influence of the electrolyte anion nature on its reductive potentials and subsequent transformations has not been found (Table 1).

But at the same time, the influence of tetraalkylammonium cation size on PTFE reductive potential and on the rate of its subsequent decay has been discovered.

A decrease in the PTFE degradation with the increase in tetraalkylammonium cation size has been found.

It is evident that the established effect depends not only on the DEL structure but on the diffusion of cations into the formed semiconductive layer on PTFE surface and on the formation of intercalation compounds taking part in electrochemical reactions as well. The cation size and rate of its diffusion into the reductive PTFE are connected antipathetically.

#### Reference

1. G.S. Shapoval, A.P. Tomilov, A.A. Pud, Extended Abstracts, 37th Meet. of International Society of Electrochemistry, Vilnius, USSR, p.IV, 1986, 119.



## MUTUAL DEPENDENCE OF CHEMISORPTION AND ELECTRON PROPERTIES OF METAL SMALL PARTICLES AND THIN FILMS

E.L.Nagaev

NPO "Kvant", Moscow

As well known, the chemisorption plays an important part in electrochemical processes. In many cases the heat and the rate of chemisorption on metal surfaces depend on the Fermi energy  $\mu$  of adsorbent. For example, for a monovalent electropositive adatom the former is a linear function of  $(E_A - \mu)$  where  $E_A$  is the valent electron energy of adatoms. Whereas for bulk samples  $\mu$  is a fixed quantity, this is not the case for small particles and thin films. Chemisorption may strongly shift  $\mu$ , and, in turn, this shift may strongly influence the chemisorption itself. Thus, an indirect interaction of a new type should appear between adatoms which, in its essence, is caused by a change in the electron density of states (DOS) under chemisorption. This means a new mechanism of the coverage dependence of the heat and the rate of chemisorption. By the same token, the chemisorption should affect such electronic properties of adsorbent as magnetic susceptibility and so on.

Mathematically, the influence of chemisorption on  $\mu$  may be related to change in boundary conditions on the electron wave function  $\psi$  which in the simplest case may be represented in the form

$$\psi|_S + \lambda \frac{d\psi}{dn}|_S = 0, \quad (1)$$

where  $\vec{n}$  is the normal vector to the surface S. Thus, the chemisorption should influence the quantity  $\lambda$ . The boundary conditions (1) lead to the spatial quantization of electron levels, so the true DOS is a singular function of the energy E. But a coarse-grained DOS may be introduced in the Born-Oppenheimer approximation which is a continuous function of the energy. The memory about the spatial quantization

manifests itself only in a surface correction to the conventional bulk DOS. The most general expression for the coarse-grained DOS in the case of (1) and the quadratic dispersion law was obtained in [1]. Using it, one obtains the surface correction  $\mu_s$  to the bulk Fermi energy  $\mu_v$ :

$$\mu = \mu_v + \mu_s, \quad \mu_v = (3\pi^2 n)^{2/3} / 2m = k_F^2 / 2m,$$

$$\mu_s = -\frac{S}{V k_F} (\mu_v + 1/2m \lambda^2) \operatorname{arctg} k_F \lambda - \mu_v / k_F \lambda -$$

$$- \frac{\pi \mu_v}{4} + \frac{\pi}{2m \lambda^2} \theta(-\lambda), \quad (2)$$

where  $S$  is the surface area and  $V$  is the volume of the sample,  $\theta(x) = 1$  for  $x > 1$  and  $\theta(x) = 0$  for  $x < 0$ ,  $h = 1$ ,  $n$  is the electron density.

As follows from (2),  $\mu_s$  being of the order of  $\mu_v / k_F L$  may reach several tenths of eV for  $L = V/S = 10$  nm, and it changes its sign from positive to negative with changing from  $\lambda = 0$  (an infinitely deep potential well) to  $\lambda \rightarrow \infty$  (the surface resonance). If  $\lambda$  falls off with increasing coverage, then  $\mu$  increases, and the heat of adsorption diminishes in the example discussed above (usually this effect is attributed to the dipole-dipole interaction). But opposite opportunity, when  $\mu$  decreases, cannot be ruled out and then the chemisorption should be self-accelerating.

The treatment just discussed assumes that the coverage dependence of  $\lambda$  is known. If it is not case another approach is developed which based on a pure microscopic model. Apart from  $E_A$ , the overlap integral  $B_B$  between the adatom and the atom of the crystal nearest to the adatom is given. A calculation is carried out which gives an expression for the one-electron retarded Green's function of which the imaginary parts gives the true DOS. After its coarse-graining a general expression was obtained for shift in DOS caused by adatoms.

As follows from this expression, if adatoms create discrete levels then the DOS is reduced inside the conduction band of the crystal. In the opposite case it is enhanced. If the Fermi energy lies not far from the conduction band bottom, then the contribution of adatoms to the Fermi energy is given by the expression

$$\mu_A = - \nu B_a^2 ( W/2 + E_A - 3 B_a^2/W )^{-1}, \quad (3)$$

where  $\nu$  is the number of adatoms per atom of the crystal,  $W$  is the conduction band width. According to (3)  $\mu_A$  may both increase and decrease with increasing coverage depending on values of  $W$ ,  $E_A$  and  $B_a$ .

#### References

1. C. Bloch, R. Balian, Ann of Phys. 60(1970), 401.

COMPACT LAYER AT THE METAL/WATER INTERFACE.  
QUANTUM CHEMICAL AND STATISTICAL APPROACH.

R. R. Nazmutdinov, M. S. Shapnik and A. Y. Tuzankin

Kazan Institute of Chemical Technology, Kazan

Recently most of self-consistent approaches treat the double electric layer in terms of the density functional technique */1/*. Attempts to extend nontraditional quantum chemical models for description of compact layer are still noticeably lacking. In particular, the results */2/* are restricted mainly to study of the water chemisorption on the uncharged metal surface. In the present work some fundamental aspects of the solvent structure at the metal/water interface have been investigated by using cluster models and the computer simulation. This approach is expected to be promising for theoretical study of the compact layer. All quantum chemical calculations were carried out in CNDO/2 - UHF approximation.

I. We assume that the structure  $c(2 \times 2)$  occurs for the water molecules adsorbed on the face (111) of copper. The water monolayer is modelled as a small ensemble including five molecules adsorbed in two extreme orientations. The metal surface is considered as the planar cluster  $Cu_{19}$ . At the potential of zero charge and under conditions of cathodic polarization ( $-15 \mu Cl/cm^2$ ) various "dipole multiplet" states were investigated. The dipole reorientation of the water molecules is computed to be possible even at the potential of zero charge. For some states of the dipole ensemble the equilibrium distance  $R(Cu-H_2O_{ads})$  depends noticeably on the surface charge. Cathodic polarization is found to have a weak effect upon the density of electronic states of the metal/water interface.

II. The influence of bulk water on the molecules adsorbed in the first monolayer is of considerable interest. To this effect the "ice-like" associates  $(H_2O)_3$  were calculated on the surface of  $Cu(100)$ .

III. The new quantum chemical model for the charged metal surface is proposed. A small planar or bilayer cluster plays the role of the electrode surface. One can vary the density of the surface charge over a wide range changing a little the metal skeleton charge. By the modification of diagonal matrix elements of a hamiltonian the field of the outer Helmholtz plane is taken into account. Our model was shown to simulate the basic features of the electrode polarization. This approach was applied to the study of chemisorption of a single water molecule on the mercury surface. The structure parameters of  $H_2O_{ads}$  were found to depend weakly on the surface charge. According to our results the electrode polarization influences noticeably on the value  $\Delta\chi^{Me}$ . The energy levels of electrons of the metal are shifted linear for any surface charge.

IV. The water structure in the compact layer at the Hg/ $H_2O$  interface was studied using Monte Carlo technique. Few types of the two-dimensional solvent lattice were simulated by various temperatures and the surface charges. To describe the metal - water bond we employed the results of quantum chemical calculations. The lateral interactions under consideration include H-bondings and electrostatic potentials, which take into account the screening effects. We investigated the influence of electric field of the compact layer on the structure of H-bondings in the first monolayer. The problem of phase transitions is also discussed.

#### References

1. A. A. Kornyshev // *Electrochim. Acta*, 34 (1989) 1829
2. An. M. Kuznetsov, R. R. Nazmutdinov, M. S. Shapnik // *Electrochim. Acta*, 34 (1989) 1821

INVESTIGATION OF THE LI/NONAQUEOUS SOLUTION INTERFACE  
BY PHOTOEMISSION TECHNIQUE

E. S. Nimon, A. V. Churikov, I. M. Gamayunova,  
A. A. Senotov, A. L. Lvov  
Saratov State University, Saratov

Properties of passivating layers (PL) formed on the lithium surface in nonaqueous electrolyte solutions influence strongly the electrochemical behaviour of the lithium electrode [1,2]. Recently [3,4] a quick-response cathodic photocurrent caused by electron photoemission from Li into PL was observed at the Li/nonaqueous solution interface. In this communication we present the results of our investigation on the effect of the Li/nonaqueous solution interface structure peculiarities and PL composition on the characteristics of photoemission current.

At sufficiently large periods of Li storage in nonaqueous solutions based on thionyl chloride (TC), propylene carbonate (PC), as well as on PC-dimethoxyethane mixtures spectral dependences of photocurrent fit the square Fowler's law [5] which is characteristic of electron photoemission from metals into low-conducting media. The work function ( $h\nu_0$ ) values of the electron transferred from Li into PL at zero potential (vs.  $\text{Li}/\text{Li}^+$  electrode) were found to be 1.0 and 1.3 eV in PC- and TC-based systems, respectively. As was also noted [3], the thermoemission current estimated on the basis of the  $h\nu_0$  value obtained may be responsible for the Li corrosion rates observed experimentally in PC solutions.

The results of photoelectrochemical measurements were found to be sensitive to alterations in PL composition on Li. Thus, storage of the Li surface in contact with dry oxygen prior to immersing the electrode into the TC-based solution or doping the PL with calcium preliminarily added to the TC solution led to a decrease of  $h\nu_0$  down to 1.0 eV or to its increase up to 1.8 eV, respectively. Long-term storage of the electrode in TC solution which was accompanied by a significant decrease of both the Ca compounds and Li oxide content in the PL resulted in restoration of the initial  $h\nu_0$  value.

Electric properties of PL on Li and the interface structure were shown to influence significantly the photoeffect characteristics. Thus, the increase of PL resistivity during storage in solution connected mainly with the decrease of concentration of mobile ionic current carriers in the PL led to a weaker influence of electrode potential on the position of the red boundary of the photoeffect. It has

also been stated that for freshly formed Li/PL interfaces in systems based on organic solvents the exponent (n) in the spectral photoemission law differs from 2. For correct estimation of n, a method proposed in Ref. [6] was used based on obtaining the logarithmic derivative of photocurrent with respect to light quantum energy allowing both  $h\nu_0$  and n to be determined simultaneously.

At short periods of Li storage in solution the exponent in the spectral law of photoemission current regularly exceeded 2 being close to 2.5. Hence, the spectral dependences of photocurrent under these conditions fit the 5/2 power law usually observed for electron photoemission from metals into concentrated ionic systems [5,7]. Similar character of spectral dependences for the emission from Li into PL points out the existence of a great number of non-equilibrium ionic current carriers in freshly formed PL, in accordance with our earlier data [2].

For studying the photoeffect kinetics, laser electrochemical technique [7] was employed. The experimental apparatus controlled by a computer included a pulse UV laser with the pulse length of  $< 10^{-8}$  s and a stroboscopic system of registration. Kinetic dependences of photocurrent (Jph) and photopotential at various periods of Li storage in the electrolyte solution were measured. In Jph, t-curves regions of quick-response amplitude growth with subsequent relatively slow decay down to zero value were observed. At sufficiently large t values photocurrent decay curves could be linearized in the coordinates  $J_{ph}, t^{-1/2}$ . The character of the kinetic dependences obtained can be explained by peculiarities of transport of photoemitted electrons in PL during their return to the lithium electrode.

#### References

1. E. Peled. In: Lithium Batteries, N. Y., Acad. Press, (1983)43.
2. E. S. Nimon, A. V. Churikov, A. A. Senotov, A. L. Lvov, I. A. Pridatko. Dokl. Akad. Nauk SSSR, 303(1988)1180.
3. E. S. Nimon, A. V. Churikov, A. L. Lvov. In: Double Layer and Adsorption at Solid Electrodes, Tartu Univ., VIII(1988)285.
4. A. L. Lvov, E. S. Nimon, A. V. Churikov, A. A. Senotov. In: 5th Int. Meet. Lithium Batteries, Beijing, China, Extended Abstracts (1990)8.
5. A. M. Brodskii, Yu. Ya. Gurevich, Yu. V. Pleskov, Z. A. Rotenberg. Modern Photoelectrochemistry, Moscow, Nauka(1974).
6. Z. A. Rotenberg, N. V. Gromova, V. E. Kazarinov. J. Electroanal. Chem., 204(1986)281.
7. V. A. Benderskii, A. M. Brodskii. Photoemission from Metals into Electrolyte Solutions, Moscow, Nauka(1977).

FORMATION OF SPACE CHARGE IN THE SYSTEM WITH FIXED CHARGES

A.V.Noskov, Yu.I.Kharkats, S.A.Lilin

Institute of Non-Aqueous Solution Chemistry, USSR Acad.Sci.,  
Ivanovo

A.N.Frumkin Institute of Electrochemistry, USSR Acad.Sci.,  
Moscow

In electrochemical kinetics the system of diffusion-migration transfer equation is resolved together with the condition of local electroneutrality that is used instead of the precise Poisson equation /1-3/, which allows to determine the coordinate distributions of potentials and concentrations. It was found elsewhere /3/ that at high enough currents, the space charge is induced in the systems containing "the background" of fixed charges together with mobile carriers.

The present paper deals with the electrodiffusion problem on the parallel transport of single-charged anions and cations in the case of homogeneous distribution of immobile background. Supposing that the Nernst-Einstein ratio for the coefficients of diffusion and mobility of the carriers is correct the initial system of equations takes the following form:

$$\begin{aligned} \frac{dC_1}{dX} + C_1 \frac{d\psi}{dX} &= j_1 = t_1 J, \\ -\frac{dC_2}{dX} + C_2 \frac{d\psi}{dX} &= j_2 = \frac{1-t_1}{\nu} J, \end{aligned} \quad (1)$$

$$C_1 = C_2 + 1 - \gamma,$$

where  $C_{1,2}$  is the concentration of mobile cations and anions scaled by  $C_0$ , which is the concentration of cations on the boundary of the diffusion layer;  $\gamma$  value characterizes the concentration of immobile negative charges which in dimensionless form equals  $1 - \gamma$ ;  $X$  coordinate is scaled by



the thickness of the diffusion layer  $L$ ;  $\Psi$  is the dimensionless electric potential (in  $kT/e$  units);  $J_{1,2}$  is the cationic and anionic current scaled by  $eD_{1,2}C_0/L$  values, respectively, where  $D_{1,2}$  denote the diffusion coefficients of cations and anions, respectively;  $J = j_1 + \nu j_2$  is the admittance current, where  $\nu = D_2/D_1$ .

The boundary conditions are as follows:

$$C_1(1) = ; ; C_2(1) = r ; \quad \Psi(1) = 0 \quad (2)$$

Integration of system (1) taking account (2) allows to obtain the implicit distribution of potential and concentration  $C_2$ :

$$\frac{2[t_1(1+r^\nu) - 1]}{t_1(\nu+1) - 1} \left[ \exp\{[t_1(\nu+1) - 1]\Psi/[t_1(\nu-1) + 1]\} - 1 \right] + (1+r)\Psi = \frac{J}{\nu} [t_1(\nu+1) - 1] (X-1) \quad (3)$$

$$2(C_2 - r) + (1-r) \frac{t_1(\nu-1)+1}{t_1(\nu+1)-1} \ln \left\{ \frac{C_2[t_1(\nu+1)-1] - (1-t_1)(1-r)}{[t_1(1+r^\nu)-1]} \right\} = \frac{J}{\nu} [t_1(\nu+1) - 1] (X-1) \quad (4)$$

The analysis shows that concentration  $C_2$  decreases with increasing admittance current  $J$  [at  $t_1 > (1+r^\nu)^{-1}$ ].

It is known that, as a rule, there is no limiting current, i.e. the concentration near electrode  $C_2(0)$  does not equal zero at any current, in the systems with fixed charges /3/. In our case, a large interval of unattainable  $C_2$  values appears. As it follows from (4), this interval has the upper limit  $C_2^{\text{max}} = (1-t_1)(1-r)/[t_1(\nu+1)-1]$ . Existence of interdicted  $C_2$  values relates physically to generation of anions occurring at  $X=0$  boundary.

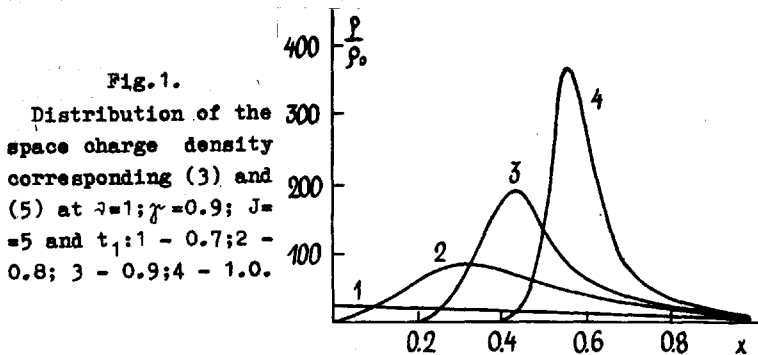
Further investigation of the distribution of the density of space charge  $\varphi(X)$  allows to obtain it by substituting (3) into the Poisson equation  $\varphi = -\epsilon/4\pi\Psi''$ :

$$\varphi = \varphi_0 (J/\nu)^2 \frac{[t_1(\nu+1) - 1]^3}{t_1(\nu-1)+1} \frac{2[t_1(\nu+1)-1]}{t_1(\nu-1)+1} \exp\{[t_1(\nu+1)-1]\Psi\}$$

$$\rho(t_1(\nu-1)+1) \left\{ \frac{2[t_1(\gamma\nu+1)-1]}{t_1(\nu-1)+1} \exp \left[ \frac{t_1(\nu+1)-1}{t_1(\nu-1)+1} \psi \right] + 1 - \gamma \right\}^3, \quad (5)$$

Here  $\rho_0 = 2eC_0(L_D/L)^2$ , where  $L_D = (\epsilon kT/8\pi e^2 C_0)^{1/2}$  is the Debye length.

The Figure shows the space charge density distributions  $\rho(X)$ , calculated using (3), (5) for a series magnitudes of the parameters. The  $\rho(X)$  dependence at high enough currents is a curve with a peak, the height and position of which are determined by the value of the admittance current  $J$ , by the transfer number  $t_1$  as well as by the ratio between the diffusion coefficients of anions and cations  $\nu$ .



The Figure shows that the increase in the anionic current ( $t_1$  decrease) is accompanied by a decreasing in space charge density. Here the corresponding  $\rho(X)$  curves are simplified and the maximum is displaced towards low magnitudes of  $X$ . At  $t_1 = (\gamma\nu + 1)^{-1}$  the  $\rho(X)$  value identically turns into zero. Further decrease in  $t_1$  results in the change of the space charge sign.

#### References

1. V.S.Markin, Yu.A.Chizmadzhev, Indutirovannyi ionnyi transport, M.: Nauka, 1974, 251 p.
2. Yu.Ya.Gurevich, Yu.I.Kharkats, Elektrokimiya, 15(1979) 94.
3. Yu.I.Kharkats, Elektrokimiya, 20 (1984) 248.

## THE INFLUENCE OF CRYSTALLOGRAPHIC ORIENTATION OF OXIDE ELECTROLYTE ON DOUBLE ELECTRICAL LAYER OF GOLD ELECTRODE

E. M. Novitskiy, I. D. Remez

Institute of Electrochemistry, Ural Science Department of the Academy of Sciences of U.S.S.R., Sverdlovsk

There are many data at present time about influence of crystallographic orientation of solid metal electrodes on properties of double electrical layer /1/. Solid electrolytes unlike solutions allow to investigate an effect of crystallographic orientation of surface of electrolyte on characteristics of double layer.

The results of the investigation of gold electrode received by slow solidification of liquid metal drop placed on flat polished surface of stabilized zirconium dioxide  $ZrO_2-0,1Y_2O_3$  (YSZ) single crystal are represented in this communication. The experiments were carried out in purified helium at 1273 K. All the samples of solid electrolyte were cutted as 1-1.3 sm. diameter half-sphere from the same piece of single crystal. The gold electrode was placed in the center of the flat electrolyte surface and its area was equal to  $1.3-1.5 \cdot 10^{-2} \text{ cm}^2$ . The spherical surface of the YSZ samples was covered with platinum powder served as counter electrode. The (110) and (100) faces of crystals were made with error less  $\pm 0,5^\circ$ . The impedance measurements in the range  $10^{-2} - 2 \cdot 10^6 \text{ Hz}$  and stationary voltammetry of the solid gold/YSZ interface were carried out by means of the automatic system /2/ supplemented by low-frequency complex admittance digital meter X-2071 /3/. The working electrode potentials were determined relatively to air reference electrode. The measurement technique was described in /4,5/ in details.

Double layer capacitance ( $C_d$ ) was measured at 100-200 kHz. The dependences  $C_d$  vs. electrode potential (E) for both crystal faces are parabolic with well pronounced minimum, however the values of  $C_d$  per-unit area are distinguished for different faces and are equal to 40-45  $\mu\text{F} \cdot \text{cm}^{-2}$  for the (110)

face having more surface package density and  $10-12 \mu\text{F}\cdot\text{cm}^{-2}$  for the (100) crystal face. Current density under anodic polarization for the (110) face is also more than for the second one, but in the cathodic region of potentials current densities are approximately equal for both crystal faces.

The relaxation processes occurring in double electrical layer on both crystal faces up to  $10^{-2}$  Hz were investigated. For this purpose the interfacial capacitance (C) vs. potential dependences were measured at 30 fixed frequencies in the same potential range. The form of the C-E curves is parabolic in general for both faces up to low frequencies. Some differences are observed at about some Hz: the second minimum of capacitance appears in more positive range of potentials than the first one and further at frequencies less 0,3 Hz the first minimum disappears completely and curves acquire a parabolic form again. For example the C vs. E plots measured at several frequencies for the (110) crystal face are represented in the Fig.

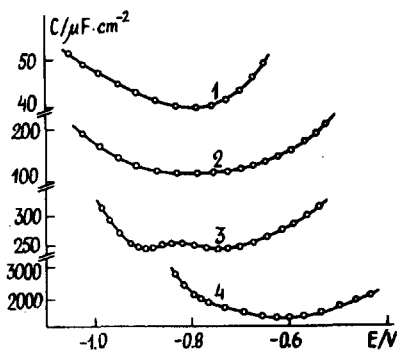


Fig. Dependence of gold/(110)YSZ interfacial capacitance on potential in helium at 1273 K. 1 - 100 kHz, 2 - 17 Hz, 3 - 1.3 Hz, 4 - 0.03 Hz.

As mentioned in [5] the minimum capacitance potential ( $E_m$ ) measured at high frequencies, when the frequency independent capacitance is recorded, corresponds to zero free

charge potential, and at low frequencies  $E_m$  approaches to the potential of the point of inflection on the stationary voltammetry curves and corresponds to zero full charge potential. Zero full charge potentials are closely spaced for both faces and equal to  $-0,79$  V and  $-0,81$  V for the (110) and (100) faces correspondingly. Minimum capacitance potential is constant when frequency decreases up to appearance of the second minimum of capacitance. The absence of displacement of  $E_m$  at frequency changes proves that specific adsorption of ions under previously mentioned conditions does not take place on the solid gold electrode/YSZ interface.

The displacement of remained second minimum to positive direction occurs when frequencies are below some Hz. Such behaviour indicates to very slow adsorption process probably connected with small mobility of the solid electrolyte cations. The minimum capacitance potentials practically coincide near  $10^{-2}$  Hz with potentials of bending point of corresponding voltammetry curves. The magnitudes of the zero full charge potentials unlike the zero free charge potentials are well distinguished for different crystal faces and make up  $-0,6$  V and  $-0,5$  V for the (110) and (100) faces correspondingly.

Thus the crystallographic orientation of YSZ solid electrolyte surface has an substantial effect on the interface impedance parameters and electrode kinetics.

#### References

1. A.N.Frumkin, Potentsialy nulevogo zarjada, Moscow, 1982.
2. I.D.Remez, Yu.S.Lukach, Rasplavy, (1989)93.
3. V.I.Kenzin, S.P.Novitskiy, Elektrokhimiya, 24(1988)184.
4. I.D.Remez, E.M.Novitskiy, Tez. dokl. V Uralskoi konferentsii po vysokotemperaturnoi fizicheskoi khimii i elektrokhemii, Sverdlovsk, 2(1989)130.
5. I.D.Remez, Yu.S.Lukach, Rasplavy, (1990)75.

# A STUDY OF THE DOUBLE LAYER AND ADSORPTION ON GOLD AND SILVER ELECTRODES IN MOLTEN SALTS BY ESTANCE-METHOD

Yu. G. Pastukhov

Inst. Electrochem. of Ural Dept. of Acad. Scie. USSR, Sverdlovsk

The interface of solid gold (silver) electrode and molten alkali halide was investigated by methods of cyclic a. and c. voltammetry and estance (differential interfacial tension  $\gamma$  /1,2/) technique. The electrode potential (E-regarding  $Pb/Pb^{2+}$  ref. el.), temperature (T), frequency (f) and salt composition were varied. The region of E where the electrode may be considered as polarizable is the more wide the lower is T of electrolyte, the greater the voltage of decomposition of salt and the more E of metal dissolution, for example in system Au-CsCl. The estance-curves for Au in all alkali metal halides and Ag-CsCl at T near melting points of salts

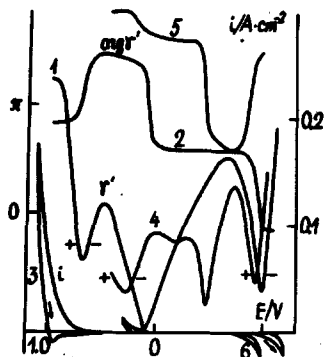


Fig.  
The experimental plots of magnitude (1,4) and phase angle (2,5) estance, current density (3,6) vs. E. 1,2,3: Au -CsCl, 2.3 kHz; 4,5,6: Ag -CsCl, 3.3 kHz; 50 mV/s, T= 932 K.

have 3 special points (zero stance-ZE) where the magnitude of full charge density ( $q$ ) influenced by the elastic surface deformation passes through zero or minimum with changing of the sign /2/:

$$(*) \quad \partial\gamma/\partial E = -q - \partial q/\partial\nu = 0,$$

$\partial v = \partial s / s$  - the relative deformation of surface,  $s$  - its area. This equation is received for equilibrium estance and for low  $f$  is true. The one ZE takes place in the region of cation discharge (cathodic -CZE), its potential shifts to more positive values by rising  $T$  and lowering  $f$ . The  $E$  of CZE depends on nature of alkali metal: the substitution of  $Cs^+$  to  $Li^+$  shifts both cathodic branch I-E curve and  $E$  of CZE to more positive values. The middle ZE (MZE) occurs in region of  $E$  where charge transfer is negligible, and the third (anodic -AZE) - in region of anodic process of anion discharge or electrode dissolution. The growing of  $E$  in shown process leads to cooling of surface owing to Peltier effect, following heat- estance  $\partial \gamma / \partial E > 0$  by these conditions. In limits of this hypothesis the integral electrocapillare curves have a maximum at MZE and two minimums in regions of adsorption of products of faradaic processes. Near MZE and up to AZE the charge of gold surface is positive, the complex anion species are adsorbed with partial charge transfer. The free charge is compensated by adatoms of halogen at AZE and full charge is equal to zero. A qualitatively simmetric situation is developed by cathodic polarisation from MZE. The negative  $q$  rised, in point of maximum the surface may keep a maximal charge, here  $\gamma'' = 0$  and admittance have the minimum. The further displacement  $E$  leads to powerful charge transfer, to rising of current and admittance also to diminishing of estance to zero. At CZE free charge is compensated by adatoms Cs. The  $E$  of maximum ECC in the series  $Cl^- - Br^- - I^-$  for Au- CsCl system is equal to 0.1, -0.1, -0.4 V, that gives evidence of growing specific adsorption of these anions /3/. The intervals between this  $E$  are close to the intervals between PZC for gold in aqueous solutions of these salts. In addition the differences of MZE for gold and silver electrodes and with  $E$  max. of ECC Pb, Bi, In in molten CsCl /4/ are compared with differences of PZC for this metals in aqueous solutions /3/. Those allow to suppose these the influence of deformation on  $q$  (second item in \*) near maximum ECC is not too big, thus it was proved for Au and Ag in aqueous solutions /2,5,6/. The growing of  $f$

alternative current leads to rising of estance magnitude in maximumes concerning heat estance and shifts E CZE to more negative and E AZE to more positive values, in analogous way the E of admittance minimums are shifted. All that is connected with going to unequilibrium estance and manifestation of growing deposit of alkali or halogen adatoms in correspondent region of E in full charge.

The increasing of T results in activation of electrodes processes: at less catodic and anodic E the charge transfer begins, the height of estance maximums diminishes, the E of CZE shifts to more positive and the E of AZE to more negative values. At T more of a certain depending on nature of metal and salt MZE gets in region of faradaic process: for Au- in region of metals dissolution, for Ag- in region of cation discharge, and at  $T \cong 1300K$  the estance curves have only CZE corresponding to overcharge on electrode with adsorbed alkali metal. The nature of alkali cation influences also adsorption of anions with partial charge transfer owing to its contrapolarizing action on anion. In series of cations  $Cs^+$ ,  $Na^+$ ,  $Li^+$  in chloride salts at constant T for Au electrode the values of E AZE increases and the T lower of that the estance curves have 3 ZE rises. The cation  $Li^+$  form the stabllest complex anions that decreases chemisorption, the charge transfer from those anions begin at more positive E and their decomposition by heating occur at more T that for cation  $Cs^+$ .

In conclusion one may note more difficulties for Ag in comparison with Au to receive reproducable estance curves that are connected with more chemical activity of the first.

#### References

1. Yu. G. Pastukhov, V. P. Stepanov, Doklady AN SSSR, 307(1989)648.
2. A. Ya. Gokhstein, Poverkhnostnoe natyashenie tverdykh tel i adsorbciya, Moscow, 1976.
3. A. N. Frumkin, Potencialy nulevogo zaryada, Moscow, 1982.
4. M. V. Smirnov, V. P. Stepanov, Electrochim. Acta, 24(1979)651.
5. A. G. Zelinskiy, R. Yu. Bek, Elektrokhimiya, 16(1980)39.
6. R. Malpas, R. Fredlein, A. Bard, J. Electroanal. Chem, 98(1979)339.



ELECTRICAL DOUBLE LAYER STRUCTURE ON THE (111), (001) AND (011) PLANES OF A BISMUTH SINGLE CRYSTAL IN 2-PROPANOL SOLUTIONS

P. Pärssimägi, K. Anni, M. Väärtnõu, E. Lust  
Tartu University, Tartu

In the electrochemical literature there is no quantitative information about the structure of the electrical double layer (edl) on single crystal planes from non-aqueous solutions, except the data of works /1,2/. But the problem of understanding the relationship between the bulk and interfacial properties of polar solvents and the crystallographic structure of electrode surface to the edl structure is still open.

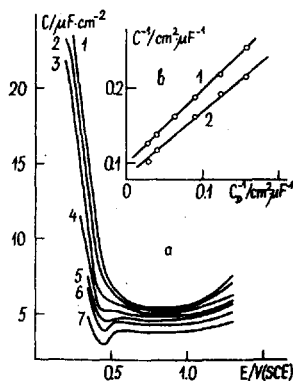
The present paper is devoted to a comprehensive study of the edl structure on the bismuth single crystal planes in the ethanolic (EtOH) and 2-propanolic (2-PrOH) surface-inactive electrolyte solutions. Preparation and surface treatment of the bismuth single crystal electrodes have already been described, as well as the capacity measurement techniques and preparation of the solutions /1-3/. The reference electrode was an aqueous saturated calomel electrode, separated from the solutions studied by the intermediate ethanolic or 2-propanolic solutions. The liquid junction between the aqueous and non-aqueous solutions was made through solution sealed taps and was kept constant in all measurements. No attempt to connect the liquid junction due to the EtOH/water and 2-PrOH/water contact has been made. The temperature was maintained at 298<sup>±</sup>1 K.

The double-layer differential admittance was measured in the range of 80 to 410 Hz. As for the aqueous solutions /3/, a slight variation of capacity C as a function of the frequency, smaller than 3-6 % for the 0.1 M solution, allows the differential admittance to be identified with the differential capacity. The potential range extended from -0.1 to -1.5 V vs. SCE. Double-layer differential capacity-potential

curves,  $C(E)$  curves, were recorded for nine concentrations of  $\text{LiClO}_4$ , from 0.5 to 0.001 M. The  $C(E)$  curves in Fig. 1 show the concentration effect of the electrolyte. The influence of the diffuse layer is visible for concentration  $c_{\text{LiClO}_4} \leq 0.01$ . The potential of the capacity minimum  $E_{mc}$  is

Fig. 1.

$C(E)$  curves (a) for the (011) plane of Bi in 2-PrOH solutions of  $\text{LiClO}_4$ , M: 1 - 0.1; 2 - 0.05; 3 - 0.02; 4 - 0.01; 5 - 0.005; 6 - 0.003; 7 - 0.001. Parsons - Zobel plots (b) at  $\sigma=0$  in 2-PrOH solutions of  $\text{LiClO}_4$  for the 1 - (011) and 2 - (001) single crystal planes of bismuth



independent of concentration of  $\text{ClO}_4^-$  anions with a relative accuracy of  $\pm 10$  mV, when the  $c_{\text{LiClO}_4}$  changes from  $10^{-3}$  to  $5 \cdot 10^{-3}$  M. As for the plane (111) in<sup>4</sup> aqueous KF solutions /3,5/, it may be assumed that no significant specific adsorption of  $\text{ClO}_4^-$  occurs at the  $E_{mc}$ , and for the most dilute  $\text{LiClO}_4$  solution the value of  $E_{mc}$  may be identified with  $E_{\sigma=0}$  for the single crystal planes of bismuth in 2-PrOH solutions (Table 1). It follows from Table 1, that the dispersion of the  $E_{\sigma=0}$  for the various single crystal planes of bismuth in 2-PrOH and EtOH is lower than in aqueous solutions /3,5/ or in acetonitrilic (AN) solutions /2/.

According to the method of Parsons and Zobel, the variation of the inverse value of double-layer capacity ( $C^{-1}$ ) at the minimum as a function of the inverse value of diffuse-layer capacity  $(C^d)^{-1}$  /4/, can be considered linear for each face, when the  $\text{LiClO}_4$  concentration decreases from 0.5 to 0.003 M. For 2-PrOH solutions the inverse slope of the

Parsons-Zobel plots  $f_{P-Z}$  is equal to 1.02 for the (111), 1.03 for the (01 $\bar{1}$ ) and 1.07 for the (001) plane of bismuth. In the absence of specific adsorption these values correspond to that of the roughness coefficient R, therefore  $1.02 < R < 1.07$  for the single crystal planes of bismuth in the 2-PrOH solutions.

Table 1

Electrical double layer parameters for bismuth single crystal planes in 2-PrOH

Electrode	$E_{\sigma=0} \pm 0.01, V$ (s.c.e.)	$f_{P-Z}$	$C_{\sigma=0}^i$ $\mu F \cdot cm^{-2}$	$C_{\sigma \ll 0}^i$ $\mu F \cdot cm^{-2}$	$D \times 10^{-14}$ atom $\cdot cm^{-2}$
(111)	-0.45	1.02	15.9	6.0	5.6
(001)	-0.41	1.07	18.4	6.8	5.3
(01 $\bar{1}$ )	-0.46	1.03	13.7	6.6	6.4
PC-Bi	-0.42	1.00	17.4	6.9	-

The inner layer capacity  $C^i$ , as a function of the electrode charge  $\sigma$  was calculated from the well-known equation applicable to the double-layer model in the absence of specific adsorption /4/

$$1/C = 1/FC^i + 1/FC^d, \quad (1)$$

where F is the fitting coefficient. The main edl parameters are given in Table 1, where the symbols have their usual meanings. The fitting coefficient F would correspond to R·f, where f represents the crystalline heterogeneity. As shown theoretically in ref. /4/ and proposed from the experiments in ref. /3,5/ for a model polycrystalline two-plane electrodes, the coefficient f depends on the dispersion of zero charge potential  $\Delta E_{\sigma=0}$  of the individual planes and on the electrolyte concentration c; and f increases as  $\Delta E_{\sigma=0}$  and c decrease. For the 2-PrOH solutions the monotonic  $C^i(\sigma)$  curve is obtained for the value of F which varies from 1.03 to 1.15 for the (111) and (01 $\bar{1}$ ) planes, and from 1.05 to 1.18 for the (001) plane, when the LiClO<sub>4</sub> concentration decreases

from 0.1 to 0.003 M. For the EtOH solutions, the values of  $F$  vary from 1.03 to 1.07 for the planes (001) and (01 $\bar{1}$ ) and from 1.02 to 1.05 for plane (111), correspondingly. The value of the roughness factor  $R$  can be estimated to be equal to 1.01-1.07 from the plot of  $F$  as a function of  $1/\sqrt{C}$  for the ethanolic and isopropanolic solutions. For the aqueous and AN solutions, the corresponding values of  $F$  are somewhat higher /3,5/ and can be ascribed to much stronger dependence of the zero charge potentials on the crystallographic structure of planes on the aqueous and AN solutions, than on the EtOH or 2-PrOH solutions.

It is clear that in EtOH and 2-PrOH, just as in water and AN /2,3,5/ in surface-inactive electrolyte solutions, at negative charges  $\sigma \ll 0$  the inner layer capacity  $C_{\sigma \ll 0}^i$  depends rather little on the crystallographic structure of the plane, being determined mainly by the dimensions of solvent molecules and by the bulk permittivity of the solvent. As the negative  $\sigma$  decreases, the  $C^i$  starts to increase due to the specific adsorption of the solvent and becomes more strongly dependent on the nature of the plane. As follows from Table 1 and data of works /2,3,5/, at all regions of  $\sigma$  the most compact principle plane has the smallest, and the most open plane the largest interfacial capacity.

#### References

1. K.L.Anni, M.G.Všártnöu, U.V.Palm, *Elektrokhimiya*, 22 (1986) 992.
2. E.J.Lust, *Elektrokhimiya*, 27 (1991) 432.
3. E.J.Lust, U.V.Palm, *Elektrokhimiya*, 24 (1988) 557.
4. I.A.Bagotskaya, B.B.Damaskin, M.D.Levi, *J. Electroanal. Chem.* 115 (1980) 189.
5. E.J.Lust, U.V.Palm, *Elektrokhimiya*, 22 (1986) 565.

## ELECTROCHEMICAL BEHAVIOUR AND CORROSION OF NICKEL IN ACID SOLUTIONS

A.P.Pchel'nikov, A.E.Kozachinskiy, Ya.B.Scuratnik, V.V.Losev  
Karpov Institute of Physical Chemistry, Moscow

The formation of both  $\alpha$ -phase (solid solution -  $\text{NiH}_{0.03}$ ) and  $\beta$ -phase (hydride -  $\text{NiH}_{0.7}$ ) is caused by the Ni absorption of hydrogen. These phases are likely to influence the electrochemical and corrosion properties of Ni. For this purpose the influence of the preliminary cathodic polarization (CP) of Ni on its anodic behaviour was studied. Moreover, the corrosion of Ni with hydrogen-evolution in deaerated solution of 1 N  $\text{H}_2\text{SO}_4$  at  $20^\circ\text{C}$  was researched into. During Ni anodic dissolution after CP or after corrosion the outer anodic current ( $i$ ) is equal to the sum of the two portion currents: Ni dissolution ( $i_{\text{Ni}}$ ) and hydrogen ionization ( $i_{\text{H}}$ ):

$$i = i_{\text{Ni}} + i_{\text{H}} \quad (1)$$

So, if we know the value  $i_{\text{Ni}}$  we could calculate  $i$ :

$$i_{\text{H}} = i - i_{\text{Ni}} \quad (2)$$

The  $i_{\text{Ni}}$  value was determined by radiotracer technique using the foreign  $T$ -isotopes  $^{58}\text{Co}$  (1).

Research was carried out by  $\mu$ computer proved system which included a three-electrode cell with electrolyte circulation between cell and measuring cuvette, detector NaI(Tl) (60x60) for continuous recording of the electrolyte radioactivity ( $N$ ), potentiostat PI-50-1 with programmer PR-8 and personal computer DVC-3m, interfaces connected with amplitude analyzer UNO 1024-90 (in some experiments AMA-CG-F1 was used) and voltmeter V7-34a. The created technique permits to define  $i_{\text{Ni}}$  directly in the experiment currency from the slope of  $N, t$ -curve and to calculate  $i_{\text{H}}$ , taking into account (2).

Slope  $N, t$ -curve (curve 1) at the Ni anodic dissolution during polarization under galvanostatic condition without preliminary CP ("initial" Ni) remains constant and the value

of  $i_{Ni}$  coincides with  $i_{Ni}$  potential (curve 3) practically does not change with time.

At the Ni dissolution after its CP (curve 2) Ni at first does not pass to the solution, i.e.  $i_{Ni}=0$ , and current is spent only on the ionization of hydrogen ( $i=i_H$ ). Then  $N,t$ -curve slope is increased with time (curve 2) testifying a gradual  $i_{Ni}$  growth and diminishing of  $i_H$ . At the moment  $t_1$   $N,t$ -curve slope (and accordingly  $i_{Ni}$ ) achieves a constant level which coincides with  $N,t$ -curve slope of the "initial" Ni, i.e. at  $t > t_1$  the outer current  $i$  is spent practically only on Ni dissolution. Immediately after reswitching from the CP to the anodic polarization Ni potential becomes equal to 0.2 V (n.h.e.) and then it moves slowly to the negative direction, reaching a constant level corresponding to the "initial" Ni dissolution (0.09 V) after 140-170 min (curve 4). If after CP Ni is dissolved at  $E=0.12$  V, so  $i$  decreases, passes through a gently sloping minimum and then increases. On the  $i$  decreasing section only hydrogen oxidizes, in minimum section  $i_{Ni}$  is 1-3 degrees below (depending on CP duration) the "initial" Ni dissolution rate at the given  $E$ . On the increasing section  $i$  is spent completely only on the Ni dissolution. In the region of  $i$  decreasing the dependence  $i-1/\sqrt{t}$  is linear and the extrapolated line passes through the origin. It is evident that hydrogen dissolution from Ni is controlled by diffusion from the Ni bulk to the Ni/solution interface.

Inhibiting hydrogen influence is explained by diffusing hydrogen atoms from Ni bulk to its surface passing from absorbing to adsorbing states and blocking the particles of Ni which are in the kink sites ("active centres") and inhibites Ni anodic dissolution.

Comparison of curves 2 and 4 shows that to the moment  $t_1$   $E$  is 60 mV more positive than in case of the "initial" Ni. This confirms that small hydrogen quantity ( $\theta_H \ll 1$ ) is enough for blocking of "active centres" on the surface of Ni and a slow Ni activation (when  $t > t_1$ ) is connected with the  $\theta_H$  decreasing on the active centres.

Ni corrosion tests showed that during 2h corrosion potential ( $E_c$ ) removes from - 0.01 to 0.06 V, corrosion current

( $i_c$ ) decreases from  $1.8 \cdot 10^{-5}$  to  $3 \cdot 10^{-6}$  A/cm<sup>2</sup>. Then  $E_c$  and  $i_c$  are practically constant. Ni corroded anodic dissolution results show that hydrogen penetrates to Ni in the corrosion tests. The investigation of anodic and cathodic behaviour shows that for the corroded Ni samples the rate of the anodic reaction decreases. This is due to the gradual increasing degree of screening by hydrogen adsorbed atoms on the "active centres" in the course of 2 h corrosion.

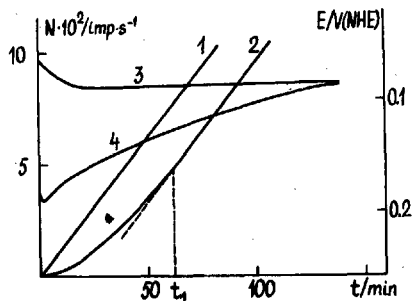


Fig.1. Time dependence of 1 N H<sub>2</sub>SO<sub>4</sub> solution radioactivity (1,2) and electrode potential (3,4) at the anodic dissolution ( $i=2 \cdot 10^{-4}$  A/cm<sup>2</sup>) of Ni "initial" (1,3) and after its preliminary CP ( $i=5 \cdot 10^{-2}$  A/cm<sup>2</sup>,  $t=2$  h) (2,4).

Therefore, hydrogen absorbing of nickel diminishes Ni anodic dissolution and corrosion at the expense of the preferable adsorption of hydrogen atom on the "active centres".

#### Reference

1. Zolotarev E , A.P.Pchel'nikov, Ya.B.Skuratnik, M.A.Dembrovskiy, N.I.Chochlov, V.V.Losev, *Zachita Metallov*, 23 (1987) 922.

## THE SYNTHETIC SEMICONDUCTING DIAMOND ELECTRODE

Yu.V.Pleskov, A.Ya.Sakharova, A.E.Sevastyanov

A.N.Frumkin Institute of Electrochemistry, USSR Acad. Sci.,  
Moscow

Diamond, being extraordinarily chemically stable, undoubtedly is a promising electrode material. Here the electrochemical behaviour of diamond was studied for first time. Thin polycrystalline films of diamond (prepared by CVD in the Institute of Physical Chemistry, Academy of Sciences of the USSR) and, for the sake of comparison, diamond-like films and a single crystal of diamond were used as electrodes. Diamond proved to be a stable electrode with quite good reproducible properties, sensitive to visible and UV lights. Its photoelectrochemical behaviour in aqueous solutions is governed by processes of the current carriers photogeneration and their separation in the space charge region near the semiconductor/solution interface. Moreover, oxygen chemisorption strongly influences the electrode properties. The flat-band potential was determined for different solution pH and the electrode pre-treatment.

Both the bulk and surface microheterogeneities in the diamond electrodes were characterized by the impedance spectroscopy. Frequency dispersion (20 Hz - 5.4 MHz) of the impedance of the film was measured for the solid-state device, i.e., the film with two ohmic contacts. The electrical conductance in the bulk of the film was quantitatively described using a model of (semi)conductive diamond grains separated by poorly conductive intercrystalline boundaries (presumably amorphous carbon).

Measurements of the electrochemical impedance in aqueous solutions<sup>✉</sup> revealed the surface heterogeneity of the films. The equivalent circuit of the electrode contains a

<sup>✉</sup> In collaboration with Nyikos Laios (Central Research Institute for Physics, Budapest, Hungary).



constant phase angle element. The dependence of the equivalent circuit elements on the concentration of the redox couple in the solution, as well as of the background electrolyte was measured. Generally, a diamond electrode proved to be less reversible in the redox solutions as compared to a platinum one.

#### SPECIAL FEATURES OF QUATERNARY AMMONIUM SALTS INFLUENCE ON IRON ANODIC DISSOLUTION IN HYDROCHLORIC ACID

M.A.Pletnev, L.L.Makarova, S.M.Reshetnikov

Udmurt State University, Izhevsk

Quaternary ammonium salts influence on the rate of electrochemical reactions is being connected with cation adsorption on the interface metal-solution and positive  $\Psi_1$ -potential appearance /1/. The adsorption of such compounds is conditioned mainly by electrostatic interaction, in the presence of halide ions the adsorption and inhibition increase. Some authors /2/ connect the inhibition of electrochemical reactions on iron in acid solutions with the influence of quaternary ammonium salt on water structure, as a result of which the Grothus transfer mechanism stops working.

In this work the influence of tetrabutylammonium chloride (TBACL) on iron anodic dissolution rate in 1 M HCl was studied. Polarization measurements were taken with potentiostat P-5827 in an argon deaired cell under different temperatures. Tetrabutylammonium salt was introduced into the cell under the potential  $-0.1$  V (NHE) after preliminary electrochemical electrode treatment.

Polarization measurements show that in the presence of TBACL the inhibition of iron anodic dissolution takes place. With the raise of the temperature the inhibition effect ( $Z_a$ ) slows down, the effect of slowing down is expressed more strongly at TBACL little concentrations. At the TBACL concentration  $c > 10^{-3}$  M the raising of the temperature leads

to the insignificant slow-down of inhibition. If we take into account that the TBACl action is conditioned by the water structure change [3] the effect can be defined by the solution conductivity measurement in the presence of tetraalkylammonium salts.

The conductivity measurements of HCl solution were carried out with the help of conductivity bridge P-568 in a thermostatic cell with platinum electrodes. The results of the measurements show that the TBACl adding slows down the specific conductivity of 0.1M HCl, the sharp slow-down is observed at the concentrations  $c = 10^{-3}$  M. This effect is observed from 25 to 85°C. It was shown in separate experiments that at the TBACl concentration  $c = 10^{-3}$  M conductivity quantities of the acid solution with and without the addition coincide at 75°C. At TBACl concentration  $c = 10^{-3}$  M the specific conductivity of 0.1 M HCl is lower than in the solution without addition at all temperatures.

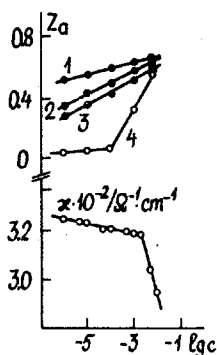


Fig. 1.

The dependence of the inhibition of iron anodic process in 1 M HCl (a) and the specific conductivity in 0.1 M HCl (b) on the TBACl concentration at the temperatures: 1 - 25; 2 - 45; 3 - 55; 4 - 65°C.

The cause of these phenomena is connected with the quaternary ammonium salts adsorption peculiarities at the different surface coverages, the quantities of which depend on TBACl volume concentration. At low and middle surface coverages the rising of temperature at the electrostatic adsorption leads to desorption of ammonium cations from the metal surface, and their inhibition effect on anodic reaction reduces. On the other hand, as the temperature rises, TBA<sup>+</sup>

oasily lose a part of the hydrate shell and solution conductivity both in the presence and absence of ammonium salt equals. At the high concentration of the quaternary ammonium salt the surface coverage of metal is approaching one /4/. In these conditions there may be a reconstruction of the adsorption layer of the phase transfer type both on iron and platinum which is accompanied by a partial cation dehydration and leads to the formation of the dimensional condensed layer /5/. Such an adsorption layer is stable, as alongside with electrostatic powers short-distance powers should appear. The formation of the dense adsorption layers promotes the resistance increase at the metal-solution interface and the reduction of the measured conductivity of system. The above mentioned monomolecular dense layer is formed at ammonium salt concentration  $c > 10^{-3}$  M. The temperature rise in the studied interval at  $c_{\text{TBACl}} > 10^{-3}$  M does not lead to a desorption and a noticeable destruction of the already formed layer. As a result of this the dependence of the effectiveness of the inhibition anodic process on the temperature at  $c_{\text{TBACl}} > 10^{-3}$  M disappears.

#### References

1. B.B.Damaskin, O.A.Petrii, Introduction to the Electrochemical Kinetics, M., Higher school, 1983, 400 p.
2. I.D.Vdovenko, A.I.Lisogor, N.A.Perekhrest, Ukr. Chem. J., 47 (1981) 1162.
3. S.G.Mairanovsky, Electrochemical Synthesis and Bioelectrochemistry, 1975, p.252.
4. M.Salve, U.Palm, Trans. Tartu State Univ., 682 (1984) 131.
5. Y.V.Michailic, B.B.Damaskin, Elektrokimiya, 15 (1979) 566.

# DETERMINATION OF ZERO CHARGE POTENTIAL IN THE PRESENCE OF ADATOMS

B.I. Podlovchenko, E.A.Kolyadko, V.I.Naumov

Chemical Faculty, Moscow State University, Moscow

The concept of the potential of zero charge is one of the fundamental ones in electrochemistry /1/. The most reliable and accurate technique for the determination of the potential of zero total charge (p.z.t.c.) of platinum group metals is based on the thermodynamic theory of hydrogen electrode /1,2 / The method of p.z.t.c. determination for solid electrodes based on measuring of the physical pendulum damped oscillations/3,4/ ( the hardness method ) is also quite well-known. In /5/ the method based on the thermodynamic theory of hydrogen electrode /1/ was proposed for p.z.t.c. determination for disperse electrodes of platinum group metals in the presence of foreign metal adatoms on the surface. The p.z.t.c of electrodeposited (e.d.) Pt and Rh with adsorbed silver atoms were determined. It was of interest to compare them with the results, obtained for the same systems in /5/ by the hardness method.

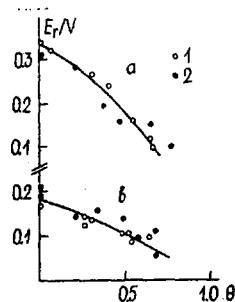
The e.d. Pt and Rh with roughness factor of 800-1000 were used. The supporting electrolyte was 1 N  $\text{Na}_2\text{SO}_4$  + 0.01N  $\text{H}_2\text{SO}_4$ . Two different cells were used: a glass one for electrochemical measurements and a Teflon one for hardness (H) measurements at a controlled potential. The hardness  $H = -1 / \left( \frac{d \ln A}{d \tau} \right)_{\tau \rightarrow 0}$  ( $\tau$  - time, A - the amplitude of oscillations.) was determined depending on  $E_r$  ( the potential referred to r.h.e.) at different degrees of surface coverage of e.d. Pt and Rh by silver adatoms,  $\theta_{\text{Ag}} \left( \theta_{\text{Ag}} = \frac{Q_{\text{H}} - Q_{\text{H}}^0}{Q_{\text{H}}^0} \right)$ , where  $Q_{\text{H}}$  and  $Q_{\text{H}}^0$  - the amount of electricity, necessary for removing  $\text{H}_{\text{ads}}$  in the absence and in the presence of  $\text{Ag}_{\text{ads}}$ ).

It is a well-known fact /3,4/ that the maximum on H, E - curves corresponds to the p.z.t.c. of studied electrodes. It was found that the hardness method is sensitive enough to study the effect of adatoms on the position of p.z.t.c. It was also found that p.z.t.c. values, obtained by the hardness method are close to those obtained earlier /5/ for the same systems by the thermodynamic method (fig.1) and

that in the presence of  $Ag_{ads}$  the p.z.t.c. of Pt and Rh shift in the cathodic direction.

Fig.1. The change of p.z.t.c. for e.d. Pt (a) and Rh (b) with the amount of adsorbed silver.

1 - obtained by the thermodynamic method ; 2 - obtained by the hardness method



The observed cathodic shift of p.z.t.c. with the growth of  $Ag$  is, apparently, caused first of all by the fact that Pt-Ag and Rh-Ag bonds are of a dipole nature with the positive end on the silver atom since the electronic work functions of Pt and Rh are larger than those of Ag. Moreover, during the Ag adsorption  $H_{ads}$ , which dipoles are directed with the positive end to the electrode, is expelled and this also has to result in the shift of p.z.t.c. in the cathodic direction. Thus the possibility to use the hardness method in order to study the effect of adatoms on the position of p.z.t.c. was demonstrated for the first time. One of the advantages of the hardness method compared to the more severe and sensitive thermodynamic method is the fact that the former can be applied to a greater number of systems with adatoms, including the systems irreversible to hydrogen and oxygen.

#### References

1. Frumkin A.N. Potentials of zero charge. M. Nauka. 1979.
2. Frumkin A.N., Petrii O.A., Damaskin B.B., J. Electroanalyt. Chem., 1970. V.27. P.81
3. Rebinder P.A., Venstrem E.K., J. Phys. Chem. (USSR) .1945. V.27. P.1.
4. Tyurin Yu.M., Naumov V.I., Smirnova L.A., Elektrokhimiya, 1979. V.15. P.1022.
5. Podlovchenko B.I., Kolyadko E.A., Elektrokhimiya, 1988. V.24. P. 1138.

ADSORPTIVE AND CATALYTIC PROPERTIES OF GLASS CARBON IN THE  
PROCESS OF OZONE SYNTHESIS IN FLUORIDE-CONTAINING SOLUTIONS.

G.F.Potapova, S.N.Kholodov, V.A.Smirnov, and V.I.Lubushkin

L.J. Karpov Institute of Physical Chemistry,  
Novocherkassk Polytechnic Institute

Ozone is known to form with high efficiency [1-3] at the anode from glass carbon during the electrolysis of concentrated solutions of fluoride-containing compounds. Much attention has been given to determining the optimal technological parameters (current density, electrolyte concentration, temperature) and to devising electrolyzers. However, information on the state of anodic surface necessary for elucidating the mechanism of ozone electrosynthesis is practically absent, aside from paper [4], which presents data based on quantitative capacitive measurements on the existence of specific adsorption of  $\text{HF}_2^-$  ions.

Thus, in concentrated solutions of fluoride-containing compounds the investigation of anodic surface, which forms in the process of ozone electrosynthesis, presents a challenging problem.

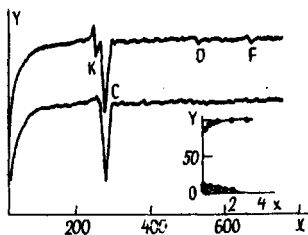


Fig. 1a. AES-spectra of glass carbon surface area after oxidation.

Plot No 1 - outer surface  
Plot No 2 - after 3 min. of ionic etchings.

X - electron energy, eV;

Y - intensity.

Fig. 1b. Element distribution profiles in the depth of glass carbon.

X - time, min.;

Y - concentration, atom %.

Fig. 1 shows electron AES-spectra and profiles of element distribution within glass carbon, oxidized at the anode in 23%  $\text{KHF}_2$  solution during 10 min. at current density of  $0.7 \text{ A.cm}^{-2}$ . Registration was performed on the "Varian" electron spectrometer in an atmosphere of xenon at pressure of  $5 \cdot 10^{-5}$  torr. AES-spectra were induced by initial electron beam with an energy of  $E_p = 3000 \text{ eV}$ , filament current of the electron gun was  $I_c = 2.91 \text{ A}$ , and the anodic current was  $I_A = 40 \mu\text{A}$ . Amplitude of modulating tension at the analyzer was  $U_m = 5 \text{ V}$ , time of potential sweep over energies in the range from 0 to 1000 eV was equal to 5 min. Detector sensitivity during spectra registration was  $25 \mu\text{V}$ , time constant was  $\tau = 0.3 \text{ s}$ . AES-profiling into the deeper parts was conducted by  $\text{Xe}^+$  ion dispersion of the surface at energy of 3000 eV. Emission current of ionic gun was 5 mA, and ionic current at the sample was  $1.5\text{--}2 \mu\text{A}$ . Maximum etching rate was  $v = 80 \text{ A.min}^{-1}$ .

As evident from data of Fig. 1, carbon, potassium, traces (1-2 atom %) of oxygen and fluorine are adsorbed on the surface of glass carbon. The latter are weakly bound to the surface, since 15 s of ionic etching eliminate them from the surface (Fig. 1a).

Oxygen coating on the glass carbon surface, that develops in the process of ozone electrosynthesis, was studied by the impulse potentiodynamic method. Cathodic potentiodynamic plots at glass carbon in 23%  $\text{KHF}_2$  solution were recorded on PI-50-1 potentiostat in an atmosphere of  $\text{N}_2$  according to the following program:  $E_{\text{inor.}}$ , V ( $\tau = 1 \cdot 10^{-3} \text{ s}$ );  $E_{\text{exp.}} = -1.2 \text{ V}, 1 \cdot 10^{-3} \text{ s}$ ;  $E_{\text{ads.}}$  from 1.0 to 3.6 V,  $1 \cdot 10^{-3} \text{ s}$ ;  $E = 1.2 \text{ V}, 1 \cdot 10^{-3} \text{ s}$ , saw-toothed potential was 50 V/s in the range of potentials from 1.2 V to -1.2 V. All potentials are shown according to the reversible hydrogen electrode in the same solution.

The amount of adsorbed oxygen-containing forms, evident from results of cathodic potentiodynamic curve processing, was 8-10 layers\* and increased linearly with time and oxidation potential. It should be noted, that no variation in the potential maximum of reduction of oxygen-containing

forms was observed neither with the change of oxidation potential nor oxidation time. Probably, the adsorption-desorption process of oxygen-containing particles occurs without the formation of definite stoichiometric compounds and with constant bonding energy.

The nature of differential capacity dependence at glass carbon on oxidation potential and current frequency in 23%  $\text{KHF}_2$  solution was studied. Measurements were done on P-5021 alternating current bridge. It was found, that in the potential range from 1.0 V to 2.2 V capacity practically does not depend on the potential and current frequency and is equal to 1-2  $\mu\text{F}\cdot\text{cm}^{-2}$ , thus indicating to the semiconductor nature of adsorbed surface compounds. Increase in differential capacity up to 12-15  $\mu\text{F}\cdot\text{cm}^{-2}$  was recorded over potential values of 2.2 V, further potential growth lead to its drop.

Obtained data reveal, that during electrolysis of concentrated solutions of fluoride-containing compounds at glass carbon the principal mean of ozone formation is the catalytic interaction of bifluoride ion oxidation products in the adsorbed layer with  $\text{H}_2\text{O}$  molecules.

---

\* redox reaction superposition on adsorption-desorption processes of oxygen-containing forms was not taken into account when the degree of filling by oxygen-containing particles was calculated.

#### REFERENCES

1. Patent U.S.A. No 4375395, C 25 B 1/00.
2. Patent U.S.A. No 4541989, C 01 B 13/11.
3. Certificate of Authorship U.S.S.R. No1321771, C 25 B 1/00.
4. Lubushkin V.A., Smirnov V.A., Proc. of the 7<sup>th</sup> Union Conference on Electrochemistry, 1988, Chernovtsy, p. 178.



THE SINGULARITIES OF DIFFUSION RELAXATION OF AN ELECTROLYTE IN THE DOUBLE ELECTRIC LAYER UPON PULSE EFFECTS

V.V. Pototskaya, A.V. Gorodyskii and N.Y. Yevtushenko

Institute of General and Inorganic Chemistry

Ukr.SSR Acad.Sci., Kiev

A mathematical model has been proposed for describing the diffusional relaxation of an electrolyte in the double electric layer upon periodic actions of pulsed rectangular potential with blocked electrodes.

The distributions of diffusion and electric fields in space and time were obtained for the binary electrolyte. The singularities of double electric layer response to the external action have been analyzed depending on duration of a pulse, period of potential pulse recurrence and parameters of the electrochemical system as well. The time of charging double electric layer is characterized by the  $LL_D / D$  value, where  $L$  is the distance between the electrodes,  $L_D$  is the Debye length,  $D$  is the diffusion coefficient of the ion. In this case the characteristic time of a change in the local field of the space charge is expressed by  $t_D = L_D^2 / D$ . The fluctuations of concentrations and field strength in the double electric layer follow external potential pulses, in case of their period  $T < LL_D / D$ . For  $T < LL_D / D$  the form of these fluctuations does not correspond to the pulsed potential waveform. The amplitude of fluctuations of ion flow density increases as moving away from the electrode surface. The most considerable fluctuations of current density take place at the exterior boundary of the diffusion double electric layer. Since the electrodes are blocked, the current at the electrode surface goes to zero. In applying a potential pulse to the electrochemical system the current density increases sharply and reaches a maximum at the end of the pulse. The double elec-

tric layer discharges during the interval, and the current density decreases slowly to some value, whose quantity depends on the pulse duration and period. The presence of local diffusion and electric fields, which do not yet disappear after stopping the external action, causes the slow of charge during the potential interval.

When moving away from the electrode surface the form of current density response to the pulsed potential becomes more and more distorted. Fig. 1 shows the dependence of current density on the distance from the electrode surface for various time values. The relaxation of the space charge is observed, caused by the finite rate of charge motion.

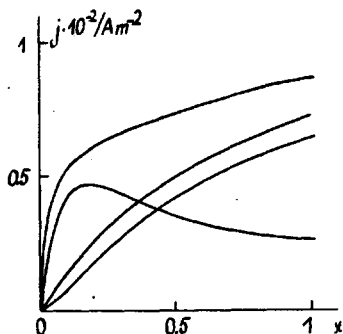


Fig. 1. The distribution of current density in the diffusion double electric layer at various of  $y$ : 1-1; 2-0,6; 3-0,5; 4-0,1;  $T=0,001$  s;  $y_1=0,5$ ;  $y$  is the unitless time in the period,  $y_1$  is the unitless pulse duration.

The study of the diffusion relaxation of electrolyte in the double electric layer allows one to choose the optimum operating conditions for pulsed electrolysis.

INFLUENCE OF PROCESS IN THE NEAR-CATHODIC LAYER  
AT THE COMPOSITION AND THE PROPERTIES OF  
HYDROXIDE DEPOSITS USED AS ANODIC MATERIALS

Y.N.Prodanov, N.V.Kozlova, M.F.Reznik, V.V.Shalaginov, A.E.Avr-  
uschenco, J.S.Lapin, D.M.Shub  
Karpov Institute of Physical Chemistry, Moscow

It is known [1-3] that the basic hydroxide compounds of metals of the ferry group show high electrocatalytic activity in the anodic process of  $O_2$  evolution. The creation of anodic materials on the base of hydroxide deposit out of Fe group metals on the another metal support became possible as a result of the study of processes in the near-cathodic layer during the reduction of metal ions.

The correlation between cathodic processes and composition of the deposits has been investigated by the method of polarisation measurements, by the finding of the correlations of pH in the near-cathodic layer both electrolysis parameters and the composition of the cathodic process. The approximate method of "flowing down" have been used to estimate pH. The composition of the received cathode deposits has been determined by optical methods - infrared spectroscopy, Raman-laser spectroscopy, and the spectroscopy of electron absorption. The anodic current-potential curves were obtained using 1M NaOH as a function of cathode deposit compositions.

It is necessary to increase pH in the near-cathodic layer so that pH in the near-cathodic layer was higher than in the main volume of the electrolyte to obtain a cathode deposit with a high content of the hydroxide phase of the metals. The adsorption and mechanical inclusions of the microparticles of the hydroxides into the cathode deposit result in the formation of the microheterogenous composition consisting of metallic matrix and containing about 40 % hydroxides. The ratio of metallic and hydroxides phases is affected by an intensity of forming of hydroxides in the near-cathodic layer and is controlled by the following factors: compositions and concentra-

tions, pH, temperature of the electrolyte, current density and deposition potential, intensity of mixing and etc. The change of pH of the nearcathodic layer is often connected with the process, discharging of the metals' ions and  $H_3O^+$  ions, which take place at the same time. The existence of side process results in decrease of the cathodic-current efficiency of the main process the electrodeposition of the metal. The increase of pH may be connected with the discharge of  $NO_3^-$  ions in the range of the potentials preceding the metal deposition. It was found, that it was necessary to rise pH by 0,5-1,0 to reach pH of the forming of hydroxides in the near-cathodic layer. Due to the reaction of the forming of the hydroxides, pH of the near-cathodic layer is stabilized.

It is necessary to have low concentrations of the metals ions, high values of pH and high current densities to ensure the formation of the hydroxides in the near-cathodic layer. The cyclic anodic polarization curves in the first cycle have characteristic maximums, or plateaus, which are not seen in the subsequent cycles. It may be connected with the processes of further oxidation of the deposits.

Thus, microheterogenous compositions, consisting of such metals as Fe, Ni, Co and mixed Fe-Ni composition with different content of hydroxide phase were obtained by using the opportunity of influencing the composition of cathode deposits through the processes in the near-cathodic layer.

The investigations of anodic behavior of microheterogenous compositions allowed us to create the new anodic material.

Reference :

1. R.E. Carbonio, V.A. Macagno, M.C. Giordano etc. // J. Applied Electrochem., 1982, v. 12, № 1, p. 121-126.
2. S.I. Cardoba, R.E. Carbonio, M. Lopez Teijlo and V.A. Macagno // Electrochem. Acta, 1986, v. 31, № 10, p. 1321-1332.
3. G. Mlynazek, M. Paszkelewicz and A. Radniecka // J. Applied Electrochem., 1984, v. 14, № 2, p. 145-149.
4. D.M. Shub, Y.N. Prodanov, I.A. Groza etc. // Avt. svid. USSR, № 1579938 ( 1990 ).

APPLICATION OF INTENSITY MODULATED PHOTOCURRENT  
METHOD IN ELECTROCHEMICAL KINETICS

Z.A.Rotenberg, O.A.Semenikhin

A.N.Frumkin Institute of Electrochemistry, USSR Acad.Sci.,  
Moscow.

Photostimulated charge separation in the electrochemical systems including either metallic ( photoemission into solution ) or semiconductor electrodes results in generation of some intermediate particles which take an active part in electrode process. Illuminating the electrode with light of different intensity it is possible to vary their concentration in order to obtain the information about the kinetics of reactions involving such particles. When the light intensity is modulated sinusoidally such information can be obtained from the analysis of frequency dependence of the real and imaginary components of the alternating photocurrent. Illuminating the electrode simultaneously with light of constant and modulated intensity it is possible to investigate the non-linear systems. Here we restrict ourselves to the consideration of the photoelectrochemical process on the semiconductor electrode where the intermediate particles are represented by the minority carriers ( "holes" for n-type semiconductor ) accepted by the surface states.

Photoexcited holes can transfer through the interface either directly from the valence band or via the surface states where they can also participate in recombination process. In this case one can obtain the following expressions for the frequency dependence of the real  $\text{Re}(j)$  and imaginary  $\text{Im}(j)$  components of photocurrent:

$$\text{Re}(j)/\Delta g = 1 - \gamma\beta - \gamma(1-\beta)k_2k/(k^2+\omega^2) \quad (1)$$

$$\text{Im}(j)/\Delta g = \gamma(1-\beta)k_2\omega/(k^2+\omega^2) \quad (2)$$

where  $\Delta g$  represents the ac component of minority carrier flux into surface,  $\omega = 2\pi f$  is a circular frequency,  $\gamma$  characterizes the fraction of holes captured by the surface

states,  $k_2$  is the rate coefficient of the surface recombination,  $k = k_1 + k_2$ , where  $k_1$  is the rate coefficient of hole injection into solution via the surface states. The coefficient  $\beta$  takes into account the dependence of the rate coefficient  $k$  on the constant light intensity. Expressions (1) and (2) are available for the system with the single surface state relaxation time. In this case the frequency response of photocurrent in complex plane is represented by the semicircle. If the relaxation times are distributed, the form of the frequency response distorts.

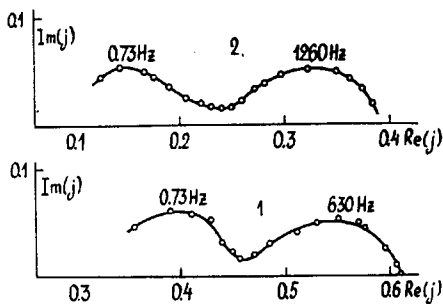


Figure. Complex plane photocurrent plots obtained for Pb/PbO/PbSO<sub>4</sub> in 1 N H<sub>2</sub>SO<sub>4</sub> at the different light intensities  $I$  ( a.u.).  $E = 0,0$  V.<sup>1</sup>

1 -  $I = 6,5$ ; 2 -  $I = 35$

The photocurrent plots in complex plane for two intensities of constant light obtained on the anodically oxidized lead electrode in 1 N H<sub>2</sub>SO<sub>4</sub> in the frequency range 1-6300 Hz with the help of the laser source of light equipped with the electrooptical modulator are shown in figure. . Both plots can be described by two overlapped ellipse arcs. Such form of frequency dependence indicates that the surface

<sup>1</sup>All potentials are given with respect to mercury sulphate reference electrode in the same solution.

state relaxation times are distributed about two mean values corresponding to the frequency at maximum of the imaginary component of photocurrent. Probably the low frequency plot of photocurrent corresponds to the slow reduction of the photoelectrolysis products and the high frequency one can be related to the surface recombination of the minority carriers. Here we take into consideration only the high frequency region where the examined model is available .

The characteristic frequency at maximum of  $\text{Im}(j)$  increases and the value of the high frequency intercept of the photocurrent plots on the real axis decreases with the light intensity thus supporting the assumption about the photoexcited electron participation in the surface recombination process. The detailed analysis of the photocurrent spectra permits us to determine the kinetic coefficients of the photoprocess. The potential dependence of the coefficient  $\gamma$  which characterizes the mechanism of charge transfer through the interface seems to be of interest. It was shown that at too negative potentials ( $E < -0,2 \text{ V}$ )  $\gamma$  is close to 1 and the photoexcited holes transfer onto acceptors mainly via the surface states while at more positive potentials the corresponding values of  $\gamma$  decrease with the potential and it is possible for holes to be injected onto acceptors directly from the valence band.

#### References

1. Li J., Peter L.M. J.Electroanalyt.Chem.,199(1987)1
2. Peat R., Peter L.M. J.Electroanalyt.Chem.,209 (1986)307
3. Pavlov D, Zanova S., Papazov G. J.Electrochem.Soc., 121(1977)1253

ON THE EFFECT OF THE TIME FACTOR ON THE COMPOSITION AND  
STRUCTURE OF THE RENEWED SURFACE OF Sn-Pb ALLOY ELECTRODES  
(based on the capacity measurement data in solutions with  
organic surface-active additives)

V.A.Safonov, M.A.Choba, D.V.Kireev

Chemical Faculty, Moscow State University, Moscow

In /1-3/ it was shown that Pb-Sn alloys are characterized by an enrichment of the surface composition with lead compared to that of the volume. In this work the method of electrochemical measurements on Pb-Sn alloy electrodes with a surface constantly renewed (by means of cutting /4/) was used in order to study the time factor ( $t$ ) effect on the potential dependence of the capacity of the electric double layer ( $C, E$ -curves) in aqueous solutions of surface-inactive electrolytes ( $\text{NaF}$  and  $\text{Na}_2\text{SO}_4$ ) with and without organic additives. The latter were presented by cyclohexanol and tetrabutylammonium cations ( $\text{TBA}^+$ ). Simultaneously a comparison of  $C, E$ -curves with those obtained on the individual Pb- and Sn-electrodes was carried out.

On  $C, E$ -curves in diluted solutions of surface-inactive electrolytes the cathodic shift of the potential of the capacity minimum, which corresponds to the potential of zero charge, was observed with the growth of  $t$ , starting from the moment of alloy surface renewing. It testifies to an increase in the Pb concentration in the surface layer.

When surface-active organic substances are present in the solution the capacity curves have characteristic peaks, corresponding to the adsorption-desorption processes of cyclohexanol molecules or  $\text{TBA}^+$  cations.

The effect of organic substances on the  $C, E$ -dependences was studied in a greater detail. It was found that on the individual metals (Pb and Sn) the cathodic capacity peaks were shifted approximately by 0.4 V in respect to each other (more negative - on Pb) and the capacity maximum on the newly generated surface of Pb-Sn alloy is located between



those peaks and shifts in cathodic direction starting from the moment of surface renewing. This result also indicates the enrichment of the electrode surface with lead atoms.;

The lack of the phenomenon of capacity maximum splitting for cyclohexanol and TBA<sup>+</sup> adsorption-desorption processes on alloy electrodes seems to be significant from the point of view of the model interpretation of the obtained data. This fact makes it possible to exclude for description of C,E-curves the application of the well-known models which are used to describe the crystallographically nonuniform polycrystalline electrodes, i.e. the models of independent electrodes and a single diffusion layer /5/.

The quantitative treatment of the obtained data was carried out within the framework of the model which is in principal analogous to one proposed by Kuznetsov *et al.* for liquid binary alloys (the review of these works one can see in /6/). According to this model the total potential jump on the alloy-solution interface at constant charge of the electrode is determined by the surface share of each of the alloy element, i.e.

$$\Delta E = E - E_G^{M_1} = (E_G^{M_1} - E_G^{M_2}) \cdot \theta, \quad (1)$$

where  $E_G^{M_1}$  and  $E_G^{M_2}$  - potentials for a given charge  $\sigma$  on individual metals,  $\Delta E$  - the potential shift at the same  $\sigma$  on the appearance of the second component on the the surface,  $\theta$  - the surface share of the second component. From the experimental C,E-dependences obtained in sufficiently concentrated NaF solutions corresponding to different  $t$  from the moment of surface renewing,  $\sigma$ ,E-curves were calculated and then, from the equation

$$\theta = (E - E_G^{Sn}) / (E_G^{Pb} - E_G^{Sn}), \quad (2)$$

$\theta$ -values and dependences of  $\theta$  on  $t$  at different  $\sigma$ =const were obtained. Assuming that the adsorption-desorption of TBA<sup>+</sup>

and cyclohexanol molecules on Sn, Pb and Sn-Pb takes place at constant  $\sigma$  for each solution the same calculations of  $\theta$  on  $t$  were made from the potentials of the capacity peaks in the solutions with surface-active additives.

It was found that all these dependences are in a good approximation linearly in  $\theta - \sqrt{t}$  coordinates and remain almost unchanged with the electrode charge. This makes it possible to assume the diffusion nature for the enrichment process of the alloy surface with lead atoms.

The comparison of the obtained data with the results of physical methods of investigation (SIMS and ESCA) made it possible to estimate the diffusion coefficient of Pb in the alloy, which amounted to  $10^{-13} - 10^{-12}$  cm<sup>2</sup>/s.

The obtained data as a whole gives weighty grounds for supposing that the main reason for the enrichment of the newly generated Pb-Sn surface under the conditions of the cathodic polarization lies in the lower values of the reversible work of surface formation on Pb as compared to Sn, and this significant difference remains valid throughout the whole studied region of potentials.

#### References

1. Yu.A.Kukk, T.H.Pyuttsepp, Dvoynoy sloy i adsorbtsiya na tverdykh elektrodakh, Tartu, 5 (1977) 124.
2. L.P.Khmelevaya, B.B.Damaskin, T.I.Vainblat, Elektrokhiimiya, 18 (1982) 1141.
3. R.P.Frankenthal, D.J.Siconolfi, Surf.Sci., 119 (1982) 331.
4. A.G.Zelinskiy, R.Yu.Bek, Elektrokhiimiya, 21 (1985) 66.
5. M.D.Levi, B.B.Damaskin, I.A.Bagotskaya, Itogi nauki i tekhniki. Elektrokhiimiya, Moskva, VINITI, 19 (1983) 3.
6. A.N.Frumkin. Potentsialy nulevogo zaryada. Moskva. Nauka. 1979, 206.

## THE METAL-ELECTROLYTE SURFACE IN THE ELECTRIC FIELD

R.Salem

D.I.Mendelev Chemical and Technological Institute, Moscow

For the purpose of studying the properties of the metal-electrolyte boundary (M/S) the simple jellium model is used nowadays. It is calculated by means of the density-functional formalism. But the self-coordination analysis of the electron structure of interface boundary M/S demands cumbersome calculation /1-3/. On the strength of this it seems very promising to utilize a semi-phenomenological approach, especially when the M/S contact in the external electric field is considered.

It is common to express the liquid metal's surface tension in the form of such specific energies as the electrostatic and the non-electrostatic (i.e. kinetic exchange, and correlational) ones /4/. Instead of analyzing all the problems when making up the microscopic electronic theories of the surface phenomena in the metals (see, for example, reviews /2/ and /3/), we only point out that we are not aware of any work which would have dealt with electrocapillarity. We can write down the change in the liquid metal's surface tension in the external electric field as the change in the Coulomb energy of the double electric layer. Then the electrostatic part of the surface energy takes the form of

$$\gamma = 1/2 \int_{-\infty}^{\infty} \varphi(z+z_0) [n(z+z_0) - n_+ \theta(-z)] dz, \quad (1)$$

where  $\varphi(z+z_0)$  is the potential jump in the double electric layer and it is the solution of the Poisson equations, and  $n(z+z_0)$ ,  $n_+ \theta(-z)$  are the distributions of the electron density at  $z > 0$  and  $z < 0$  correspondingly,  $z$  being the coordinate along the normal to the surface,  $z_0$  is the shift of the electron system (as a whole) in the external field  $E$  which is perpendicular to the M/S boundary.

The noncompensated charge leads to the electric field which can be written down as the one of a plane capacitor

if the charge density  $\delta_e = \pm en_+ z_e / 2, 3/$ . Here  $\delta_e$  is a free parameter.

The equation

$$\Delta \gamma = 2\pi n_D^2 (en_+ kR_S^2 \delta_e - k^2 R_S^2 \delta_e^2) \quad (2)$$

was obtained in /5/ for the electrocapillary curve when Fridel's oscillations together with the change in the barrier in the external field had been taken into consideration.

We clearly can see in (2) that a parabola represents the dependence of the surface-tension drop upon the charge. Its ascending and descending branches are not symmetrical relatively to the sign of  $\delta_e$ .

Our model takes into consideration the noticeable shift of phase ( $\Delta$ ) of Fridel's oscillations (in the dependence of the external field) as well as the change in the electron density ( $n_+, z=0$ ) and shielding radius ( $R_S$ ). Thus, the model has the quantum nature and it is essential for its being adequate to the experiment.

#### References

1. Theory of the Inhomogeneous Electron Gas, ed. by S.Lundquist and N.H.March, Plenum Press, N.Y.-London, 1983.
2. V.F.Ukhov, R.M.Kobeleva, G.V.Dedkov, A.J.Temrokov, Electron-Statistical Theory of Metals and of Ion Crystals, Nauka, Moscow, 1982.
3. A.M.Brodsky, M.I.Urbakh, Electrodynamics of the Metal/Electrolyte Boundary, Nauka, Moscow, 1989.
4. G.Paash, M.Wohn, Phys. St. Sol., 70 (1975) 555.
5. R.R.Salem, Zhurnal Fiz. Khim. 64 (1990) 2836.

STUDY OF EFFECT OF PASSIVATING SUBSTANCES UPON INITIAL  
STAGE SILVER AND PLATINUM ELECTROCRYSTALLIZATION FROM  
MOLTEN SALTS

N.A.Saltykova, L.T.Kosikhin, A.N.Baraboshkin,  
O.V.Portnyagin, N.O.Esina

Institute of Electrochemistry of the USSR  
Academy of Sciences, the Ural Division, Sverdlovsk

The nucleation of silver crystals on platinum microcathodes in silver nitrates melts, containing passivating substances, at 230-360°C has been studied by galvanostatic and potentiostatic methods. The study of initial stage of platinum electrocrystallization was carried out on glassy-carbon microcathodes in the melts of ternary eutectic NaCl-KCl-CsCl, containing platinum chlorides, at 500-700°C by galvanostatic technique. In order to maintain cathode surfaces in stable state electrode was preliminary polarized as anode at +5; +20 mV. Melt  $\text{AgNO}_3$  acquired passivating properties after preliminary overheating of the melt 20-110°C above the electrolysis temperature, leading to the formation of silver oxycompounds in the melt (for example,  $3 \text{Ag}_2\text{O} \cdot \text{AgNO}_3$ ). In a galvanostatic regime passivation in  $\text{AgNO}_3$  melt leads to increase in both the overvoltage maximum of crystal nucleation  $\eta_m$  and the time of its reaching, and also to increase of the growth overvoltage of the nuclei originated (Fig. 1 a, b).

Maximal overvoltage of the nucleation of silver crystals  $\eta_m$  in passivating  $\text{AgNO}_3$  melts reached 60 mV (in non-passivating 40 mV). Platinum electrode capacity in passivating  $\text{AgNO}_3$  melts is much higher than in non-passivating ones and it can reach 1000 F/cm<sup>2</sup>. Increase of electrode capacity in passivating melts occurs apparently due to the increase in silver ad-atoms concentration (at equilibrium silver potential).

One should pay attention to capacity decrease with growth of current density. The exchange current of silver deposition-dissolution, determined by the method /1/, for conditions of nucleation and growth of a single nucleus (average radius  $2 \cdot 10^{-4}$  cm) is by an order lower than in non-

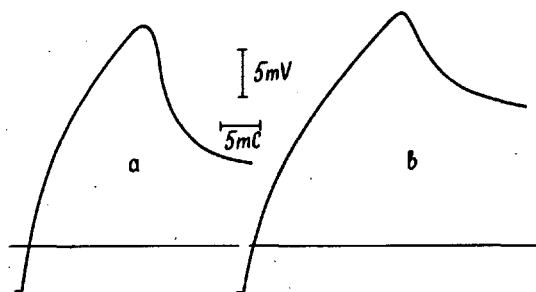


Fig 1. Oscillograms  $\eta - t$  for non-passivating (a) and passivating (b) melts of  $\text{AgNO}_3$ ,  $i = 7,6 \cdot 10^{-4} \text{A/cm}^2$  a-250°C, b-250/300°C (overheating of the melt up to 300°C, 30 min.)

-passivating melts and is equal to 30-50  $\text{A/cm}^2$ . Considerable dependence of silver nucleation upon anode potential magnitude preliminarily applied to cathode and upon exposure time of this potential before cathode current impulse has been established.

The nucleation of a single silver crystal has been studied by potentiostatic technique with application of "autopotentiostat" of original construction [2]. Time of a single crystal arising depends upon magnitude, temperature and state of the substrate. We have maximum in the histograms of times of arising of the first nucleus, that evidences of non-stationary behaviour of the nucleation process both in non-passivating and passivating melts. Non-stationary state is connected with changes substrate state or of ad-atom concentration in the process of nucleation.

Magnitudes of the nucleation constants in Volmer equation for passivating melts are much greater than in non-passivating ones that is explained by the passivator influence not only over depositing substance but on the state of platinum substrate as well.

The investigation of the nucleation of platinum crystals at glassy carbon cathodes from  $\text{NaCl-KCl-CsCl}$  has

shown that at the same time with retaining of general objective laws of nucleation process (increase in the maximal overvoltage and number of nuclei with current density increase, decrease of  $\eta_m$  with increase in the electrolysis temperature, etc) a series of features has been found. In spite of higher electrolysis temperature maximal overvoltage can reach 600 mV. The influence of oxygen-containing impurities in the chloride melt over nucleation parameters has been established. Maximal overvoltage increases at low content of impurities in comparison with pure melts, but at large concentration of oxycompound impurities one can observe decrease of  $\eta_m$  magnitude (on 200-300 mV) that can be the consequence of activation of glassy carbon cathode. One of the reasons of activation of glassy carbon surface is spontaneous chemical deposition of platinum crystals and Pt-C compounds under interaction of oxygen ions with platinum ions (II) and carbon. On the grounds of the experimental curves  $\eta$ -t and the data of number of platinum crystals at the cathode the exchange currents of platinum discharge-ionization process and electrode capacity have been estimated. The exchange current magnitude increases with current density (2-100 A/cm<sup>2</sup>) and electrode capacity drops. Dependence of the exchange current density on the current density can be connected with the dimensions and structure of the crystal nuclei surface. The exchange current magnitude on flat faces should be expected to be lower than on atomic-rough faces. For discussion of experimental results we have proposed model about the influence of foreign substances over the silver and platinum nucleation in molten salts.

1. A.N.Baraboshkin, L.T.Kosikhin, N.A.Saltykova. Doklady of the USSR Academy of Sciences, 160 (1965) 145.
2. A.N.Baraboshkin, L.T.Kosikhin. The Transactions of the Institute of Electrochemistry of the USSR Academy of Sciences, the Ural Division (Sverdlovsk), 18 (1972) 69.

ON THE APPLICATION OF CHRONOCOULOMETRY IN STUDIES OF IONIC  
ADSORPTION ON THE BISMUTH DROP ELECTRODE

V.Semevsky, P.Pärsimägi, M.Väärtnõu, A.Alumaa  
Tartu University, Tartu

The most popular methods in studies of electrical double layer and adsorption phenomena are the measuring of electrode surface tension and differential capacity. The methods based on the direct measurement of electrode charge  $q$  have been used considerably less. However, in recent years a method named chronocoulometry has been applied in studies of adsorption of organic compounds on solid electrodes /1,2/. The essence of that method is as follows: a potential step  $\Delta E$  is produced on the electrode and the dependence of current due to charging of the electrical double layer on time is measured. Integration of current-time dependence during the potential step yields the corresponding change in electrode charge  $\Delta q$ . As has been shown in /1/, the values of differential capacity  $C$  obtained on solid electrodes are often non-equilibrium ones even at very low frequencies of alternate current. However, by the aid of chronocoulometry it is possible to obtain the equilibrium values of  $q$ . This conclusion is proved by the independence of the measured  $\Delta q$  of the measuring time. On the other hand, the application of chronocoulometry requires considerably more complicated equipment, since the values of current must be measured in very short time intervals.

The device for the investigation of adsorption phenomena by the aid of chronocoulometry in our laboratory has been constructed by the firm "Abakus". The initial parameters are introduced and the results registered on an Apple II+ computer. The device permits to produce the potential steps with certain lengths and heights, measure the variation of current in time and after that find the alteration in electrode charge by integration of current-time dependences. The device consists of a potentiostat, current amplifier and integrator,



which work under the control of a microprocessor. The device is characterized by the following parameters: polarizing voltage up to  $\pm 20$  V; polarizing current up to  $\pm 10$  mA; accuracy of keeping of electrode potential  $\pm 2$  mV; the range of potentials on electrode  $+0.3 \dots -2.5$  V; the current in the potential measuring circuit  $< 10^{-9}$  A; the duration of transition period  $< 500$  ns; the range of measuring of current  $0.1 \mu\text{A} \dots 16$  mA; the time of measuring (length of potential step)  $10 \dots 500$  ms. The block-scheme of measuring system is represented in the following figure.

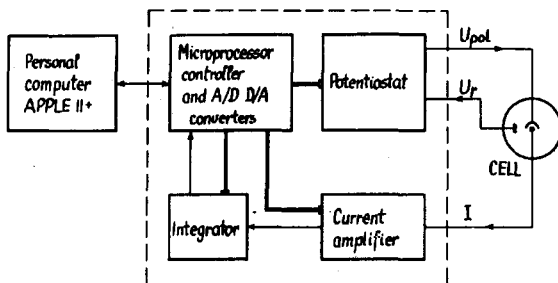


Fig.1. Scheme of the measuring system.

To control the operation of the described device, the adsorption of chloride anions from constant ionic strength solutions  $0.1\text{M LiCl} + 0.1(1-m)\text{M LiClO}_4$  ( $0.01 > m > 1$ ) in ethanol on the solid bismuth drop electrode has been chosen as the subject of investigation because this system has been very thoroughly studied by means of differential capacity measurements [5]. The reference electrode was a saturated calomel electrode. Two different modes have been used for obtaining the  $\Delta q$  values. In first case, the potential step with a constant height  $\Delta E = 100$  mV has been used and the initial potential has been moved continuously towards positive direction. In the second case the initial potential has

been kept constant (-1.0 V) and various  $\Delta E$  have been applied. The range of studied potentials was between -1.4 and 0...-0.2 V (dependent on value of  $m$ ) and the total time of measuring of one  $\Delta q, E$ -curve was less than one minute. After that the  $\Delta q$  values were summarized and the scale of  $q$  changed so that zero coincided with the zero charge potential of bismuth. It has been found that two modes of obtaining the  $\Delta q$  values give very close results (differences in  $\Delta q$  do not exceed 0.2...0.3  $\mu C \cdot cm^{-2}$  for  $|q| < 10 \mu C \cdot cm^{-2}$ ). To find the charge of adsorbed  $Cl^-$ -ions  $q_1$ , the obtained  $q, E$ -curves have been treated according to Hurwitz-Parsons method /3,4/ (analogously to  $q, E$ -curves that were obtained by integration of  $C, E$ -curves).

It has been found that the charge  $q_1$  obtained by chronocoulometry is somewhat less than the same quantity obtained from differential capacity measurements, but the difference is not essential (less than 1...1.5  $\mu C \cdot cm^{-2}$ ). The  $q_1$  values were fitted to virial isotherm and the parameters characterizing the inner layer calculated according to the Grahame-Parsons model. The values of the obtained quantities are presented in the following table. For comparison, analogous values obtained from differential capacity measurements /5/ are also presented. The parameters in the table are as follows:  $B$  - adsorption equilibrium constant;  $B$  - coefficient of the mutual interaction of adsorbed ions;  $K_{02}$  and  $K_{12}$  - integral capacities of the inner layer;  $x_1$  and  $x_2$  - distances of inner and outer Helmholtz planes from electrode surface.

Table 1  
Quantities characterizing the adsorption of  $Cl^-$  ions

Method	$\ln B$	$B/nm^2 \cdot ion^{-1}$	$K_{02}/\mu F \cdot cm^{-2}$	$K_{12}/\mu F \cdot cm^{-2}$	$(x_2 - x_1) \cdot (x_2)^{-1}$
$Q, E$	3.5	3.4	30	73	0.41
$C, E$	3.8	4.2	28	61	0.46

As can be seen from the table, there are no qualitative differences in quantities obtained by different methods.

However, the numerical values differ more than can be caused by measuring errors. We suggest that the values of  $q$  obtained by chronocoulometry are closer to the equilibrium ones than those obtained by integration of C,E-curves, but the differences are by no means so large that the conclusions made previously on the ground of differential capacity measurements can be considered doubtful.

#### References

1. J.Richer, J.Lipkowski, J.Electrochem.Soc., 133 (1986) 121.
2. J.Richer, J.Lipkowski, J.Electroanal.Chem., 251 (1988) 217.
3. H.D.Hurwitz, J.Electroanal.Chem., 10 (1965) 35.
4. E.Dutkiewicz, R.Parsons, J.Electroanal.Chem., 11 (1966) 100.
5. U.Palm, M.Väärtnõu, M.Salve, J.Electroanal.Chem., 86 (1978) 35.

#### ADSORPTION PROPERTIES AND SELECTIVITY OF MANGANESE DIOXIDE IN SEA WATER ELECTROLYSIS

V.V.Shalaginov, M.F.Reznik, E.N.Shchitovskaya, N.B.Kondrikov  
Karpov Institute of Physical Chemistry, Moscow  
Far East State University, Vladivostok

The investigation of the sea water electrolysis with oxygen and hydrogen evolution reactions is of great interest. It has been well known that there are two kinds of processes in sea water (dilute brine) electrolysis: hydrogen-oxygen evolutions reactions and hydrogen-chlorine evolutions reactions. Most anodic materials have higher oxygen overpotentials and a high activity for chlorine evolution.

Sometimes the evolution of chlorine is undesirable, there are difficulties in the utilization of chlorine. In this case the anodes with high selectivity for oxygen evolution should be used. There are only few anodic materials having these properties. The selective properties of these anodes are far from being completely understood. Recent research has been mainly directed to the study of the correlation between adsorption properties and selectivity of the electrodes.

The preparation of the  $MnO_2$  samples was carried out by different methods: by thermal decomposition of  $Mn(NO)_2 \cdot 4H_2O$  and by galvanic deposition under different conditions. Some samples were prepared by anodic deposition, and then these ones were heated for 1 hour at  $350^\circ C$ . The  $MnO_2$  electrodes have different crystallographic structures. The behavior of  $MnO_2$  electrodes has been compared with that of  $RuO_2$ - $TiO_2$ -anodes (DSA).

The study of the selectivity was carried out in solutions with low chlorine concentrations. The  $NaCl$  concentration was 30 g/l, temperature  $25^\circ C$ , the anodic current density 100 mA/cm<sup>2</sup>.

The experiments with the  $MnO_2$  electrodes show that the samples prepared by different methods have different selectivities in dilute brine. The oxygen gas content is 60-98 % and for  $RuO_2$ - $TiO_2$ -anode 30 %, correspondingly.

The cyclic voltammetry characteristics for  $RuO_2$ - $TiO_2$  and  $MnO_2$  electrodes differ significantly. For DSA the electrode reactions of dissolved chlorine (formed at higher overvoltages) influence the  $i$ - $E$  curves profiles. In the cathodic half-cycle, one (or two) well-expressed peaks are observed, which are associated with the reduction of molecular chlorine. The peak current increases with increasing anodic potential in the range from 1.3 to 1.5 V. There is a strong dependence of the cathodic peak current on the hydrodynamic conditions. The peak can be ascribed to either the adsorption or desorption process. But the system is more complicated. The charge that has been determined by integration of  $i$ - $E$

curves is much greater than that for the reduction of a monolayer adsorbate /1/.

For  $MnO_2$  electrodes with different selectivities there are no cathodic peak currents on the  $i$ - $E$  curves.

It has been shown that the preparation parameters, the heat and chemical treatment of the samples and another factors has influence on the selectivity of electrodes.

The stability of the selective properties of  $MnO_2$  electrodes has been studied for a long time.

The data obtained lead us to the supposition that the selective properties of the coatings are conditioned by their crystallochemical structure.

#### Reference

1. V.V.Shalaginov, D.M.Shub, E.V.Kasatkin, Proc. 8th Symp. on Double Layer and Adsorption on Solid Electrodes, Tartu, 1988, p.418.

## INVESTIGATION OF THE WATER CHEMISORPTION ON THE INDIUM SURFACE

M. S. Shapnik, R. R. Nazmutdinov and O. I. Malyucheva

Kazan Institute of Chemical Technology, KAZAN

The chemisorption of a single water molecule on the surface of low index face of indium was studied on the base of cluster models for the metal. Quantum chemical calculations were carried out by using the spin-polarized CNDO/2 programme. The analysis of surface orbitals of the cluster  $In_9$  allows to predict some optimal orientations for  $H_2O_{ads}$ .

1. According to our results the water adsorption on the In surface is nondissociative and the bond O-H stretching does not occur.

2. Two basic types of adsorption sites were found to be possible on the metal surface. The monolayer of water molecules adsorbed in hollow positions by two extreme orientations may be considered as the structured lattice  $c(2 \times 2)$ . Such dipoles contribute essentially to the surface potential drop. Other molecules ( on-top position ) have a more remarkable orientational freedom.

3. The calculations predict the increase in work function for In as a result of the water adsorption. The change of the surface potential drop ( $\Delta\chi^{In}$ ) was estimated in light of well known Frumkin conception /1/. This value ( 0,19V ) is in a good agreement with experimental data.

4. The thickness of the compact layer ( $d_H$ ) at the In/ water interface in NaF solutions is calculated to be about 0,212 nm. The value  $d_H$  obtained is less than one for mercury and does not contradict to capacitance characteristics known for these metals.

5. By comparison of our data with results /2/ the position of indium in the "microscopical" row of the metal hydrophilicity may be proposed:



Attempts to explain the experimental capacitance curves /3/ have been also undertaken.

## References

1. A. N. Frumkin "Potentials of zero charge" Moscow, Nauka, 1982. 260p.
2. An. Kuznetsov, R. R. Nazmutdinov, M. S. Shapnik // Electrochim. Acta, 34 (1989) 1821
3. N. B. Grigorjev, I. A. Gedvillo, N. G. Bardina // Elektrokhimiya, 8 (1972) 409

THE KINETICS OF THE CATHODIC AND ANODIC PROCESSES ON  
THE EUTECTIC ALLOYS OF SILICON AND GERMANIUM WITH  
3d-TRANSITION METALS

A.B.Shein, R.G.Aitov

Perm State University, Perm

New electrode materials with the unique corrosion and electrochemical behaviour are of great importance for the applied electrochemistry. In this aspect the "metal-non-metal" alloys, intermetallic compounds and composition materials are of special interest.

In our recent investigations it has been shown /1-4 / that such compounds, as 3d-transition metal silicides, are very prospective as the materials for the creation of cathodes for the process of hydrogen generation.

In this work the results of the investigation of the cathodic and anodic behaviour of some metal silicides and germanides as well as the eutectic alloys (MeSi-Si, MeGe-Ge) in sulphuric acid are presented.

Intermetallic compounds  $Me_xGe_y$ ,  $Me_xSi_y$  (Me=Fe, Co, Ni) and the eutectic alloys were prepared of pure materials: semiconducted zone-refined germanium (99,99%Ge), electrolytic cobalt (99,98%Co), nickel (99,98%Ni) and iron (99,98% Fe). The investigated electrodes are polycrystalline and single crystals with the surfaces (100), (110), (111) and (210). Before the electrochemical measurements the test electrodes were prepared as in /1/, and then they were placed in the solution of  $H_2SO_4$  in triply distilled water, which was deaerated before and during measurements by bubbling pure  $N_2$ . The polarization and impedance measurements were made with the help of PI-50-1 and R 5021 and structural investigations - with the help of Neophot and JEOL 35 Sm.

The results of the polarization and impedance measurements show, that the main role in the mechanism and kinetics of the cathodic process plays the metallic component of the intermetallides. The role of the non-metallic component (Si, Ge) becomes essential only for the intermetallides with high content of silicon and germanium, for example,  $CoSi_2$ ,  $FeGe_2$ , etc. For such eutectic alloy, as Ge-

-FeGe<sub>2</sub>, the rate of the cathodic reaction is smaller, than for the intermetallic compound FeGe<sub>2</sub>, and it is almost equal to the rate for pure Ge.

The electrocatalytic activity of the surface in regard to the H<sub>2</sub> evolution reaction has been discovered for CoSi. The cathodic currents  $i_c$  (at potential E=const) for CoSi are greater than for pure Co, the Tafel coefficient  $b_c = 0,100-0,110$  V and it is dependent weakly on the crystallographic orientation of the CoSi-electrode surface.

The role of the crystallographic orientation of the surface was investigated for such systems as CoSi, NiSi, FeSi and others. It was shown, that different surface orientation influences mainly on the kinetics, but not on the mechanism of the cathodic process.

The kinetics of the anodic process on the intermetallides and the eutectic alloys was also investigated. It was shown, that the corrosion resistance of MeSi is greater than that of Me and Si. At the very initial moment the rates of the anodic dissolution of MeSi and Me are almost equal. But after some time the anodic currents for MeSi become much weaker than for pure Me, because of the high protective properties of the passive layer of SiO<sub>2</sub>. It was shown that the minimal rate of the anodic dissolution in the range FeSi, CoSi, NiSi is characteristic for CoSi. This fact can be explained in the following way. In the case of CoSi the passive film is formed at the anodic potentials, which consists practically only of SiO<sub>2</sub>. At the same time, in the case of FeSi a mixed oxide (SiO<sub>2</sub>+Fe<sub>2</sub>O<sub>3</sub>) is formed, which is less compact and possesses weak protective properties. The role of the crystallographic orientation of the electrode surface in anodic process is not essential.

The rate of the anodic dissolution of metal germanides, as MeGe, and the eutectic alloys (MeGe-Ge) is smaller than that of metal silicides, because of the weak protective property of GeO and GeO<sub>2</sub>. By the interaction of MeGe-alloys with the solutions, the dissociative adsorption of water molecules occurs, first of all, on the atoms with greater affinity for oxygen (in our case, on Ge-atoms). So, one must expect the weakening of the bond of solution components with some other atoms in alloy (Me-atoms). This weakening of the bond of wa-



ter molecules with Me-atoms makes the process of passivation difficult, which is clearly observed for  $\text{FeGe}_2$  and  $\text{FeGe}_2\text{-Ge}$ .

In the case of such range, as Fe,  $\text{FeGe}_2$ ,  $\text{FeGe}_2\text{-Ge}$  and Ge, the attempt of the quantitative definition of the role of each component of the system (MeGe-Ge) in the kinetics of the cathodic and anodic processes was made. It was shown that the electrochemical properties of the intermetallic  $\text{FeGe}_2$ -electrode differ from the properties of  $\text{FeGe}_2$ -phase in eutectic alloy. The corrosion resistance of  $\text{FeGe}_2$ -phase in the eutectic  $\text{FeGe}_2\text{-Ge}$  alloy is greater, than those of Ge-phase and of pure intermetallic  $\text{FeGe}_2$ .

It was concluded that the principle of independence of electrochemical reactions for each phase and for each component of this phase cannot be used for the analysis of the electrochemical behaviour of two-phase Me-Ge alloys.

The results of the polarization measurements in combination with the surface observation of the dissolving electrodes by SEM show that unlike pure iron, Fe-Ge alloys have not tendency to passivation. The absence of the passive state region, that is conditioned in the case of Fe by the protective properties of  $\text{Fe}_2\text{O}_3$ , makes it possible to assume, that  $\text{Fe}_2\text{O}_3$  is not formed in significant amounts on the surface of the dissolving  $\text{FeGe}_2$ -phase.

Such investigated alloys as NiGe-Ge,  $\text{CoGe}_2\text{-Ge}$  and Ge- $\text{Cu}_3\text{Ge}$  are not passivated in sulphuric acid either.

Some of the investigated materials are suggested to use for the creation of the cathodes, possessing high corrosion resistance in acidic media (CoSi is the best material).

#### References

1. A.B.Shein, *Elektrokhimiya*, 24(1988)1335.
2. R.G.Aitov, A.B.Shein, *Elektrokhimiya*, 26(1990)241.
3. A.B.Shein, *Korrosion (DDR)*, 19(1988)171.
4. A.B.Shein, J.Heyrovsky Centennial Congress/41 st Meeting  
ISE, Prague, August 20.-25.1990, 1990, Fr.-51.

EFFECT OF THE SOLUTION pH AND ADSORPTION OF I<sup>-</sup> IONS ON THE HYDROGEN OVERVOLTAGE ON TANTALUM IN ACIDIC SULPHATE MEDIA

I.N.Sherstobitova

Perm State University, Perm

The polarization measurements were carried out on Ta wire (99.95 %) annealed in vacuum ( $10^{-5}$  mm Hg, 850° C, 2h). To standardize the Ta electrodes surface state, the latter were pretreated in a uniform manner and cathodically polarized in 1 N H<sub>2</sub>SO<sub>4</sub> at current density of about  $1 \cdot 10^{-1}$  A/cm<sup>2</sup> for 1 h; then the polarization curve was recorded in 1 N H<sub>2</sub>SO<sub>4</sub>. Investigating the pH effect, the solution was replaced with one of the solutions as follows: 0.1 N H<sub>2</sub>SO<sub>4</sub> + 0.9 N K<sub>2</sub>SO<sub>4</sub>, pH=1.18; 0.05 N H<sub>2</sub>SO<sub>4</sub> + 0.95 N K<sub>2</sub>SO<sub>4</sub>, pH=2.4; 0.01 N H<sub>2</sub>SO<sub>4</sub> + 0.99 N K<sub>2</sub>SO<sub>4</sub>, pH=3.74. Each of these solutions was pre-deaerated for 1 h with electrolytically obtained hydrogen. To investigate the effect of I<sup>-</sup> ions adsorption, potassium iodide was added in step-by-step increasing portions to 1 N H<sub>2</sub>SO<sub>4</sub> after recording the polarization curve in this solution.

Table 1

Effect of the solution pH on the hydrogen evolution reaction (HER) parameters on Ta in H<sub>2</sub>SO<sub>4</sub> solutions

pH range	Tafel slope, mV·decade <sup>-1</sup>	Transfer coefficient	$\left(\frac{dE}{dpH}\right)_i$ , mV	$\left(\frac{d\eta}{dpH}\right)_i$ , mV
0.3-1.18	200	0.3	198-200	139-141
1.18-2.4	200-240	0.3-0.245	105-110	46-51
2.4-3.74	240-270	0.245-0.22	70-75	11-16

As it is seen from the Table 1, first, the Tafel slope is pH dependent and increases from 0.2 at pH=0.3 up to 0.27 at pH=3.74 and, secondly, the change in pH value results in the (dE/dpH) value change. At pH ranging from 0.3 up to 1.18 the observed value  $(dE/dpH)_i \approx 200-230$  mV can be explained

from the point of view of the slow discharge theory and of the slow electrochemical desorption theory, which is more probable for Ta [1]. According to these theories:

$$\eta = \text{const} - \frac{1-\alpha}{\alpha} \frac{2.3RT}{F} \lg a_{\text{H}_3\text{O}^+} .$$

Since the hydrogen electrode potential (overvoltage is measured regarding it) also depends on the solution pH, then

$$\left( \frac{dE}{dpH_1} \right) = \frac{1-\alpha}{\alpha} \frac{2.3RT}{F} pH + \frac{2.3RT}{F} pH .$$

At  $\alpha \approx 0.3$  (this value corresponds to the Tafel slope of 0.2 V), one obtains

$$\left( \frac{dE}{dpH_1} \right) = 196 \text{ mV}, \quad \text{and} \quad \left( \frac{d\eta}{dpH_1} \right) = 137 \text{ mV}$$

These results are in accordance with the experimental data.

At pH ranging from 1.18 up to 2.4 a considerable decrease of  $d\eta/dpH$  is observed in comparison with the theoretical value for the slow electrochemical desorption, and at pH of about 3.74 the overvoltage can be regarded to be independent of pH. This fact points to the change of the HER mechanism from the slow electrochemical desorption to the slow recombination, and to the gradual surface passivation enhancement at the solution acidity decreasing more probable for Ta, as well. Indeed, the oxide film thickness increase results in the Me-H bond energy ( $E_{\text{Me-H}}$ ) decrease that should accelerate the hydrogen evolution rate and reduce the overvoltage at increase of the pH of the solution. Therefore, the effects of pH raising and  $E_{\text{Me-H}}$  lowering compensate each other. A considerable decrease in  $E_{\text{Me-H}}$  should cause a decrease of the transfer coefficient  $\alpha$  and, hence, the increase of the Tafel slope. The experiments have corroborated the theory. Thus, on the Ta surface passivation enhancement at pH increasing more than 1, our assumptions seem to be confirmed.

The polarization curves recorded on Ta-electrode in the presence of  $\text{I}^-$  ions are presented in the Figure 1. These anions influence the HER actively raising the hydrogen over-

voltage. This effect is more pronounced at lower cathodic potentials where the Ta surface positive charge is greater.

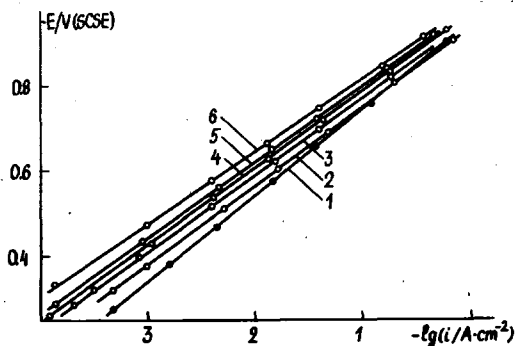


Fig.1. The cathodic polarization curves on Ta electrode in 1 N  $H_2SO_4$  at the  $I^-$  ions concentration as follows (in mole/l): (1) 0; (2)  $3 \cdot 10^{-3}$ ; (3)  $1 \cdot 10^{-2}$ ; (4)  $3 \cdot 10^{-2}$ ; (5)  $1 \cdot 10^{-1}$ ; (6)  $3 \cdot 10^{-1}$ .

The specifically adsorbed  $I^-$  ions decrease the surface coverage with  $H_{ads}$  and  $E_{Me-H}$  and shift the  $\psi'$  potential to more negative values. The first effect results in the hydrogen evolution inhibition at slow electrochemical desorption. The second and the third effects result in the HER acceleration. The first effect seems to be expressed to a greater extent, which is quite possible at a considerable Ta surface coverage with  $H_{ads}$  in the absence of the  $I^-$  ions.

#### Reference

1. B.B.Damaskin, O.A.Petrii. Introduction to the Electrode Kinetics. Moscow, Higher School Publishing House, 1975, p.361.

STATE OF SURFACE OF HIGH-TEMPERATURE ALLOY ZHS6-KP  
AND ITS BASIC COMPONENTS AT ANODIC HIGH-SPEED DISSOLUTION  
IN NON-AQUEOUS PERCHLORATE SOLUTIONS

G.F.Shpak, S.A.Lilin

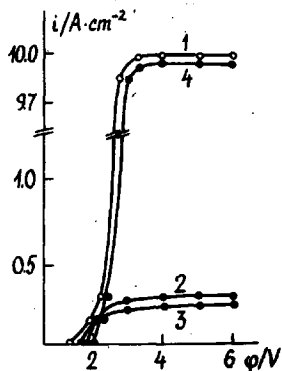
S.Iaso Polytechnical Institute, Kishinev  
Institute of Non-Aqueous Solution Chemistry, USSR Acad. Sci.  
Ivanovo

Behaviour of metals in electrolyte solutions at electrochemical dissolution is dependent enough on the state of anode surface. This refers essentially to the processes of electrochemical finishing in non-aqueous and water-organic solutions of electrolytes.

The dependence of the electrochemical behaviour of alloy ZHS6-KP on the solution nature is visually illustrated by the data shown in the Figure.

Fig.

Potentiostatic polarization curves of dissolution of alloy ZHS6-KP in 1 M solution of  $\text{NaClO}_4$  in various solvents: 1 - water, 2 - formamide (FA), 3 - dimethylformamide (DMFA), 4 - acetonitrile (AN). Rotation speed of disk electrode is 2000 rev/min; solution temperature is 293 K.



The state of surface of alloy ZHS6-KP and that of nickel and chromium (as its basic components) was investigated

Table 1

Dependence of electrophysical parameters of the surface films on ZhS6-KP alloy at its high-speed anodic dissolution in 1 M solution of  $\text{NaClO}_4$  on solvent nature and potential magnitude

Solvent	$\varphi$ , V	$V_{PEP}$ , mV	$W$ , $\Omega \cdot \text{cm}^2 \text{c}^{-1/2}$	$C_1$ , $\mu\text{F} \cdot \text{cm}^{-2}$	$C_2$ , $\mu\text{F} \cdot \text{cm}^{-2}$	Character of surface
Water	1.8	-	-	-	-	Existence of thick black film
	4.0	-	-	-	-	the same
	6.5	0.5	129	77	76	the same
FA	1.8	0.075	-	-	-	the same
	4.0	0.080	258.4	9	20	smooth, bright
DMFA	6.5	0.085	431.7	9.7	14	the same
	1.8	0.25	-	-	-	Existence of thick black film
	4.0	0.3	699.7	9.9	9	smooth, bright
AN	6.5	0.55	521.9	10	20	the same
	1.8	0.08	258.6	5.2	18	the same
	4.0	0.05	877.9	5.7	10	the same
	6.5	0.05	877.9	5.7	10	the same

Note: The magnitudes of the electrophysical parameters of the surface film on ZhS6-KP formed in air:  $V_{PEP} = 0.18$  mV;  $W = 2058 \Omega \text{cm}^2 \text{c}^{-1/2}$ ;  $C_1 = 3.3 \mu\text{F} \cdot \text{cm}^{-2}$ ;  $C_2 = 6.4 \mu\text{F} \cdot \text{cm}^{-2}$ .

by photoelectropolarization (PEP) and impedance spectroscopy methods according to the technique described elsewhere /1/. The results obtained are given in the Table.

As it is shown elsewhere /1/ for the studies on the process of electrochemical finishing of aluminium, capacity  $C_1$  interrelates with the thickness of the surface film. The value of capacity  $C_2$  reflects the degree of the surface pitting (i.e., quality of its finishing). The value of Warburg diffusion impedance (W) characterizes the efficiency of inhibiting, the transfer of metal cations through the film.

Similar results are obtained for nickel and chromium.

It follows from the comparison of the data shown in the Figure and Table 1 that there is a correlation between the parameters of equivalent scheme and the characteristics of electrochemical formation (process productivity and quality of the surface finished). Besides, there is a direct evidence of the differences between the characteristics of the film oxidized in air and the one existing on the surface of anodically dissolved metal.

#### Reference

1. Studies on electrophysical characteristics of surface anodic films on aluminium by the methods of electrode impedance and photoelectropolarization, E.I.Vinogradov, E.P.Grishin, O.I.Nevsky, E.M.Rumyantsev. Ivanovo, 1986. Dep. ONIITECHIM 09.06.86, N 841-khp86.

## THE ELLIPSOMETRIC STUDY OF POLYPYRROLE FILMS

T. Silk, A. Hallik, J. Tamm

Tartu University, Tartu

Polypyrrole (PP) is one of the most studied conducting polymers thanks its good stability to temperature and to acids /1/. PP films can be easily generated electrochemically on various substrates. There have been several ellipsometric studies of conducting polymer films: polyaniline /2/, polyvinylferrocene /3/, polypyrrole /4/, polythionine /5/, polythiophene /6/. In most cases the complex refractive index ( $n-ik$ ) has been determined from the ellipsometric angles  $\Delta$  and  $\Psi$ . According to the majority of investigations the refractive index shows only a slight dependence on the thickness  $d$  of polymeric films, i.e. the films seem to be homogeneous. But it is known that such films have complicated structure: the polymeric chains may be either fibrillar or globular; the dopant ions distribution is not uniform; according to SEM pictures the film is porous etc. This contradiction probably springs from the fact that the authors have been determined the parameters only at some limited thickness range or at relatively large  $d$  values (above 100 nm). It is very important by the computing of  $n$  and  $k$  values to know the exact film thickness, since it can be easily shown that in case of conducting films ( $k \neq 0$ ) we can find greatly different quantities for the parameters depending on the assumptive  $d$ . In most cases the  $d$ -values are calculated from coulometric data, assuming a full current efficiency which may not be correct. According to /7/, where the  $d$  of freestanding PP films were determined from cross sections by SEM the slope of the charge-thickness dependence changes with the synthesis potential. The actual  $d$  can fluctuate ca. 1.5 times at the same amount of charge.

Another difficulty in interpreting the ellipsometric data is caused by the influence of surface roughness. Taking into account the actual roughness is a very serious problem in ellipsometry. Therefore it is necessary to try to realize the measurements on as smooth surfaces as possible. For the ellipsometric studies of conducting polymer films it means



that the  $d$  cannot exceed a certain value  $\sqrt{8}$ .

In present investigation the PP films parameters  $n$  and  $k$  at  $d=20, 40, 70, 100, 150, 200, 400$  and  $700$  nm were determined. The PP in oxidized state was formed electrochemically on a mirror-finished surface of Pt-electrode from acetonitrile solution, containing  $0.1$  M of pyrrole and  $0.15$  M  $\text{NaClO}_4$  as a supporting electrolyte under galvanostatic conditions ( $i=1$  mA/cm<sup>2</sup>). The reduced state of PP was formed in the same solution applying the potential  $-0.6$  V in respect to the saturated aqueous AgCl reference electrode throughout 1 and 5 minutes. We expect to obtain the thickness of  $1$   $\mu\text{m}$  with the passage of  $0.4$  C/cm<sup>2</sup> according to  $\sqrt{8}$ . A L119 ellipsometer equipped with a L118RA automatic rotating analyzer interfaced to a HP-85 desk-top computer was employed. All measurements were performed in air at the wavelength of  $632.8$  nm and the angles of incidence were  $60^\circ$  and  $70^\circ$ .

Experimentally obtained trajectories on the  $\Delta, \Psi$ -plane cannot be described in the framework of homogeneous model, i.e. the  $n$  and  $k$  must be changed with  $d$ , especially in the vicinity of the electrode. The measurements on reduced PP show that in the same region ( up to  $100-150$  nm from the electrode ) a alteration of properties takes place. We should note that the scattering of  $\Delta$  and  $\Psi$  values was greater for reduced PP than for oxidized state.

In order to model the PP films behaviour we used a multilayer model with a layer thickness of  $5$  nm with several regions. The functional dependence of  $n$  and  $k$  upon  $d$  in each region was proposed in the form  $n = n_i + (n_f - n_i) \exp[-ad_x^b]$ , where  $n_i$  and  $n_f$  are the initial and final values, respectively;  $d_x$  - relative thickness in given region and  $a, b$  are formal parameters determining the shape and position of the transition from  $n_i$  to  $n_f$ . In this way we were able to simulate the experimental data with a satisfactory accuracy using 3-6 different regions. We have detected that in all cases there is a deep minimum in  $n, k$ -values at range of  $40-100$  nm from the electrode and the optical constants achieve a more or less fixed values at  $200$  nm. The reduction affects mainly the  $k$ , which decreases 4-5 times in the vicinity of the electrode, the  $n$ -minimum becomes deeper and the maximum

at  $\sim 100-150$  nm appears. It is known that the quantity of  $k$  is connected with the conductivity of the films. Consequently the diminishing of  $k$  may be associated with the decrease in the dopant concentration. This is in accordance with the influence of reduction time on such a behaviour. On the other hand, the removal of dopant ions affects strongly the diameter of polymer fibres which may decrease up to 3 times/B/. It also influences the values of optical parameters.

To summarize the results of simulation of the experimental data we can deduce that the transition from the conducting state to nonconducting one begins at the electrode-polymer interface and propagates to the direction of the solution. The synthesized PP films have complicated structures and thus are to considerable extent inhomogeneous, or at least close to the electrode surface. The ellipsometry is applicable to detect the alterations which take place in the polymeric films of various thicknesses.

#### References

1. G.B. Street, in T.A. Skotheim (Ed.), Handbook of Conducting Polymers, V.1, Marcel Dekker, N.Y. 1986, Ch. 8.
2. S. Gottesfeld, A. Redondo, S. W. Feldberg, J. Electrochem. Soc., 134(1987)272.
3. C. M. Carlin, L. J. Kepley, A. J. Bard, J. Electrochem. Soc., 132(1985)353; G. C. Winston, C. M. Carlin, J. Electrochem. Soc., 135(1988)789.
4. C. Lee, J. Kwak, A. J. Bard, J. Electrochem. Soc., 136(1989)3720
5. C. Lee, J. Kwak, L. J. Kepley, A. J. Bard, J. Electroanal. Chem., 282(1990) 239; A. Hamnett, A. R. Hillman, J. Electroanal. Chem., 195(1985)189.
6. J. Zerbino, W. J. Plieth, G. Kossmehl, J. Electroanal. Chem., 260(1989)361; W. J. Plieth, J. Zerbino, C. Lahmann, G. Kossmehl, J. Electroanal. Chem., 274(1989)213.
7. T. Osaka, K. Naoi, S. Ogano, S. Nakamura, J. Electrochem. Soc., 134(1987)2096.
8. G. Tourillon, in T.A. Skotheim (Ed.), Handbook of Conducting Polymers, V.1, Marcel Dekker, N.Y. 1986, Ch. 9.
9. A. F. Diaz, J. I. Castillo, J. A. Logan, W. Y. Lee, J. Electroanal. Chem., 129(1981)1115; C. S. Choi, H. Tachikawa, J. Am. Chem. Soc., 112(1990) 1757.

## PHOTOEFFECTS AT THE INTERFACE Cu/Cu(II), GLYCINE, $\alpha$ - OR $\beta$ -ALANINE

A. Survila, P. Kalinauskas

Institute of Chemistry and Chemical Technology, Lithuanian Academy of Sciences; Vilnius University, Vilnius

According to [1], the phase  $\text{Cu}_2\text{O}$  layers may be formed on the surface of non-polarized Cu electrodes which are in contact with solutions containing 0.01 M Cu(II) and 0.04 M of glycine either  $\alpha$ - or  $\beta$ -alanine. The thermodynamic probability of these processes may be attained at  $\text{pH} > 4$ , 3.5 and 3.3, respectively, for the series of ligands mentioned. The existence of such surface layers has been confirmed by potentiometric [2], ellipsometric and X-ray spectroscopic data [3].

Compact  $\text{Cu}_2\text{O}$  may be related to the semiconductors of p-type. However, the cuprous oxides formed as thin films under various conditions may gain both hole and electron conductivity.

In order to investigate the photoelectrochemical properties of Cu electrode, the argon laser JTH-406 has been made use of. The laser beam power density was altered from 0.03 to 3  $\text{W cm}^{-2}$  with a wave length ranging from 0.4579 to 0.5145  $\mu\text{m}$ .

In the case of  $\beta$ -alanine system the typical response of electrode potential to a laser beam perturbation takes the following configuration. A sharp fall of the electrode potential from dark value  $E_d$  to minimum one  $E_{\text{min}}$  results from the switching of a laser beam on. The former  $E$  may be described by Nernst equation for the second kind electrode, i.e. taking into account the existence of the  $\text{Cu}_2\text{O}$  layer.  $E_{\text{min}}$  was found to be on the 0.125 V level with no clearly expressed dependence on pH in the pH range from 5 to 8.

The next shift of electrode potential involves rather a slow (within several seconds) rise from  $E_{\text{min}}$  to the steady-state  $E_s$  value. The latter is close to the equilibrium potential of the first kind electrode.

So, at low overvoltages the phase layers in  $\beta$ -alanine system exhibit the properties of n-type semiconductor. The inversion of photocurrent sign is observed at the cathodic polarization of 150 mV order (Fig. 1). The type of layer conductivity also changes in this case.

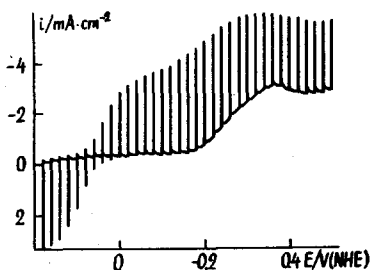


Fig. 1  
The typical response to laser beam pulses of  $\beta$ -alanine system containing 0.01 M Cu(II), 0.1 M ligand and 0.3 M  $K_2SO_4$  at pH = 7

The response of electrode potential exactly reiterates the shape of laser signal, the intensity of which is modulated up to the frequency of 3 kHz (higher frequencies have not been investigated).

In contrast to the  $\beta$ -alanine solutions the positive photopotentials and negative photocurrents prevail at low overvoltages in the case of glycine and  $\alpha$ -alanine systems. The photoeffects are weaker, which is in accordance with the evaluation of thermodynamic probability of  $Cu_2O$  formation.

The different photoelectrochemical properties observed in the systems under investigation can be related to the deviations from stoichiometry of the surface oxide layers. Both the degree and the sign of these deviations depend on the ligand nature as well as on the electrode cathodic polarization value.

#### References

1. A.A. Survila. Electrode processes in systems of labile complexes of metals. Vilnius: Mokslas, 1989.
2. A.A. Survila, V.A. Uksienė, *Elektrokhimiya*, **25**(1989)952.
3. V.A. Uksienė, V.D. Reipa, A.A. Survila. Investigations in the metal deposition field. Vilnius, 1989. P. 33.

## HYDROGEN EVOLUTION REACTION ON THE METALS OF IRON GROUP

J. Tamm, L. Tamm, P. Vares, J. Arold

Tartu University, Tartu

The hydrogen evolution reaction on the metals of iron group has been studied in many works, but it is very difficult to generalize the experimental results obtained. The number of factors which influence the kinetics of the cathodic hydrogen evolution on iron, cobalt and nickel is much larger than for mercury type metals, however this fact is often not been taken into account. A systematic study of the effect of the chemical nature and structure of the metal, the surface state of the electrode, the electrolyte composition and temperature has been carried out in the work to be reported. The electrodes were prepared from different kinds of metals: poly- and single crystal iron and nickel, electrochemically deposited cobalt and nickel. The surface of the electrodes has been polished mechanically, chemically or electrochemically.

It has been established that the rate of the hydrogen evolution reaction depends not only on the nature and structure of the metal, but also on the method of preparing the electrode's surface and on the polarization treatment. In the case of nickel, the most essential factor is the pretreatment of the electrode: the rate of the hydrogen evolution on mechanically polished surface exceeds that on chemically polished surface 50-100 times /1/. The rates on iron electrodes with differently prepared surfaces differ only 5 times, but the purity of the metal has a much stronger influence /2/. If the purity of iron or nickel is high enough, the overvoltage depends only slightly on the structure and purity of the metal.

According to the great number of experimental data nickel is considered to have highest catalytic activity among the metals of iron group. However, the results of our measurements on chemically polished electrodes show that the exchange current densities increase in the sequence Ni Co Fe.

These results can be explained if to assume that hydrogen absorbs into the metal during the cathodic polarization. Hydrogen absorption should decrease the metal-hydrogen bond energy and increase the hydrogen overvoltage. Some experimental data support this supposition. It has been established /1/ that the special surface state with low hydrogen overvoltage can be realized on polycrystalline nickel electrodes, annealed in hydrogen. After the polarization with high cathodic current density this surface state disappeared. A remarkable rise of the hydrogen overvoltage in time after switching on the cathodic polarization is probably also connected with the absorption of hydrogen /3/.

It has been established that for all the electrodes investigated, the dependence of the hydrogen overvoltage on the pH of the solution is less than that proposed by the theory of slow discharge of protons. Obviously the nature of the metal-solution interface in the case of the metals of iron group is mainly determined by the metal-water bond rather than by the electrostatic interactions between ions and the metal surface.

Essential differences in the regularities of the hydrogen evolution on the metals of iron group become also evident in the different influence of the temperature on the hydrogen overvoltage. According to the theory of the elementary act of electrochemical reactions the overvoltage might have an effect mainly on the value of apparent heat of activation. The most unusual results were obtained on mechanically polished nickel: the overvoltage has a major effect on the value of the preexponential factor and influences very slightly the apparent heat of activation. The results on iron electrodes were as proposed by the theory - overvoltage influences mainly the apparent heat of activation.

#### References

1. L.Tamm, J.Tamm, V.Past, Trans. Tartu State Univ., 332 (1974) 3.
2. J.Tamm, P.Vares, *Elektrokhimiya*, 23 (1987) 1269.
3. J.Arold, J.Tamm, *Elektrokhimiya*, 25 (1989) 418.

## OXYGEN REDUCTION ON GOLD

K. Tammeveski, T. Tenno  
Tartu University, Tartu

At present time in the case of amperometric oxygen sensors, cathodes are mainly made of noble metals, of platinum and gold preferably. In the present work the electroreduction of oxygen on gold-covered glassy carbon electrodes has been examined, using the rotating disc electrode technique. A thin layer of gold was applied by means of vacuum evaporation. The measurements were carried out in KOH and KCl solutions. All potentials are given versus saturated calomel electrode (SCE). The solutions were saturated by air oxygen. To obtain reproducible results the working electrode was cycled several times between potentials +0.1 and -1.2 V.

Voltammetry curves for oxygen reduction are shown in the Figure. They are characterized by two waves in 0.1 M and 1.0 M solutions of KOH. The second wave is not well formed. In the potential range from -0.4 to -0.8 V the experimental values of current are higher than required for  $2\bar{e}$  process of oxygen reduction. Additional current was considered due to partial reduction of  $\text{HO}_2^-$  in the region of the first wave [1,2]. The results obtained by Adžić et al. on gold single crystal electrodes testify to the essential dependence of oxygen and hydrogen peroxide reduction process on the surface structure [3-5]. The second wave in current-potential (i,E) curve, which begins at potential -0.8 V is characterized by a gradual rise of the current. At the potential of -1.2 V current gains the value, close to the diffusion limited  $4\bar{e}$  process.

In the solutions of 0.1 M and 1.0 M KCl the same measurements were carried out. In the i,E curve only one wave can be observed. There is a large region of potentials from -0.6 V to -1.2 V, where oxygen reduction current is diffusion limited. This is evident from the plot of  $i^{-1}$  vs.  $\omega^{-1/2}$  ( $\omega$ -rotation rate), where linear dependence is gained, the

approximation of which will pass through the zero.

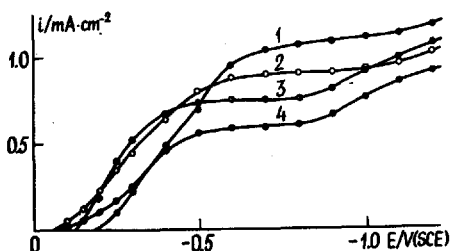


Fig. Voltammetry curves for oxygen reduction on gold covered glassy carbon electrodes in air saturated solutions of: 1- 0.1 M KCl; 2- 1.0 M KCl; 3- 0.1 M KOH; 4- 1.0 M KOH. Sweep rate  $10 \text{ mV}\cdot\text{s}^{-1}$ , rotation rate 1850 rpm.

#### References

1. R. W. Zurilla, R. K. Sen, E. Yeager, *J. Electrochem. Soc.*, **125** (1978) 1103.
2. M. R. Tarasevich, K. A. Radyushkina, V. Yu. Filinovskii, R. Kh. Burshtein, *Elektrokhimiya*, **6** (1970) 1522.
3. R. R. Adžić, N. M. Marković, V. B. Vešović, *J. Electroanal. Chem.*, **165** (1984) 105.
4. N. M. Marković, R. R. Adžić, V. B. Vešović, *J. Electroanal. Chem.*, **165** (1984) 121.
5. N. A. Anastasijević, S. Štrbac, R. R. Adžić, *J. Electroanal. Chem.*, **240** (1988) 239.



SPECIFIC FEATURES OF THE ADSORPTION OF  
MACROHETEROCYCLES ON A METAL ELECTRODE

M.R.Tarasevich, L.A.Khanova, L.F.Lafi

A.N.Frumkin Institute of Electrochemistry, USSR Acad. Sci.,  
Moscow

It has been shown by the example of chlorophyll (Chl), pheophytin (Phe), tetraphenylporphyrin ( $H_2TPP$ ), Zn-tetraphenylporphyrin (ZnTPP), Zn-ethioporphyrin (ZnEP), coproporphyrin ( $H_2CP$ ) and iron dicarbonyl ( $FeCb_2$ ) that substances with developed conjugated systems of delocalized electrons exhibit irreversible adsorption on a metal surface. This effect is observed not only for  $\pi$ -conjugated macrocycles (porphyrins), but also for an electron-deficient compound iron dicarbonyl.

Adsorption was carried out from aqueous and aprotic solvents: from aqueous solutions of Chl, Phe,  $H_2TPP$ , ZnTPP,  $H_2CP$ , ZnEP solubilized with acetone; Chl solutions in acetone, butyrolactone, propylene carbonate, solutions of  $H_2TPP$ , ZnTPP in acetone, aqueous solutions of  $FeCb_2$ . Solubilized solutions are monomeric nonequilibrium systems; solutions of porphyrins in the aprotic solvents mentioned are true solutions. In spite of the fact that solutions of different nature were used, irreversible adsorption was observed in all the cases. No new products were formed during adsorption, destruction and polymerization products in particular.

The adsorption cannot be explained by the hydrophobic nature of the substances studied, since, for example, after thorough washing off with acetone, dibenzo-18-crown-6, which is readily adsorbed on an amalgamated platinum electrode, is completely removed from the surface.

The specific features of irreversible nondestructive adsorption of porphyrine and  $FeCb_2$  differ qualitatively both from those of reversible physical adsorption and irreversible destructive adsorption. The irreversible adsorption of porphyrins is characterized by the concentration-independent adsorption in a certain concentration range and by presence

of several states of adsorbed substances depending on the adsorption conditions (substance concentration, potential and solvent nature). It is shown that transition from one adsorbed state to another is possible. There being no equilibrium between the dissolved and adsorbed substances, adsorption on the surface can occur in states which are not energetically the most favorable ones. The solvent nature, concentration of the substance being adsorbed and electrode potential create different conditions for the molecule present in the layer adjacent to the electrode at the moment of adsorption. The irreversible adsorption on the electrode fixes these metastable states. In passing to more negative potentials during measurement of the current-voltage curve, a transition from a less to more energetically favorable state is possible.

The electrochemical reactions of adsorbed porphyrins have been studied. As the potential of the redox reaction of a strongly adsorbed substance differs from that of the redox reaction of the unadsorbed substance, it is possible to make use of this property for studying electron tunnelling processes. The possibility of electron tunnelling through a cetyl alcohol monolayer (2 nm thick) on an amalgamated platinum electrode in a dark redox reaction of iron dicarbonyl has been proved with the use of qualitative criteria.

ON THE REASON OF THE ONSET OF ZERO ESTANCE IN THE  
INTERFACE "REVERSIBLE ELECTRODE/SOLID ELECTROLYTE"

A.Ya.Tarasov, A.T.Filyayev

Institute of Electrochemistry, Ural Department of the USSR  
Acad. of Sci., Sverdlovsk

Studying the estance of the interfaces  $\text{Ag}/\alpha\text{-AgI}$  ( $\text{AgCl}$ ,  $\text{AgBr}$ ,  $\text{Ag}_4\text{RbI}_5$ ,  $\text{Ag}_6\text{I}_4\text{WO}_4$ ) /1/ and  $\text{Cu}/\text{CuBr}$  ( $\text{Cu}_4\text{RbCl}_3.25\text{I}_{1.75}$ ) a discovery was made that after several cyclic variations of potential in the range  $0 \leq \varphi \leq 0.6$  V in respect to a corresponding reference electrode, the estance curves that take place in a segment of values that are more positive than  $\varphi = 0.02$  V (silver electrode) and  $\varphi = 0.04$  V (copper electrode) drop to the zero line, and then at  $\varphi \geq 0.05$  V (Ag) and  $\varphi \geq 0.09$  V (Cu) the estance is zero everywhere. Since these reference electrodes always have metal oxides on their surface, and the processes of overvoltage and "undervoltage" in electrodisolution and electrodeposition occur /1/ that can introduce corresponding changes to the forms of estance curves, then the further studies (that are more correct) were carried out on the electrochemical system  $\text{Ag}/\text{Ag}_{2.5}\text{S}/\text{SEL}$  (solid electrolyte)/ $\text{Ag}_{2.5}\text{S}/\text{Ag}$  with maximum saturation with silver of  $\text{Ag}_{2.5}\text{S}$  ( $\delta = \delta_{\text{max}}$ ) that executed functions of reversible silver electrode. Saturation of silver sulfide with silver at  $T > 450$  K results in the onset of mixed electron-ionic conductivity in it, the electron conductivity being very high /2/. Results of studying the estance of this system fully agree with those obtained in respect to the interface  $\text{Ag}/\text{SEL}$  (Fig.1).

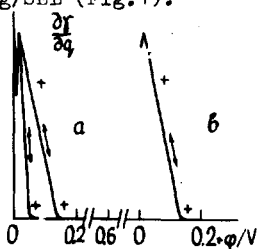


Fig.1

Dependences of the estance modulus on potential of the interface  $\text{Ag}/\text{AgBr}$  at  $T=683$  K,  $V=10^{-3}$  V/s,  $f_e=3.62$  kHz (a) and  $\text{Ag}/\text{Ag}_2\text{S}/\text{AgBr}$  at  $T=683$  K,  $V=10^{-3}$  V/s,  $f_e=3.28$  kHz (b).

Let us consider the reasons that result in the zero dependence of the estance on potential.

Run of alternating current through half element  $Ag/Ag_{2+\delta}S/SEL$  is accompanied by the onset of temperature difference between the silver electrode and SEL. This is caused by Joule's and Peltier's heat effects. Joule's heat is estimated from the strength of the current passing through the resistance of silver sulfide:  $Q=I^2 \cdot R$ . But there is no necessity to estimate it, since we have two identical in thickness layers of  $Ag_2S$  that are disposed symmetrically to the soundguide (SEL) /3/, and this is the reason why the arising heat deformations in these layers are levelled. The thermodynamical essence of Peltier's heat is caused by the difference in values  $\Delta H$  and  $\Delta Z$  for the electrode process  $Ag^+ + \bar{e} \rightleftharpoons Ag_{ads} - W_1$ , i.e.  $\Delta Z - \Delta H = -T\Delta S = T(\partial E/\partial T) = W_1$ , where  $\Delta Z$ ,  $\Delta H$ ,  $\Delta S$  are variations in isobar potential, the reaction enthalpy (heat effect) and the process entropy, respectively;  $\partial E/\partial T$  (Seebeck's coefficient) is the thermal potential of thermogalvanic element  $Ag/AgX/Ag$  ( $X$  stands for halogen) with values of  $AgX$  for  $\alpha$ - $AgI$ ,  $AgCl$  and  $AgBr$  taken from /4/. Since under the temperatures of the study and at  $\delta=0$  the electron conductivity of  $Ag_{2+\delta}S$  is high (the more so, as  $\delta = \delta_{max}$  that is a degree of deviation from stoichiometry), then in the interface  $Ag_{2+\delta}S/SEL$ , with positive polarization (by constant current) of silver electrode, the oxidation of halogen (as at  $Ag$  electrode) will occur:  $X_{el}^- - \bar{e}_{el-de}(Ag_2S) \rightarrow X_{ads}$ . This will be accompanied by the transition of cations  $Ag^+$  from silver sulfide to SEL. With superposition of variable component onto the mean potential (constant current) the energy of the interphase layer will undergo changes and generate mechanical oscillations on both electrodes (bipolar electrode /3/) recorded by piezoelectric element. Since the ionic conductivity of  $Ag_2S$  is considerably poorer than the electron one, then in the interface of silver sulfide/SEL, reversible reaction  $Ag - \bar{e} \rightleftharpoons Ag^+ + W_1$  must unequivocally occur, with heat effect  $W_1$  (in the field of alternating current), i.e. heat fluctuations on each half-element of the electrochemical system shall be synchronous: one of the half-element's electrodes is cooled ( $\Delta q > 0$ ), which cor-

responds to the increase in the surface tension ( $\Delta\gamma > 0$ ), and the other one is heated ( $\Delta q < 0$ ), which corresponds to the decrease in the surface tension ( $\Delta\gamma < 0$ ). In this case, the estance curve (everywhere positive) must be raised above the zero line by the value of the reaction heat effect  $W_1/5$ . But this is not observed. Reaction  $X^- - \bar{e} \rightleftharpoons X_{ads} + W_2$  can not level this heat effect, if only for the simple reason that  $W_2$  strongly exceeds  $W_1$  in the absolute value. On the other hand, this is a slow relaxation process.

It is known from the literature, e.g., that the process of dissolution of bromine in SEL AgBr proceeds via the reaction  $Br \rightarrow Br^- + [e^+] + W_3$  with heat effect  $W_3$  that is equal in the absolute value to that of the reversible reaction of silver but with the opposite sign (at  $T=683$  K,  $W_3=0.44$  V /6/ and  $W_1=0.44$  V, a ratio of  $1V=23.06$  kcal/faraday being admitted here),  $[e^+]$  stands for electron hole. Let us imagine now that negative half-wave of sinusoidal component, on one of the electrodes of half-element of the electrochemical system, reaction  $Ag^+ + \bar{e} \rightleftharpoons Ag_{ads} - 0.44$  V takes place. Simultaneously, at the same electrode, reaction  $Br \rightleftharpoons Br^- + [e^+] + 0.44$  V occurs (countercurrent of electron holes and silver cations). Hence, the total process  $Ag^+ + \bar{e} + Br_{ads} \rightleftharpoons Ag_{ads} + Br^- + [e^+]$  occurring at one of the electrodes has no heat effect, and, consequently, the estance is zero. It is for this reason that in numerous measurements of impedance // at reversible electrodes, parallel to Faraday's process, a circuit arises that refers to non-basic charge carriers.

#### References

1. A.Ya.Tarasov, S.V.Karpachev and other, Dokl. AN SSSR, 30 1 (1988) 389.
2. C.Wagner, J.Chem.Phys, 21 (1953) 1819.
3. V.A.Prusov, A.T.Filyayev, A.Ya.Tarasov, Avt.svid.N1242766 B.I.N 25, 1986.
4. B.F.Markov, Ye.B.Kuzyakin, Tez.dokl.IV Vsesoyuz.sov.fiz.khimii i elektrokhimii raspl.solei i shlakov, Kiev, 1971.
5. A.Ya.Gokhstein, Poverkhnostnoye natyazheniye tverdykh tel i adsorbtsiya, M.: Nauka, 1976.
6. D.O.Raleigh, J.Phys.Chem.Sol., 26 (1965) 329.
7. Ye.A.Ukshe, N.G.Bukun, Tverd.elektrolity, M.: Nauka, 1977.

ADSORPTIVE AND ELECTROCHEMICAL PROPERTIES OF PLATINUM FILM  
OF DIFFERENT DISPERSION DEPOSITED ON TITANIUM BASE

Yu.V.Telepnya, D.M.Shub

Karpov Institute of Physical Chemistry, Moscow

The study of correlation between dispersion properties of electrodes and the conditions of their production arouses interest in connection with decision of electrocatalytic problems, as the platinum film anode has a wide range of application. It is known that the composition and properties of electrolyte solution nature and state of cations and anions, character of chemisorbed oxide layers, pH and promoters influence both electrochemical activity and selectivity of platinum electrode in the case of peroxydisulphate-anion synthesis /1/. However, the regularities of electrochemical properties' change of platinum film anode with different true surfaces have been studied insufficiently /2/.

The kinetics of  $\text{PtCl}_6^{2-}$  complexes reduction was investigated by pulse potentiodynamics and steady-state polarization curve (PC) methods. The deposition of platinum on titanium base from acidic electrolytes in the range of the hydrogen section of potentiodynamic curve (PDC) and at more negative potentials was investigated. The conditions have a great effect on the roughness factor (RF) of the platinum deposits. The RF increases while the current density, platinum complexes concentration and temperature rise.

Obviously, the properties of the electrolytic platinum deposits and the degree of their roughness depend on the relation between the formation rate of platinum atoms and their inclusion into crystal lattice.

Shift of PC for the electrodes with high RF in direction of higher rates of oxygen evolution reaction was discovered by polarization measurements on electrodes with different RF (3, 40, 120, 300) in 3.3 M  $(\text{NH}_4)_2\text{SO}_4 + 0.1 \text{ M H}_2\text{SO}_4$  electrolyte. The high slopes of E-I curves are connected with semiconductor changes of the oxidized surface state and semiconductor nature of oxygen layers formed at anodic potentials. The in-

crease in ohmic losses on the electrode with  $RF=40$  may be connected with an additional resistance in pores and on the borders of "grains" of the platinum film anode. It leads to the lowering of the potential possible to realize on the electrode and of the efficiency of electrosynthesis connected with this potential. It was found from balance experiments in the sulphate solution that with the RF increase in the range from 3 to 300 the rate of peroxydisulphate formation and the current efficiency decrease rapidly from 75 to 1.5. It was interesting to study the composition and properties of oxygen coverages, formed at high anodic potentials under these conditions.

The peculiarities of hydrogen adsorption-desorption processes and oxygen chemisorption in the range of potentials from 1.2 to 3.6 V (NHE) were investigated by cathodic potentiodynamics. After computer treatment of the results the correlation between the degree of the oxygen species coverage (CO-1.3 and CO-2 forms) and the RF was found. The increase in oxygen evolution rate at potentials 2.5-3.6 V in sequence of electrodes with RF values 3, 40, 120, 300 is connected with the rise of labile oxygen share for the CO-2 form. It correlates with strengthening of the CO-2 species bond observed in potentiodynamic experiments (the shift of reduction peak to more cathodic potentials).

The change of the adsorption surface properties and the differences in oxygen evolution reaction rate of the Ti/Pt electrodes with various dispersions is evidently the cause of different selectivity in peroxydisulphate-anion synthesis.

#### References

1. V.I.Veselovsky, A.A.Rakov, E.V.Kasatkin.A.A.Yakovleva.in Adsorption and Electric Double Layer in Electrochemistry, ed. by A.N.Frumkin and B.B.Damaskin, Nauka,Moscow, 1972, p.132.
2. G.A.Seryshev, Chemistry and Technology of Hydrogen Peroxide, Khimiya, Leningrad, 1984, p.48.

## THE DISTRIBUTION OF GAS COMPONENT IN THE INTERPHASAL BOUNDARY

T. Tenno, A. Mashirin  
Tartu University, Tartu

The application of amperometric diffusion limited sensor of soluble gas guarantees measuring of its contents in the units of effective concentration [1]. For the environments with different thermodynamic properties (organic liquids, water, salt solutions and others) the same values of effective concentration  $c_e$  express one and the same level of physical interaction between the soluble gas and the membrane of the sensor through the interphasal boundary. This interaction functions through equilibrium distribution of the given gas component between boundary phases (environment - sensor membrane). The effectivity coefficient  $k_h$  ( $c_e = k_h c$ , where  $c$  is concentration) is expressed with regard to gas environment as basic.

The equilibrium distribution of gas components between the phases is attained by means of equal and opposite flows of gas components through boundary interphasal surface, e.g., between gas (g) and liquid (s) phases:

$$j_{gs} = j_{sg} \quad (1)$$

where  $j_{gs} = k_{gs} * j_{gd}$  is the equilibrium gas flow density from the gas phase into the liquid phase,  $j_{sg} = k_{sg} * j_{sd}$  - equilibrium gas flow density from the liquid phase into the gas phase,  $k_{gs}$  and  $k_{sg}$  are probability coefficients of transition of gas component molecules from the gas phase into the liquid phase and vice versa,  $j_{gd}$  and  $j_{sd}$  are the flow densities of the gas component self-diffusion in the gas and liquid phases.

The coefficients  $k_{gs}$  and  $k_{sg}$  are connected with the average energy of transition of gas molecules through interphasal boundary, but the parameters  $j_{gd}$  and  $j_{sd}$  - are connected with the diffusion characteristics of these phases:



$$j_{gd} = c_g (\bar{v}_g)_x m, \quad (2)$$

$$j_{sd} = c_s (\bar{v}_s)_x m, \quad (3)$$

where  $c_g$  and  $c_s$  denote the concentration of gas component in gas and liquid phases,  $(\bar{v}_g)_x$  and  $(\bar{v}_s)_x$  are the average velocities of diffusion translation of gas component to interphasal surface (along a given axis) from gas and liquid phase,  $m$  - is the mass of gas component molecule.

Thus in establishing the equilibrium distribution of gas component between the phases, their diffusion characteristics are also participating. Besides, it is necessary to mention that in equation (1) only the  $c_g$  and  $c_s$  characterize the content of gas component in the gas and liquid phases. We can assume that by establishing equilibrium state the partial pressure of the gas component in the gas phase appears as a measure concentration, on the one hand. On the other hand, as an energy parameter, the partial pressure may participate in the total change of the energetic state of gas component by its transition through the boundary phases and influence the value of coefficients of probability of transitions  $k_{gs}$  and  $k_{sg}$ .

As a result of the presented discussion, we could conclude that immediate physical factors of establishing equilibrium distribution of gas component in the heterogeneous system are:

- diffusion characteristics of phases of the heterogeneous system,
- energetic probabilities of transition of gas component through the interphasal boundary.

The above-mentioned physical factors characterize the soluble state of gas component and permit to widen the comprehension about effective concentration as a physical parameter by determining the contents of soluble gas component.

#### References

1. V. Past, T. Tenno, K. Bergmann, *Electrochimija*, 17(1981), 1094

## DEPOSITION POTENTIAL AND ZERO CHARGE POTENTIAL AS ELECTROCRYSTALLIZATION PARAMETERS OF METALS

Yu.M.Tjurin, V.V.Izotova, V.I.Naumov, T.V.Sazont'eva

Nizhny Novgorod Polytechnical Institute, Nizhny Novgorod

Considerable advances have been made up to now in the area of the electrocapillarity theory, including unbalanced electrodes under conditions of the surface layer conversions governed by the oxide and crystal formation, by corrosion etc. /1,2/. The surface forming work, depending, according to this theory, on  $E$ ,  $\Gamma_i$ ,  $\mu_i$  and zero charge potential position, appears in the main kinetic, energetic and structural relationships of the electrocrystallization theory. The simultaneous discussion of electrocapillary and electrocrystallization theories is not found in the literature and consideration of electrocapillary phenomena covers mainly the adsorption range of the surface active substances.

In this report from that point of view, the relationships between the surface formation work, surface tension, wettability, soldering ability, lustre, microhardness, internal stresses, porosity, structure and morphology for the series of commercial and electrodeposited metals (Ag, Cu, Ni, Sn and their alloys with Bi and Pb) at the boundary metal/solution and metal/air and polarization potential ( $E_{pol}$ ) and deposition potential ( $E_{dep}$ ) are analyzed. The objects were selected so that their electrocrystallization potentials would be in the range of electrodeposition.

As substantiated, the quantitative measure of the surface work ( $\sigma$ ) is the Rebinder hardness, the surface tension ( $\gamma$ ) is the linear electrode deformation under polarization conditions and  $\sigma, E_{pol}$  curves proper are the unbalanced analogues of the electrocapillary curves. It was found that a common property of hard electrodes in a wide range of cathodic potentials is the polyextremal behaviour of  $\sigma, E_{pol}$  and  $\gamma, E_{pol}$  relations. The maxima for  $\sigma, E_{pol}$  curves are identified as zero charge potentials, while the minima as the

area of crossing of adjacent electrocapillary curves where the sign of the surface charge is not determined as a single-valued function. The fact of realization of several electrocapillary curves and, correspondingly, zero charge potentials on the same metals (for the Cu, Ni and Sn - Bi alloy there are two such values; for the Pb, Sn and Sn - Pb alloy in acidic solutions there is one value for each; for the alkaline solutions there are two or more; for the Ag in the neutral solution there are four values) allows one to define the problem of the zero charge potentials multiplicity for the hard metals and to clarify some debated issues of the problem already on this stage of the studies. Interpretation of realization mechanisms for the zero charge potentials and electrocapillary curves is proposed.

It has been found in the studies of metals and alloys that the zero charge potential plays the role of a parameter governing the value of the excess surface energy of the electrochemical deposit. The surface forming work relationship to  $E_{dep}$  is the representation of the corresponding  $\sigma$ ,  $E_{pol}$  curves (Fig. 1) and the deposits having formed potentiometrically in the vicinity of the depositing metal zero charge potential, show the maximum value not only for the work of forming but also for the adhesive tension, wettability and soldering ability as well. The further investigation of the electrochemical deposit characteristics allowed one to classify the properties of deposit that are in the cause- and consequence relationship with the work of forming and the surface charge and not correlated with the change of  $\sigma$ . It has been shown, that the orientation, size and form of grains, surface roughness, internal tensions and microhardness of electrolytic deposits do not define conclusively the character of the surface forming work relationship to  $E_{dep}$  and in turn, they are not governed by this relationship. On the contrary, relationships of the number of surface defects (etching dots), porosity, hydrogen evolution reaction exchange current and surface forming work to  $E_{dep}$  are similar. It has also been found that the absolute maxima for deposit lustre are observed in the area of ascending

branches of potentials of  $\sigma, E_{pol}$  curves that correspond to the positive surface charges and predominant anion adsorption potentials which most likely are of levelling behaviour.

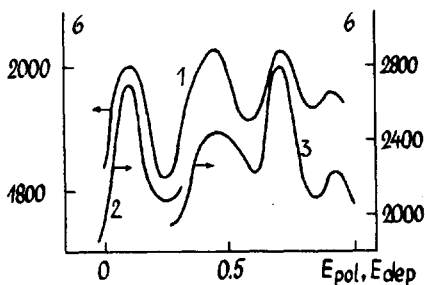


Fig.1. Surface forming work for the commercial (curve 1) and electrodeposited (curves 2,3) silver samples as a function of  $E_{pol}$  at the background of 0.5 M  $Na_2SO_4$  (curve 1) and  $E_{dep}$  (curve 2 - thiosulfate, curve 3 - ferric ferrocyanide silvering electrolyte).

As a result, a new effect of maximum hardness realization, surface forming work, surface adhesive tension at electrodeposition of metals in the vicinity of their zero charge potential was found, that can be used for having the desired influence on wettability, soldering ability, electrocatalytic and anodic (corrosive) activity and other functional properties of electrodeposited coatings.

#### References

1. Yu.M.Tjurin, V.I.Naumov, L.A.Smirnova, *Elektrokhimiya*, 15 (1979) 1022.
2. V.I.Naumov, T.V.Sazont'eva, Yu.M.Tjurin, *Elektrokhimiya*, 24 (1988) 1455.

SPECTRAL PROPERTIES OF ELECTROCHEMICALLY  
GENERATED CUPRATE FILMS

G.A.Tsirlina, R.M.Lazorenko-Manevich, L.A.Sokolova,  
O.A.Petrii

Moscow State University, Moscow  
Karpov Physicochemical Institute, Moscow

It is known that cuprate and cuprite films have interesting photoelectrochemical properties /1,2/. However, the partially hydrated thin oxide layers on Cu were investigated only in aqueous alkaline solutions containing alkali metal cations. Nowadays in view of anodic electrosynthesis of Cu-based high temperature superconductors /3/ such films attract great attention, especially those containing heavy cations, i.e. alkali-earth metals, Tl, Bi, Pb and some others.

In present communication some new data are presented concerning optical and electrochemical properties of Cu-Ba- and Cu-Tl-mixed oxide films on the polished Cu surface and their comparison with pure cuprate films.

According to the cyclic voltammograms and stationary polarization curves, the presence of  $Ba^{2+}$  in the solution strongly influences the kinetics of copper passivation and dissolution. The peak height of active dissolution decreases and the current in the passive region increases in comparison with those in NaOH solutions at the same values of pH.

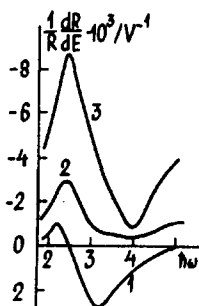
The addition of  $Tl^+$  salts leads to the appearance of anodic currents of  $Tl_2O_3$  deposition in the region of Cu oxidation, resulting in the Tafel relationship with the slope about 130 mV which holds up to oxygen evolution potential.

The electroreflection spectra ( $dR/RdE, \hbar\omega$ ) (figure) were measured in 0,46 M NaOH solution on the copper rodes previously anodized in basic solutions of NaOH (curve 1), NaOH +  $Tl_2SO_4$  (curve 2) and  $Ba(OH)_2$  (curve 3).

The main tendencies observed are growth of negative signal peak at 2,1-2,4 eV and the disappearance of positive signal peak at 3,2 eV with the cationic modification of film. Incorporation of cations ( $Ba^{2+}$  or  $Tl^{3+}$ ) into cuprate

was detected by Auger spectroscopy. It was shown that negative signal peak height vs potential curves have maxima at potentials which differ from each other for the films of various compositions.

Fig.  
Electroreflection spectra (real part) of Cu-(1), Cu-Ba(2) and Cu-Tl(3) containing oxide films (see text) measured in 0,46 M NaOH solution at 1,3 V (RHE). Modulation - 70 mV, 15 Hz.



As for acetonitrile solutions, electroreflection signals for all cuprate films are lower than  $10^{-4} \text{ V}^{-1}$  in a wide spectral region. The existence of peaks only in aqueous solutions gives evidence that the appearance of these peaks is caused by  $\text{H}_2\text{O}$  and (or) oxygen adsorption on the oxide surface. Hence, the data presented in the figure show a significant difference between the adsorption behaviour of pure and modified cuprate films.

The shape of spectra of cuprates is typical for the spectra of passive oxide films on different metals and is in qualitative agreement with the idea of water chemisorption on inhomogeneous oxide surface developed earlier /4/.

#### References

1. U. Collisi, H.-H. Strehblow, J. Electroanal. Chem., 210(1986)213.
2. J. Drogg, C. Alderliesten, P. Alderliesten, G. Bootsma, J. Electroanal. Chem., 111(1980)61.
3. G.A. Tsirlina, S.N. Putilin, O.A. Petrii et al, Sverkhprovodimost, 5(1991), in press.
4. R.M. Lazorenko-Manevich, L.A. Sokolova, Zashchita Metallov, 27(1991), in press.

THE DIFFERENTIATION OF THE SURFACE ACTIVE CENTRES  
RESPONSIBLE FOR CHEMICAL AND ELECTROCHEMICAL  
METAL DISSOLUTION

L.E.Tsygankova

Tambov State Pedagogical Institute, Tambov

The differentiation of the surface active centres on  $G_{ads}$  of a solvent molecules /1/ results in operation of chemical and electrochemical ionization mechanisms of a metal. Being different sides of a single process, these mechanisms differ in many kinetic parameters. However, this phenomenon does not allow to consider their ionization occurring on the energetically different surface active centres. This problem can be resolved under conditions of estimation of the inhibitor effect on the kinetics of the chemical and electrochemical ionization:

- solvent takes part in metal ionization directly;
- surface-active substances (SAS) are adsorbed on dissolving metal surface forcing out solvent molecules from it.

Both statements hold for solvophilic metals only.

The experimental verification of the ideas being developed was made under conditions of ionization of steel 12X18H10T and steel Ct.3 (the choice was stimulated by an essential difference of effects observed on them) in ethyleneglycol solution of HCl. Iodide-ions were used as SAS.

Bringing  $7.9 \cdot 10^{-5}$  mole/l of iodide-ions in 3.0 M ethyleneglycol solutions of HCl (80°) gives a sixfold decrease in the rate of chemical dissolution ( $i_x$ ) of stainless steel in the potential range of  $E_{COR}$  ( $\pm 0.15V$ ) together with a very feeble slow down of the electrochemical ionization (anodic area, rate  $i_a$ ). Further increasing of the  $c_{I^-}$  by three orders of magnitude does not practically change  $i_x$  and decreases  $i_a$  essentially. At the same time,  $i_x$  does not equal zero at the corrosion potential but on the contrary,  $i_x \gg i_a$  in the  $c_{I^-}$  interval studied.

A different picture in all respects is observed on Ct.3

in the same solutions ( $20^{\circ}$ ). The presence of  $7.9 \cdot 10^{-5}$  mole/l iodide ions leads to a twofold decrease of  $i_x$  and to the increase in  $i_a$  by approximately one order of magnitude (anodic polarization). It is evident that adsorption of iodide ions in the same active centres cannot lead to such different effects. An  $i_a$  decrease in comparison with the background one is observed in the presence of  $7.9 \cdot 10^{-2}$  mole/l iodide ions only. At the same time, increase of  $C_{I^-}$  to  $7.9 \cdot 10^{-3}$  mole/l does not change  $i_x$  in spite of forcing out solvent molecules by inhibitor not far from all active centres being characterized by the known interval  $\Delta \Delta G_{ads} / 1$ . The latter statement is proved by the following:  $i_x \gg i_a$  and  $i_x$  determine the rate of steel ionization.

Raising temperature of the solution to  $80^{\circ}$  increases the absolute values of  $i_a$  and  $i_x$  but decreases the inhibitive ability of iodide ions with respect to  $i_a$  and  $i_x$  to zero, i.e. iodide ions are incompetent with respect to the ethyleneglycol molecules adsorption in all adsorption centres.

The experimental data presented in this report have given rise to the following conclusions:

- chemical and electrochemical metal dissolution take place in different active centres under conditions studied;
- inhibitor particles cannot force out the solvent molecules from all active centres inside the determinate range of  $\Delta \Delta G_{ads}$ ;
- the correlation between free adsorption energies of solvent molecules and inhibitor particles or inhibitor fragments is not defined by the nature of the latter only, but by the relative energetic activity of adsorption centres;
- a special interest in the conditions of the energetic non-uniformity represents the combined inhibitors. Their components can be adsorbed differently on the active centres with different values of  $\Delta G_{ads}$ , slowing down the chemical ionization because of ones components and the electrochemical ionization because of other components. Such inhibitors have proved to be most effective inside definite intervals of active centres  $\Delta \Delta G_{ads}$ .



## Reference

1. V.I.Vigdorovich, L.E.Tsygankova, Chemistry and Chemical Technology, 32 (1989) 3.

## CONSTANT PHASE SHIFT AS A CONSEQUENCE OF THE FRACTAL CHARACTER OF ION TRANSPORT

A.E.Ukshe

Institute of Chemical Physics, Chernogolovka

When studying relaxation processes in solid electrolytes in the band of low and infra-low frequencies at non-harmonic interactions and long observation times, one can observe, besides the double layer capacity overcharge, the relaxation corresponding to the constant phase angle  $/1/$ , i.e. a CPA-element with the frequency response:

$$Y = A(j\omega)^P \quad (1)$$

or with the time response

$$A = bt^{1-P}, \text{ where } 0 < p < 1 \quad (2)$$

Dependences (1) and (2) are connected through the Laplace transformation.

At present there are two hypotheses to explain the physical nature of such an element.

1. There are strong local inhomogeneities with static fractal structure of the electrode/electrolyte interface.

2. Limitation and deformation of the surface layer of solid electrolyte caused by non-zero ion radii. This hypothesis was reported by me at the previous symposium.

What is the essence of this hypothesis? As the ions have non-zero sizes, their number in the surface monolayer is limited. This limitation is especially strong in the case of a solid electrolyte when ion transport can take place only along the rigid sublattice channels, occupying an inconsider-

able part of the volume. The relaxation of the volume charge arising from ion excess is supposed to follow the plastic deformation mechanism.

The presence of the critical charge that accounts for the change in the electrode/solid electrolyte interface behaviour was detected experimentally. However, some other peculiarities were also discovered. There has recently been a tendency to explain all slow relaxation in solid electrolytes by the CPA effect. Our investigation proved that this was not the case. It was discovered for the  $\text{Pt}|\text{H}_3\text{PMo}_{12}\text{O}_{40}$  and  $\text{Au}|\text{Ag}_4\text{RbI}_5$ , that in the case of frequencies at which the charge transferring over the interface during on half period of measurement signal has a lower value than a certain critical one, the cell equivalent scheme includes the double layer capacity and the diffusion impedance of Warburg. Thus, the double layer is considered a plane capacitor and the relaxation takes place due to the diffusion of secondary carriers. At lower frequencies, when the charge is higher than the critical value, a CPA element is switched on consecutively to the double layer capacity, i.e. the relaxation mechanism is changed.

We consider that the phenomena connected with geometric limitations of charge density and, probably, with the channel structure of a solid electrolyte should lead directly to the fractal character of ion transport.

Let's consider the transport of ion along an isolated one-dimensional channel of conductivity where an ion can jump to the next position with probability  $p$  in the positive and  $1-p$  in the negative direction under the random motion. In the presence of electrical field  $p$  is not equal to  $1-p$ . Since at random moments of time the channel happens to be blocked up in random places by other ions, probabilities  $p$  for different knots are independent and distributed according to the "binary" law

$$p(p) = q\delta(p-p_0) + (1-q)\delta(p-p_0)$$

In case a one-dimensional channel is blocked, it completely stops the transport. However, as there actually are two-dimensional or three-dimensional channel net the blocking is dynamical, we can introduce probability  $p_b$  for an ion to get into the blocked up position.

Now considering the frequency of jumps constant, we may apply to the above system the results obtained by the Monte-Carlo method by J. Bernasconi and W. Schneider /2/, who showed that the displacement of the particle in such a system is in fractal dependence on time:

$$x(t) = t^\nu F(\beta^{-1} \ln t), \quad 1 < \nu < 1/2 \quad (3)$$

Upon averaging on time and a large number of ions the periodic function  $F$  disappears:

$$F(\beta^{-1} \ln t) = \text{const} = F, \quad \text{and} \quad x(t) = Ft^\nu \quad (4)$$

Therefore, the ion transport in a randomly blocked channel has a fractal character. When the current runs in the volume of superionic, the probability of channel blocking, i.e. decomposing of an infinite cluster, is close to zero, as the number of positions is several times larger than that of ions. Besides, for current flow the charge displacement is significant, while the character of the transport of a separate ion does not play any important role (e.g. a transfer mechanism of transport may take place). In the region of a space charge the above mechanism would work, since under the effect of electric field the thickness of this charge will change in time in proportion to an average ion displacement, i.e.

$$d = at^\nu \quad (5)$$

If we accept that the bulk charge capacity is inversely proportional to its thickness and apply the Heavyside transformation for producing a response to the harmonic current /3/, we may conclude that the admittance of such a bulky charge is

$$Y = A\omega^p \exp(j p/2), \quad \text{where } p = 1 - \nu \quad (6)$$

Admittance (6) corresponds to (1), i.e. we have obtained the CPA element.

We have obtained a fractal time dependence of ion distribution in transport process with computer simulation based on the ideas which have been discussed.

#### References

1. G.Brug, A. van den Eeden et al , J.Electroanal.Chem., 176 (1984) 275.
2. Fractal in Physics, ed. by L.Piotronero and E.Tossatty, Amsterdam, 1986, 670 p.
3. A.E.Ukshe, Fiz. Tverd. Tela, 30 (1990) 671.

#### THE OVER-CHARGE EFFECT IN DOUBLE ELECTRICAL LAYER

E.A.Ukshe

New Chemical Problems Institute, USSR Acad.Sci.,  
Chernogolovka

It has been shown in numerous investigations that DEL capacitance in molten salts, concentrated aqueous solutions and solid electrolytes is very high and increases with increasing of electrode potential and temperature. These peculiarities are not in agreement with the well known Helmholtz and Gouy-Chapman approximations. Such a behaviour of the DEL in condensed ionic systems can be caused by alternation of the charge sign in the ionic layers near the electrode which can be conditioned by a specific character of the radial distribution function.

For generation of the sign-alternating ionic structure, first of all it is necessary to form an excess charge or, respectively, excess number of certain ions in the first near-electrode ionic layer. If the charge of the electrode

surface is  $q_m$  and the effective total charge of the first ionic layer is  $-q_s$ , then owing to the specific adsorption, the inequality  $|q_s| > q_m$  can be realized.

Excess charge in the first ionic layer has to be compensated in next layers when moving off from the electrode surface. It is worth noting that the first layer ionic overcharge  $|q_s - q_m|$  might not be connected with any electric charge in the condensed phase as a whole. This overcharge is formed only because of the redistribution of ions in the ordered structure, i.e. in the short-order region of concentrated liquid electrolytes or in crystal lattice of solid electrolytes. The compensation of the excess charge of the first ionic layer can be realized by means of a gradual monotonous charge attenuation in some following ionic layers or by alternating charge attenuation. As a result, the measured capacitance is the effective total value for the series circuit of the interdependent capacitors as it is shown in Fig.1.

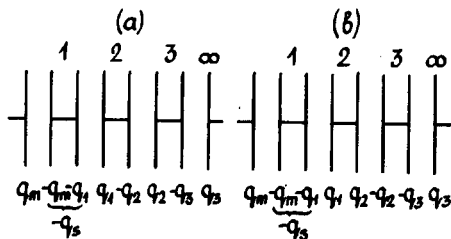


Fig.1. Charge distribution among the ionic layers arranged parallel to positively charged metallic surface.

It can be get for the capacitance of the DEL with monotonous charge attenuation

$$c_a = \frac{\epsilon \epsilon_0}{a_s} (1 - \beta - \beta^2 - \beta^3 - \dots)^{-1} = \frac{\epsilon \epsilon_0}{a_s} \frac{1 - \beta}{1 - \beta(ks+1)}$$

and for alternating charge attenuation

$$c_b = \frac{\epsilon \epsilon_0}{a_s} (1 - \beta + \beta^2 - \beta^3 + \dots)^{-1} = \frac{\epsilon \epsilon_0}{a_s} \frac{1 + \beta}{1 - \beta(ks-1)}$$

Here  $\epsilon_0 = 8.8 \cdot 10^{-12} \text{ F}\cdot\text{m}^{-1}$  is dielectric permeability of vacuum,  $\epsilon$  is dielectric constant of ionic phase,  $a_s$  is effective thickness of the first ionic layer (i.e. the layer of adsorbed ions),  $k = a_v/a_s$ , where  $a_v$  is the mean thickness of the ionic layers except the first one,  $s = q_1/\beta q_m$  and  $\beta = q_{n+1}/q_n$  are over-charge coefficients for the first and following ionic layers, respectively. Hereby, the charge of the first ionic layer equals  $q_s = q_m + q_1$ .

The origin of the over-charge is connected with ionic adsorption at the electrode surface. But the extending of its compensation for several ionic layers arises from the particles orderliness and from the limiting of the number of vacant sites in the structure of the condensed electrolyte. Both these phenomena are connected with strong electrostatic and covalent interactions of the ions.

At the first approximation we can assume that  $k=2$ . Besides, the inequalities

$$\beta < 1, \quad s\beta < 1 \quad \text{and} \quad s > 1$$

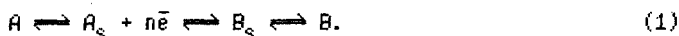
have to be satisfied. Then it is easy to see that the calculated values of  $c_a$  and  $c_b$  can be larger than the capacitance of the Helmholtz dense layer.

ABOUT ACCOUNTING OF REAGENT SPECIFIC ADSORPTION WHEN  
 DETERMINING THE KINETIC PARAMETERS OF THE ELECTROCHEMICAL  
 REACTIONS

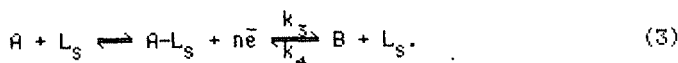
V.F.Vargalyuk, S.A.Kagolovskij

Dnepropetrovsk State University, Dnepropetrovsk

The problem of the electrode process kinetics investigation under the conditions of the reagent specific adsorption has been discussed in literature. There are known the kinetic equations derived by K.Golub [1] and P.Delahay [2] for the galvanostatic and potentiostatic regime of electrolysis, which account the adsorption of the particles reacted and are useful for the reaction of the following type



However, it is practically impossible to use them for the analysis of the particular electrochemical systems because due to the extensive formulation of the initial problem the relations deduced have not a real analytical form at all. Besides, the participation of only the compound adsorbed in the electrochemical reaction is not the most common case. Most often a parallel reduction of the diffusing and specifically adsorbed particles proceeds as in the electrochemical processes involving the organic compounds being slowly adsorbed or the discharge of the aquoions of metals and their complexes with the surfactant ligands



For such systems we have determined the constants of the charge transfer rates for reactions (2) and (3) under the potentiostatic conditions. Assuming that  $\Gamma_B \rightarrow 0$  gives the

following relation

$$i = H_1 \exp(H_2^2 t) \operatorname{erfc}(H_2 \sqrt{t}) + \left[ C_{d1} - H_3 - H_4 \sum_{p=0}^{\infty} \frac{t^{p+\frac{1}{2}}}{(p+\frac{1}{2})p!} \right] \frac{dE}{dt}. \quad (4)$$

As the generalized constants  $H_1 - H_4$  of equation (4) involve both the known quantities ( $n, F, D_A, D_B, C_A^0, C_B^0$ ) and a large number of the unknown parameters ( $k_1, k_2, k_3, k_4, K_A = \partial \Gamma_A / \partial C_A, K_B = \partial \Gamma_B / \partial C_B, K_E = \partial \Gamma_A / \partial E$ ), to determine the last ones, the complex processing of a number of the chronoamperograms recorded at various values of  $E, C_A^0, C_B^0$  and  $C_L^0$  is used.

In order to increase the initial information quantity it is suggested to differentiate and integrate  $i, t$ -curves recorded. It is shown, that the combination of  $di/dt, t$ - and  $q, t$ -curves recorded with the initial  $i, t$ -relations makes it possible to determine the kinetic parameters of the electrochemical reaction, the parameters not being affected by adsorption phenomena. In this case a set of the relations characterizing the very adsorption process ( $C_{d1}-E, \Gamma_A-E, \Gamma_A-C_A^0$  and  $\Gamma_A-C_B^0$ ) is obtained as an intermediate result.

The method developed is used to study the nature of the effects produced by some surfactants on the acceleration of the electroreduction of metal ions. The electroreduction of cadmium ions at the presence of iodide and oxalate ions illustrates that in the first case the charge is transferred to the complexes reacting by the bridge mechanism and in the second one the process rate increases mainly due to the reagent adsorption increase resulting from surface complexing.

#### References

1. K. Golub, J. Electroanal. Chem., 17(1968)277.
2. G. G. Susbielles, P. Delahay, J. Electroanal. Chem., 17(1968)289.



ON THE RELATION BETWEEN THE INTERACTION OF ADSORBATE MOLECULES  
WITH ELECTRODE SURFACE AND ITS IONIZATION POTENTIAL

M. Väärtnõu, A. Alumaa  
Tartu University, Tartu

Existence of a connection between chemisorption and the first ionization potential  $I$  of the adsorbate molecule can be considered justified in the case of the aromatic compounds whose interaction energy with the electrode surface appears to be a significant part of the adsorption energy. As a result of that specific interaction, a considerable charge transfer from adsorbate molecules to the electrode takes place already in the adsorption region near the zero charge potential  $E_{q=0}$  of the electrode /1,2/. As the potential moves to the positive direction, the coefficient of the partial charge transfer increases and in the case of platinum electrode in non-aqueous medium the oxidation potential  $E_{ox}$  can be reached, at which a complete electron transfer takes place. It must be noted that in many studies /3-5/ a linear relationship between  $E_{ox}$  and  $I$  in vacuum has been found. These quantities are related by the following equation /2/

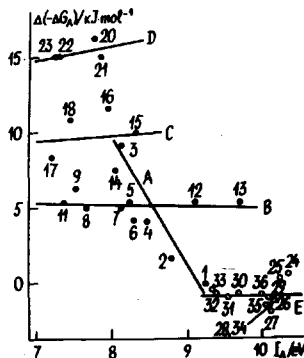
$$E_{ox} = -\phi + E_{q=0} - \Delta G_s^+ + \Delta G_s + I, \quad (1)$$

where  $\phi$  is the electron work function, by which the ion formation energy diminishes on electrode surface,  $-\Delta G_s$  and  $-\Delta G_s^+$  are the free energies of solvation of neutral and ionized forms of organic compound in a solution. Thus, a physically justified linear correlation between  $E_{ox}$  and  $I$  may be expected only for compounds with analogous structures (equal number of functional groups or aromatic rings and other factors) and similar solvation effects. These principles for grouping of the observed compounds were regarded as a basis also in looking for relation between the adsorption of organic compounds and their ionization in vacuum. Besides, it seems to be justified to seek a correlation not on the basis of the total free energy of adsorption  $-\Delta G_A$ , as it was done in works /6,7/, but on the basis of that part of it which is directly

related to the specific interaction of adsorbate with the electrode surface. This interaction may be quite well characterized by the profit in the free adsorption energy  $\Delta(-\Delta G_A)$  of an organic compound at transition from free solution surface to the boundary bismuth/solution /B,9/.

Fig.1.

The dependence of profit in the free adsorption energy of organic compounds  $\Delta(-\Delta G_A)$  at transition from free solution surface to the boundary Bi/solution on the first ionization potential  $I$  in vacuum: A - aromatic hydrocarbons, B - mono-functional derivatives of benzene, C - difunctional derivatives of benzene, D - monofunctional derivatives of naphthalene, E - aliphatic compounds.



The following compounds correspond to the numbers in the figure: 1 - benzene, 2 - toluene, 3 - naphthalene, 4 - phenol, 5 - o-cresol, 6 - m-cresol, 7 - p-cresol, 8 - aniline, 9 - o-toluidine, 10 - m-toluidine, 11 - p-toluidine, 12 - benzyl alcohol, 13 - benzoic acid, 14 - pyrocatechol, 15 - resorcinol, 16 - hydroquinone, 17 - o-phenylenediamine, 18 - m-phenylenediamine, 19 - p-phenylenediamine, 20 - 1-naphthol, 21 - 2-naphthol, 22 - 1-naphthylamine, 23 - 2-naphthylamine, 24 - acetic acid, 25 - propionic acid, 26 - butyric acid, 27 - valeric acid, 28 - hexanoic acid, 29 - heptanoic acid, 30 - acetone, 31 - methyl ethyl ketone, 32 - methyl propyl ketone, 33 - methyl butyl ketone, 34 - ethyl acetate, 35 - propyl acetate, 36 - butyl acetate.

The results of the correlation analysis are plotted in Fig.1. As it can be seen, in the case of aliphatic compounds (line E), no evident relation occurs between  $\Delta(-\Delta G_A)$  and  $I$ . This result is quite natural, since no significant specific

interaction of adsorbate molecules with electrode surface and partial charge transfer from adsorbate molecules to electrode has been found on electrodes with high hydrogen overvoltage.

However, any correlation between  $\Delta(-\Delta G_A)$  and  $I$  has not been found for polar aromatic compounds either. As can be seen in Fig 1. (lines B,C,D), in spite of a considerable charge transfer in the adsorption process of aromatic compounds on electrodes, the expected strengthening of the  $\pi$ -electron interaction between the adsorbate and the electrode surface at decrease of  $I$  as the electronic characteristic of adsorbate molecule, does not take place. Thus, in respect to the interaction between the adsorbate molecules and electrode surface in the region of zero-charge potential of bismuth, the determining factors are such structural characteristics of molecules as the existence, number and mutual arrangement of functional groups and also the number of aromatic rings in adsorbate molecules. The dependence of  $\Delta(-\Delta G_A)$  on  $I$  in the case of aromatic hydrocarbons (line A) is different just because that the change of  $I$  at transition from benzene to naphthalene is accompanied by an increase in the number of aromatic rings.

There are various action mechanisms showing how the structural factors of the adsorbate molecules are determining their interaction with electrode surface. It is necessary to emphasize the influence of the functional group in the adsorbate molecule on its orientation in the adsorbed layer and therefore also on creating conditions for surface-adsorbate interaction. For this reason, only a satisfactory correlation has been found between  $\Delta(-\Delta G_A)$  and the total excess of the  $\pi$ -electron density  $\sum \Delta q_\pi$  on carbon atoms in aromatic rings (the correlation coefficient for compounds with one aromatic ring is 0.874). The values of  $\sum \Delta q_\pi$  were obtained by quantum chemical calculation in CNDO/2 approximation /10/.

The analysis of the dependence of free energy of adsorption  $-\Delta G_A$  on  $I$  yields unjustified results because  $-\Delta G_A$  contains both the energy of structural squeezing out of adsorbate from bulk solution and the interaction energy with electrode surface /6,7/. In our opinion, the values of  $I$  at

the maxima of these dependences may in no way be interpreted as the resonance potentials to which correspond the compounds chemically interacting with the electrode surface.

#### References

1. A.R.Alumaa, U.E.Past, U.V.Palm, *Elektrokhimiya*, 23 (1988) 1558.
2. D.Rolle, J.W.Schultze, *Electrochim.Acta*, 31 (1986) 991.
3. L.L.Miller, C.D.Nordbom, E.A.Mayeda, *J.Org.Chem*, 37 (1972) 916.
4. A.B.Lutskii, Yu.I.Beilis, V.I.Fedorenko, *Zh.org.khimii*, 42 (1972) 2535.
5. A.E.Lutskii, Yu.I.Beilis, V.I.Fedorenko, *Zh.org.khimii*, 43 (1973) 101.
6. E.A.Netshayev, *Elektrokhimiya*, 14 (1978) 1403.
7. A.E.Shcherbakov, V.P.Kuprin, F.I.Danilov, *Elektrokhimiya*, 26 (1990) 116.
8. U.V.Palm, B.B.Damaskin, *Itogi Nauki i Tehn., Ser. Elektrokhim.*, 12 (1977) 99.
9. J.Ehrlich, T.Ehrlich, U.Palm, *Trans.Tartu State University*, 441 (1978) 76.
10. J.A.Pople, D.L.Beveridge, *Approximate Molecular Orbital Theory*, McGraw-Hill, New York, 1970.

KINETICS OF REACTIONS WITH PARTICIPATION OF A REAGENT  
AS A STIMULATOR OF ACTIVE DISSOLUTION AND A PASSIVATOR  
OF METAL IN PARALLEL PROCESSES

M.V.Vigdorovich, V.I.Vigdorovich

All-Union Scientific Research and Design Technological  
Institute on Machinery and Oil-products Utilization in  
Agriculture, Tambov

On the basis of the ideas developed in /1/, one can see that the solution components of the same kind can act either as activators or passivators (inhibitors) of metal ionization under different conditions. Moreover, this phenomenon is connected with energetic nonuniformity of adsorption centres /2/ and with the existence of attractive interaction of the adsorbate. The  $H_2O$  molecules and chloride ions, in particular, have such a double nature under conditions of iron ionization /3/.

Let us consider the ionization of an active and passive metals, whose rates are  $j_1$  and  $j_2$ , respectively, with participation of substance A:

$$j_1 = k_1 \theta C_A^m \exp[\beta_1(E - \psi_1)F/RT] \quad (1)$$

$$j_2 = k_2(1 - \theta)C_A^n \exp[\beta_2(E - \psi_1)F/RT]. \quad (2)$$

$\beta_1$  and  $\beta_2$  are either seeming (for polystage reactions) or true transfer coefficients;  $\theta$  and  $(1-\theta)$  are the fractions of active and passive surface, respectively.

Orders on A can differ very much because of the different nature of the intermediate adsorbed complexes in the case of the ionization of active and passive metals. If  $T = \text{const}$  and the electrode potential and solution composition are invariables ( $\psi_1 = \text{const}$ ), the common rate of reaction is as follows:

$$j = k_1 \theta C_A^m + k_2(1-\theta)C_A^n. \quad (3)$$

Seeming order on A will remarkably change with an increase in the passive surface contribution. Let us estimate it, ta-

king  $j$  as the primary value if  $\Theta=1$ , then increasing of  $(1-\Theta)$  brings about a decrease in  $j$

$$\Delta j = k_1 C_A^m - k_1 C_A^m \Theta - k_2 C_A^n (1-\Theta) = (k_1 C_A^m - k_2 C_A^n)(1-\Theta). \quad (4)$$

The seeming order of the reaction of  $W$  regarding  $A$  can be expressed as follows:

$$W = \frac{d(\ln \Delta j)}{d(\ln C_A)} = \frac{d(\ln \Delta j)}{dC_A} \cdot \frac{dC_A}{d(\ln C_A)} = \frac{d(\ln \Delta j)}{dC_A} \cdot C_A \quad (5)$$

To get  $W=W(C_A)$ , the analysis has been carried out under  $A$ -sorption submission to the Langmuire-, Freundlich- and Frumkin isotherms for both the uniform and nonuniform surface, and under conditions of the attractive interaction, accordingly.

The Langmuire isotherm

$$\Theta = \frac{BC_A}{BC_A + 1} \quad (6)$$

Combining (4) and (6), we have

$$\Delta j = \frac{k_1 C_A^m - k_2 C_A^n}{BC_A + 1} \quad (7)$$

Taking into account (5), one can get

$$W = \frac{mk_1 C_A^m - nk_2 C_A^n}{k_1 C_A^m - k_2 C_A^n} - \frac{BC_A}{BC_A + 1} \quad (8)$$

For the numerical calculation of the magnitude of  $\Delta C_A$ , where experimental dependence  $\ln \Delta j = f(\ln C_A)$  can be approximated by a straight line equation with the necessary accuracy, equation (8) can be used.

Freundlich isotherm

$$\Theta = BC_A^{\alpha_1}, \quad 0 < \alpha_1 < 1 \quad (9)$$

$$\Delta j = (k_1 C_A^m - k_2 C_A^n)(1 - BC_A^{\alpha_1}) \quad (10)$$

The function  $W = f(C_A)$  has the following form according to (5):

$$W = \frac{m \int C_A^{m-n} - n}{\int C_A^{m-n} - 1} - \frac{B\alpha_1 C_A^{\alpha_1}}{1 - BC_A^{\alpha_1}} \quad (5)$$

The Frumkin isotherm

$$BC_A = \frac{\theta}{1 - \theta} \exp(-2\alpha\theta) \quad (11)$$

The presentation of the exponent in (11) according to Taylor if  $\theta \rightarrow \theta_0$  ( $0 < \theta_0 < 1$ ) results in the following expression:

$$B_1 C_A = \frac{\theta}{1 - \theta} (1 + 2\alpha\theta_0 - 2\alpha\theta), \quad B_1 = Be^{2\alpha\theta_0}$$

$$W = \frac{m \int C_A^{m-n} - n}{\int C_A^{m-n} - 1} - \sqrt{\frac{B_1 C_A}{(B_1 C_A + 2\alpha\theta_0 + 1)^2 - 8\alpha B_1 C_A}} \quad (12)$$

If the sign before the square root is positive then the solutions of equation (12) in case  $\alpha < 0$  have physically non-sensical values ( $\theta < 0$ ).

The results on numerical calculations of  $W$  on the borders of concentration intervals  $\Delta C_A$  of different lengths are given for all isotherm pointed out in the report.

Generally, the correlation  $W=W(C_A)$  has the following form:

$$W = \frac{m \int C_A^{m-n} - n}{\int C_A^{m-n} - 1} - f(C_A), \quad f(C_A) > 0 \quad (13)$$

By experimental defining of the character of  $f(C_A)$  one can obtain the true adsorption isotherm which is not limited by the boundaries of the original model. If  $\theta = g(C_A)$ , then

$$W = \frac{m \int C_A^{m-n} - n}{\int C_A^{m-n} - 1} - \frac{C_A g'(C_A)}{1 - g(C_A)} \quad (14)$$

Combining (13) and (14), one can obtain

$$f(C_A) = \frac{C_A g'(C_A)}{1 - g(C_A)} \quad \text{and} \quad \theta = 1 - e^{-\int_{C_A}^{\theta} [f(C_A)/C_A] dC_A}$$

References

1. Ya.M.Kolotyркин, Works of Moscow Institute of Chemical Machinebuilding, M., 67 (1975) 5.
2. Ya.M.Kolotyркин, Proc. 5th Europ. Symp. Corrosion Inhibitors, Ferrara, 1980, p. 1157.
3. F.M.Micheeva, G.M.Floryanovich, Zashita Metallov, 23 (1987) 33.

INVESTIGATION OF THE INFLUENCE OF THE POROUS STRUCTURE,  
INTERFACE CAPACITY, KINETIC AND DIFFUSION CHARACTERISTICS  
ON THE DISCHARGE-CHARGE CURVES OF POLYANILINE ELECTRODES

Yu.M.Vol'fkovich, A.V.Shlepakov, T.K.Zolotova,  
S.D.Bobe, A.A.Zaitsev

A.N.Frumkin Institute of Electrochemistry, USSR Acad. Sci.,  
Moscow

This study is concerned with the influence of the porous structure, interface capacity, kinetic and diffusion characteristics on the discharge-charge curves of polyaniline electrodes. The standard porosimetry method (SPM) /1/ was used for the first time for investigation of the structural-sorption properties of electrodes from polyaniline (PAN) in the working state in aqueous medium. We studied the structure of PAN films electrodeposited on carbographite cloth and platinum gauze as well as that of chemically synthesized PAN powders. Electrosynthesis is possible only on cloths with graphite surfaces. It was found that electrodeposited films and chemically synthesized powder particles have an internal porous structure with the specific surface  $S = 50-100 \text{ m}^2/\text{g}$  and the porosity of 15 - 30 %. The most characteristic pore radius range ( $r$ ) is from 10 to 400 Å. Therefore, a PAN film is to be treated as a porous electrode, which has not practically been done previously. Apart from pores, water in PAN is present in a still higher energy state - in the hydration shells of counterions. It is shown that in water PAN undergoes swelling, increasing its surface several times. The pores of chemically synthesized PAN powder show a maximum on the differential porogram in the range of  $r = 10-400 \text{ Å}$  with a peak at 60 Å. For a chemically synthesized PAN powder the pore radius range is mainly 100-6000 Å with a peak at 350 Å, i.e. the peak is shifted into the range of larger pores.

A macrokinetic model of the operation of a porous PAN electrode (PANE) has been developed. This electrode con-



sists in contacting cylindrical PAN fibers with the mean radius  $R$ , the pores between them being filled with electrolyte. During discharge and charge of PANE a nonsteady-state diffusion of counterions occurs along the radial axis in a PAN cylinder.

$$\frac{1}{D} \frac{\partial c}{\partial \tau} = \frac{\partial^2 c}{\partial \varrho^2} + \frac{2}{\varrho} \frac{\partial c}{\partial \varrho} \quad (1)$$

with the initial and boundary conditions

$$c(\tau=0, \varrho) = c_H; \quad \left( \frac{\partial c}{\partial \varrho} \right)_{\varrho=0} = 0;$$

$$n_{FD} \left( \frac{\partial c}{\partial \varrho} \right)_{\varrho=R} = \pm \left[ i_0 \left( \frac{c_0}{c_H} \right) e^{\alpha_0 \tilde{E}} - e^{-(1-\alpha_0) \tilde{E}} \right] = i_p, \quad (2)$$

where the signs "+" and "-" are for the PANE discharge and charge, respectively,  $\tilde{\tau}$  is the time,  $c$ ,  $c_0$ ,  $c_H$  are the counterion concentrations at  $\varrho = \varrho$ ,  $\varrho = R$  and  $\tau = 0$ , respectively,  $i_0$  is the exchange current density,  $\tilde{E} = E/RT$ ,  $E$  is the polarization,  $D$  is the diffusion coefficient of counterions in PAN,  $i_0$  is the current density of the electrochemical reaction, equal to

$$i_0 = i - i_3, \quad (3)$$

where  $i_3 = C_e (\partial E / \partial \tilde{\tau})$  is the charge current density of the PAN/solution interface,  $C_e$  is the specific electric capacity of this surface,  $i$  is the total local current density. The potential distribution across PANE (coordinate  $x$ ) is given by the equation

$$d^2 E / dx^2 = (\tilde{\varrho}_e + \tilde{\varrho}_s) \text{Si}(\tilde{E}) \quad (4)$$

with the boundary conditions

$$(dE/dx)_{x=0} = \tilde{\varrho}_s I; \quad (dE/dx)_{x=L} = \tilde{\varrho}_e I, \quad (5)$$

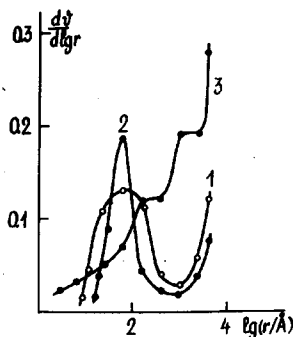
where  $I$  is the integral current density per unit visible surface of PANE,  $\tilde{\varrho}_e$  and  $\tilde{\varrho}_s$  are the effective resistances with respect to the liquid phase (electrolyte) and solid phase (with respect to PAN and electroconducting additives if they are used),  $L$  is PANE thickness,  $S$  is the specific surface measured just as  $R$ , by SPM. The macrokinetic model under consideration can, in principle, also be used for electrodes

from other conducting polymers.

The set of differential equations (1) and (5), similar to that considered in /2/, was numerically solved with a computer using a different method. By means of Fourier transforms it was transformed into a set of integral equations. This method of solution has an advantage, since the equations show better convergence and differentiability.

Fig.1.

Differential porogram: 1 - PAN/carbographite cloth; 2 - PAN/platinum gauze; 3 - PAN/powder.



By comparing the calculated and experimental discharge and charge curves, it is possible with the use of the above model to estimate such fundamental characteristics of PAN as  $C_e$ ,  $D$ ,  $i_0$ . Thus, we obtained for PAN:  $D = 10^{-19} \text{ cm}^2/\text{s}$ ,  $i_0 = 3 \cdot 10^{11} \text{ A/cm}^2$ ,  $C_e = 10^{-3} \text{ F/cm}^2$ . It is demonstrated that the model describes satisfactorily the experimental data. We have also examined the influence of various factors on the discharge and charge curves which are S-shaped. We have found the influence of  $C_e$  on the discharge curve to be particularly strong in its initial and final parts. At large  $C_e$  the discharge curve improves, i.e. it becomes flatter with increasing  $D$  and  $S$ . With increasing  $i_0$  and decreasing  $\rho_e$  and  $\rho_s$ ,  $E$  decreases.

#### References

1. Yu.M.Vol'fkovich, V.S.Bagotzky, V.E.Sosenkin, E.I.Shkol'nikov, *Elektrokimiya*, 16 (1980) 1620.
2. Yu.M.Vol'fkovich, O.A.Petrii, A.A.Zaitsev, I.V.Kovrigina,

THEORY OF EQUILIBRIUM AND KINETIC PHENOMENA  
IN ELECTRON-CONDUCTING POLYMER FILMS

M.A. Vorotyntsev

A.N. Frumkin Institute of Electrochemistry, USSR Acad. Sci.,  
Moscow

Synthesis and practical applications of electrodes covered by electron-conducting polymer films.

Discussion of the modern state of the theory.

*Structural changes at doping/dedoping process:*

a dielectric/electron-conducting phase transition (variation of the electronic state of polymer molecules, electron transfer across the metal/film boundary, ionic and solvent transport inside the film, reversibility at doping), conductivity of the doped film (high concentration of electronic mobile charge carrier, polarons and bipolarons, ion-polaron couples, electrochemical reactions of solute species).

*Potential and charged species distributions inside the film:*

dissociation of ionogenic groups and specific binding of ions by polymer groups, models of a homogeneous medium and a fixed charge, film-solution ionic equilibrium, field screening in the film, typical regimes of potential distribution, effects of electron transfer from the metal, dependence of the interfacial potential and concentrations of the film charge species on the electrode potential, effect of an upper limit for the polaron and ionic concentrations inside the film.

*Interpretation of alternating current and polarisation data:*

typical voltammograms of the film doping/dedoping process and an electrochemical reaction of solute redox species at the film surface, quasi-thermodynamic theory of these phenomena, hysteresis and interfacial charge transfer, interphasial capacitance contribution and anodic plateau of voltammograms, impedance of the metal/film/solution system with account of slow electron-ion transport inside the film and charge transfer across both interfaces.

# INDIVIDUAL AND COMBINED ADSORPTION OF CORROSION INHIBITORS ON FERRUM

Yu.M.Vyzhimov

Kazan Institute of Chemical Technology, Kazan

The corrosion inhibitors of combined type are being widely used in industry due to their versatility and effectiveness. While investigating such systems there arise questions concerning the comparative analysis of the protective action of separate mixture components on corrosion mechanism and regularities of its change.

In the present work the coadsorption of corrosion inhibitors (CI) of alkyl-pyridinebromide (APB) and isononylphenol (OP-10) from aqueous solution on ferrous electrode has been investigated. This combination has obvious feature of individual adsorption and depending on conditions one might expect intensification of adsorption of both CI as well as preferential adsorption of one of the mixture components.

To solve the problem, the authors used the procedure of measurement of the ferrous electrode incremental capacitance in a wide range of potentials and radio-isotope method at corrosion potential. Radioisotopic method was used to determine the partial electrode surface coverage by the component under investigation.

The experimental isotherms of individual and combined adsorption on ferrous electrode from aqueous solution with hydrogen sulphide addings (100 mg/l) are given in the figure. As is seen from the figure, by adding hydrogen sulphide into the system the adsorption of APB increases several times. Synergetic effect of  $H_2S$  can be explained by the fact that anions  $HS^-$  adsorbed on ferrum act as bridges, facilitating the adsorption of corrosion inhibitors of cation type  $R^+$ , APB being one of them. As a result of interaction of the intermediate complex  $Fe(HS^-)$  with organic cation, a relatively stable surface compound  $Fe(H-S-R)$  appears on the metal surface.

The adding of the OP-10 type CI influences greatly the

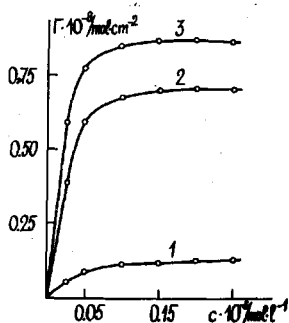


Fig. 1.

Isotherms of adsorption of alkyipyridine bromide from water solution with addings: 1 - individual adsorption; 2 - APB + H<sub>2</sub>S (100 mg.l<sup>-1</sup>); 3 - APB + OP-10 + H<sub>2</sub>S.

adsorption of APB on the surface of metal samples. In small concentrations when the total partial degree of filling is less than one, the adding of OP-10 intensifies the sorption of APB. At high concentrations the competitive effects are displayed, and the isotherm of combined adsorption practically coincides with the individual isotherm of APB. On the basis of the facts described above, one can see a higher competitive ability of APB for adsorption on ferrum and it is possible to suppose that the combined layer of two coadsorbates consists only of the APB molecules. In experiments concerning the investigation of adsorption of OP-10 type CI marked by carbon C-14 and in conditions of combined addition, the effect of intensifying sorption of OP-10 in the presence of APB is noticed as well. These results testify to the increasing sorption of both components and the adsorbing layer consists of molecules of both components.

The results obtained by radioisotopic method were compared with the data obtained by the method of incremental capacitance. Such a comparison makes it possible to identify a much more complex character of the interaction of APB and OP-10 at high volumetric concentrations of adsorbate displayed in complementary effects of capacitance lowering. The depression of capacitance in combined adsorption reaches abnormally low values. On the basis of experimental data, the model structure of adsorption layer as two parallel layers consisting of adsorbate molecules of various types can be supposed.

THE CONNECTION BETWEEN THE  $\text{CO}_3^{2-}$ -ION ADSORPTION PROCESS ON Pt,Rh,Ir AND THE KINETICS OF THE PEROXYDICARBONATE SYNTHESIS

A.A.Yakovleva, E.A.Nashivin

Karпов Institute of Physical Chemistry, Moscow

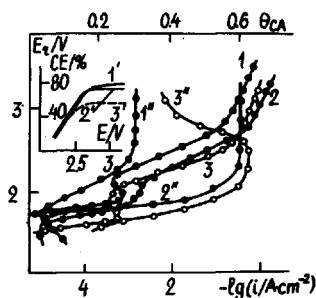
Kinetic regularities of the peroxydicarbonate-anion (PDCA) synthesis are studied insufficiently /1,2/. The correlation of the selectivity of the  $\text{C}_2\text{O}_6^{2-}$  production with the adsorption properties of the anodic films on platinum metals has not been considered before. This reaction is of great interest both as a source of an ecologically pure oxidizer and for the investigation of the influence of the anion composition and pH on the electrocatalytic properties of anode materials.

The complex of experimental methods including the methods of radioactive trace, impedance and pulse potentiodynamics were applied for studying of such kind of connections.

Polarization curves, current efficiency (CE) - potential and carbonate-anion (CA) coverage - E dependences on Pt (1, 1', 1''), Rh (2, 2', 2'') and Ir (3, 3', 3'') are shown in Fig.1.

Fig.1.

The  $E_r - \lg i$  curves,  $CE_{\text{PDCA}} - E$  and  $\theta_{\text{CA}} - E_r$  dependences on Pt (1, 1', 1''), Rh (2, 2', 2'') and Ir (3, 3', 3'') in 1 M  $\text{K}_2\text{CO}_3$  at 15°C.



Exceeding the value of 2.1 V (r.h.e.), the synthesis of PDCA takes place at a considerable rate on all anodes. Strong inhibition of the anode processes was observed at potentials over 2.5 V (ohmic losses were determined by current interac-

tion method). After sharp rise of the polarization curves at current densities  $>0.1 \text{ A/cm}^2$  the current efficiencies of PDCA formation achieve maximum values of 75, 69, 50 % for Pt, Rh, Ir correspondingly. In more concentrated solutions ( $3 \text{ M K}_2\text{CO}_3$ ), the selectivities of Pt, Rh, Ir are almost equal (CE - 95, 89, 85 %). In the range of the potentials of the effective PDCA synthesis the adsorption of CA species reaches the limited values for Pt and Rh, but decreases when Ir is used. That is caused by a stronger inhibition of the anode process. It is interesting that the increase in the CA adsorption in the range of the potentials of 1.7-2.1 V corresponds to the region of the transition from the oxygen evolution reaction to PDCA synthesis. Opposite to acidic solutions /3/, for the CA adsorption in alkaline carbonate system (pH = 12.5) the polyextremum phenomena at potentials higher than 2.0 V are not found. That is connected with the low polarizability of the oxide layers on these metals. The strength of the bond between the CA species and the anode surface at high anodic potentials was estimated by means of the pulse electrochemical exchange method /4/.

It was shown that at high potentials there are two types of CA species. About 80 % of CA are exchanged at the first second of polarization, at the same time it takes about 30 min to exchange 10-20 % of the strongly-bonded particles. The kinetics and the selectivity of PDCA synthesis are connected with the behaviour of the weakly-bonded particles.

Table 1

Exchange degree of the CA species during a short period of the anodic polarization and current efficiencies of PDCA synthesis on Pt, Rh, Ir in  $1 \text{ M K}_2\text{CO}_3$  at  $15^\circ\text{C}$

Anode	E = 2.4 V			E = 2.9 V		
	Exchange time, s		CE % PDCA	Exchange time, s		CE % PDCA
	0.01	0.06		0.01	0.06	
Pt	26	48	37	40	50	75
Rh	20	50	40	35	47	69
Ir	28	50	40	28	35	55

The data of CA exchange kinetics are shown in Table 1. The equal selectivities of Pt, Rh, Ir at 2.4 V correspond to the equal amount of exchange particles, but at 2.9 V the decrease in the current efficiency of the PDCA synthesis in series Pt > Rh > Ir is connected with reducing the exchange degree of weakly-bonded CA.

Complex experimental data allow us to suggest that the weakly-bonded CA species are included in the active centers and form the surface structures favorable for the discharge of the same kind of species in solution. It was shown that for Pt, Rh, Ir the polarization curves of PDCA formation coincide, assuming that only the part of the electrode surface occupied by CA with a rapid exchange rate is active in this process. This result confirms our supposition about formation of the active centers as a result of the CA adsorption on the oxidized electrode surface. It has been shown by impedance and potentiodynamics that one of the main causes of the different adsorptivity of the CA species could be the differences in semiconductive properties and electron structure of the oxide layers of these metals.

#### References

1. N.E.Homutov, M.F.Sorokina, Zh. Fiz. Khim., 40 (1966) 44.
2. P.M.Wiel, L.J.J.Janssen, J.G.Hoogland, Electrochim. Acta, 16 (1971) 1217.
3. Ya.M.Kolotyrkin, A.A.Yakovleva, I.L.Kuvinova, J. Electroanal. Chem. 180 (1984) 241.
4. E.A.Nashivin, A.A.Yakovleva, Electrochim. Acta, 26 (1990) 724.



THE STUDY OF THE INTERFACE STRUCTURE AND OF THE FLOTATION REAGENTS' ADSORPTION ON THE MINERAL/SOLUTION INTERFACE

G.M.Yashina, S.S.Bobov, V.M.Rudoy

Institute "Unipromed", Sverdlovsk

It is a known fact that the interaction of semiconductive sulphide minerals and oxygen as well as other reagents in flotation and hydrometallurgy is greatly affected by electrochemical reactions.

However, due to the lack of a more exact information as to the processes taking place on the mineral/solution interface, their influence can hardly be evaluated properly.

The method widely used for studying the adsorption of organic compounds on different metals, is known as an impedance method. But this method does not give reliable results on the adsorption of surface active species on minerals because not all characteristics of the mineral/solution interface are taken into account.

However, the use of the impedance method to define the flotation reagents' adsorption on mineral surface, provided all the characteristics and the structure of the interface are taken into consideration, can give the data, necessary for modelling the optimal theoretical scheme for the selective separation of pyrite and chalcopyrite.

In the present work, using the alternating current method, by means of the bridge P-5021 there was established a frequency dependence of mineral components on mineral/electrolyte ( $\text{Na}_2\text{SO}_4$ ) interface in air and purified inert gas (argon). The results show that the capacity of minerals in air is much less than in the inert gas.

The decrease in the differential capacity of pyrite in air is governed by the adsorption pseudocapacity, which is the result of the adsorption of oxygen on the mineral surface and of the low rate of its oxydation.

Upon addition of potassium xanthate the capacity and thickness of the electrical double layer are changed.

This change is caused by layer-by-layer adsorption on mineral surface: first of xanthate anion and then of the products of the reaction. These products are copper/iron xanthate, if the reaction takes place in the inert atmosphere, and dixanthogenide, if the reaction takes place in air.

Relation between these 2 forms of sorption of collectors on mineral surface affects the activity of flotation of sulphide minerals.

The structure of mineral/solution interface in flotation was studied in 2 equivalent schemes: one consisted of 6 elements, the other - of 7. These schemes are usually identified with the use of graphoanalytic methods based on the analysis of frequency dependence of impedance components.

However, these methods do not able us to quantify the elements in these schemes, that is why the methods of computation mathematics are recommended (for receiving the values of electrochemical impedance).

The present study involves the multiple simplex algorithm, according to which the deviation is minimized.

Simplex method provides a detailed description of the mineral/solution interface structure, quantifies the values of electrochemical and semi-conductive characteristics of the interface.

Thus, the impedance method is quite effective for controlling the flotation reagents' adsorption on the mineral surface.

The received data on the structure of the interface may be used for prognosticating the optimum concentration of reagents in selective separation of contacting minerals in ores.

INFLUENCE OF COPPER ON ELECTROCATALYTIC PROPERTIES  
OF HIGH-DISPERSED Pd/C ELECTRODES

N.A.Zakarina, M.Yu.Yusupova

Institute of Organic Catalysis and Electrochemistry,  
Kazakh SSR Acad. Sci., Alma-Ata

It is known that adsorption and electrocatalytic properties of high-dispersed metals differ from those of massive metals. Therefore, control of the active metal dispersity is one of the routes to production of electrode materials with specified properties. From this standpoint, synthesis of bimetallic colloidal particles of a definite dispersity with their subsequent attachment to a support seems rather promising. The present work aims at studying hydrogen adsorption and dissolution by Pd-Cu electrodes based on bimetallic Pd-Cu sols with controlled dispersity.

Hydrogen adsorption and dissolution in Pd-Cu electrodes supported on "Sibunit" grade coal ( $S = 549 \text{ m}^2 \cdot \text{g}^{-1}$ ; pore radius =  $40 \text{ \AA}$ , pore volume =  $0.35 \text{ cm}^3 \cdot \text{g}^{-1}$ ) were studied by the method of charging curves and by potentiometric method. The potential sweep rate was varied from  $0.04$  to  $1.00 \text{ mV} \cdot \text{s}^{-1}$ . Measurements were carried out in  $1 \text{ N H}_2\text{SO}_4$  solution. Mono-dispersed palladium sols were prepared by liquid-phase reduction of  $\text{PdCl}_2$  by citrate solution at  $373 \text{ K}$ . Control of the particle dispersity in sols was effected by means of electron microscopy  $\text{ЭМ-1005}$  with magnifying power  $140000$ . The electron microscopy study of Pd-Cu sols shows them to be metallic particles of spherical shape with closely spaced sizes. On introduction of copper into palladium sols differing in particle sizes, there occurs a slight increase in particles. However, sols preserve uniformity of particle distribution. Bimetallic Pd-Cu sols with a different particle size have been synthesized. The content of the given-size particles in them is  $64$ - $85\%$ .

It is shown that introduction of copper into sols al-

ters considerably the adsorption and dissolution of hydrogen. On increasing the copper content, on the charging curves one observes a more and more increasing potential drop upon current switch-on, and reduction in the length of the first portion of  $\alpha$ - $\beta$  junction "platform". This is indicative of the deceleration of the process of hydrogen ionization on Pd-Cu/C electrodes and of a decrease in its amount. Potentiodynamic curves of Pd-Cu/C electrodes are characterized by a small "platform" of dissolved hydrogen ionization and a maximum of the adsorbed hydrogen ionization, an increase in the copper content causing a sharp decrease in hydrogen sorbed by electrodes. A decrease in the dissolved hydrogen content is sharper than that of the adsorbed hydrogen. At 16.7 at.% copper-content Pd-Cu/C electrodes contain no dissolved hydrogen, whereas full cessation of hydrogen adsorption occurs only at 37,5% copper content.

It is shown that control of the size of metal particles and concentration of the introduced copper make it possible to synthesize bimetallic particles homogeneous in phase composition, possessing specified adsorption and electrocatalytic properties.

Optimal compositions and metal particle sizes in Pd-Cu system have been determined for the reaction of acetylene compound hydrogenation.

#### INFLUENCE OF SOLVENT ON THE ADSORBABILITY OF 1-(2-PROPIONITRILE)-PYRROLIDINE AND 1-(3-AMINOPROPYL)- -PYRROLIDINE ON PLATINUM AND NICKEL ELECTRODES

T.A.Zerina, A.A.Michri

A.N.Frumkin Institute of Electrochemistry, USSR Acad. Sci.,  
Moscow

Solvent adsorption is known to have a significant effect on the adsorbability of a number of organic compounds

and on the kinetics of electrocatalytic processes involving them. In particular, it was shown in /1/ that fairly strong adsorption of water molecules on the surface of an electrode - catalyst suppresses practically completely the adsorption process of a number of organic compounds (ethylene, simplest aliphatic alcohol) on a nickel electrode. In /2, 3/ studies were made on the adsorption on Pt and Ni electrodes (in alkaline electrolyte) of much more complex organic compounds - PNP and its hydrogenation product APP, and this permits comparison of the results.

It is known that adsorption of water and organic compounds is of a competitive nature and, therefore, at a large enough bond energy between an organic particle and metal, the water molecules adsorbed on it would be expected to be displaced and thus conditions would be provided for organic substance adsorption.

It was established that PNP is adsorbed both on Pt and on Ni, whereas APP is adsorbed only on Pt. The differences in the adsorbability of PNP and APP on Ni are bound up with those in the adsorption mechanism of these compounds. To elucidate the question of the nature of the bond of an irreversibly chemisorbed organic substance on a Ni electrode, the adsorbabilities of PNP, APP and pyrrolidine were comparatively studied. It was found that an irreversibly chemisorbed substance is formed only with PNP. It should be noted that, generally speaking, PNP adsorption can occur due either to the interaction with metal surface of an unshared electron pair on the nitrogen atom (both in heterocycle and in nitrile group), hydrogenation of the  $-CH_2-$  chain or by breaking of multiple bonds in nitrile group. Occurrence of PNP adsorption (whose molecule has a nitrogen atom,  $-CH_2-$  chain and multiple bond in nitrile group) in the absence of APP adsorption (which has an unshared electron pair and  $-CH_2-$  chain) and pyrrolidine (which has only an unshared electron pair) indicates that displacement of water molecules from Ni surface becomes possible only when a sufficiently strong bond is formed due to hybridization of the  $\sigma$ -bond of nitrile group and is energetically disadvantageous for

adsorption processes following the mechanism of hydrogenation and bond formation by means of an unshared electron pair.

The fast potentiodynamic pulses method was used to investigate the dependence of the surface coverage with irreversibly chemisorbed organic substance on potential during adsorption of PNP and APP on Pt electrode. It follows from the obtained data that in the hydrogen adsorption range  $\Theta_{APP}$  is twice as large as  $\Theta_{PNP}$ . When the potential shifts in the anodic direction,  $\Theta_{APP}$  remains practically constant, whereas  $\Theta_{PNP}$  increases and at the potential of  $\sim 0.9$  V proves to be equal to  $\Theta_{APP}$ . In the whole potential range studied,  $\Theta_{APP}$  does not depend on potential. These results can be interpreted on the assumption that in the hydrogen adsorption range PNP adsorption proceeds by breaking the multiple bond in nitrile group. When the potential shifts in the anodic direction, the dehydrogenation processes of  $-CH_2-$  chain become more and more pronounced and fairly high anodic potentials, when the degree of hydrogenation reaches its maximum, the structure of adsorbed particles formed during PNP and APP adsorption (adsorbed by the dehydrogenation mechanism) becomes identical.

It is evident from the obtained data that on metals with fairly strongly adsorbed water molecules (e.g. Ni) only those adsorption mechanisms of organic compounds can be realized, whose energetics ensure displacement of water molecules from the surface.

#### References

1. A.G.Pshenichnikov, A.A.Michri, *Itogi nauki i tekhniki, Elektrokimiya*, M., VINITI, 1986. V.23, P.101.
2. T.A.Zerina, A.A.Michri, *Elektrokimiya*, 26 (1990) 548.
3. T.A.Zerina, A.A.Michri, A.G.Pshenichnikov, L.N.Ivanovskaya, *Abstr. of papers XII All-Union Conf. on the Electrochem. of Org. Compounds*, 1990, Moscow-Karaganda, 85.

## AUTHOR INDEX

Afanasiev B.N.	3	Dzhumabekova Kh.K.	5
Aitov R.G.	182		
Alpatova N.M.	83	Ehrlich J.	112
Altayev N.K.	5	Ekilik V.V.	21
Al'tentaller L.I.	85	Esina N.O.	172
Alumaa A.	7,51,175,224		
Anni K.	109,144	Fedorova O.V.	94
Arold J.	196	Fedorovich N.V.	39
Arulepp M.	104	Fevraleva V.A.	21
Avruchenko A.E.	162	Filyayev A.T.	202
Avrutskaya I.A.	11		
		Gamayunova I.M.	133
Babak E.A.	14	Gelovani G.A.	41
Bagotskaya I.A.	15	Gilmanshina S.I.	43
Baraboshkin A.N.	172	Gorelik V.E.	45
Barbin N.M.	18	Gorodyskii A.V.	160
Berezhnaya A.G.	21	Grigoryev V.P.	45
Bobe S.D.	230	Guseva L.T.	48
Bobov S.S.	239		
Bostanov V.	24	Hallik A.	51,191
Boytsov V.G.	15		
Bozhenko L.G.	94	Itov G.U.	11
Bukun N.G.	27	Ivanovsky L.E.	18
Burkal'tseva L.A.	88	Izotova V.V.	209
Bykova L.V.	3		
		Jänes A.	53
Chernyshov S.F.	85		
Choba M.A.	167	Kagolovskij S.A.	222
Chumakov I.V.	30	Kalinauskas P.	194
Churaev N.V.	122	Kaplan G.I.	59
Churikov A.V.	133	Karasevskii A.I.	58
		Kasatkin E.V.	59
Daikhin L.I.	33	Kavardakov N.I.	62
Danilov F.I.	35,90	Kazarinov V.E.	15,65
Dobrenkov G.A.	43,48	Khanova L.A.	200
Dzhavakhidze P.G.	37	Kharkats Yu.I.	67,135

Kholodov S.N.	157	Lubushkin V.I.	157
Kichigin V.I.	62	Lust E.	53, 109, 112, 116, 144
Kireev D.V.	167	Lust K.	116
Kolesnichenko I.I.	70,	Lvov A.L.	133
Kolyadko E.A.	155		
Kondratiev V.V.	79	Makarova L.L.	152
Kondrikov N.B.	178	Malycheva O.I.	180
Kornyshev A.A.	37	Man'ko L.Yu.	93
Korshin G.V.	72	Manuyrov I.R.	72
Kosikhin L.T.	172	Marsagishvili T.A.	119
Kostin N.A.	77	Mashirin A.	207
Kozachinskiy A.E.	148	Maslii A I.	24
Kozlova N.V.	162	Mazin V.M.	122
Kravtsov V.I.	79	Michri A.A.	242
Kriksunov L.B.	81	Mikulina O.E.	125
Kris R.E.	58		
Krishtalik L.I.	83	Nagaev E.L.	128
Kryukov Yu.I.	85	Nashivin E.A.	236
Kublanovskii V.S.	14	Naumov V.I.	155, 209
Kucherenko S.S.	94	Nauryzbaev M.K.	5
Kucherov S.S.	11	Nazmutdinov R.R.	131, 180
Kudryavtseva Z.I.	88	Neburchilova E.B.	59
Kuprin V.P.	90	Nechaeva O.N.	45
Kuznetsov An.M.	93	Nekrasov V.N.	18
Kuznetsov V.V.	94	Nekrassova N.A.	51
Kvaratskheliya G.R.	97	Nimon E.S.	133
Kvaratskheliya R.K.	97	Noskov A.V.	135
		Novitskiy E.M.	138
Lafi L.F.	200		
Lapin J.S.	162	Obraztsov V.B.	35
Laushera S.	99	Obretenov W.	24
Lazorenko-Manevich R.M.	212	Ovsyannikova E.V.	83
Levi M.D.	102		
Liebsch A.	37	Panov E.V.	58
Lilin S.A.	135, 188	Parfjonov Yu.A.	35
Loodmaa V.	104	Pärsimägi P.	144, 175
Losev V.V.	148	Pastukhov Yu.G.	141
Loshkaryov Yu.M.	106	Pchel'nikov A.P.	148



Petrii O.A.	212	Shilotkach G.D.	43
Petukhov A.A.	72	Shlepakov A.V.	230
Pleskov Yu.V.	151	Shpak G.F.	188
Pletnev M.A.	152	Shub D.M.	162,205
Podlovchenko B.I.	155	Silk T.	191
Popova A.A.	45	Skobochkina Yu.P.	3
Portnyagin O.V.	172	Smirnov V.A.	157
Potapova G.F.	157	Sobolev V.D.	122
Pototskaya V.V.	160	Sokirko A.V.	67
Prodanov Y.N.	162	Sokolova L.A.	212
Pshenichnikov A.G.	70	Stenina E.V.	99
Pud A.A.	125	Survila A.	194
Pullerits R.	53		
		Tamm J.	51,191,196
Remez I.D.	138	Tamm L.	196
Reshetnikov S.M.	152	Tammeveski K.	198
Reznik M.F.	162,178	Tarasevich M.R.	200
Rotenberg Z.A.	164	Tarasov A.Ya.	202
Rudoy V.M.	239	Tatishvili G.D.	119
		Telepnya Yu.V.	205
Safonov V.A.	167	Tenno T.	198,207
Sakharova A.Ya.	151	Tikhomirov A.V.	30
Salem R.	170	Tjurin Yu.M.	209
Saltykova N.A.	172	Tkachenko S.V.	39
Salve M.	116	Tomilov A.P.	125
Sazont'eva T.V.	209	Tsirlina G.A.	212
Scuratnik Ya.B.	148	Tsygankova L.E.	214
Semenikhin O.A.	164	Tüür A.	104
Semevsky V.	175	Tuzankin A.Y.	131
Senotov A.A.	133		
Sevastyanov A.E.	151	Ukshe A.E.	216
Shalaginov V.V.	162,178	Ukshe E.A.	219
Shapnik M.S.	131,180	Urbakh M.I.	37
Shapoval G.S.	125		
Shcherbakov A.B.	90	Vares P.	196
Shchitovskaya E.N.	178	Vargalyuk V.F.	222
Shein A.B.	182	VÄärtnou M.	144,175,224
Sherstobitova I.N.	185	Vigdorovich M.V.	227

Vigdorovich V.I.	227	Yevtushenko N.Y.	160
Vishnyakova N.A.	11	Yusupova M.Yu.	241
Vol'fkovich Yu.M.	122,230		
Vorotyntsev M.A.	233	Zaitsev A.A.	230
Vyzhimov Y.M.	48,234	Zakarina N.A.	241
		Zerina T.A.	242
Yakovleva A.A.	236	Zhamierashvili M.G.	97
Yashina G.M.	239	Zhuravlev A.N.	11
Yemets V.V.	15	Zolotova T.K.	230

## CONTENTS

B.N.AFANASIEV, L.V.BYKOVA, Yu.P.SKOBOCHKINA. Forecasting of Tetraalkylammonium Cations' Influence of Hydroxonium Cation and Oxygen Molecules' Discharge Kinetics. . . . .	3
N.K.ALTAYEV, Kh.K.DZHUMABEKOVA, M.K.NAURYZBAYEV. On Statistical Theory of Organic Surfactants' Influence on the Kinetics of Cations Electroreduction . . . . .	5
A.ALUMAA. Adsorption of Organic Compounds on a Bismuth Electrode from Ethylene Glycol. . . . .	7
I.A.AVRUTSKAYA, S.S.KUCHEROV, A.N.ZHURAVLEV, G.V.ITOV, N.A.VISHNYAKOVA. Voltammetry of Organic Compounds on the Glassy Carbon Electrode in the Presence of Lead Ions . . . . .	11
E.A.BABAK, V.S.KUBLANOVSKII. Parameters of Double Layer Charging. . . . .	14
I.A.BAGOTSKAYA, V.V.YEMETS, V.G.BOYTSOV, V.E.KAZARINOV. The Influence of Metal Nature on the Structure of the Electric Double Layer in N-Methylformamide in the Solution of Inactive Electrolyte. . . . .	15
N.M.BARBIN, V.N.NEKRASOV, L.E.IVANOVSKY. The Effect of Electro-Oxidation of Oxide-Containing Ions on the Adsorption Capacity of the Chlorine Glass-Carbon Electrode and on the Chloride Ion Charge. . . . .	18
A.G.BEREZHNYAYA, V.V.EKILIK, V.A.FEVRALEVA. On the Role of Adsorption Process in Inhibition of Anodic Dissolving of Alloys NiZn and SnIn . . . . .	21
V.BOSTANOV, A.I.MASLII, W.OBRETENOV. Influence of the Surfactants' Adsorption on the Propagation Rate of Monoatomic Layers during Electrocrystallization of Silver. . . . .	24
N.G.BUKUN. Electrode Potentials and Work Functions . . . . .	27
I.V.CHUMAKOV, A.V.TIKHOMIROV. On the Mechanism of Electroreduction of Acrylonitrile on Mercury, Cadmium and Lead. . . . .	30

L.I.DAIKHIN. The Theory of the Protonic Acid Doping of Polyaniline with Changeable Level of Oxidation. . .	33
F.I.DANILOV, V.B.OBRATSOV, Yu.A.PARFJONOV. Temperature Effect on the Adsorption of the Homologues of Aliphatic Alcohols and Acids . . . . .	35
P.G.DZAVAKHIDZE, A.A.KORNYSHEV, A.LIEBSCH, M.I.URBAKH. Theory of Nonlinear Optical Response of the Electrochemical Interface: Second Harmonic Generation. .	37
N.V.FEDOROVICH, S.V.TKACHENKO. The Electroreduction of Nitrate-Anion on Single Crystalline Silver Electrodes. . . . .	39
G.A.GELOVANI. On the Existence of Adsorption in Halogeneous Molten Systems. . . . .	41
S.I.GILMANSHINA, G.D.SHILOTKACH, G.A.DOBRENKOV. The Adsorption of Tirozine Cations on the Bismuth (Plane 111) and Mercury Electrodes . . . . .	43
V.P.GRIGORYEV, O.N.NECHAIEVA, V.E.GORELIK, A.A.POPOVA. On Possible Relationship Between the Potentials of Start of Passivation and Zero Charge of Transition Metals. . . . .	45
L.T.GUSEVA, Y.M.VYZHIMOV, G.A.DOBRENKOV. Modelling of Adsorption Layers of Organic Compounds on Bismuth and Mercury Electrodes. . . . .	48
A.HALLIK, N.A.NEKRASSOVA, A.ALUMAA, J.TAMM. Formation and Properties of Polypyrrole and Polythiophene Films on Pt and Au. . . . .	51
A.JÁNES, E.LUST, R.PULLERITS. Adsorption of Cyclohexanol on the (111) and (001) Faces of Antimony. . . . .	53
A.I.KARASEVSKII, R.E.KRIS, E.V.PANOV. The Formation of the Quasi-Metallic Layer on the Metal-Molten Salt Interface . . . . .	58
E.V.KASATKIN, E.B.NEBURCHILOVA, G.I.KAPLAN. Study of the Chemisorbed Surface Layers Formed at High Anodic Potentials on the Faces of Platinum Monocrystal . . .	59
N.I.KAVARDAKOV, V.I.KICHIGIN. The Impedance of the Cathodic hydrogen Evolution on Copper in Acidic Sulfate Solutions . . . . .	62
V.E.KAZARINOV. Electric Double Structure and Adsorption	

at Electrodes Modified by Electron-Conducting Polymer Films . . . . .	65
Yu.I.KHARKATS, A.V.SOKIRKO. Generation of Variable Sign Space Charge in a Diffusion Layer for Electrode Process with Subsequent Homogeneous Reaction. . .	67
I.I.KOLESNICHENKO, A.G.PSHENICHNIKOV. Intensification of Hydrogen Transport across a Pd Membrane by Modification of the Electrode/Electrolyte Interface	70
G.V.KORSHIN, I.R.MANYUROV, A.A.PETUKHOV. Investigation of Double Electric Layer on Glassy Carbon Electrode by Electroreflectance Method. . . . .	72
I.N.KOSENKO, V.V.TROFIMENKO. Kinetics and Mechanism of Monolayer Silver Electrodeposition from Rhodanide Solution. . . . .	74
N.A.KOSTIN. Influence of Pulse Polarization on Surface-Active Substances Adsorption in Metal Electroplating . . . . .	77
V.I.KRAVTSOV, V.V.KONDRATIEV. On the Influence of Supporting Electrolyte Concentration on the Electroreduction Rate of Dipyrophosphate Metal Complexes	79
L.B.KRIKSUNOV. Influence of Double Layer Structure on the Hydrogen Evolution Reaction at High Temperatures . . . . .	81
L.I.KRISHTALIK, N.M.ALPA TOVA, E.V.OVSYANNIKOVA. Electrostatic Interaction of Ions with a Solvent. . .	83
Yu.I.KRYUKOV, S.F.CHERNYSHOV, L.I.AL'TENTALLER. Adsorption and Electrocatalytic Properties of Sulfur-Containing Compounds of Iron Group Metals . . . .	85
Z.I.KUDRYAVTSEVA, L.A.BURKAL'TSEVA. Specific Features of the Formation of Subsurface Oxides on Nickel and Iridium Electrodes. . . . .	88
V.P.KUPRIN, F.I.DANILOV, A.B.SHCHERBAKOV. On the Prediction of the Non-Specific Adsorption in the Organic Molecule - Metal - Water System . . . . .	90
An.M.KUZNETSOV, L.Yu.MAN'KO. A Monte Carlo Simulation of the Interaction of Hydrated Ions with the Metal Surface . . . . .	93
V.V.KUZNETSOV, L.G.BOZHENKO, S.S.KUCHERENKO, O.V.FEDO-	

ROVA. Role of Adsorption Phenomena in Cadmium and Cupric Ions Discharge Kinetics in Mixed Solvents. . . . .	94
R.K.KVARATSKHELIYA, G.R.KVARATSKHELIYA, M.G.ZHAMIERAS-HVILI. Voltammetry and IR Spectroscopy of Nitrogen (5+) in High-Basic Media. . . . .	97
S.LAUSHERA, E.V.STENINA. To the Ising Model Application for Adsorption Description of Two-Dimensional Condensed Layers of Organic Substances on Electrode/Solution Interface. . . . .	99
M.D.LEVI. Equilibrium Double Layer Structure and Electrode Kinetics at Electron-Conducting Polymers. . . . .	102
V.LOODMAA, M.ARULEPP, A.TÜÜR. The Effect of Temperature on the Output Signal of Ammonia Gas Sensor. . . . .	104
Yu.M.IOSHKARYOV. Adsorption of Surfactants and Metal Electrodeposition Kinetics. . . . .	106
E.LUST, K.ANNI. Electrical Double Layer on the Single Crystal Antimony Electrodes in the Ethanolic Surface Inactive Electrolyte Solutions . . . . .	109
E.LUST, J.EHRLICH. Electrical Double Layer and Adsorption of Cyclohexanol on the (0001) and (11 $\bar{2}$ 0) Faces of Cadmium. . . . .	112
K.LUST, M.SALVE, E.LUST. Adsorption of Cl <sup>-</sup> , Br <sup>-</sup> , I <sup>-</sup> and SCN <sup>-</sup> Anions on Single Crystal Planes of Bismuth Electrodes . . . . .	116
T.A.MARSAGISHVILI, G.D.TATISHVILI. Structure of Double Electric Layer and Radiation of Radiowaves. . . . .	119
V.M.MAZIN, Ju.M.VOLFKOVICH, V.D.SOBOLEV, N.V.CHURAEV. Investigation of the Electric Double Layer at the Ion-Exchange/Electrode Interface and Inside Ion-Exchange Membrane . . . . .	122
O.E.MIKULINA, G.S.SHAPOVAL, A.P.TOMILOV, A.A.PUD. The Influence of Supporting Electrolyte Composition on Electrochemical Reactions and Subsequent Degradation of Solid-Phase Polymeric Dielectrics. . . . .	125
E.L.NAGAEV. Mutual Dependence of Chemisorption and Electron Properties of Metal Small Particles and Thin Films. . . . .	128
R.R.NAZMUTDINOV, M.S.SHAPNIK, A.Y.TUZANKIN. Compact	

Layer at the Metal/Water Interface Quantum Chemical and Statistical Approach. . . . .	131
E.S.NIMON, A.V.CHURIKOV, I.M.GAMAYUNOVA, A.A.SENOTOV, A.V.LVOV. Investigation of the Li/Nonaqueous Solution Interface By Photoemission Technique . . .	133
A.V.NOSKOV, Yu.I.KHARKATS, S.A.LILIN. Formation of Space Charge in the System with Fixed Charges . .	135
E.M.NOVITSKY, I.D.REMEZ. The Influence of Crystallographic Orientation of Oxide Electrolyte on Double Electrical Layer of Gold Electrode. . . . .	138
Yu.G.PASTUKHOV. A Study of the Double Layer and Adsorption on Gold and Silver Electrodes in Molten Salts by Estance-Method . . . . .	141
P.PÄRSIMÄGI, K.ANNI, M.VÄÄRTNÖU, E.LUST. Electrical Double Layer Structure on the (111), (001) and (01 $\bar{1}$ ) Planes of a Bismuth Single Crystal. . . . .	144
A.P.PCHELNIKOV, A.E.KOZACHINSKIY, Ya.B.SCURATNIK, V.V.LOSEV. Electrochemical Behaviour and Corrosion of Nickel in Acid Solutions. . . . .	148
Yu.V.PLESKOV, A.Ya.SAKHAROVA, A.E.SEVASTYANOV. The Synthetic Semiconducting Diamond Electrode . . . . .	151
M.A.PLETNEV, L.L.MAKAROVA, S.M.RESHETNIKOV. Special Features of Quaternary Ammonium Salts Influence on Iron Anodic Dissolution in Hydrochloric Acid. . .	152
B.I.PODLOVCHENKO, E.A.KOLYADKO, V.I.NAUMOV. Determination of Zero Charge Potential in the Presence of Adatoms . . . . .	155
G.F.POTAPOVA, S.N.KHOLODOV, V.A.SMIRNOV, V.I.LUBUSHKIN. Adsorptive and Catalytic Properties of Glass Carbon in the Process of Ozone Synthesis in Fluoride-Containing Solutions. . . . .	157
V.V.POTOTSKAYA, A.V.GORODYSKII, N.Y.YEVTUSHENKO. The Singularities of Diffusion Relaxation of an Electrolyte in the Double Electric Layer upon Pulse Effects . . . . .	160
Y.N.PRODANOV, N.V.KOZLOVA, M.F.REZNIK, V.V.SHALAGINOV, A.E.AVRUSCHENCO, J.S.LAPIN, D.M.SHUB. Influence of Process in the Near-Cathodic Layer at the Compo-	

sition and the Properties of Hydroxide Deposits Used as Anodic Materials. . . . .	162
Z.A.ROTENBERG, O.A.SEMENIKHIN. Application of Inten- sity Modulated Photocurrent Method in Electro- chemical Kinetics . . . . .	164
V.A.SAFONOV, M.A.CHOBA, D.V.KIREEV. On The Effect of the Time Factor on the Composition and Struc- ture of the Renewed Surface of Sn-Pb Alloy Elec- trodes (Based on the Capacity Measurement Data in Solutions with Organic Surface-Active Addi- tives). . . . .	167
R.SALEM. The Metal-Electrolyte Surface in the Elec- tric Field. . . . .	170
N.A.SALTYKOVA, L.T.KOSIKHIN, A.N.BARABOSHKIN, O.V.POR- TNYAGIN, N.O.ESINA. Study of Effect of Passi- vating Substances upon Initial Stage Silver and Platinum Electrocrystallization from Molten Salts . . . . .	172
V.SEMEVSKY, P.PÄRSIMÄGI, M.VÄÄRTNÖU, A.ALUMAA. On the Application of Chronocoulometry in Studies of Ionic Adsorption on the Bismuth Drop Electrode. . . . .	175
V.V.SHALAGINOV, M.F.REZNIK, E.N.SHCHITOVSKAYA, N.B. KONDRIKOV. Adsorption Properties and Selectivi- ty of Manganese Dioxide in Sea Water Electroly- sis . . . . .	178
M.S.SHAPNIK, R.R.NAZMUTDINOV, O.I.MALYUCHEVA. Inves- tigation of the Water Chemisorption on the In- dium Surface. . . . .	180
A.B.SHEIN, R.G.AITOV. The Kinetics of the Cathodic and Anodic Processes on the Eutectic Alloys of Silicon and Germanium with 3d-Transition Metals . . . . .	182
I.N.SHERSTOBITOVA. Effect of the Solution pH and Ad- sorption of $I^-$ Ions on the Hydrogen Overvoltage on Tantalum in Acidic Sulphate Media. . . . .	185
G.F.SHPAK, S.A.LILIN. State of Surface of High-Tempe- rature Alloy ZrS6-KF and Its Basic Components at Anodic High-Speed Dissolution in Non-Aqueous Perchlorate Solutions . . . . .	188



T.SILK, A.HALLIK, J.TAMM. The Ellipsometric Study of Polypyrrole Films . . . . .	191
A.SURVILA, P.KALINAUSKAS. Photoeffects at the Interface Cu/Cu(II), Glycine, $\alpha$ - or $\beta$ -Alanine. . .	194
J.TAMM, L.TAMM, P.VARES, J.AROLD. Hydrogen Evolution Reaction on the Metals of Iron Group. . . . .	196
K.TAMMEVESKI, T.TENNO. Oxygen Reduction on Gold. . .	198
M.R.TARASEVICH, L.A.KHANOVA, L.F.LAPI. Specific Features of the Adsorption of Macroheterocycles on a Metal Electrode . . . . .	200
A.Ya.TARASOV, A.T.FILYAYEV. On the Reason of the Onset of Zero Estance in the Interface "Reversible Electrode/Solid Electrolyte". . . . .	202
Yu.V.TELEPNYA, D.M.SHUB. Adsorptive and Electrochemical Properties of Platinum Film of Different Dispersion Deposited on Titanium Base . . . . .	205
T.TENNO, A.MASHIRIN. The Distribution of Gas Component in the Interphasal Boundary. . . . .	207
Yu.M.TJURIN, V.V.IZOTOVA, V.I.NAUMOV, T.V.SAZONT'EVA. Deposition Potential and Zero Charge Potential as Electrocrystallization Parameters of Metals. . . . .	209
G.A.TSIRLINA, R.M.IAZORENKO-MANEVICH, L.A.SOKOLOVA, O.A.PETRII. Spectral Properties of Electrochemically Generated Cuprate Film. . . . .	212
L.E.TSYGANKOVA. The Differentiation of the Surface Active Centres Responsible for Chemical and Electrochemical Metal Dissolution . . . . .	214
A.E.UKSHE. Constant Phase Shift as a Consequence of the Fractal Character of Ion Transport. . . . .	216
E.A.UKSHE. The Over-Charge Effect in Double Electrical Layer . . . . .	219
V.F.VARGALYUK, S.A.KAGOLOVSKIJ. About Accounting of Reagent Specific Adsorption When Determing the Kinetic Parameters of the Electrochemical Reactions . . . . .	222
M.VÄÄRTNÖU, A.ALUMAA. On the Relation between the Interaction of Adsorbate Molecules with Electrode Surface and Its Ionization Potential. . . . .	224

M.V.VIGDOROVICH, V.I.VIGDOROVICH. Kinetics of Reactions with Participation of Reagent as a Stimulator of Active Dissolution and a Passivator of Metal in Parallel Processes . . . . .	228
Yu.M.VOL'FKOVICH, A.V.SHLEPAKOV, T.K.ZOLOTOVA, S.D.BOBE, A.A.ZAITSEV. Investigation of the Influence of the Porous Structure, Interface Capacity, Kinetic and Diffusion Characteristics on the Discharge-Charge Curves of Polyaniline Electrodes. . . . .	231
M.A.VORONTYNTSEV. Theory of Equilibrium and Kinetic Phenomena in Electron-Conducting Polymer Films. . . . .	234
Y.M.VYZHIMOV. Individual and Combined Adsorption of Corrosion Inhibitors on Ferrum. . . . .	235
A.A.YAKOVLEVA, E.A.NASHIVIN. The Connection between the $\text{CO}_3^{2-}$ -Ion Adsorption Process on Pt, Rh, Ir and the Kinetics of the Peroxydicarbonate Synthesis . . . . .	237
G.M.YASHINA, S.S.BOBOV, V.M.RUDOY. The Study of the Interface Structure and of the Flotation Reagents' Adsorption on the Mineral/Solution Interface. . . . .	240
N.A.ZAKARINA, M.Yu.YUSUPOVA. Influence of Copper on Electrocatalytic Properties of High-Dispersed Pd/C Electrodes. . . . .	242
T.A.ZERINA, A.A.MICHRI. Influence of Solvent on the Adsorbability of 1-(2-Propionitrile)-Pyrrolidine and 1-(3-Aminopropyl)-Pyrrolidine on Platinum and Nickel Electrodes . . . . .	243
AUTHOR INDEX . . . . .	246